VISION IN CEPHALOPODS, VOLUME II

EDITED BY: Daniel Osorio, Chuan-Chin Chiao and Frederike Diana Hanke
PUBLISHED IN: Frontiers in Physiology

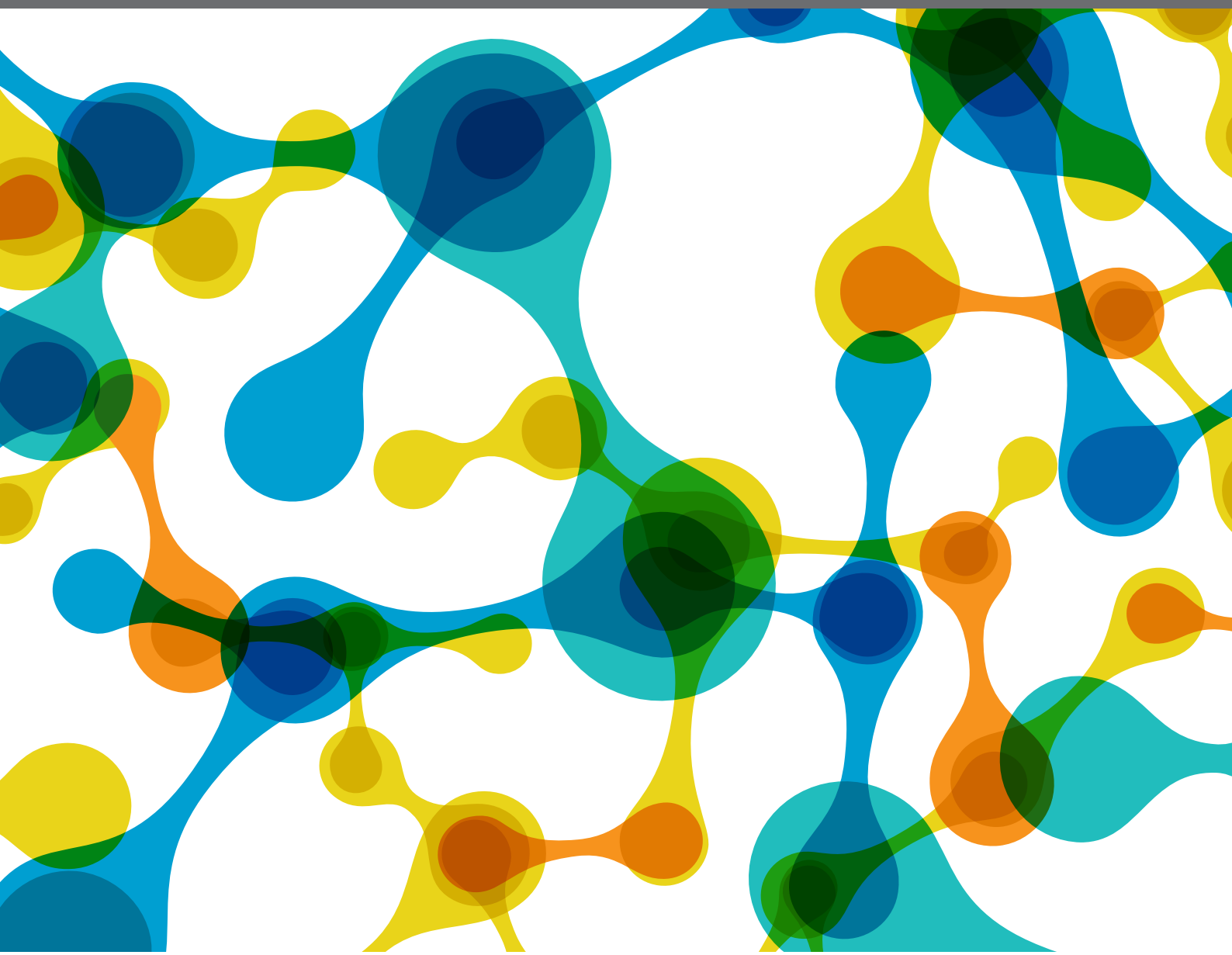

frontiers Research Topics

ISSN 1664-8714
ISBN 978-2-88971-407-0
DOI 10.3389/978-2-88971-407-0

About Frontiers

Frontiers is more than just an open-access publisher of scholarly articles: it is a pioneering approach to the world of academia, radically improving the way scholarly research is managed. The grand vision of Frontiers is a world where all people have an equal opportunity to seek, share and generate knowledge. Frontiers provides immediate and permanent online open access to all its publications, but this alone is not enough to realize our grand goals.

Frontiers Journal Series

The Frontiers Journal Series is a multi-tier and interdisciplinary set of open-access, online journals, promising a paradigm shift from the current review, selection and dissemination processes in academic publishing. All Frontiers journals are driven by researchers for researchers; therefore, they constitute a service to the scholarly community. At the same time, the Frontiers Journal Series operates on a revolutionary invention, the tiered publishing system, initially addressing specific communities of scholars, and gradually climbing up to broader public understanding, thus serving the interests of the lay society, too.

Dedication to Quality

Each Frontiers article is a landmark of the highest quality, thanks to genuinely collaborative interactions between authors and review editors, who include some of the world's best academicians. Research must be certified by peers before entering a stream of knowledge that may eventually reach the public - and shape society; therefore, Frontiers only applies the most rigorous and unbiased reviews.
Frontiers revolutionizes research publishing by freely delivering the most outstanding research, evaluated with no bias from both the academic and social point of view. By applying the most advanced information technologies, Frontiers is catapulting scholarly publishing into a new generation.

What are Frontiers Research Topics?

Frontiers Research Topics are very popular trademarks of the Frontiers Journals Series: they are collections of at least ten articles, all centered on a particular subject. With their unique mix of varied contributions from Original Research to Review Articles, Frontiers Research Topics unify the most influential researchers, the latest key findings and historical advances in a hot research area! Find out more on how to host your own Frontiers Research Topic or contribute to one as an author by contacting the Frontiers Editorial Office: frontiersin.org/about/contact

VISION IN CEPHALOPODS, VOLUME II

Topic Editors:
Daniel Osorio, University of Sussex, United Kingdom
Chuan-Chin Chiao, National Tsing Hua University, Taiwan
Frederike Diana Hanke, University of Rostock, Germany

Citation: Osorio, D., Chiao, C.-C., Hanke, F. D., eds. (2021). Vision in Cephalopods, Volume II. Lausanne: Frontiers Media SA. doi: 10.3389/978-2-88971-407-0

Table of Contents

frontiers in Physiology

EDITORIAL
published: 02 August 2021
doi: 10.3389/fphys.2021.731780

Editorial: Vision in Cephalopods: Part II

Frederike D. Hanke[1]*, *Chuan-Chin Chiao*[2] *and Daniel C. Osorio*[3]

[1] Institute for Biosciences, Neuroethology, University of Rostock, Rostock, Germany, [2] Department of Life Science, National Tsing Hua University, Hsinchu, Taiwan, [3] School of Life Sciences, University of Sussex, Brighton, United Kingdom

Keywords: eye, optics, visual system, visual adaptations, octopus, sepia

Editorial on the Research Topic

Vision in Cephalopods: Part II

Coleoid cephalopods are much like fish, with single chambered eyes, large visual brain areas, and complex behaviors, but they have evolved independently, and their locomotion—inspiration to the field of soft robotics (Calisti et al., 2011; Kim et al., 2013), adaptive coloration, and polarization vision are quite unlike those of vertebrates (Hochner et al., 2006; Hanlon and Messenger, 2018). What then do these fascinating molluscs, often said to be intelligent, reveal about chance and necessity in the evolution of brains and behavior?

Our 2018 Frontiers in Physiology Research Topic "Vision in cephalopods" (https://www.frontiersin.org/research-topics/4856/vision-in-cephalopods) showed that cephalopod vision research is a small but flourishing field. The present collection of eight research articles and one review demonstrates the strength and significance of the field, encompassing subjects such as phototransduction (Bonadè et al.), psychophysics of polarization vision (Nahmad-Rohen and Vorobyev), visual development (Groeger et al.) and two of the most distinctive cephalopod behaviors—prey capture (Wu et al.; Brauckhoff et al.) and adaptive coloration (Hadjisolomou et al.). Cephalopods are best known in neuroscience for the squid giant axon and octopus cognition, but the present collection finds cuttlefish of the genus *Sepia* as the subject of all but two on *Octopus* and one on a squid.

Most cephalopods are color blind (but c.f. Stubbs and Stubbs, 2016), but polarization vision might substitute color vision (Pignatelli et al., 2011), allowing them to judge surface properties, and to mitigate the effects of scatter in turbid water. However, whereas most animals process color and luminance in separate visual pathways, Nahmad-Rohen and Vorobyev find that octopus use the same system for polarization, and luminance. Polarization patterns—which are invisible to the human eye—feature in the repertoire of visual cephalopod communication signals. Here, López Galán et al. highlight the richness of these signals, and the dynamics in courtship displays of the cuttlefish *Sepia plangon*, which has 57 body pattern components deployed in 18 body patterns. Many of these patterns are displayed only briefly, and an attempt to test these small cuttlefish with 3D printed models of conspecifics failed because the models lacked the dynamics of the visual signals. It would be interesting to know how far learning and motor skill play a part in the function of these elaborate visual signals as they do in bird song (Marler, 1990). Dynamic patterns are possible because cephalopods' color change is mediated by chromatophores, which are directly innervated by motoneurons (Messenger, 2001), allowing rapid change and the production of moving patterns known as passing cloud displays. Here Hadjisolomou et al. show that individual chromatophores of the squid *Doryteuthis pealeii* can respond to a flash with a mean latency of only 50 ms. Visual movement is also important in prey capture when both prey and predator move, and Wu et al. find that the cuttlefish *Sepia pharaonis* can extract the speed and direction from their moving prey to track prey and to select the visual hunting strategy most appropriate for the specific situation.

OPEN ACCESS

Edited and reviewed by:
Klaus H. Hoffmann, University of Bayreuth, Germany

***Correspondence:**
Frederike D. Hanke
frederike.hanke@uni-rostock.de

Specialty section:
This article was submitted to Invertebrate Physiology, a section of the journal Frontiers in Physiology

Received: *28 June 2021*
Accepted: *09 July 2021*
Published: *02 August 2021*

Citation:
Hanke FD, Chiao C-C and Osorio DC (2021) Editorial: Vision in Cephalopods: Part II. Front. Physiol. 12:731780. doi: 10.3389/fphys.2021.731780

Turning to visual ecology, Goerger et al. investigate how turbidity affects visual development of the cuttlefish *Sepia officinalis*; surprisingly a low level of turbidity during larval development improves polarization sensitivity. Cephalopods also have to cope with changes in ambient luminance. The common octopus *Octopus vulgaris* can adapt to sudden changes in luminance with a rapid pupillary response (Soto et al.). With the characterization of the dynamics of the pupil of *Octopus vulgaris*, our understanding of vision in this cephalopod species, that is/has been widely used in visual (discrimination) experiments, was advanced (for review see Hanke and Kelber). While a mobile pupil can be of advantage in an inhomogeneous light environment, ambient luminance also changes with a daily cycle. Although some cephalopod species are active during the day, Brauckhoff et al. show that the cuttlefish can hunt in dim light conditions but not in complete darkness.

Where next? In the 1930's, Young (1938) already highlighted the potential of *Octopus* for neuroscience leading to wonderful anatomical work, behavioral studies, and began investigations of the squid giant axon, but nevertheless research on "simple" nervous systems mostly focused on insects and gastropod molluscs. Modern physiological methods offer the potential for recording from cephalopod brain to understand the visual motor control circuitry, learning and more. We are unlikely to attract the support offered to key model organisms or for clinical applications, but, as Young already realized, cephalopods offer unique insight into principles of sensory-motor control, cognition and evolutionary neuroscience that are of the widest significance.

AUTHOR CONTRIBUTIONS

All authors listed have made a substantial, direct and intellectual contribution to the work, and approved it for publication.

REFERENCES

Calisti, M., Giorelli, M., Levy, G., Mazzolai, B., Hochner, B., Laschi, C., et al. (2011). An octopus-bioinspired solution to movement and manipulation for soft robots. *Bioinspir. Biomimetics* 6:036002. doi: 10.1088/1748-3182/6/3/036002

Hanlon, R. T., and Messenger, J. B. (2018). *Cephalopod Behaviour*. Cambridge: Cambridge University Press. doi: 10.1017/9780511843600

Hochner, B., Shomrat, T., and Fiorito, G. (2006). The octopus: a model for a comparative analysis of the evolution of learning and memory mechanisms. *Biol. Bull.* 210, 308–317. doi: 10.2307/4134567

Kim, S. H., Laschi, C., and Trimmer, B. (2013). Soft robotics: a bionspired evolution in robotics. *Trends Biotechnol.* 31, 287–294. doi: 10.1016/j.tibtech.2013.03.002

Marler, P. R. (1990). Song learning: the interface between behaviour and neuroethology. *Philo. Transact. R. Soc. B: Biol. Sci.* 329, 109–114. doi: 10.1098/rstb.1990.0155

Messenger, J. B. (2001). Cephalopod chromatophores: neurobiology and natural history. *Biol. Rev.* 76, 473–528. doi: 10.1017/S1464793101005772

Pignatelli, V., Temple, S. E., Chiou, T.-H., Roberts, N. W., Collin, S. P., and Marshall, N. J. (2011). Behavioural relevance of polarization sensitivity as a target detection mechanism in cephalopods and fishes. *Philo. Transact. R. Soc. Lond. B Biol. Sci.* 366, 734–741. doi: 10.1098/rstb.2010.0204

Stubbs, A. L., and Stubbs, C. W. (2016). Spectral discrimination in color blind animals via chromatic aberration and pupil shape. *PNAS* 113, 8206–8211. doi: 10.1073/pnas.1524578113

Young, J. Z. (1938). The functioning of the giant nerve fivres of the squid. *J. Experi. Biol.* 15, 170–185. doi: 10.1242/jeb.15.2.170

Conflict of Interest: The authors declare that the research was conducted in the absence of any commercial or financial relationships that could be construed as a potential conflict of interest.

frontiers in Physiology

REVIEW
published: 14 January 2020
doi: 10.3389/fphys.2019.01637

The Eye of the Common Octopus (*Octopus vulgaris*)

Frederike D. Hanke[*†] and Almut Kelber*

Lund Vision Group, Department of Biology, Lund University, Lund, Sweden

Octopus vulgaris, well-known from temperate waters of the Mediterranean Sea and a well-cited model species among the cephalopods, has large eyes with which it scans its environment actively and which allow the organism to discriminate objects easily. On cursory examination, the single-chambered eyes of octopus with their spherical lenses resemble vertebrate eyes. However there are also apparent differences. For example, the retina of the octopus is everted instead of inverted, and it is equipped with primary rhabdomeric photoreceptors rather than secondary ciliary variety found in the retina of the vertebrate eye. The eyes of octopus are well adapted to the habitat and lifestyle of the species; the pupil closes quickly as a response to sudden light stimuli mimicking a situation in which the octopus leaves its den in shallow water during daytime. Although the many general anatomical and physiological features of octopus vision have been described elsewhere, our review reveals that a lot of information is still missing. Investigations that remain to be undertaken include a detailed examination of the dioptric apparatus or the visual functions such as brightness discrimination as well as a conclusive test for a faculty analogous to, or in lieu of, color vision. For a better understanding of the octopus eye and the functions mediated by it, we suggest that future studies focus on knowledge gaps that we outline in the present review.

Keywords: vision, cephalopods, octopoda, visual function, optics

OPEN ACCESS

Edited by:
Graziano Fiorito, Stazione Zoologica Anton Dohrn, Italy

Reviewed by:
David B. Edelman, Dartmouth College, United States
Justin Marshall, University of Queensland, Australia
Eve Seuntjens, KU Leuven, Belgium

****Correspondence:***
Frederike D. Hanke
frederike.hanke@uni-rostock.de

†Present address:
Frederike D. Hanke, Neuroethology, Institute for Biosciences, University of Rostock, Rostock, Germany

Specialty section:
This article was submitted to Invertebrate Physiology, a section of the journal Frontiers in Physiology

Received: *19 October 2019*
Accepted: *30 December 2019*
Published: *14 January 2020*

Citation:
Hanke FD and Kelber A (2020) The Eye of the Common Octopus (Octopus vulgaris). Front. Physiol. 10:1637. doi: 10.3389/fphys.2019.01637

INTRODUCTION

If you have ever encountered an octopus, the way the animal looks at you is striking; you feel as if you are being scanned. The eyes are one of the prominent characteristics of the octopus but also of cephalopods in general. Already from outside, the eyes appear to be special. They are usually rather large with a diameter of approximately 20 mm (see section "Eye Size and Ocular Dimensions"), and their pupils often have conspicuous shapes (see **Figure 1** and, for example, photos in Douglas, 2018). If one takes a closer look at eye morphology, the coleoid cephalopod eyes attract attention, as parallels can be drawn between the design of the camera type eyes of these molluscs and the design of vertebrate eyes, particularly those of fish (von Lenhossék, 1894; Packard, 1972). At the neuronal level, large parts of the cephalopod brain are dedicated to the processing of visual information as indicated by the size of their optic lobes (Young, 1960, 1971; Wells, 1966a; Maddock and Young, 1987).

In numerous studies on the eyes of many of the approximately 800 known species of cephalopods (Jereb and Roper, 2005, 2010; Jereb et al., 2014), we have learned a lot about specialized eye designs, for example, the pinhole eye of *Nautilus* (Hensen, 1865; Griffin, 1900; Wiley, 1902; Merton, 1905; Hurley et al., 1978; Muntz and Ray, 1984; Muntz, 1991; Barber, 2010), the asymmetrical eyes of *Histioteuthis* (Denton and Warren, 1968; Young, 1975; Wentworth and Muntz, 1989; Thomas et al., 2017) and the largest eyes on Earth, found in *Architeuthis* and

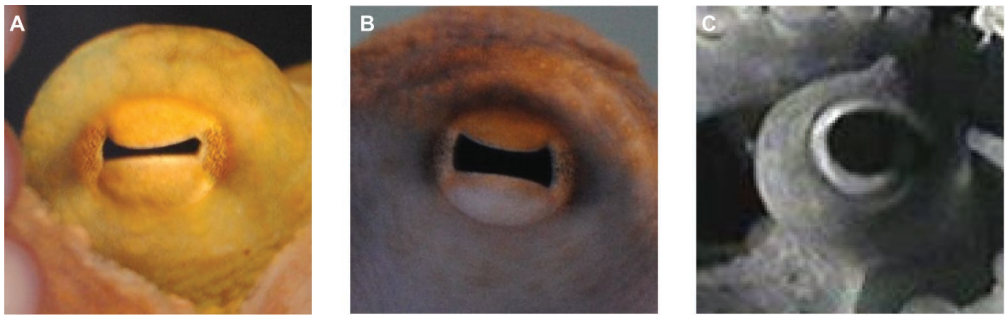

FIGURE 1 | Pupil of *Octopus vulgaris*. **(A)** Constricted horizontal slit pupil in bright light, **(B)** intermediate pupil size, and **(C)** fully dilated pupil in dim light conditions.

Mesonychoteuthis (Nilsson et al., 2012), just to mention a few examples. In addition to reports regarding peculiar eye designs, researchers have worked on many aspects of the visual system in more common cephalopod genera such as *Octopus*, *Eledone*, *Sepia*, and *Loligo*. Young (1962a) pointed out basic similarities among the eyes of these genera, but at the same time, mentioned important differences between them. Because of these apparent differences, neither generalizing conclusions from one species to another, nor combining data from different species to derive overarching conclusions should be the method of choice.

This review aims to summarize the present knowledge regarding the eye and vision of a well-studied cephalopod, the common octopus, *Octopus vulgaris*. Thus, when we are referring to octopus in the text, data collected with *Octopus vulgaris* are considered; if data from other cephalopod species are included for comparison, the species name is indicated. We set out to collect information on vision in the common octopus as it is a prominent model species among cephalopods and has probably been the most-studied cephalopod species for more than 150 years. Especially in the mid-20th century, many studies were designed to unravel the discriminatory and cognitive abilities of this species using behavioral tests with visual stimuli (for example, see work by Boycott, Mackintosh, Messenger, Sutherland, Wells, and Young such as Boycott and Young, 1956; Young, 1956; Sutherland, 1957; Wells, 1960; Mackintosh, 1963; Messenger, 1968a). However, our understanding of vision in octopus is still patchy and has never been summarized specifically for this species. After a short, general introduction to *Octopus vulgaris* in general, it is the aim of the current review to gather, to the best of our knowledge, all information available on the eye of the common octopus. The collection of references can then form the basis for future investigations of vision and the visual faculties of this species. Accordingly, we will mention such future avenues in the text.

GENERAL INTRODUCTION TO *OCTOPUS VULGARIS*

Octopus vulgaris, first described by Cuvier in 1797, belongs to the family *Octopodidae* encompassing more than 200 species. The genus *Octopus* constitutes a "catchall" genus (Jereb et al., 2014) for all species that possess two rows of suckers on the eight arms and an ink sac. The distribution of *Octopus vulgaris sensu stricto* (Jereb et al., 2014) covers the Mediterranean Sea, as well as the central and north-east Atlantic Ocean. The common octopus is said to be nocturnal (Woods, 1965; Altman, 1966; Kayes, 1974; Jereb et al., 2014), but it has been seen to shift its activity phase, for example in the presence of prey or predators (Meisel et al., 2013), and thus some studies report crepuscular or even diurnal activity (Mather, 1988; Meisel et al., 2003, 2006). In the presence of one of its many predators (Sanchez et al., 2015), the soft-shelled octopus either hides in dens, camouflages to the background with the help of a sophisticated system of pigment-filled chromatophores, electron-dense leucophores, and reflecting iridophores, or exhibits distinct behavioral displays (Packard and Sanders, 1971). The dens are inhabited only temporarily for a couple of days or weeks (Kayes, 1974; Mather and O'Dor, 1991). Octopus uses natural crevices or holes as hiding places or accumulates rocks and shells to build its own den. As a bottom feeder, foraging often seems to be tactile (Jereb et al., 2014), involving exploration of the surroundings with its arms, in search for crustaceans, fish, shelled molluscs or polychaetes (Mather, 1991; Boyle and Rodhouse, 2005; Mather et al., 2012; Sanchez et al., 2015). In addition, visual and chemical cues are most likely used to find prey (Boyle and Rodhouse, 2005). *Octopus vulgaris* is solitary, and the sexes only meet during mating (Hanlon and Messenger, 2018) when the male transfers spermatophore packages with its heterocotylus, an enlarged sucker on one of the arms, into the mantle cavity and oviduct of the female. At the end of the life cycle, the female lays 100,000–500,000 eggs bound together and glued to the ceiling of a den or to a rock. The female stays with the eggs for the duration of development, which can last up to 5 months, continuously caring for and defending the eggs. The female octopus does not feed during this period, digesting its own musculature in this last phase of its life (Jereb et al., 2014; Hanlon and Messenger, 2018). As a consequence, the female dies shortly after the eggs hatch. The 1–2 mm sized transparent hatchlings, called paralarvae, undergo a planktonic phase mostly in shallow (i.e., pelagic) waters that can last weeks to months before they settle on the sediment. The subsequent adult life stage can last up to 2 years during which octopus adopts a general benthic lifestyle but is still commonly found in pelagic waters. Specimens of *Octopus vulgaris* can reach a mantle length of up to 250 mm, a total length of over 1 m, and a body weight of more than 2 kg (Jereb et al., 2014).

Reader interested in the biology of cephalopods, including *Octopus vulgaris,* are referred to Hanlon and Messenger (2018), or to Jereb et al. (Jereb and Roper, 2005, 2010; Jereb et al., 2014, 2015).

EYE SIZE AND OCULAR DIMENSIONS

Often, the eye of *Octopus vulgaris* (**Figure 2**) is described as large. In several studies, external eye dimensions are given. Beer (1897) measured an eye length (most likely axial eye length) of 17 mm in an octopus individual weighing 607 g. Additionally, Hanlon and Messenger (2018) documented an eye diameter of 20 mm in an individual weighing 205 g. Both values are within the range of eye diameters of 15–20 mm given by Fröhlich (1914a) for *Eledone moschata*, *Octopus macropus,* and *Octopus vulgaris*. According to Packard (1969), a really large octopus can have an eye with a diameter larger than 20 mm; however 'really large' is not further specified by this author. For comparison, the eyes of humans are, on average, 24 mm in diameter (Augusteyn et al., 2012). Given that adult humans weigh far more than an octopus, the octopus indeed has a large eye relative to body size/mass. The octopus eye is large even when compared to a nocturnal bird such as the tawny owl (*Strix aluco*), which weighs 400–800 g, and has an eye diameter of 23–29 mm (Brooke et al., 1999).

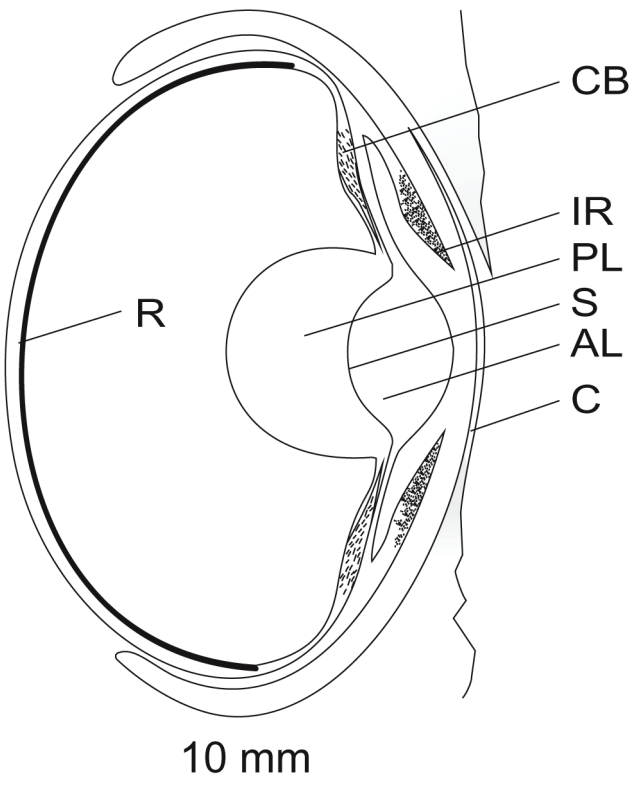

FIGURE 2 | Schematic of the eye of *Octopus vulgaris* (longitudinal vertical section). Light falling on the eye of octopus first hits the cornea (C). Beyond the cornea, the light passes the anterior chamber and the pigmented mobile iris (IR) before it is refracted by the spherical lens. The lens, composed of an anterior (AL) and a posterior part (PL) separated by a septum (S), is suspended by the ciliary body (CB). Finally, the light hits the everted retina (R) in the back of the eye. A detailed description of the ocular structures is given in the text. The figure was adapted from frozen sections of an octopus eye and from Figure 1 in Budelmann (1994) and Figure 5 in (Wells, 1966b) displaying an eye of *Octopus* spec. Scale 10 mm.

Beside external eye dimensions, no information on internal parameters such as ocular dimensions, radii of curvature, refractive indices or absorption coefficients of ocular media is available for octopus. These data would be required in order to develop detailed and informative optical models of the eye of octopus to further increase our understanding of how and what the octopus sees.

VISUAL FIELDS AND EYE MOVEMENTS

The eyes of octopus are placed laterally and can be moved independently, with the eye axes occasionally deviating by up to 180 degrees (Heidermanns, 1928). To date, no measurements of visual field size are available for this species. From the eye placement of octopus, one could assume that octopus possesses a small binocular visual field, to the front and possibly to the back; however, Budelmann et al. (1997) dispute the existence of a binocular field in octopods. In any case, octopus certainly has large monocular visual fields, the space in which objects can be seen with one eye. This is consistent with the animals watching or tracking objects preferable with one eye (Heidermanns, 1928; Muntz, 1963; Byrne et al., 2002, 2004). The size of the monocular visual field is likely similar to that of *Sepia officinalis*. Model calculations in *Sepia* revealed that the visual field is limited by pupil size and that it is much smaller (Schaeffel et al., 1989) than the 177 degrees estimated by Messenger (1968b) for the horizontal plane.

The octopus can modify the space it can oversee by retracting and bulging out its eyes, or by rotational eye movements. The rotational eye movements that can turn the eye up to 80 degrees sideways in either direction (Budelmann and Young, 1984) are mediated by four oblique muscles that pass halfway around the eyeball. In total, each octopus eye has seven extra-ocular muscles, each innervated by a separate nerve (Glockauer, 1915; Budelmann and Young, 1984). In contrast, decapod cephalopods have up to 14 eye muscles that are innervated by only four nerves (Glockauer, 1915; Budelmann and Young, 1993).

Octopus also shows reflexive eye movements. When stimulated by a large field vertical grating rotating on an optokinetic drum, the animals perform compensatory eye, head, and body movements (Packard, 1969).

Future studies of the visual fields of octopus are highly desirable, particularly those that provide measurements of the putative binocular visual field and evaluate its implications for binocular depth perception, the monocular visual field, and the dynamic visual field, taking eye movements into account. Regarding eye movements, it remains to be determined whether the octopus can also turn its eyes upwards and downwards, and if so, to what degree.

EYE LID AND CORNEA

As is likely the case with all octopods, octopus possesses a ring-shaped muscular skin fold or bulge around the eye that can close in a manner comparable to an eye lid (von Lenhossék, 1894; Magnus, 1902). This eye lid-like structure closes over a cornea (**Figure 2**) which is hardly visible in the living octopus. This cornea has also been referred to as pseudo-cornea (Schöbl, 1877) or pseudo-corneal fold (Amoore et al., 1959). According to previous studies (Beer, 1897; Magnus, 1902), which are supported by our own observations, the cornea is not a component of the eye, meaning that the cornea cannot be extracted together with the underlying ocular structures. Moreover, it has a dorsal opening which brings the anterior chamber — the compartment between cornea and lens — in contact with the surrounding sea water (Amoore et al., 1959; Wells, 1966b); although this finding is not undisputed. As expected, the fluid within the anterior chamber has the same sodium concentration as seawater, however the potassium concentration has been found to be higher (Amoore et al., 1959).

A detailed analysis of the cornea is required to determine the functional role of the cornea in the eye of the octopus. Interesting insight in this often neglected structure could also be obtained by studying the histological fine structure of the cornea or its development during ontogeny.

PUPIL AND IRIS

One of the most prominent features of the octopus eye is its pupil (**Figure 1**). The cephalopod pupil is mobile, in contrast to the pupil of fishes, excluding the elasmobranchs (Douglas, 2018). The pupil of octopus is circular in darkness (**Figure 1C**), while in bright light, it constricts to a horizontal slit (**Figures 1A,B**) corresponding to the orientation of the central stripe of increased photoreceptor density on the retina (Muntz, 1977; and see section "Retina and Visual Function"). Compared to other cephalopods that can have U- or W-shaped pupils (e.g., cuttlefish), a slit-shaped pupil is a rather simple pupil design (Douglas, 2018).

In general, the octopus pupil adapts the eye to changes in ambient light. The advantage of the pupillary reaction is that it is faster than the alternative adaptation mechanisms which, in octopus, are pigment migration and the contraction/enlargement of the photoreceptors (Babuchin, 1864; Young, 1963). Pupil dynamics were recently examined in an octopus by Soto (2018). The individual studied, with a mantle length of approximately 6.5 cm, had a pupil area of 33 mm^2 when the pupil was fully dilated. Pupil area decreased to approximately 4 mm^2, or 12% of the dark-adapted pupil area, when the eye was exposed to bright light. Constriction of the octopus pupil was thus similar to or a little weaker than in other cephalopod species (Douglas et al., 2005; Bozzano et al., 2009; Matsui et al., 2016) such as *Sepia officinalis* or *Eledone cirrhosa* that constrict their pupils to 3% of the maximal area (Douglas et al., 2005). It took the octopus pupil 0.5–1.3 s to reach half maximum constriction defined as the t_{50} value. Most other cephalopod pupils examined so far also constricted quickly upon light exposure with t_{50} values ranging from 0.3 to 3 s (Douglas et al., 2005; McCormick and Cohen, 2012; Matsui et al., 2016). Thus, these pupils are adapted to fast light changes also occurring in the habitat of octopus, for instance when they are leaving the den in shallow water during daytime hours. In contrast, pupil constriction took 90 s in *Nautilus pompilius* (Hurley et al., 1978), a species that is most likely not experiencing drastic variations in ambient light in its habitat. The same probably holds true for *Japetella diaphana*, a deep sea octopus, whose pupil takes approximately 6 s to constrict (Douglas, 2018). In addition, the range of light intensities to which the pupil of *Octopus vulgaris* reacts with intermediate pupil sizes is narrow (Hess, 1905; Soto, 2018); the pupil already fully constricts in response to a luminance of approx. 20 cd/m^2.

Axial light has a stronger effect on pupillary dilation than light from above (Soto, 2018), as described generally for cephalopods by Hess (1909, 1910) or McCormick and Cohen (2012). This "shadow effect" of the pupil for light from above might result in a more constant intensity of the retinal image than the illumination in the natural environment, in which most light is coming from above; this effect has so far only been described for *Sepia officinalis* (Mäthger et al., 2013).

Pupil dilation seems highly variable and individual (Magnus, 1902), and is also affected by factors other than ambient illumination (Weel and Thore, 1936). Octopus might constrict its pupil to camouflage the eye, allowing the animal to blend into the substrate, and the dilated pupil could serve as intra-specific deimatic signal, making the animal appear larger and more threatening to potential predators (Douglas, 2018).

Octopus does not show a consensual pupil response (Magnus, 1902; Weel and Thore, 1936). If only one eye is illuminated, only the pupil of this eye constricts, not the pupil of the non-illuminated eye. A non-consensual pupil response is adaptive in a species that has laterally placed eyes and watches objects predominantly with one eye (Heidermanns, 1928; Muntz, 1963; Byrne et al., 2002, 2004).

The octopus usually keeps the pupil horizontal, a reaction mediated by the statocysts that are required for the animal to maintain proper body and eye orientation (Boycott, 1960; Wells, 1960; Boycott et al., 1965). Only if the pupil is horizontal, and thus the orientation of the retinal receptors is fixed relative to the external world (see section "Retina and Visual Function"), the octopus is able to discriminate stimuli differing in orientation (Boycott and Young, 1956; Sutherland, 1957, 1963a; Wells, 1960; Young, 1960). This suggests that visual and proprioceptive input is not integrated in the brain.

The octopus pupil is bounded by the iris. According to Hess (1909), the cephalopod iris is not a structure of the inner eye but instead lies in form of a lobe in front/on top of the posterior chamber (**Figure 2**). The iris consists of five cell layers (Froesch, 1973): the external epithelium, a chromatophore and iridocyte layer, a layer of muscles and collagen strands, and the pigment epithelium. The chromatophores and the pigment epithelium absorb, while the iridophores reflect light, thereby changing the appearance of the eye, for instance when a threatened animal displays the dark eye bar over the eyes (Packard and Sanders, 1971). The muscles found in the iris are most likely

sphincters, however, Froesch (1973) was unable to distinguish between sphincter and dilator. Brain regions and nerves involved in the pupillary reaction were described by Magnus (1902) as well as Weel and Thore (1936).

Soto (2018) described the pupillary reactions of only one octopus individual. It would be interesting to analyze more individuals to assess whether the data already obtained are representative for the species; in this case, the non-consensual pupil reaction could also be quantified. A future challenge might also be to further characterize the role of the pupil shape in modulating optical properties or for camouflaging the eye. Regarding the latter, an interesting study of pupil shape-mediated camouflage in skates was recently published (Youn et al., 2019).

LENS AND ACCOMMODATION

At first glance, the octopus lens, the main refracting structure within its eye, seems to be spherical (**Figure 2**). However, as the lens of *Octopus vulgaris* has not been measured, it might be slightly ellipsoidal, as is the case in other cephalopods (Sivak, 1982, 1991; Sroczynski and Muntz, 1985; Sivak et al., 1994). Fishes also have spherical lenses: however, in contrast to fish, the lens of octopus consists of an anterior and a posterior part divided by a septum (**Figure 2**; Budelmann, 1996). Each component is comprised of onion-like layers (Budelmann et al., 1997).

The lens develops from the lentigenic body, called "corpus epithelia" in early studies (Arnold, 1967). The cells of the lentigenic body are characterized by their larger size, prominent nuclei, intensely stained nucleoli, and cytoplasmic RNA. The lentigenic body lies in the front of the optic vesicle. Fine cytoplasmic processes of the lentigenic body form the lens primordium, which increases in size through the addition of further lentigenic processes to the surface (Arnold, 1967). Studies of the octopus lens have so far mainly focused on lens development and lens proteins (Arnold, 1967; Bon et al., 1967; Dohrn, 1970; Brahma, 1978) with the aim of understanding the convergent evolution of cephalopod and vertebrate lenses.

Beer (1897) examined accommodation in numerous cephalopod species including *Octopus vulgaris* and concluded that the octopus eye can, indeed, accommodate or adjust its focus. According to Beer, the octopus is myopic or short-sighted, in its resting state; thus its eyes are well-adapted to seeing objects nearby. Beer found that when the eye was electrically stimulated, refraction changed to a status close to emmetropia i.e., normal-sightedness. This change was not accompanied by a change in the curvature of the lens, but by a positional change as in fish (Land and Nilsson, 2002): the lens moved closer to the retina. The retraction of the lens was caused by the contraction of a ring-shaped muscle at the equator of the bulbus which is firmly associated with the ciliary body (**Figure 2**) that is a section of the uvea and serves to suspend the lens. Upon contraction, the ciliary body and lens are pulled against the retina. A prerequisite for these movements is that the eye bulbus of octopus is very soft and flexible.

Beer (1897) also assumed a myopic resting refractive state for *Sepia officinalis*. However, retinoscopic measurements in *Sepia officinalis* revealed emmetropia or slight hyperopia (Schaeffel et al., 1999). In the latter study, it was also speculated that the accommodation mechanism in *Sepia* involves the lens moving laterally, thus perpendicular relative to the pupillary axis of the eye. It is likely that new investigations of visual accommodation in octopus would also reveal a resting refractive state close to emmetropia. In general, octopus might not need elaborate accommodation abilities as its spherical lens with a short focal length, in conjunction with long receptor cells (see section "Retina and Visual Function") most likely provide a large depth of focus (Budelmann et al., 1997).

There are a number of open questions related to the octopus lens, beginning first with the previously mentioned spherical shape of the lens. The second question relates to ocular transmittance. According to Denton and Warren (1968), octopus lenses should absorb ultraviolet (UV) light as octopus live close to the surface, whereas cephalopods living in the deep sea seem to have transparent lenses. However, this aspect needs to be studied in greater detail, as the statement by Denton and Warren (1968) is in contrast to a note by Hess (1910) in his work regarding the lenses of *Eledone* and *Sepia* which, according to his measurements, do not absorb light of any wavelength. As no details of the measurement procedure are given by Hess, we must assume that he was only able to measure in the visible part of the spectrum. Thus his note has to be treated with caution.

Third, very little is known about the optical properties of the lens of octopus. According to a side note in Sutherland (1963b), the lens is not astigmatic, thus the different meridians do not possess different refractive power. Most likely, it possesses a graded refractive index that compensates for longitudinal spherical aberration, such that axial and non-axial light rays are focused in the same focal plane, as in *Octopus pallidus* and *Octopus australis* (Jagger and Sands, 1999) or with some residual spherical aberration as in other cephalopod lenses (Sroczynski and Muntz, 1985, 1987; Sivak, 1991; Sivak et al., 1994; Kröger and Gislen, 2004; Sweeney et al., 2007); the lens of *Illex illecebrosus* seems to be overcorrected for spherical aberration (Sivak, 1982). In contrast to spherical aberration, the lenses of *Octopus* spec. do not seem to be corrected for chromatic aberration (Heidermanns, 1928; Jagger and Sands, 1999). In this regard, the nature of chromatic aberration — that is, a condition in which light of different wavelengths is focused differently — has to be re-evaluated in the context of color vision (see section "Visual Pigment and Color Vision").

Finally, regarding the development of the split cephalopod lens, it is still unknown how the growth of the two components is coordinated. This question was already posed by Jacob and Duncan (1981) in the case of *Sepiola atlantica*, in which the anterior and posterior part of the lens are not closely electrically coupled. These authors also suggested studying whether the anterior and posterior halves of the lens are built from the same lens proteins.

RETINA AND VISUAL FUNCTION

Although the eyes of vertebrates and coleoid cephalopods are similar in many aspects (Packard, 1972), the retinal designs of these two animal groups differ drastically. Cephalopods have

everted retinae with the rhabdomeric photoreceptors pointing towards the light (Fröhlich, 1914a) in contrast to the inverted retinae with ciliary photoreceptors in vertebrates. Moreover, in contrast to the multilayered vertebrate retinae, cephalopod retinae mainly contain the photoreceptors. Cephalopod photoreceptors are primary receptor cells, each with its own axon, whereas the vertebrate photoreceptors are secondary receptor cells derived from epithelial cells. The axons of octopus photoreceptors project directly to the large optic lobes, where the visual information is processed (Young, 1960, 1971; Wells, 1966a; Maddock and Young, 1987). In vertebrates, the processing of the visual information already begins in the inner retina, before visual signals pass into the brain *via* the optic nerve.

We will now describe the retina of *Octopus vulgaris* in detail (**Figure 3**). A limiting membrane shields the retina towards the posterior chamber. The limiting membrane might be a secretion of the supporting cells (von Lenhossék, 1894) that lie between the rhabdoms in the distal retina; there are about as many supporting cells as rhabdoms (Young, 1963).

The retina itself is densely packed with photoreceptors; their density is highest in a central horizontal stripe (Young, 1960, 1962b, 1963, 1971). At its distal end, oriented towards the light, each photoreceptor carries two rhabdomeres facing opposite sides. Four rhabdomeres belonging to four photoreceptors form a square rhabdom (**Figure 3**), which is analogous to the rhabdom of arthropods. The square arrangement of the rhabdoms is very regular, although there are also some cells which are particularly small that are not organized in arrangements of four (Young, 1963). Despite this very regular receptor arrangement, as well as corresponding regular distributions of the dendrites in the plexiform layer in the optic lobe (Young, 1960), the octopus is only able to discriminate stimuli differing in orientation (Boycott and Young, 1956; Sutherland, 1957, 1963a; Wells, 1960; Young, 1960) when the eye is oriented such that the pupil is horizontal, that is when the statocysts are functioning normally (Boycott, 1960; Wells, 1960; Boycott et al., 1965). The regular receptor arrangement plays an important role for the polarization sensitivity of the eye of octopus (see section "Dichroism of the Retina and Polarization Sensitivity").

The two rhabdomeres of each photoreceptor are separated by screening pigment in the cell body (**Figure 3**). Additional pigment is found in the processes of the supporting cells between the distal segments of the photoreceptors. The migration of this screening pigment to the bases/tips of the photoreceptor and perhaps also the supporting cells (Babuchin, 1864; Young, 1963), in combination with enlargement/contraction of the photoreceptors and the constriction/dilation of the pupil (see **Figure 1** and section "Pupil and Iris"), serves to dark- or light-adapt the eye. Pigment migration does not seem to be uniformly fast throughout the entire retina; in the photoreceptors within the central stripe, which have less pigment than the cells in other retinal regions (Young, 1962b), pigment migration is slower during light adaptation, but faster during dark adaptation than in the remainder of the retina (Hess, 1905; Young, 1963).

In *Octopus fangsiao (O. ocellatus)*, dopaminergic efferents from the optic lobe seem to cause screening pigment migration during the dark adaptation process (Gleadall et al., 1993). In *O. vulgaris*, this has yet to be studied.

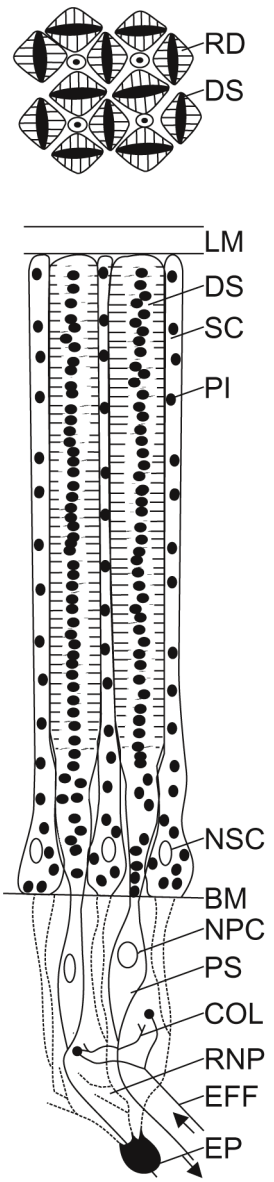

FIGURE 3 | Schematic diagram of the retina of *Octopus vulgaris*. A limiting membrane (LM) shields the retina towards the posterior chamber. In the distal part of the retina are found the distal segments (DS) of the photoreceptors and supporting cells (SC). Pigment granules (PI) can be found within the photoreceptors and the supporting cells. The cross section through the distal retina (upper diagram), shows the regular arrangement of the distal segments of the photoreceptors (DS) that possess two rhabdomeres (RD) each, facing opposite sides of the cell, and separated by pigment (PI). Four rhabdomeres from four neighboring receptors form a rhabdom. While the nuclei of the supporting cells (NSC) are situated in the distal retina, the nuclei of the photoreceptor cells (NPC) are found in their proximal segments (PS) in the proximal retina, beyond the basal membrane (BM). In the proximal retina, within the retinal nerve plexus (RNP), photoreceptors are interconnected by collateral fibers (COL) from the proximal segments of the photoreceptors, and photoreceptors interact with efferents (EFF) from the optic lobe. Epithelial cells (EP), considered to be retinal glia cells, seem to form processes (dashed lines) that lie between the inner segments of the retinal cells. The schematic diagram of the octopus retina was adapted from previously published drawings (Babuchin, 1864; Schultze, 1867; Grenacher, 1884; Wolken, 1958; Moody and Parriss, 1960, 1961; Young, 1960, 1962b, 1971; Boycott et al., 1965; Yamamoto et al., 1965).

The photoreceptors of the octopus retina narrow before passing the basement membrane that separates their distal parts from the proximal segments that carry the cell nuclei (**Figure 3**). Finally, the photoreceptors give rise to axons. Within this region, called the retinal plexus, two types of interactions can be found: (1) interactions between photoreceptors, mediated by fine collateral fibers branching from the proximal part of the photoreceptors, and (2) interactions between centrifugal cells, which are efferents from the plexiform zone of the optic lobes, and photoreceptors (Young, 1962b; Boycott et al., 1965; Tonosaki, 1965; Lund, 1966; Patterson and Silver, 1983). In the central stripe of the retina, the proximal segments of the photoreceptors are longer, and the retinal plexus is thicker than in the rest of the retina (Young, 1963). Three studies have described synapses and transmitters in the retina of *Octopus vulgaris*, among other species (Gray, 1970; Lam et al., 1974; Silver et al., 1983). There is accumulating evidence that the photoreceptors are cholinergic, whereas the centrifugal cells are dopaminergic.

The axons of the photoreceptors leave the eye in bundles of approximately 20 axons, each through holes in the sclera (Patterson and Silver, 1983). Before these axon bundles enter the optic lobe, the bundles decussate: the dorsal retina projects to the ventral optic lobe and vice versa (Boycott et al., 1965; Lettvin and Maturana, 1965; Patterson and Silver, 1983). The optic lobes are composed of the cortex and a central medulla, and most photoreceptors axons terminate in the outer plexiform zone of the cortex of the optic lobe (Young, 1960, 1962a, 1971; Dilly et al., 1963).

Dichroism of the Retina and Polarization Sensitivity

The rhabdomeres of the photoreceptors are arranged either horizontally or vertically. Each rhabdomere consists of densely packed straight microvilli that, because of the regular arrangement of the rhabdomeres, are oriented perpendicular to each other (Wolken, 1958; Young, 1960, 1971). With the alignment of the visual pigment with the long axis of the tubules (Roberts et al., 2011), each rhabdomere is a dichroic analyzer that absorbs light polarized parallel to the tubules maximally. This regular retinal arrangement is thus most likely the basis for the ability of octopus to perceive polarized light (Moody and Parriss, 1960, 1961; Rowell and Wells, 1961; Lettvin and Pitts, 1962; Moody, 1962; Tasaki and Karita, 1966; Sugawara et al., 1971; Shashar and Cronin, 1996).

Numerous functions of polarization sensitivity have already been described for cephalopods in general, including object detection or recognition, communication or navigation, among other (for review see Mäthger et al., 2009; Shashar, 2014). However, it still remains to be determined what role polarization sensitivity plays in *Octopus vulgaris* in particular, as most evidence in this respect has been collected in other cephalopod species, so far. Additionally, it remains to be determined whether octopus possesses true polarization vision as proposed by Shashar and Cronin, 1996, a view that has been challenged by Nilsson and Warrant (1999).

Photoreceptor Density, Spatial, and Temporal Resolution

Given an eye size of approximately 2 cm (see section "Eye Size and Ocular Dimensions"), the octopus retina covers an area of 1–4 cm^2 (Wolken, 1958; Young, 1963). In this retina, 2–3 × 10^7 photoreceptors cells are found with a cell density varying between 18,000–22,000 cells/mm^2 in the periphery and approximately 55,000 cells/mm^2 in the central stripe (Young, 1960, 1962b, 1963, 1971). In the central stripe, the rhabdoms are longer and thinner than in the periphery; rhabdom diameters as small as 4 μm have been found in the stripe, while rhabdoms in the periphery had diameters of up to 10 μm (Young, 1963). The higher rhabdom density in the central retinal stripe is strongly indicative of higher spatial resolution in this area, even though this has not been measured directly with electrophysiological methods; for electrophysiological studies in octopus, the reader is referred to previous studies (Tasaki et al., 1963a,b; Boycott et al., 1965; Lettvin and Maturana, 1965; Hamasaki, 1968a,b; Tsukahara et al., 1973). In accordance with the foregoing, a horizontal area of increased spatial resolution would be highly adaptive in bottom-living animals (Muntz, 1977; Talbot and Marshall, 2010).

Visual acuity was assessed with two different behavioral approaches, in a discrimination experiment using gratings (Sutherland, 1963b) as well as in an optomotor study (Packard, 1969). The first approach assessed visual acuity as 1.7 cycles/degrees or better for animals weighing 250–500 g. The second assessed visual acuity as 0.6–1.1 cycles/degrees for two groups of very small animals with average weights of 0.27 g and 2.7 g, and 1.1 cycles/degrees or better for animals weighing 17 g; all values are estimates based on the assumption that the animals were in the center of the optokinetic drum. Due to several aspects related to the experimental procedure, these studies may have underestimated the visual acuity of octopus. This possibility is supported by another discrimination experiment on grating visual acuity in *Octopus pallidus* and *Octopus australis* whose visual acuity was assessed as 3.1–6.8 cycles/degrees (Muntz and Gwyther, 1988). Considering this acuity range, the octopus visual acuity would be comparable to the visual acuity of cats or fowls (Rahmann, 1967). Generally, the visual acuity of octopus might vary with illumination, as the receptive field of single receptors will probably be smaller when the pigment has migrated to the distal tip of the receptors in bright light (Lettvin and Pitts, 1962; Sutherland and Carr, 1963; Young, 1963); an aspect that still needs to be fully worked out in octopus.

The temporal resolution of the eye, as measured by flicker fusion frequency, has been determined in both *Octopus vulgaris* and *Octopus briareus* as 72 Hz with a stimulus intensity of 4.5 × 10^6 cd/m^2 by Hamasaki (1968b). The flicker fusion frequency decreases relatively fast reaching only 20 Hz when stimulus intensity was decreased by 4 logarithmic units. As the values given are averages from the two species of octopus, it would be interesting to document the flicker fusion frequency for *Octopus vulgaris* in particular.

Visual Pigment and Color Vision

Octopus vulgaris possesses only one visual pigment within its photoreceptors, an R-type-opsin (Cronin and Porter, 2014)

which absorbs maximally at 475 nm with a β-band at 360 nm (Brown and Brown, 1958; Kropf et al., 1959; Hamasaki, 1968a). Generally, the visual pigments of octopods seem to be less well matched to the light environment than the pigments of squids and cuttlefish. It is speculated that a fine-tuning of the pigments might not be under selective pressure in octopods in contrast to squids and cuttlefish as other senses such as haptics or chemoreception might be more important than vision in these benthic animals (Chung and Marshall, 2016).

In line with the presence of only one visual pigment, most studies have concluded that *Octopus vulgaris* is color-blind (Piéron, 1914; Bierens de Haan, 1926; Messenger et al., 1973; Messenger, 1977; Kawamura et al., 2001), though the work of Fröhlich, Goldsmith, and Kühn suggest otherwise (Fröhlich, 1914a,b; Goldsmith, 1917a,b; Kühn, 1950). However, in these old color vision studies, either experiments were not adequately controlled for the brightness of the stimuli or stimuli were adjusted in brightness on the basis of a human brightness discrimination ability that likely differs from the brightness discrimination ability of octopus. Moreover, these studies were not designed to examine a color vision mechanism recently simulated for *Octopus australis* by Stubbs and Stubbs (2016a). This color vision mechanism exploits the longitudinal chromatic aberration of the lens; thus, even monochromats should be able to obtain color information this way. Although this mechanisms has been questioned (Gagnon et al., 2016; Stubbs and Stubbs, 2016b), it would be interesting to test it in the context of the mystery of color-blind camouflage and the question of what role the eyes and/or photoreceptors in the skin (Ramirez and Oakley, 2015) play in background matching by cephalopods generally. Stubbs and Stubbs speculate that this mechanism might also help to explain why some cephalopods have developed colorful intra-specific signals (Stubbs and Stubbs, 2016b).

To date, the only cephalopod known to possess more than one pigment, the classic precondition for color vision, is *Watasenia scintillans*; it has three visual pigments based on vitamin A1 (λ_{max} = 484 nm), vitamin A2 (λ_{max} = 500 nm), and 4-hydroxyretinal (λ_{max} = 470 nm) (Matsui et al., 1988a,b; Seidou et al., 1990; Kito et al., 1992; Michinomae et al., 1994). A putative color vision faculty in the firefly squid is supported by the existence of a banked retina that compensates for this animal's lens not being corrected for longitudinal chromatic aberration (Kröger and Gislen, 2004).

DISCUSSION

This review demonstrates that several aspects of vision of *Octopus vulgaris* have been investigated in some detail. Nevertheless, large gaps remain in our understanding of vision for this species, notwithstanding the fact that the common octopus has been an object of scientific study for more than 150 years. In our opinion, one of the largest gaps in our knowledge stems from the poor understanding of the dioptric apparatus of octopus. In addition, the primary functions of vision — including visual acuity, brightness discrimination, depth perception, motion detection, polarization and color vision — have not been conclusively investigated, and thus some enduring mysteries (in particular, color-blind camouflage) persist to the present day.

Taken together, the current array of published studies on the eye of *Octopus vulgaris* — many of which are reviewed here — helps us to understand adaptations of the visual system to lifestyle and habitat. To provide some examples, characteristics of the visual system of octopus such as specifics of the pupil or the retina mirror the benthic lifestyle of adult octopus which can even inhabit shallow water: an environment in which it experiences high light intensities from above and drastic light changes when leaving its den during the day. Moreover, the large eye movements and aspects that camouflage the animal or the eye specifically reinforce the fact that octopus is a soft-bodied animal that falls prey to many animals. Future studies will allow completion of a picture of vision in *Octopus vulgaris*. Detailed insight will thus be obtained regarding the world of a fascinating invertebrate which otherwise spends its life in a habitat that is still not easily accessible to humans.

AUTHOR CONTRIBUTIONS

FH wrote the first version of the manuscript. AK contributed comments and suggestions. Both authors approved the final version of the manuscript.

FUNDING

This review was supported by a grant from the Deutsche Forschungsgemeinschaft to FH (HA 17891/2–1). We furthermore acknowledge the financial support of the Deutsche Forschungsgemeinschaft and the University Rostock/University medicine Rostock within the funding program Open Access Publishing.

ACKNOWLEDGMENTS

The authors would like to thank Frank Schaeffel for commenting on the manuscript.

REFERENCES

Altman, J. S. (1966). *The behaviours of Octopus vulgaris Lam. In its natural habitat: A pilot study.* Vol. 2. Underwater Association of Malta. Carshalton, UK: T.G.W. Industrial & Research Promotions.

Amoore, J. E., Rodgers, K., and Young, J. Z. (1959). Sodium and potassium in the endolymph and perilymph of the statocyst and in the eye of octopus. *J. Exp. Biol.* 36, 709–714.

Arnold, J. M. (1967). Fine structure of the development of the cephalopod lens. *J. Ultrastruct. Res.* 17, 527–543. doi: 10.1016/S0022-5320(67)80139-4

Augusteyn, R. C., Nankivil, D., Mohamed, A., Maceo, B., Pierre, F., and Parel, J.-M. (2012). Human ocular biometry. *Exp. Eye Res.* 102, 70–75. doi: 10.1016/j.exer.2012.06.009

Babuchin, A. (1864). Vergleichend histologische Studien - über den Bau der Cephalopodenretina. *Würzburger Naturwiss. Z.* 5, 127–140.

Barber, V. C. (2010). "The sense organs of nautilus" in *Nautilus - the biology and paleobiology of a living fossil.* Vol. 6. eds. N. H. Landman and P. I. Harries (Dordrecht, Heidelberg, London, New York: Springer).

Beer, T. (1897). Die Accommodation des Kephalopodenauges. *Pflügers Arch. Physiol.* 67, 541–587.

Bierens de Haan, J. A. (1926). Versuche über den Farbensinn und das psychische Leben von *Octopus vulgaris*. *Z. Vgl. Physiol.* 4, 766–796. doi: 10.1007/BF00342382

Bon, W. F., Dohrn, A., and Batink, H. (1967). The lens proteins of a marine invertebrate *Octopus vulgaris*. *Bichim. Biophys. Acta* 140, 312–318.

Boycott, B. B. (1960). The functioning of the statocysts of *Octopus vulgaris*. *Proc. R. Soc. B Biol. Sci.* 152, 78–87.

Boycott, B. B., Lettvin, J. Y., Maturana, H. R., and Wall, P. D. (1965). Octopus optic responses. *Exp. Neurol.* 12, 247–256. doi: 10.1016/0014-4886(65)90070-1

Boycott, B. B., and Young, J. Z. (1956). Reactions to shape in *Octopus vulgaris* Lamarck. *Proc. Zool. Soc. London* 126, 491–547.

Boyle, P. R., and Rodhouse, P. G. K. (eds.) (2005). "Coastal and shelf species" in *Cephalopods - ecology and fisheries* (Oxford: Blackwell Science), 161–175.

Bozzano, A., Pankhurst, P. M., Moltschaniwsky, N. A., and Villaneuva, R. (2009). Eye development in southern calamary, *Sepioteuthis australis*, embryos and hatchlings. *Mar. Biol.* 156, 1359–1373. doi: 10.1007/s00227-009-1177-2

Brahma, S. K. (1978). Ontogeny of crystallins in marine cephalopods. *J. Embryol. Exp. Morpholog.* 46, 111–118.

Brooke, M. L., Hanley, S., and Laughlin, S. R. (1999). The scaling of eye size with body mass in birds. *Proc. R. Soc. Lond. B* 266, 405–412. doi: 10.1098/rspb.1999.0652

Brown, P. K., and Brown, P. S. (1958). Visual pigments of the octopus and cuttlefish. *Nature* 182, 1288–1290. doi: 10.1038/1821288a0

Budelmann, B. U. (1994). Cephalopod sense organs, nerves and the brain: adaptations for high performance and lifestyle. *Mar. Freshw. Behav. Physiol.* 25, 13–33.

Budelmann, B. U. (1996). Active marine predators: the sensory world of cephalopods. *Mar. Freshw. Behav. Physiol.* 27, 59–75. doi: 10.1080/10236249609378955

Budelmann, B. U., Schipp, R., and von Boletzky, S. (1997). "Cephalopoda" in *Microscopic anatomy of invertebrates - Mollusca II.* Vol. 6A, eds. F. W. Harrison and A. J. Kohn (New York, Chichester, Brisbane, Toronto, Singapore, Weinheim: A John Wiley & Sons Inc. Publication), 119–414.

Budelmann, B. U., and Young, J. Z. (1984). The statocyst-oculomotor system of *Octopus vulgaris*: extraocular eye muscles, eye muscle nerves, statocyst nerves and the oculomotor centre in the central nervous system. *Philos. Trans. R. Soc. Biol. Char.* 306, 159–189.

Budelmann, B. U., and Young, J. Z. (1993). The oculomotor system of decapod cephalopods: eye muscles, eye muscle nerves, and the oculomotor neurons in the central nervous system. *Philos. Trans. R. Soc. Biol. Char.* 340, 93–125.

Byrne, R. A., Kuba, M., and Griebel, U. (2002). Lateral asymmetry of eye use in *Octopus vulgaris*. *Anim. Behav.* 64, 461–468. doi: 10.1006/anbe.2002.3089

Byrne, R. A., Kuba, M. J., and Meisel, D. V. (2004). Lateralized eye use in *Octopus vulgaris* shows antisymmetrical distribution. *Anim. Behav.* 68, 1107–1114. doi: 10.1016/j.anbehav.2003.11.027

Chung, W.-S., and Marshall, N. J. (2016). Comparative visual ecology of cephalopods from different habitats. *Proc. R. Soc. B Biol. Sci.* 283:20161346. doi: 10.1098/rspb.2016.1346

Cronin, T. W., and Porter, M. L. (2014). "The evolution of invertebrate photopigments and photoreceptors" in *Evolution of visual and non-visual pigments*. eds. D. M. Hunt, M. W. Hankins, S. P. Collin, and N. J. Marshall (New York: Springer), 105–135.

Denton, E. J., and Warren, F. J. (1968). Eyes of the Histioteuthidae. *Nature* 219, 400–401. doi: 10.1038/219400a0

Dilly, P. N., Gray, E. G., and Young, J. Z. (1963). Electron microscopy of optic nerves and optic lobes of *Octopus* and *Eledone*. *Proc. R. Soc. B Biol. Sci.* 158, 446–456.

Dohrn, A. (1970). Distribution and electrophoretic mobility of proteins in samples taken from different layers of vertebrate and invertebrate lenses. *Exp. Eye Res.* 9, 297–299. doi: 10.1016/S0014-4835(70)80087-2

Douglas, R. H. (2018). The pupillary light response of animals; a review of their distribution, dynamics, mechanisms and functions. *Prog. Retin. Eye Res.* 66, 17–48. doi: 10.1016/j.preteyeres.2018.04.005

Douglas, R. H., Williamson, R., and Wagner, H.-J. (2005). The pupillary response of cephalopods. *J. Exp. Biol.* 208, 261–265. doi: 10.1242/jeb.01395

Froesch, D. (1973). On the fine structure of the *Octopus* iris. *Z. Zellforsch.* 145, 119–129. doi: 10.1007/BF00307193

Fröhlich, F. W. (1914a). Beiträge zur allgemeinen Physiologie der Sinnesorgane. *Z. Sinnesphysiol.* 48, 28–164.

Fröhlich, F. W. (1914b). Weitere Beiträge zur allgemeinen Physiologie der Sinnesorgane. *Z. Sinnesphysiol.* 48, 354–438.

Gagnon, Y. L., Osorio, D., Wardiff, T. J., Marshall, N. J., Chung, W.-S., and Temple, S. E. (2016). Can chromatic aberration enable color vision in natural environments? *Proc. Natl. Acad. Sci. USA* 113, E6908–E6909. doi: 10.1073/pnas.1612239113

Gleadall, I. G., Ohtsu, K., Gleadall, E., and Tsukahara, Y. (1993). Screening pigment migration in the *Octopus* retina includes control by dopaminergic efferents. *J. Exp. Biol.* 185, 1–16.

Glockauer, A. (1915). Zur Anatomie und Histologie des Cephalopodenauges. *Z. Wiss. Zool.* 113, 325–360.

Goldsmith, M. (1917a). Psychologie animale. Quelques réactions sensorielles chez le poulpe. *Comptes rendus hebdomadaire des séances de l'Académie des sciences* 164, 448–450.

Goldsmith, M. (1917b). Quelques réactions du poulpe. Contributions à la psychologie des invertébrés. *Bull. Inst. Gén. Psychol.* 17, 24–44.

Gray, E. G. (1970). A note on synaptic structure of the retina of *Octopus vulgaris*. *J. Cell Sci.* 7, 203–215.

Grenacher, H. (1884). Abhandlungen zur vergleichenden Anatomie des Auges. I. Die Retina der Cephalopoden. *Abh. Naturforsch. Ges. Halle* 16, 1–50.

Griffin, L. E. (1900). *The anatomy of Nautilus pompilius. Vol 8*. Washington: Memoirs of the National Academy of Science, Government Printing Office.

Hamasaki, D. (1968a). The ERG-determined spectral sensitivity of the octopus. *Vis. Res.* 8, 1013–1021.

Hamasaki, D. I. (1968b). The electroretinogram of the intact anesthetized octopus. *Vis. Res.* 8, 247–258.

Hanlon, R. T., and Messenger, J. B. (2018). *Cephalopod behaviour*. Cambridge: Cambridge University Press.

Heidermanns, C. (1928). Messende Untersuchungen über das Formensehen der Cephalopoden und ihre optische Orientierung im Raume. *Zool. Jahrb. Abt. Allg. Zool. Physiol.* 45, 346–349.

Hensen, V. (1865). Über das Auge einiger Cephalopoden. *Z. Wiss. Zool.* 15, 155–242.

Hess, C. (1905). Beiträge zur physiologie und anatomie des cephalopodenauges. *Pflügers Arch. Gesamte Physiol.* 109, 393–439.

Hess, C. (1909). Die accommodation der cephalopoden. *Arch. Augenheilkd.* 64, 125–152.

Hess, C. (1910). Neue untersuchungen über den lichtsinn bei wirbellosen tieren. *Pflügers Arch. Gesamte Physiol.* 136, 282–367.

Hurley, A. C., Lange, G. D., and Hartline, P. H. (1978). The adjustable "pinhole camera" eye of *Nautilus*. *J. Exp. Zool.* 205, 37–44. doi: 10.1002/jez.1402050106

Jacob, T. J. C., and Duncan, G. (1981). Electrical coupling between fibre cells in amphibian and cephalopod lenses. *Nature* 290, 704–706. doi: 10.1038/290704a0

Jagger, W. S., and Sands, P. J. (1999). A wide-angle gradient index optical model of the crystalline lens and eye of the octopus. *Vis. Res.* 39, 2841–2852. doi: 10.1016/S0042-6989(99)00012-7

Jereb, P., Allcock, A. L., Lefkaditou, E., Piatkowski, U., Hastie, G. J., and Pierce, G. J. (2015). *Cephalopod biology and fisheries in Europe: II. Species accounts vol report no. 325*. Copenhagen: ICES International Council for the Exploration of the Sea.

Jereb, P., and Roper, C. F. E. (2005). *Cephalopods of the world - an annotated and illustrated catalogue of species known to date. Volume 1. Chambered nautiluses and sepioids*. Rome: FAO Fisheries Synopsis, 1–13.

Jereb, P., and Roper, C. F. E. (2010). *Cephalopods of the world - an annotated and illustrated catalogue of species known to date. Volume 2. Myopsid and oegopsid squids*. Rome: FAO Fisheries Synopsis, 1–13.

Jereb, P., Roper, C. F. E., Norman, M. D., and Finn, J. K. (2014). *Cephalopods of the world - an annotated and illustrated catalogue of cephalopod species known to date. Volume 3. Octopods and vampire squids*. Rome: FAO Fisheries Synopsis.

Kawamura, G., Nobutoki, K., Anraku, K., Tanaka, Y., and Okamoto, M. (2001). Color discrimination conditioning in two octopus *Octopus aegina* and *O. vulgaris*. *Nippon Suisan Gakkai.* 67, 35–39. doi: 10.2331/suisan.67.35

Kayes, R. J. (1974). The daily activity pattern of *Octopus vulgaris* in a natural habitat. *Mar. Behav. Physiol.* 2, 337–343.

Kito, Y., Partridge, J. C., Seidou, M., Narita, K., Hamanaka, T., Michinomae, M., et al. (1992). The absorbance spectrum and photosensitivity of a new synthetic visual pigment based on 4-hydroxyretinal. *Vis. Res.* 32, 3–10. doi: 10.1016/0042-6989(92)90106-S

Kröger, R. H. H., and Gislen, A. (2004). Compensation for longitudinal chromatic aberration in the eye of the firefly squid, *Watasenia scintillans*. *Vis. Res.* 44, 2129–2134. doi: 10.1016/j.visres.2004.04.004

Kropf, A., Brown, P. K., and Hubbard, R. (1959). Lumi- and metarhodopsins of squid and octopus. *Nature* 183, 446–448.

Kühn, A. (1950). Über Farbwechsel und Farbensinn von Cephalopoden. *Z. Vgl. Physiol.* 32, 572–598.

Lam, D. M. K., Wiesel, T. N., and Kaneko, A. (1974). Neurotransmitter synthesis in cephalopod retina. *Brain Res.* 82, 365–368. doi: 10.1016/0006-8993(74)90621-0

Land, M. F., and Nilsson, D.-E. (2002). *Animal eyes*. Oxford: Oxford University Press.

Lettvin, J. Y., and Maturana, H. R. (1965). Octopus vision. *MIT Q. Prog. Rep.*, 194–212.

Lettvin, J. Y., and Pitts, W. H. (1962). Neapolitan studies. *MIT Q. Prog. Rep.* 64, 288–290.

Lund, R. D. (1966). Centrifugal fibers to the retina of *Octopus vulgaris*. *Exp. Neurol.* 16, 100–112.

Mackintosh, N. J. (1963). The effect of irrelevant cues on reversal learning in the rat. *Br. J. Psychol.* 54, 127–134. doi: 10.1111/j.2044-8295.1963.tb00868.x

Maddock, L., and Young, J. Z. (1987). Quantitative differences among the brains of cephalopods. *J. Zool.* 212, 739–767. doi: 10.1111/j.1469-7998.1987.tb05967.x

Magnus, R. (1902). Die Pupillarreaction der Octopoden E Pflüger. *Arch. Physiol.* 92, 623–643. doi: 10.1007/BF01790186

Mather, J. A. (1988). Daytime activity of juvenile *Octopus vulgaris* in Bermuda. *Malacologia* 29, 69–76.

Mather, J. A. (1991). Foraging, feeding and prey remains in middens of juvenile *Octopus vulgaris* (Mollusca: Cephalopoda). *J. Zool.* 224, 27–39. doi: 10.1111/j.1469-7998.1991.tb04786.x

Mather, J. A., Leite, T. S., and Batista, A. T. (2012). Individual prey choices of octopuses: are they generalist or specialist? *Curr. Zool.* 58, 597–603. doi: 10.1093/czoolo/58.4.597

Mather, J. A., and O'Dor, R. K. (1991). Foraging strategies and predation risk shape the natural history of juvenile *Octopus vulgaris*. *Bull. Mar. Sci.* 49, 256–269.

Mäthger, L. M., Hanlon, R. T., Hakansson, J., and Nilsson, D.-E. (2013). The W-shaped pupil in cuttlefish *(Sepia officinalis)*: functions for improving horizontal vision. *Vis. Res.* 83, 19–24. doi: 10.1016/j.visres.2013.02.016

Mäthger, L. M., Shashar, N., and Hanlon, R. T. (2009). Do cephalopods communicate using polarized light reflections from their skin? *J. Exp. Biol.* 212, 2135–2140. doi: 10.1242/jeb.020800

Matsui, S., Seidou, M., Horiuchi, S., Uchiyama, I., and Kito, Y. (1988a). Adaptation of a deep-sea cephalopod to the photic environment - evidence for three visual pigments. *J. Gen. Physiol.* 92, 55–66.

Matsui, S., Seidou, M., Uchiyama, M., Sekiya, N., Hiraki, K., Yoshihara, K., et al. (1988b). 4-Hydroxyretinal, a new visual pigment chromophore found in the bioluminescent squid, *Watasenia scintillans*. *Biochim. Biophys. Acta* 966, 370–374.

Matsui, H., Takayama, G., and Sakurai, Y. (2016). Physiological response of the eye to different colored light-emitting diodes in Japanese flying squid *Todarodes pacificus*. *Fish. Sci.* 82, 303–309. doi: 10.1007/s12562-015-0965-5

McCormick, L. R., and Cohen, J. H. (2012). Pupil light reflex in the Atlantic brief squid, *Lolliguncula brevis*. *J. Exp. Biol.* 215, 2677–2683. doi: 10.1242/jeb.068510

Meisel, D. V., Byrne, R. A., Kuba, M., Griebel, U., and Mather, J. A. (2003). "Circadian rhythms in *Octopus vulgaris*" in *Coleoid cephalopods through time*. Vol. 3, eds. K. Warnke, H. Keupp and S. V. Boletzky (Berlin: Berlin Paläobiologische Abhandlung), 171–177.

Meisel, D. V., Byrne, M., Kuba, M., Mather, J. A., Ploberger, W., and Reschenhofer, E. (2006). Contrasting activity patterns of two related octopus species, *Octopus macropus* and *Octopus vulgaris*. *J. Comp. Psychol.* 120, 191–197. doi: 10.1037/0735-7036.120.3.191

Meisel, D. V., Kuba, M., Byrne, R. A., and Mather, J. A. (2013). The effect of predatory presence on the temporal organization of activity in *Octopus vulgaris*. *J. Exp. Mar. Biol. Ecol.* 447, 75–79. doi: 10.1016/j.jembe.2013.02.012

Merton, H. (1905). Über die Retina von Nautilus und einigen dibranchiaten Cephalopoden. *Z. Wiss. Zool.* 79, 325–396.

Messenger, J. B. (1968a). Monocular discrimination of mirror images in *Octopus*. *Pubbl. Staz. Zool. Nap.* 36, 103–111.

Messenger, J. B. (1968b). The visual attack of the cuttlefish, *Sepia officinalis*. *Anim. Behav.* 16, 342–357.

Messenger, J. B. (1977). Evidence that *Octopus* is colour blind. *J. Exp. Biol.* 70, 49–55.

Messenger, J. B., Wilson, A. B., and Hedge, A. (1973). Some evidence for colour-blindness in *Octopus*. *J. Exp. Biol.* 59, 77–94.

Michinomae, M., Masuda, H., Seidou, M., and Kito, Y. (1994). Structural basis for wavelength discrimination in the banked retina of the firefly squid *Watasenia scintillans*. *J. Exp. Biol.* 193, 1–12.

Moody, M. F. (1962). Evidence for the intraocular discrimination of vertially and horizontally polarized light by *Octopus*. *J. Exp. Biol.* 39, 21–30.

Moody, M. F., and Parriss, J. R. (1960). Discrimination of polarized light by *Octopus*. *Nature* 186, 839–840. doi: 10.1038/186839a0

Moody, M. F., and Parriss, J. R. (1961). The discrimination of polarized light by *Octopus*: a behavioural and morphological study. *Z. Vgl. Physiol.* 44, 268–291. doi: 10.1007/BF00298356

Muntz, W. R. A. (1963). Intraretinal transfer and the function of the optic lobes in octopus. *Q. J. Exp. Psychol.* 15, 116–124.

Muntz, W. R. A. (1977). "Pupillary response of cephalopods" in *Symposium of the Zoological Society of London*. Vol. 38, 277–285.

Muntz, W. R. A. (1991). Anatomical and behavioural studies on vision in *Nautilus* and *Octopus*. *Am. Malacol. Bull.* 9, 69–74.

Muntz, W. R. A., and Gwyther, J. (1988). Visual acuity in *Octopus pallidus* and *Octopus australis*. *J. Exp. Biol.* 134, 119–129.

Muntz, W. R. A., and Ray, U. (1984). On the visual system of *Nautilus pompilius*. *J. Exp. Biol.* 109, 253–263.

Nilsson, D.-E., and Warrant, E. J. (1999). Visual discrimination: seeing the third quality of light. *Curr. Biol.* 9, R535–R537. doi: 10.1016/S0960-9822(99)80330-3

Nilsson, D.-E., Warrant, E. J., Johnson, S., Hanlon, R., and Shashar, N. (2012). A unique advantage for giant eyes in giant squid. *Curr. Biol.* 22, 683–688. doi: 10.1016/j.cub.2012.02.031

Packard, A. (1969). Visual acuity and eye growth in *Octopus vulgaris* Lamarck. *Monitore Zool. Ital.* 3, 19–32.

Packard, A. (1972). Cephalopods and fish: the limits of convergence. *Biol. Rev.* 47, 241–307. doi: 10.1111/j.1469-185X.1972.tb00975.x

Packard, A., and Sanders, G. D. (1971). Body patterns of *Octopus vulgaris* and maturation of response disturbance. *Anim. Behav.* 19, 780–788. doi: 10.1016/S0003-3472(71)80181-1

Patterson, J. A., and Silver, S. C. (1983). Afferent and efferent components of *Octopus* retina. *J. Comp. Physiol.* 158, 381–387.

Piéron, H. (1914). Contribution à la psychologie du poulpe; la mémoire sensorielle. *Ann. Psychol.* 20, 182–185.

Rahmann, H. (1967). Die Sehschärfe bei Wirbeltieren. *Naturwiss. Rundsch.* 1, 10–14.

Ramirez, M. D., and Oakley, T. H. (2015). Eye-independent, light-activated chromatophore expansion (LACE) and expression of phototransduction genes in the skin of *Octopus bimaculoides*. *J. Exp. Biol.* 218, 1513–1520. doi: 10.1242/jeb.110908

Roberts, N. W., Porter, M. L., and Cronin, T. W. (2011). The molecular basis of mechanisms underlying polarization vision. *Philos. Trans. R. Soc. Biol. Char.* 366, 627–637. doi: 10.1098/rstb.2010.0206

Rowell, C. H. F., and Wells, M. J. (1961). Retinal orientation and the discrimination of polarized light by octopuses. *J. Exp. Biol.* 38, 827–831.

Sanchez, P., Villanueva, R., Jereb, P., Guerra, A., Gonzalez, A. F., Sobrino, I., et al. (2015). "Octopus" in *Cephalopod biology and fisheries in Europe: II. Species accounts*. eds. P. Jereb, L. Allcock, and E. Lefkaditou (Copenhagen: ICES International Council for the Exploration of the Sea), Report No. 325: 13–28.

Schaeffel, F., Murphy, C. J., and Howland, H. C. (1989). Accommodation and visual optics in the cuttlefish (*Sepia officinalis*). *Investig. Ophthalmol. Vis. Sci.* 30(Suppl), 508.

Schaeffel, F., Murphy, C. J., and Howland, H. C. (1999). Accommodation in the cuttlefish (*Sepia officinalis*). *J. Exp. Biol.* 202, 3127–3134.

Schöbl, J. (1877). Über die Blutgefäße des Auges der Cephalopoden. *Arch. Mikrosk. Anat.* 15, 215–243.

Schultze, M. (1867). Die Stäbchen in der Retina der Cephalopoden und Heteropoden. *Arch. Mikrosk. Anat.* 5, 1–24.

Seidou, M., Sugahara, M., Uchiyama, M., Hiraki, K., Hamanaka, T., Michinomae, M., et al. (1990). On the three visual pigments in the retina of the firefly squid, *Watasenia scintillans*. *J. Comp. Physiol. A* 166, 769–773.

Shashar, N. (2014). "Polarization vision in cephalopods" in *Polarized light and polarization vision in animal sciences*. Vol. 2, ed. G. Horvath (Berlin, Heidelberg: Springer), 217–224.

Shashar, N., and Cronin, T. W. (1996). Polarization contrast vision in *Octopus*. *J. Exp. Biol.* 199, 999–1004.

Silver, S., Patterson, J. E., and Mobbs, P. G. (1983). Biogenic amines in cephalopod retina. *Brain Res.* 273, 366–368. doi: 10.1016/0006-8993(83)90864-8

Sivak, J. G. (1982). Optical properties of a cephalopod eye (the short finned squid, *Illex illecebrosus*). *J. Comp. Physiol. A* 147, 323–327. doi: 10.1007/BF00609666

Sivak, J. G. (1991). Shape and focal properties of the cephalopod ocular lens. *Can. J. Zool.* 69, 2501–2506. doi: 10.1139/z91-354

Sivak, J. G., West, J. A., and Campbell, M. C. (1994). Growth and optical development of the ocular lens of the squid (*Sepioteuthis lessoniana*). *Vis. Res.* 34, 2177–2187. doi: 10.1016/0042-6989(94)90100-7

Soto, C. (2018). *Der Pupillenreflex des gemeinen Kraken Octopus vulgaris*. Master's thesis. Rostock, Germany: University of Rostock.

Sroczynski, S., and Muntz, W. R. A. (1985). Image structure in *Eledone cirrhosa*, an *Octopus*. *Zool. Jahrb. Abt. Allg. Zool. Physiol.* 89, 157–168.

Sroczynski, S., and Muntz, W. R. A. (1987). The optics of oblique beams in the eye of *Eledone cirrhosa*, an *Octopus*. *Zool. Jahrb. Abt. Allg. Zool. Physiol.* 91, 419–446.

Stubbs, A. L., and Stubbs, C. W. (2016a). Spectral discrimination in color blind animals via chromatic aberration and pupil shape. *Proc. Natl. Acad. Sci. USA* 113, 8206–8211. doi: 10.1073/pnas.1524578113

Stubbs, A. L., and Stubbs, C. W. (2016b). Reply to Gagnon et al.: all color vision is more difficult in turbid water. *Proc. Natl. Acad. Sci. USA* 113:E6910. doi: 10.1073/pnas.1614994113

Sugawara, K., Katagiri, Y., and Tomita, T. (1971). Polarized light responses from octopus single retinular cells. *J. Fac. Sci.* 17, 581–586.

Sutherland, N. S. (1957). Visual discrimination of orientation and shape by the octopus. *Nature* 179, 11–13. doi: 10.1038/179011a0

Sutherland, N. S. (1963a). The shape-discrimination of stationary shapes by octopuses. *Am. J. Psychol.* 76, 177–190.

Sutherland, N. S. (1963b). Visual acuity and discrimination of stripe widths in *Octopus vulgaris* Lamarck. *Pubbl. Staz. Zool. Nap.* 33, 92–109.

Sutherland, N. S., and Carr, A. E. (1963). The visual discrimination of shape by *Octopus*: the effect of stimulus size. *Q. J. Exp. Psychol.* 15, 225–235.

Sweeney, A. M., Des Marais, D. L., Ban, Y.-E. A., and Johnson, S. (2007). Evolution of graded refractive index in squid lenses. *J. R. Soc. Interface* 4, 685–698. doi: 10.1098/rsif.2006.0210

Talbot, C. M., and Marshall, J. (2010). Polarization sensitivity in two species of cuttlefish - *Sepia plangon* (Gray 1849) and *Sepia mestus* (Gray 1849) - demonstrated with polarized optomotor stimuli. *J. Exp. Biol.* 213, 3364–3370. doi: 10.1242/jeb.042937

Tasaki, K., and Karita, K. (1966). Intraretinal discrimination of horizontal and vertical planes of polarized light by *Octopus*. *Nature* 209, 934–935. doi: 10.1038/209934a0

Tasaki, K., Norton, A. C., and Fukuda, Y. (1963a). Regional and directional differences in the lateral spread of retinal potentials in the *Octopus*. *Nature* 198, 1206–1208.

Tasaki, K., Oikawa, T., and Norton, A. C. (1963b). The dual nature of the octopus electroretinogram. *Vis. Res.* 3, 61–72.

Thomas, K. N., Robinson, B. H., and Johnson, S. (2017). Two eyes for two purposes: in situ evidence for asymmetric vision in the cockeyed squids *Histiothethis heteropsis* and *Stigmatoteuthis dofleini*. *Philos. Trans. R. Soc. Biol. Sci.* 372:20160069. doi: 10.1098/rstb.2016.0069

Tonosaki, A. (1965). The fine structure of the retinal plexus in *Octopus vulgaris*. *Z. Zellforsch.* 67, 521–532. doi: 10.1007/BF00342584

Tsukahara, Y., Tamai, M., and Tasaki, K. (1973). Oscillatory potentials of the *Octopus* retina. *Proc. Jpn. Acad.* 49, 57–62. doi: 10.2183/pjab1945.49.57

von Lenhossék, M. (1894). Zur Kennnis der Netzhaut der Cephalopoden. *Z. Wiss. Zool.* 58, 636–660.

Weel, P. B., and Thore, S. (1936). Über die Pupillarreaktion von *Octopus vulgaris*. *Z. Vgl. Physiol.* 23, 26–33.

Wells, M. J. (1960). Proprioception and visual discrimination of orientation in *Octopus*. *J. Exp. Biol.* 37, 489–499.

Wells, M. J. (1966a). "The brain and behavior of cephalopods" in *Physiology of mollusca*. Vol. II, eds. K. M. Wilbur and C. M. Yonge (New York, London: Academic Press), 547–590.

Wells, M. J. (1966b). "Cephalopod sense organs" in *Physiology of mollusca*. Vol. II, eds. K. M. Wilbur and C. M. Yonge (New York, London: Academic Press), 523–545.

Wentworth, S. L., and Muntz, W. R. A. (1989). Asymmetries in the sense organs and central nervous system of the squid *Histiotheuthis*. *J. Zool.* 219, 607–619. doi: 10.1111/j.1469-7998.1989.tb02603.x

Wiley, A. (1902). *Contribution to the natural history of the pearly Nautilus. A. Wiley's zoological results, part VI*. Cambridge, UK: Cambridge University Press.

Wolken, J. (1958). Retinal structure. Mollusc, Cephalopoda: *Octopus, Sepia*. *J. Biophys. Biochem. Cytol.* 4, 835–838. doi: 10.1083/jcb.4.6.835

Woods, J. (1965). Octopus-watching off Capri. *Animals* 7, 324–327.

Yamamoto, T., Tasaki, K., Sugawara, Y., and Tonosaki, A. (1965). Fine structure of the octopus retina. *J. Cell Biol.* 25, 345–359. doi: 10.1083/jcb.25.2.345

Youn, S., Okinaka, C., and Mäthger, L. M. (2019). Elaborate pupils in skates may help camouflage the eye. *J. Exp. Biol.* 222:jeb195966. doi: 10.1242/jeb.195966

Young, J. Z. (1956). Visual responses by octopus to crabs and other figures before and after training. *J. Exp. Biol.* 33, 709–729.

Young, J. Z. (1960). The visual system of *Octopus* (1) regularities in the retina and optic lobes of *Octopus* in relation to form discrimination. *Nature* 186, 836–839. doi: 10.1038/186836a0

Young, J. Z. (1962a). The optic lobes of *Octopus vulgaris*. *Philos. Trans. R. Soc. Biol. Char.* 245, 19–65.

Young, J. Z. (1962b). The retina of cephalopods and its degeneration after optic nerve section. *Philos. Trans. R. Soc. Biol. Char.* 245, 1–18.

Young, J. Z. (1963). Light- and dark-adaptation in the eyes of some cephalopods. *J. Zool.* 140, 255–272.

Young, J. Z. (1971). *The anatomy of the nervous system of Octopus vulgaris*. Oxford: Clarendon Press.

Young, R. E. (1975). Function of the dimorphic eyes in the midwater squid *Histioteuthis dofleini*. *Pac. Sci.* 29, 211–218.

Conflict of Interest: The authors declare that the research was conducted in the absence of any commercial or financial relationships that could be construed as a potential conflict of interest.

frontiers in Physiology

ORIGINAL RESEARCH
published: 28 April 2020
doi: 10.3389/fphys.2020.00379

Spatial Contrast Sensitivity to Polarization and Luminance in Octopus

Luis Nahmad-Rohen[1] *and Misha Vorobyev*[2]*

[1] Leigh Marine Laboratory, Institute of Marine Science, University of Auckland, Auckland, New Zealand, [2] Optometry and Vision Science, Faculty of Medical and Health Sciences, University of Auckland, Auckland, New Zealand

While color vision is achieved by comparison of signals of photoreceptors tuned to different parts of light spectra, polarization vision is achieved by comparison of signals of photoreceptors tuned to different orientations of the electric field component of visible light. Therefore, it has been suggested that polarization vision is similar to color vision. In most animals that have color vision, the shape of luminance contrast sensitivity curve differs from the shape of chromatic contrast sensitivity curve. While luminance contrast sensitivity typically decreases at low spatial frequency due to lateral inhibition, chromatic contrast sensitivity generally remains high at low spatial frequency. To find out if the processing of polarization signals is similar to the processing of chromatic signals, we measured the polarization and luminance contrast sensitivity dependence in a color-blind animal with well-developed polarization vision, *Octopus tetricus*. We demonstrate that, in *Octopus tetricus,* both luminance and polarization contrast sensitivity decrease at low spatial frequency and peak at the same spatial frequency (0.3 cpd). These results suggest that, in octopus, polarization and luminance signals are processed via similar pathways.

Keywords: octopus vision, octopus behavior, polarization vision, contrast sensitivity, polarization sensitivity, chromatic vision

OPEN ACCESS

Edited by:
Daniel Osorio,
University of Sussex, United Kingdom

Reviewed by:
Thomas Cronin,
University of Maryland, Baltimore County, United States
PrimoŽ Pirih,
University of Ljubljana, Slovenia

***Correspondence:**
Misha Vorobyev
m.vorobyev@auckland.ac.nz

Specialty section:
This article was submitted to Invertebrate Physiology, a section of the journal Frontiers in Physiology

Received: *16 November 2019*
Accepted: *30 March 2020*
Published: *28 April 2020*

Citation:
Nahmad-Rohen L and Vorobyev M (2020) Spatial Contrast Sensitivity to Polarization and Luminance in Octopus. Front. Physiol. 11:379. doi: 10.3389/fphys.2020.00379

INTRODUCTION

Polarization sensitivity is widespread among invertebrates with rhabdomeric photoreceptors, such as arthropods and cephalopods, because rhabdomeric photoreceptors are inherently polarization sensitive by virtue of their microvillar structure (Moody and Parriss, 1960; Young, 1971). Polarization vision is particularly important to cephalopods, a group of animals that lack color vision, as it plays an important role in navigation (Shashar et al., 2002; Cartron et al., 2012), contrast enhancement (Shashar and Cronin, 1996; Shashar et al., 2002; Temple et al., 2012; Cartron et al., 2013b), detection of transparent prey (Shashar and Hanlon, 1998; Cartron et al., 2013a), and communication (Shashar and Cronin, 1996; Boal et al., 2004; Mäthger et al., 2009; Shashar et al., 2011). Furthermore, it seems that polarization contrast alone might be sufficient for both object detection and motion perception (Glantz and Schroeter, 2006; Pignatelli et al., 2011; Temple et al., 2012). It is possible that polarization vision could have an advantage over color vision in underwater environments, as the light spectrum is variable and long wavelengths (reds) are lost rapidly with depth, whereas the background polarization is relatively constant in angle and degree (Waterman, 1954; Marshall and Cronin, 2011), allowing for small changes in polarization to be easily detected in this almost noise-free environment (Cronin et al., 2003; Pignatelli et al., 2011).

It has been proposed that polarization vision is analogous to color vision in that it allows the viewer to divide a scene into regions based on the differences in polarization in the same way that color vision discriminates between chromaticities (Bernard and Wehner, 1977; Nilsson and Warrant, 1999; Cronin et al., 2003). Both polarization vision and color vision require a comparison between receptor signals: color vision is achieved through comparison of signals of photoreceptors tuned to different parts of the light spectrum (Vorobyev, 2007), whereas polarization vision is achieved through comparison of signals of photoreceptors tuned to different orientations of the electric field component of visible light.

If polarization vision were indeed analogous to color vision, a similar neural processing of both may be expected. One way to test this is through a contrast sensitivity function (CSF)—the dependence of sensitivity on the spatial frequency of a stimulus. The shape of the contrast sensitivity function depends on the neural processing of receptor signals (Barlow, 1961; Atick, 1992; Laughlin, 1994; Wandell, 1995). While the achromatic (luminance) contrast sensitivity function generally has a bell-like shape and decreases at both low and high spatial frequencies, chromatic sensitivity does not decrease at low spatial frequency and decreases at the high spatial frequency earlier than the achromatic contrast sensitivity function does (Cornsweet, 1970; Wandell, 1995). This difference between chromatic and achromatic contrast sensitivity has been demonstrated for humans, birds, fish, and insects (Mullen, 1985; Giurfa and Vorobyev, 1997; Lind and Kelber, 2011; Siebeck et al., 2014). The relationship between the shape of the contrast sensitivity and neural processing of visual signals is well-understood (Campbell and Robson, 1968; Cornsweet, 1970; Northmore and Dvorak, 1979; Rovamo et al., 1999; Pelli and Bex, 2013). While the decrease of sensitivity at low spatial frequency is a consequence of lateral inhibition, the lack of decrease of sensitivity at low spatial frequency is a consequence of spatial summation. A quantitative theory explaining the shape of contrast sensitivity has been developed for processing of luminance and chromatic information by human retinal ganglion cells (Rovamo et al., 1999).

In a previous paper we have demonstrated that the octopus luminance contrast sensitivity decreases at low spatial frequency (Nahmad-Rohen and Vorobyev, 2019). Here we compare luminance and polarization contrast sensitivity in *Octopus tetricus* (Gould, 1852). The lack of decrease of polarization sensitivity at low spatial frequency would be an indication of the similarity between processing of polarization in octopus and chromatic information in animals possessing color vision. On the other hand, the similarity of the shape of luminance and polarization sensitivity would indicate that luminance and polarization signals are conveyed via similar pathways.

Octopus photoreceptors are arranged in the form of parallel tubes packed into groups called rhabdomeres, the microvilli of which lie perpendicular to those of adjacent rhabdomeres and parallel to those of opposite ones. Such orthogonal arrangement provides polarization sensitivity as it strongly favors (and thus allows them to distinguish between) rays polarized at vertical and horizontal direction (Moody and Parriss, 1960, 1961; Young, 1971; Nilsson and Warrant, 1999). Octopuses are capable of discriminating between objects based on whether they show polarization contrast or not, and can detect variation in polarization patterns within a single object. Furthermore, they are able to identify objects through polarization cues alone, using the particular polarization patterns of each object to tell them apart (Shashar and Cronin, 1996; Cronin et al., 2003).

The polarization visual acuity of cephalopods has been measured through discrimination training (Shashar and Cronin, 1996), reflex method experiments (Temple et al., 2012), and optomotor tests (Cartron et al., 2013a). Discrimination tests have shown that octopuses can differentiate between polarization patterns with an *e*-vector variation of 20° (Shashar and Cronin, 1996). By presenting a polarized stimulus simulating an approaching predator and observing changes in body coloration as a response to it, Temple and colleagues reported that the minimum polarization angle difference detectable by octopus was 10° (Temple et al., 2012). Cephalopods have shown both optomotor and optokinetic responses in temporal resolution experiments designed specifically for polarization vision (Talbot and Marshall, 2010; Cartron et al., 2013a), and it was observed that, as with brightness, polarization sensitivity increases with age, albeit having a slower development (Cartron et al., 2013a).

However, thorough polarization contrast sensitivity measurements have not been made for octopuses. This may have been a very difficult (if not impossible) task to accomplish in the past, but it is now possible to do so by using a Liquid Crystal Display (LCD) screen. By removing the output polarizing filter, an image consisting of polarization patterns can be produced (Glantz and Schroeter, 2006; Foster et al., 2018). This technique has previously been used to present cuttlefish and squid with stimuli simulating either an approaching predator or a prey item and elicit the appropriate response (Pignatelli et al., 2011; Temple et al., 2012; Cartron et al., 2013b), as well as to present a looming stimulus to fiddler crabs (How et al., 2012). Another technique used for presenting butterflies with polarized stimuli includes using a digital light processing projector with a spinning linear polarizer (Stewart et al., 2017). Here we use a modified LCD screen to present octopuses with sinusoidal gratings to obtain a polarization contrast sensitivity function (PCSF).

Generally sensitivity depends on background. For example, in human observers, the sensitivity to changes of chromaticity decreases as the chromaticity of background increases, i.e., it is easier to detect small increase in chromaticity against achromatic backgrounds than against chromatic backgrounds due to the saturation of chromatic mechanisms (Krauskopf and Gegenfurtner, 1992). To find out if the ability of octopus to detect polarization depends on the polarization of background light, we test octopuses using unpolarized and 50% horizontally polarized background. The underwater light is horizontally polarized (Waterman, 1981; Marshall and Cronin, 2011), and the degree of polarization is typically below 50% and rarely exceeds 60%, even under exceptional conditions (Waterman, 1981; Marshall and Cronin, 2011). Therefore, the polarization of background

Abbreviations: LCSF, luminance contrast sensitivity function; PCSF, polarization contrast sensitivity function.

light used in our experiments is within the range of variability of polarization of background light in the octopus habitat.

A novel method based on a reflex response was used to collect behavioral data from psychophysics experiments in a non-invasive way. This reflex response provides advantages over discrimination training methods, as it eliminates variables that can otherwise affect the test subject's choice, such as mood, confusion, and even handedness/preference for one side (Northmore and Yager, 1975; Byrne et al., 2002; Cartron et al., 2013a). Moreover, even when the conditioned response is well-established, curious animals can at times pick the wrong choice intentionally (Shashar and Cronin, 1996).

METHODS

Animals and Housing

Ten octopuses (*Octopus tetricus*) (41–191 g) were captured with pot traps in Hauraki Gulf, New Zealand, and housed in individual tanks of 90 cm × 45 cm × 40 cm (L × W × H) with a 6 mm thick glass wall at the Leigh Marine Laboratory. Tanks had a constant flow of 200 μm filtered seawater from the Goat Island Marine Reserve, and were provided with an additional aeration system. Each tank was illuminated with overhanging fluorescent lights. Tanks were provided with an enriched, semi-natural environment (algae, rocks, and oyster shells), as well as a PVC pipe for octopuses to build their dens in. Animals were given live food (mussels and snails) 3–4 times/week. Individuals were given 2–3 days of acclimatization after capture before beginning experiments. Octopuses were kept for 2–3 months for experiments, after which they were released back into Hauraki Gulf.

All animal handling and experiments were carried out under approval of the University of Auckland Animal Ethics Committee (ref. 001761).

Experimental Setup and Procedure

Vertical sinusoidal gratings of different spatial frequencies and varying contrast were used to measure the luminance and polarization contrast sensitivity of octopuses. The experimental procedure was based on that of Nahmad-Rohen and Vorobyev (2019).

Octopuses were presented with a stimulus consisting of vertically oriented sinusoidal gratings of five different spatial frequencies [12, 4, 1, 0.3, and 0.1 cycles per degree (cpd)] on an LCD screen to measure their contrast sensitivity to both luminance and polarization. The sinusoidal grating alternated between two positions by changing phase by 180° twice per second (temporal frequency of 2 Hz) to reduce habituation to the stimulus (Zeil, 2000). Depending on stimulus intensity, the octopus flicker-fusion frequency varies between 20 and 70 Hz (Hamasaki, 1968). We do not know which temporal frequency for the stimulus would be optimal for octopus vision. However, we empirically found that the frequency chosen (2 Hz) yields a reliable response. This alternating stimulus as opposed to a moving one was used to avoid confusion between contrast and motion sensitivity. Stimuli were created through MATLAB [version 7.12.0.635 (R2011a)] running Psychophysics Toolbox function interface (version 3.0.12 for Apple OS X, http://psychtoolbox.org).

The distance between the octopus and the tank edge was measured for each individual before beginning trials, and total distance was input into the script in order to generate the correct stimuli. Correction for the air-water interface was done by dividing the desired spatial frequency of the stimulus by the refractive index of seawater—1.34.

Black corrugated plastic was placed around the tank, as well as from the edge of the tank to the LCD monitor on the top, bottom, left, and right sides as a screen in order to restrict the octopus field of view of anything other than the monitor, so as to avoid any distractions or other visual stimuli. For this purpose, the aeration system was turned off during experiments. Furthermore, the lights above the tank were diffused, thus ensuring that the main light source was the LCD screen (see **Figure 1**).

The screen was located at 1 m from tank and always kept at conventional orientation. For luminance sensitivity measurements, the polarizer filter of the screen (DELL UltraSharp 1907FP, 19″) was, by manufacturer settings, oriented at 45° with respect to horizontal (0°) or vertical (90°) orientations. For polarization sensitivity measurements, the polarizer of the screen (DELL UltraSharp 1905FP, 19″), which was vertically oriented (90°) by manufacturer settings, was removed. The luminous intensity of the background against which the stimuli were presented was 86.7 for luminance sensitivity (50% gray), and 354.5 in the case of the screen with removed polarizer (the polarizing filter attenuates light emitted from the screen). The screen with the removed polarizer produces polarization patterns that do not have intensity contrast and hence are completely invisible to non-polarization sensitive animals. Thus, a maximum amplitude grating corresponded to perpendicular *e*-vector angles. By decreasing contrast, the degree of polarization difference in the grating is decreased. In the screen with the removed polarizer, pixel value 255 (white) corresponded to the vertical direction and pixel value 0 (black) corresponded to the horizontal direction.

To calibrate the modified LCD screen, a PR655 spectroradiometer (Photo Research Inc.) with affixed vertical (90°), horizontal (0°), and oblique (45° and 135°) polarizing filters was used to measure monitor output spectra at different pixel values (**Figures A1-A,A2**). The intensity values were obtained by multiplying spectra by the octopus spectral sensitivity (Brown and Brown, 1958) (**Figure A1-B**) and subsequent integration over wavelength. During calibration no change in intensity was observed at 45° and 135° for all pixel values, and measurements of the angle of polarization were constant across all intensities, meaning that changes in contrast or intensity correspond to changes in degree of polarization rather than to changes in *e*-vector orientation (see **Appendix 1**—Polarization Monitor Calibration). The pixel value at which the vertically and horizontally polarized light produced the same level of intensity determined the intensity corresponding to zero degree of polarization (see **Figure A3**). Gamma correction was introduced to ensure intensity linearity.

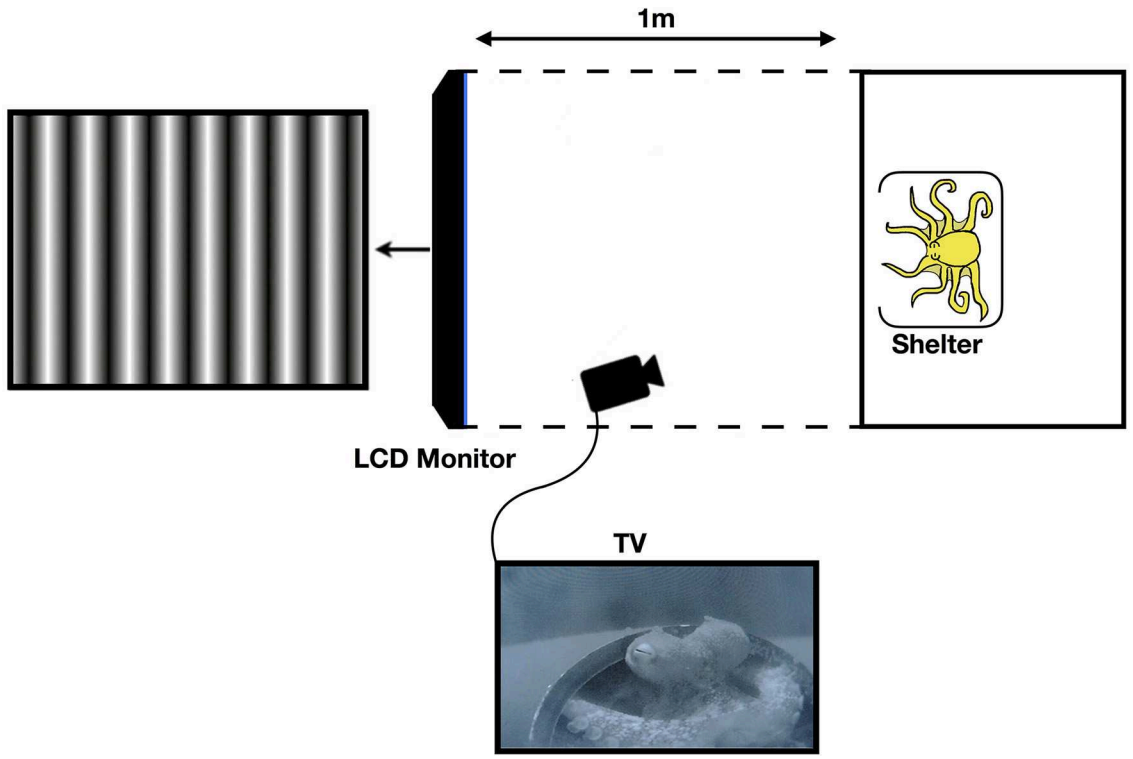

FIGURE 1 | Diagram of the experimental setup (not to scale). The black corrugated plastic tunnel blocks any stimulus outside of the tank apart from the LCD monitor. Reprinted with permission from Nahmad-Rohen and Vorobyev (2019).

For the polarization contrast sensitivity measurements, two backgrounds were used: one with zero degree of polarization, the other with 50% polarization with a dominant horizontal *e*-vector orientation. The monitor settings used to achieve 50% polarization corresponded to the settings used for gray background in luminance experiments.

The uniform background (50% gray for unmodified LCD screen, unpolarized/50% polarization for modified screen) was shown for 1 h before the experiment began so that the octopuses became accustomed to it. Stimuli were presented for 2 s, shifting phase by 180° with a temporal frequency of 2 Hz. After stimulus presentation the programme remained idle, showing the uniform gray background, until given instruction to show the next one. A window of at least 20 s was used between stimulus presentations. To avoid habituation, frequencies were presented in random order. Each spatial frequency was presented a minimum of 30 times. To avoid habituation resulting from a stimulus with high Michelson contrast, the initial contrast for the procedure was 5%. Contrast was capped at 10% for the luminance experiment, and at 16% polarization for all frequencies except the highest one (12 cpd), which was capped at 28.6% polarization, for the polarization experiment. Thus, sensitivity values below 10 for luminance and 6.1 (or 3.5 for 12 cpd) for polarization cannot be reliably estimated. Minimum contrast, based on hardware limitations, was 0.7%.

Whether an octopus would see the stimulus or not was determined by whether a "fixation response" was shown—expansion of the chromatophores in and around the eye occurring as a result of accommodation, resulting in a momentary darkening around the pupil—(Turnbull, 2014; Nahmad-Rohen and Vorobyev, 2019). Because the fixation response is an uncontrolled reflex it does not require training, and preliminary tests in which the grating was shown at 100% contrast (see Nahmad-Rohen and Vorobyev, 2019—**Supplementary Materials**) showed that it is a reliable determinant of whether the grating is resolved by the subject.

The fixation response was monitored through a CCTV camera (Panasonic CCTV WV-BL200) placed outside the tank facing the octopus's eye. The camera provided live feed to a tv screen, making it possible to assess the presence or absence of a fixation response in real time. With each positive (fixation response present) or negative (no expansion of the chromatophores) response, contrast was decreased or increased, respectively, based on an adaptive staircase procedure with a Weibull approximation of the psychometric function (QUEST; Watson and Pelli, 1983). This procedure uses data from previous stimulus presentations to guide further testing. For each step, the adaptive staircase procedure uses the information from all previous trials to determine the contrast level of the next stimulus presentation and estimate the position of a threshold. This method allows us to establish a threshold reliably using only a limited number of trials

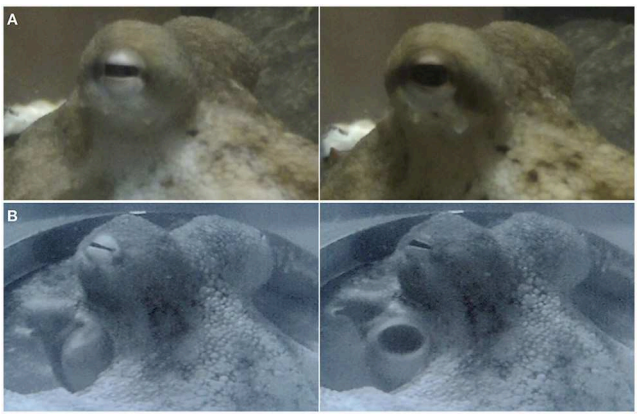

FIGURE 2 | Two examples of octopus fixation reflex. (Left) Stimulus not present. (Right) Pupil expands along with chromatophores around the eye as a response to the appearance of the sinusoidal grating. The different features of the fixation response can be expressed at various degrees of intensity: **(A)** shows a strong pupil expansion and expression of the "eye bar," whereas **(B)** shows a good example of the "dark eye ring." **(B)** Reprinted with permission from Nahmad-Rohen and Vorobyev (2019).

(Watson and Pelli, 1983). The staircase was run until a contrast threshold was established, and a minimum of 30 presentations were done for each spatial frequency. Luminance sensitivity was defined as the inverse of the contrast threshold, and polarization sensitivity as the inverse of degree of polarization threshold.

It is important to note that, given the nature of the methods, we recorded attention threshold rather than minimal detectable contrast.

Data Analysis

For each stimulus presentation, a Weibull psychometric function was applied to estimate the probability of stimulus detection:

$$\Psi\left(C; C_t\right) = \gamma + (1 - \gamma - \delta)\left(1 - exp\left(-\left(\frac{C}{C_t}\right)^{\beta}\right)\right), \quad (1)$$

where γ is the false alarm rate (number of fixation responses in the absence of a stimulus), δ is the proportion of trials with blind responses (presentations in which the stimulus is resolvable by the individual—based on the contrast level—but still fails to respond), β is the slope of the psychometric function, C corresponds to the contrast presented, and C_t is the contrast threshold parameter searched for by the staircase procedure. We use the following values for false alarm rate and proportion of blind responses: $\gamma = 0.0569$, $\delta = 0.3058$ (Nahmad-Rohen and Vorobyev, 2019). These values were obtained by presenting stimuli to two octopuses at 100% contrast. The proportion of blind responses was defined as the number of cases when the octopus did not respond to the 100% contrast grating divided by the total number of presentations. The false alarm rate was defined as the number of fixation responses when no stimulus was present divided by the total duration of the trial (Nahmad-Rohen and Vorobyev, 2019). The value for β (3) was based on suggestions from literature (Watson and Pelli, 1983).

Once the QUEST staircase procedure was finished, the threshold parameter C_t was calculated along with the error estimate for each spatial frequency. The local maximum of a likelihood function was then found while keeping parameters γ, δ, and β constant. The likelihood function L is:

$$L = \sum_{i=1}^{n} (y_i log(\Psi(C_i, C_t)) + (1 - y_i) log(1 - \Psi(C_i, C_t))), \quad (2)$$

where n is the total number of presentations for each given spatial frequency and y is the sequence of responses (0 if negative, 1 if positive) for each of the contrasts C at which the sinusoidal grating was presented. The value of the parameter C_t that maximized the likelihood function (i.e., for which the maximum value of the likelihood function was found) provides the contrast threshold. This was found using the "FindMaximum" function in Wolfram Mathematica©.

After obtaining the contrast threshold estimate, a parametric bootstrap procedure (Wichmann and Hill, 2001) was used to obtain error bars (**Figures 4**, **5**). This procedure was chosen because it takes into account the noise of the original data (Wichmann and Hill, 2001). In our case, the causes of noise can include factors such as changes in attention or distraction due to floating debris in the water. Assuming a binomial distribution of the data from the psychophysical experiments, and based on the probability of stimulus detection obtained from the Weibull psychometric function, a new set of data was created using a random number generator. In this virtual experiment, the stimulus was detected if the random number obtained was smaller than the probability of detection, and not detected if it was larger. Thus, a new sequence of responses y was obtained, in turn generating a new threshold C_t by maximizing the likelihood function with the virtual sequence of responses. For each spatial frequency, this procedure was repeated 10,000 times (obtaining different results of the virtual psychophysical experiment each time) to obtain a sequence of thresholds. The interquartile range of this threshold sequence is displayed as error bars in the contrast sensitivity graphs (**Figures 4**, **5**).

All data analysis was done in Wolfram Mathematica (version 11.3 for Mac OS X).

It is important to keep in mind that false alarms can occur as a result of different circumstances, such as floating debris in the water or neural noise. It is possible that the false alarm rate and proportion of blind responses vary between individuals.

Relation Between Degree of Polarization and Contrast

We define the direction of polarization of the maximum signal (white, pixel value 255) as 0° and the direction of minimal signal (black, pixel value 0) as 90°. Let I_0 and I_{90} be the intensities of light polarized at 0° and 90° orientations, respectively. Then, the degree of polarization is defined as:

$$P = \frac{I_0 - I_{90}}{I_0 + I_{90}}\, 4 \quad (3)$$

The degree of polarization, so defined, ranges from +1 to −1, with 0 corresponding to unpolarized light. Let I_0^0 and I_{90}^0 be the

FIGURE 3 | Octopus unilateral body pattern display.

intensities corresponding to the background and $P^0 = \frac{I_0^0 - I_{90}^0}{I_0^0 + I_{90}^0}$, then $\frac{2I_0^0}{I_0^0+I_{90}^0} = 1 + P^0$, $\frac{2I_{90}^0}{I_0^0+I_{90}^0} = 1 - P^0$. Note that, in the case of a screen with the removed polarizer, $I_0 + I_{90} = I^0$ is constant. Therefore, when contrast C is presented against the background the light intensities are given by

$$I_0 = I_0^0 + CI_0^0 = I^0 \frac{\left(1 + P^0\right)(1 + C)}{2}, \tag{4}$$

$$I_{90} = I_{90}^0 - CI_0^0 = I^0 \left(1 - \frac{\left(1 + P^0\right)(1 + C)}{2}\right), \tag{5}$$

and substitution of Equation (5) into Equation (4) gives:

$$P = \frac{I_0^0 - I_{90}^0 + 2CI_0^0}{I_0^0 + I_{90}^0} = P_0 + C\left(1 + P^0\right). \tag{6}$$

Therefore, the change of degree of polarization is given by:

$$P = C\left(1 + P^0\right) \tag{7}$$

RESULTS

The fixation response is comprised of three separate elements: expansion of the pupil, which can aid in estimating distances and which occurs in cephalopods when fighting or viewing food (Douglas et al., 2005); expression of the "dark eye ring" behavior, which can be seen in octopuses when disturbed by an object suddenly appearing or approaching the octopus (Borrelli et al., 2006); and expression of the "eye bar" (Packard and Sanders, 1971; Forsythe and Hanlon, 1985; Borrelli et al., 2006) (see **Figure 2** and **Supplementary Material Movie 1**). Each one of these features can be displayed at various degrees of intensity, and they occur simultaneously. In some cases the dominant response is an expansion of the pupil, in others it is the darkening around the eye (dark eye ring and/or eye bar). However, it is difficult to specify in each case which one is dominant. During experiments it was observed that occasionally octopuses would not show a fixation response when a stimulus appeared on the screen, but would respond to it by displaying a unilateral body pattern—a conspicuous pattern in which one side of the body becomes dark while the other half remains pale (van Heukelem, 1966; Packard and Sanders, 1971; Forsythe and Hanlon, 1985; Borrelli et al., 2006) (see **Figure 3**). Contrary to the body pattern description by Forsythe and Hanlon (1985) and Packard and Sanders (1971), the dark side was not always the side facing the stimulus. Also, unlike Van Heukelem's description (van Heukelem, 1966), this color change was not frequent, and was only seen occasionally and clearly linked to the appearance of the sinusoidal grating. Most octopuses presented this pattern during the polarization experiments, and only one during the luminance experiments. These unilateral body pattern expressions were counted as "positive" responses for staircase procedure purposes.

Luminance contrast sensitivity curves were obtained for three octopuses, and polarization contrast sensitivity curves were obtained for seven octopuses (three of which were the same as those for which luminance sensitivity curves were obtained). Three luminance contrast sensitivity thresholds from Nahmad-Rohen and Vorobyev (2019) are also presented here (octopuses 1–3: Atha, Tmienja, and Wassakib) Luminance contrast sensitivity peaked at 0.3 cpd and decreased at lower spatial frequencies in all six animals (see **Figure 4**). The mean contrast sensitivity at the maximum was 30.1 [contrast threshold = 3.32 ± 1.61% (mean ± SD)] and was in the range from 57.8 (contrast threshold = 1.73%) to 17 (contrast threshold = 5.87%) (see **Table 1**). By comparison, the best value for human contrast sensitivity is around 100 (contrast threshold = 1%) (Mullen, 1985).

Polarization contrast sensitivity also peaked at 0.3 cpd for six out of seven animals (see **Figure 4**). For one octopus (Tseebii) the polarization sensitivity at 1 cpd was higher (but not significantly) than that at 0.3 cpd. The staircase procedure was repeated for 1 cpd, yielding a much lower sensitivity (see **Figure 4**). Polarization contrast sensitivity was measured with unpolarized (3 animals: Tekyu, Ahtapot, Tuktujk) and 50% polarized (4 animals: Tseebii, Atocatl, Xhono, Sha'tekon) background. The degree of polarization sensitivities corresponding to the peak sensitivity (0.3 cpd) are equal to 59.2 [polarization threshold = 1.69 ± 0.5% (mean ± SD)] and 46.3 [polarization threshold = 2.16 ± 1.34% (mean ± SD)] for unpolarized and polarized backgrounds, respectively. The difference between sensitivities for polarized and unpolarized background was not significant ($p = 0.84$, t-test). The data from two groups were pooled together giving a mean polarization sensitivity of 51 [polarization threshold = 1.96 ± 1.02% (mean ± SD)]. The range of the polarization sensitivity was from 87.3 (polarization threshold = 1.15%) to 24.6 (polarization threshold = 4.07%) (see **Table 1**). The difference between the peak values of luminance and polarization thresholds was not statistically significant ($p = 0.11$, t-test).

Comparison between luminance and polarization sensitivity curves from the three octopuses (Tekyu, Ahtapot, and Tuktujk) allowed us to investigate the difference between the luminance and polarization sensitivity in more details (**Figure 5**). The sensitivity maximum at 0.3 cpd was higher for polarization than for luminance for each of the three individuals (see **Figure 5** and **Table 1**): 69.3, 69, and 42.7 for polarization vs.

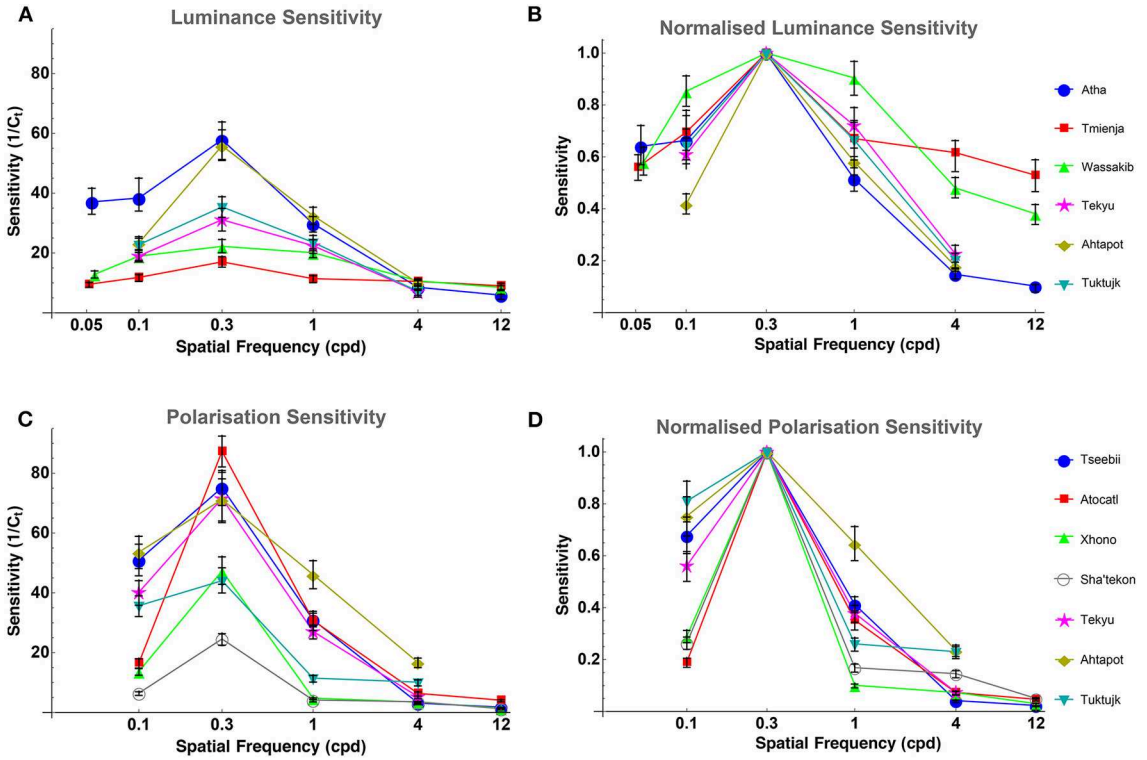

FIGURE 4 | (A) Octopus LCSF. All octopuses show the same bell-like shape of the sensitivity curve, and all peak at 0.3 cpd. Sensitivity is defined as the inverse of the contrast threshold. The error bars indicate bootstrap interquartile range. **(B)** Octopus LCSF normalized to the peak sensitivity value of each curve (at 0.3 cpd) for easier comparison between them. **(C)** Octopus PCSF. All octopuses show the same bell-like shape of the polarization sensitivity curve as the ones from the luminance sensitivity experiment. Sensitivity is defined as the inverse of the contrast of the degree of polarization. The error bars indicate bootstrap interquartile range. **(D)** Octopus PCSF normalized to the peak sensitivity value of each curve (at 0.3 cpd) for easier comparison between them.

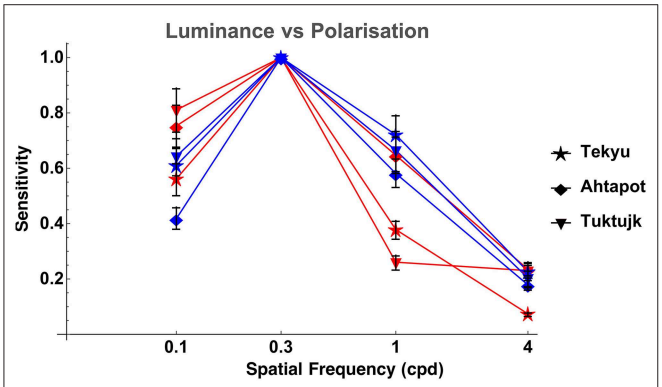

FIGURE 5 | Comparison of LCSF (blue) and PCSF (red) of three octopuses (normalized to the peak sensitivity value of each curve at 0.3 cpd). The error bars indicate bootstrap interquartile range. It can be appreciated that the shapes of the sensitivity curves are quite similar, although the differences between them are inconsistent: polarization sensitivity is higher than luminance sensitivity for two octopuses (Ahtapot and Tuktujk) at low spatial frequency (0.1 cpd), and lower than luminance sensitivity at a higher spatial frequency (1 cpd) for two out of three octopuses (Tekyu and Tuktujk).

31.1, 55.9, and 35.4 for luminance for Tekyu, Ahtapot, and Tuktujk, respectively. On the other hand, the difference in the shape was inconsistent. For two octopuses (Ahtapot and Tuktujk), polarization sensitivity was higher than luminance sensitivity at the lowest spatial frequency (0.1 cpd), and at a higher spatial frequency (1 cpd), polarization sensitivity was lower than luminance sensitivity for two octopuses (Tekyu and Tuktujk) (see **Figure 5**). To quantify the difference in the shape of contrast sensitivity curves, we normalized contrast sensitivity to its maximum at 0.3 cpd in all six luminance and seven polarization contrast sensitivity curves (see **Figure 4**). The normalized contrast sensitivities are characterized by the sensitivity at three frequencies (0.1, 1, and 3 cpd). The differences were assessed using a generalization of t-test to multidimensional data—the Hotteling T^2-test followed by a Bonferroni *post-hoc* test. We detected a small but statistically significant difference ($p = 0.026$, $n_1 = 6$, $n_2 = 7$) between the shapes of the polarization and luminance contrast sensitivity (**Figure 4**). We found that the luminance sensitivity is significantly higher than the polarization sensitivity at 1 cpd ($p = 0.007$, Bonferroni *post-hoc* test), and no statistically significant differences for the other spatial frequencies.

DISCUSSION

We compared the contrast sensitivity to luminance and polarization in octopus and demonstrated that, in contrast to

TABLE 1 | Contrast thresholds and sensitivity for luminance and polarization.

Octopus	Contrast thresholds (%) and sensitivity ($1/C_t$) at 0.3 cpd	
	Luminance	**Polarization**
1. Atha	1.73 (57.8)	–
2. Tmienja	5.87 (17.0)	–
3. Wassakib	4.5 (22.2)	–
4. Tseebii*	–	1.33 (75.2)
5. Atocatl*	–	1.15 (87.3)
6. Xhono*	–	2.11 (47.3)
7. She'tekon*	–	4.07 (24.6)
8. Tekyu	3.21 (31.1)	1.44 (69.3)
9. Ahtapot	1.79 (55.9)	1.45 (69)
10. Tuktujk	2.82 (35.4)	2.34 (42.7)
Mean	3.32 (30.1)	1.96 (51)
SD (σ)	1.61 (17)	1.02 (21.8)

Sensitivity is presented in brackets. For polarization sensitivity, octopuses marked with an asterisk (octopuses 4–7) were tested at 50% polarization background, while the others were tested at unpolarized background.

chromatic sensitivity, which generally does not decrease at low spatial frequency (Mullen, 1985; Giurfa et al., 1997; Lind and Kelber, 2011), octopus polarization sensitivity decreases at low spatial frequency. Therefore, we conclude that the processing of polarization signals in octopus is not analogous to the processing of chromatic signals in animals with color vision. Moreover, the shape of octopus polarization sensitivity is very similar to the shape of luminance sensitivity—both peak at the spatial frequency of 0.3 cpd. This indicates that luminance and polarization pathways are similar.

The difference in the processing of luminance and chromaticity can be explained in two different ways. (i) While luminance vision is achieved by summation of photoreceptor signals, chromatic vision is achieved by subtraction. This implies that chromatic vision suffers from the noise originating in photoreceptors to a higher degree than luminance vision. Therefore, chromatic vision has lower spatial resolution than luminance vision because spatial summation improves the signal-to noise ratio. Similar reasoning may explain the differences in the degree of lateral inhibition between luminance and chromatic vision. The lateral inhibition reduces the redundancy in the signal and hence improves the information transfer via channels with limited capacity (Barlow, 1961; Atick, 1992). However, when the signal-to-noise ratio is high it is beneficial to reduce or remove the lateral inhibition (Atick, 1992). (ii) Chromatic and achromatic vision are used for different purposes. Luminance vision is used for border detection, while chromatic vision is used for detecting the changes of material and identification of material properties (Rubin and Richards, 1982; Maximov, 2000). High spatial resolution and lateral inhibition facilitate border detection, but are not required for identification of material properties. Therefore, whereas chromatic vision is tuned to large visual angles, luminance (or achromatic) vision is tuned for detecting fine details in smaller visual angles (Giurfa et al., 1997; Lind and Kelber, 2011).

Because polarization vision is based on the comparison of two noisy signals, polarization vision may require larger spatial summation than luminance vision. Indeed, the only statistically significant difference between luminance and polarization sensitivity was a slightly lower contrast sensitivity for polarization at 1 cpd (see **Figures 4**, **5**), which can be attributed to an increase of spatial summation for polarization vision compared to luminance vision. However, unlike chromatic vision, polarization vision cannot be used for identification of material properties because the perceived polarization depends on viewing conditions such as mutual positions of the observer and the object (Waterman, 1981; How and Marshall, 2014). Cephalopods use polarization vision for tasks that are similar in their nature to those associated with luminance vision. It has been demonstrated that cephalopods use polarization vision to detect transparent prey (Shashar and Hanlon, 1998; Cartron et al., 2013a) which usually consists of small, planktonic organisms with highly birefringent bodies (and therefore produce high polarization contrast) (Shashar and Hanlon, 1998; Johnsen et al., 2011). Polarization vision is also used by cephalopods for communication: depending on the individual's activity, polarization patterns in their bodies change (Boal et al., 2004; Chiou et al., 2007; Mäthger et al., 2009). These polarization patterns have fine details (Boal et al., 2004; Chiou et al., 2007; Mäthger et al., 2009). Hence, the similarity between luminance and polarization contrast sensitivity and the presence of lateral inhibition in polarization vision is consistent with the similarity of tasks of luminance and polarization vision. However, it cannot be excluded that polarization vision can be also used for tasks that do not require high spatial resolution, such as polarization-based navigation (Shashar et al., 2002; Cartron et al., 2012). While it is well-established that, in terrestrial habitats, insects use polarization vision for navigation (Labhart, 2016), the utility of polarization cues for navigation are not well-understood. It has been argued that polarization-based navigation underwater is restricted to very shallow waters, and could be limited to shore detection (Shashar et al., 2011).

Due to the limitations of the methods, polarization sensitivity was measured at a higher light intensity than that used to measure luminance sensitivity. This can contribute to a possible difference in the maximal sensitivities to luminance and polarization (note that the difference in the maximal sensitivity between luminance and polarization was not statistically significant). However, the differences in the light levels at which the experiments were performed cannot explain the decrease of polarization sensitivity at 1 cpd because with the increased light level the sensitivity to high frequency should increase due to decrease of spatial summation (Atick, 1992). We performed experiments polarized and 50% polarized background and did not detect any significant difference. Because natural background polarization very rarely exceeds 50% (Waterman, 1981; Marshall and Cronin, 2011), we conclude that polarization sensitivity is unlikely to saturate in natural conditions.

Cartron et al. (2013a) noted that, in insects "polarized and unpolarized information are coded differently and are processed by different type of neurons in the optic lobe," and provide the hypothesis that "In cephalopods [...] polarization is not a

simple modulation of luminance information, but rather that it is processed as a distinct channel of visual information." Our results do not confirm this hypothesis and indicate that the processing of polarization and luminance signals in octopus are largely similar.

DATA AVAILABILITY STATEMENT

All datasets generated for this study are included in the article/**Supplementary Material**.

ETHICS STATEMENT

The animal study was reviewed and approved by University of Auckland Animal Ethics Committee (ref. 001761).

AUTHOR CONTRIBUTIONS

MV designed the experiment. LN-R performed the experiments. Both authors analyzed the data and wrote the manuscript.

FUNDING

This research was partly funded by Consejo Nacional de Ciencia y Tecnologia, Fellow CVU no. 516833, and by Royal Society Marsden Grant 19-UOA-104-3718652.

ACKNOWLEDGMENTS

The authors would like to thank Errol Murray for his help in setting the tanks, building the traps, and capturing the octopuses, Stefan Spreitzenbarth for his assistance in the field, and Veronica Rohen & Jessica Campbell for their help with the statistical analysis.

SUPPLEMENTARY MATERIAL

The Supplementary Material for this article can be found online at: https://www.frontiersin.org/articles/10.3389/fphys.2020.00379/full#supplementary-material

Supplementary Material Movie 1 | Octopus fixation reflex.

REFERENCES

Atick, J. J. (1992). Could information theory provide an ecological theory of sensory processing? *Netw. Comput. Neural Syst.* 3, 213–251. doi: 10.1088/0954-898X_3_2_009

Barlow, H. (1961). "The coding of sensory messages," in *Current Problems in Animal Behaviour,* eds W. H. Thorpe, and O. L. Zangwill (Cambridge: Cambridge University Press), 331–360.

Bernard, G. D., and Wehner, R. (1977). Functional similarities between polarization vision and color vision. *Vision Res.* 17, 1019–1028. doi: 10.1016/0042-6989(77)90005-0

Boal, J. G., Shashar, N., Grable, M. M., Vaughan, K. H., Loew, E. R., and Hanlon, R. T. (2004). Behavioral evidence for intraspecific signaling with achromatic and polarized light by cuttlefish (*Mollusca: Cephalopoda*). *Behaviour* 141, 837–861. doi: 10.1163/1568539042265662

Borrelli, L., Gherardi, F., and Fiorito, G. (2006). *A Catalogue of Body Patterning in Cephalopoda*. Firenze: Firenze University Press. Avaliable online at: https://www.torrossa.com/it/catalog/preview/2251219

Brown, P. K., and Brown, P. S. (1958). Visual pigments of the octopus and cuttlefish. *Nature* 182, 1288–1290. doi: 10.1038/1821288a0

Byrne, R. A., Kuba, M., and Griebel, U. (2002). Lateral asymmetry of eye use in octopus vulgaris. *Anim. Behav.* 64, 461–468. doi: 10.1006/anbe.2002.3089

Campbell, F. W., and Robson, J. G. (1968). Application of fourier analysis to the visibility of gratings. *J. Physiol.* 197, 551–566. doi: 10.1113/jphysiol.1968.sp008574

Cartron, L., Darmaillacq, A.-S., Jozet-Alves, C., Shashar, N., and Dickel, L. (2012). Cuttlefish rely on both polarized light and landmarks for orientation. *Anim. Cogn.* 15, 591–596. doi: 10.1007/s10071-012-0487-9

Cartron, L., Dickel, L., Shashar, N., and Darmaillacq, A.-S. (2013a). Maturation of polarization and luminance contrast sensitivities in cuttlefish (*Sepia officinalis*). *J. Exp. Biol.* 216, 2039–2045. doi: 10.1242/jeb.080390

Cartron, L., Josef, N., Lerner, A., McCusker, S. D., Darmaillacq, A.-S., Dickel, L., et al. (2013b). Polarization vision can improve object detection in turbid waters by cuttlefish. *J. Exp. Mar. Biol. Ecol.* 447, 80–85. doi: 10.1016/j.jembe.2013.02.013

Chiou, T.-H., Mäthger, L. M., Hanlon, R. T., and Cronin, T. W. (2007). Spectral and spatial properties of polarized light reflections from the arms of squid (*Loligo pealeii*) and cuttlefish (*Sepia officinalis* L). *J. Exp. Biol.* 210, 3624–3635. doi: 10.1242/jeb.006932

Cornsweet, T. N. (1970). *Visual Perception, 1st Edn*. New York, NY: Academic Press.

Cronin, T. W., Shashar, N., Caldwell, R. L., Marshall, N. J., Cheroske, A. G., and Chiou, T.-H. (2003). Polarization vision and its role in biological signaling. *Integr. Comp. Biol.* 43, 549–558. doi: 10.1093/icb/43.4.549

Douglas, R. H., Williamson, R., and Wagner, H.-J. (2005). The pupillary response of cephalopods. *J. Exp. Biol.* 208(Pt. 2), 261–265. doi: 10.1242/jeb.01395

Forsythe, J. W., and Hanlon, R. T. (1985). Aspects of egg development, post-hatching behavior, growth and reproductive biology of octopus burryi voss, 1950 (*Mollusca: Cephalopoda*). *Vie et Milieu* 35, 273–282.

Foster, J. J., Temple, S. E., How, M. J., Daly, I. M., Sharkey, C. R., Wilby, D., et al. (2018). Polarisation vision: overcoming challenges of working with a property of light we barely see. *Sci. Nat.* 105, 1–27. doi: 10.1007/s00114-018-1551-3

Giurfa, M., and Vorobyev, M. (1997). The detection and recognition of color stimuli by honeybees: performance and mechanisms. *Isr. J. Plant Sci.* 45, 129–140. doi: 10.1080/07929978.1997.10676679

Giurfa, M., Vorobyev, M., Brandt, R., Posner, B., and Menzel, R. (1997). Discrimination of coloured stimuli by honeybees: alternative use of achromatic and chromatic signals. *J. Comp. Physiol. A* 180, 235–243. doi: 10.1007/s003590050044

Glantz, R. M., and Schroeter, J. P. (2006). Polarization contrast and motion detection. *J. Comp. Physiol. A* 192, 905–914. doi: 10.1007/s00359-006-0127-4

Hamasaki, D. I. (1968). The electroretinogram of the intact anesthetized octopus. *Vis. Res.* 8, 247–258. doi: 10.1016/0042-6989(68)90012-6

How, M. J., and Marshall, N. J. (2014). Polarization distance: a framework for modelling object detection by polarization vision systems. *Proc. Royal Soc. B.* 281:20131632. doi: 10.1098/rspb.2013.1632

How, M. J., Pignatelli, V., Temple, S. E., Marshall, N. J., and Hemmi, J. M. (2012). High e-vector acuity in the polarisation vision system of the fiddler crab Uca vomeris. *J. Exp. Biol.* 215, 2128–2134. doi: 10.1242/jeb.068544

Johnsen, S., Marshall, N. J., and Widder, E. A. (2011). Polarization sensitivity as a contrast enhancer in pelagic predators: lessons from *in situ* polarization imaging of transparent zooplankton. *Philos. Trans. R. Soc. Lond. B Biol. Sci.* 366, 655–670. doi: 10.1098/rstb.2010.0193

Krauskopf, J., and Gegenfurtner, K. (1992). Color discrimination and adaptation. *Vis. Res.* 32, 2165–2175. doi: 10.1016/0042-6989(92)90077-v

Labhart, T. (2016). Can invertebrates see the e-vector of polarization as a separate modality of light? *J. Exp. Biol.* 219, 3844–3856. doi: 10.1242/jeb.139899

Laughlin, S. B. (1994). Matching coding, circuits, cells, and molecules to signals: general principles of retinal design in the fly's eye. *Prog. Retin. Eye Res.* 13, 165–196. doi: 10.1016/1350-9462(94)90009-4

Lind, O., and Kelber, A. (2011). The spatial tuning of achromatic and chromatic vision in budgerigars. *J. Vis.* 11:2. doi: 10.1167/11.7.2

Marshall, N. J., and Cronin, T. W. (2011). Polarisation vision. *Curr. Biol.* 21, R101–R105. doi: 10.1016/j.cub.2010.12.012

Mäthger, L. M., Shashar, N., and Hanlon, R. T. (2009). Do cephalopods communicate using polarized light reflections from their skin? *J. Exp. Biol.* 212, 2133–2140. doi: 10.1242/jeb.020800

Maximov, V. V. (2000). Environmental factors which may have led to the appearance of colour vision. *Philos. Trans. R. Soc. Lond. B Biol. Sci.* 355, 1239–1242. doi: 10.1098/rstb.2000.0675

Moody, M. F., and Parriss, J. R. (1960). Discrimination of polarized light by octopus. *Nature* 186, 839–840. doi: 10.1038/186839a0

Moody, M. F., and Parriss, J. R. (1961). The discrimination of polarized light by octopus: a behavioural and morphological study. *Z. Vgl. Physiol.* 44, 268–291. doi: 10.1007/BF00298356

Mullen, K. T. (1985). The contrast sensitivity of human colour vision to red-green and blue-yellow chromatic gratings. *J. Physiol.* 359, 381–400. doi: 10.1113/jphysiol.1985.sp015591

Nahmad-Rohen, L., and Vorobyev, M. (2019). Contrast sensitivity and behavioural evidence for lateral inhibition in octopus. *Biol. Lett.* 15:20190134. doi: 10.1098/rsbl.2019.0134

Nilsson, D.-E., and Warrant, E. J. (1999). Visual discrimination: seeing the third quality of light. *Curr. Biol.* 9, R535–R537. doi: 10.1016/s0960-9822(99)80330-3

Northmore, D. P. M., and Dvorak, C. A. (1979). Contrast sensitivity and acuity of the goldfish. *Vis. Res.* 19, 255–261. doi: 10.1016/0042-6989(79)90171-8

Northmore, D. P. M., and Yager, D. (1975). "Psychophysical methods for investigations of vision in fishes," in *Vision in Fishes*, *1st Edn.*, ed M. A. Ali (New York, NY: Plenum Press), 689–704.

Packard, A., and Sanders, G. D. (1971). Body patterns of octopus vulgaris and maturation of the response to disturbance. *Anim. Behav.* 19, 780–790. doi: 10.1016/S0003-3472(71)80181-1

Pelli, D. G., and Bex, P. (2013). Measuring contrast sensitivity. *Vis. Res.* 90, 10–14. doi: 10.1016/j.visres.2013.04.015

Pignatelli, V., Temple, S. E., Chiou, T.-H., Roberts, N. W., Collin, S. P., and Marshall, N. J. (2011). Behavioural relevance of polarization sensitivity as a target detection mechanism in cephalopods and fishes. *Philos. Trans. R Soc. B Biol. Sci.* 366, 734–741. doi: 10.1098/rstb.2010.0204

Rovamo, J. M., Kankaanpää, M. I., and Kukkonen, H. (1999). Modelling spatial contrast sensitivity functions for chromatic and luminance-modulated gratings. *Vis. Res.* 39, 2387–2398. doi: 10.1016/s0042-6989(98)00273-9

Rubin, J. M., and Richards, W. A. (1982). Color vision and image intensities: when are changes material? *Biol. Cybern.* 45, 215–226. doi: 10.1007/bf00336194

Shashar, N., and Cronin, T. W. (1996). Polarization contrast vision in octopus. *J. Exp. Biol.* 199, 999–1004.

Shashar, N., and Hanlon, R. T. (1998). Polarization vision helps detect transparent prey. *Nature* 393, 222–223. doi: 10.1038/30380

Shashar, N., Johnsen, S., Lerner, A., Sabbah, S., Chiao, C.-C., Mäthger, L. M., et al. (2011). Underwater linear polarization: physical limitations to biological functions. *Philos. Trans. R. Soc. B Biol. Sci.* 366, 649–654. doi: 10.1098/rstb.2010.0190

Shashar, N., Milbury, C. A., and Hanlon, R. T. (2002). Polarization vision in cephalopods: neuroanatomical and behavioral features that illustrate aspects of form and function. *Mar. Freshw. Behav. Physiol.* 35, 57–68. doi: 10.1080/10236240290025617

Siebeck, U. E., Wallis, G. M., Litherland, L., Ganeshina, O., and Vorobyev, M. (2014). Spectral and spatial selectivity of luminance vision in reef fish. *Front. Neural Circuit.* 8:118. doi: 10.3389/fncir.2014.00118

Stewart, F. J., Kinoshita, M., and Arikawa, K. (2017). A novel display system reveals anisotropic polarization perception in the motion vision of the butterfly *Papilio Xuthus. Integr. Comp. Biol.* 57, 1130–1138. doi: 10.1093/icb/icx070

Talbot, C. M., and Marshall, N. J. (2010). Polarization sensitivity in two species of cuttlefish - sepia plangon (gray 1849) and sepia mestus (gray 1849) - demonstrated with polarized optomotor stimuli. *J. Exp. Biol.* 213, 3364–3370. doi: 10.1242/jeb.042937

Temple, S. E., Pignatelli, V., Cook, T., How, M. J., Chiou, T.-H., Roberts, N. W., et al. (2012). High-resolution polarisation vision in a cuttlefish. *Curr. Biol.* 22, R121–R122. doi: 10.1016/j.cub.2012.01.010

Turnbull, P. (2014). *Emmetropisation in the Camera-Type Eye of the Squid*. Auckland: University of Auckland.

van Heukelem, W. F. (1966). *Some Aspects of the Ecology and Ethology of Octopus Cyanea (Gray)*. Honolulu, HI: University of Hawaii.

Vorobyev, M. (2007). "Color in invertebrate vision," in *The senses: A Comprehensive Reference, 1st Edn*, eds R. H. Masland and T. Albright (Oxford: Academic Press), 205–210.

Wandell, B. A. (1995). *Foundations of Vision, 1st Edn*. Sunderland: Sinauer Associates.

Waterman, T. H. (1954). Polarization patterns in submarine illumination. *Science* 120, 927–932. doi: 10.1126/science.120.3127.927

Waterman, T. H. (1981). "Polarization sensitivity," in *Handbook of Sensory Physiology, Vol. VII/6B*, ed H. Autrum (Berlin: Springer), 281–469.

Watson, A. B., and Pelli, D. G. (1983). QUEST: a bayesian adaptive psychometric method. *Percept. Psychol.* 33, 113–120. doi: 10.3758/bf03202828

Wichmann, F. A., and Hill, N. J. (2001). The psychometric function: II. Boostrap-based confidence intervals and sampling. *Percept. Psychol.* 63, 1314–1329. doi: 10.3758/BF03194545

Young, J. Z. (1971). *The Anatomy of the Nervous System of Octopus Vulgaris, 1st Edn.* Oxford: Clarendon Press, 417–442.

Zeil, J. (2000). Depth cues, behavioural context, and natural illumination: some potential limitations of video playback techniques. *Acta Ethol.* 3, 39–48. doi: 10.1007/s102110000021

Conflict of Interest: The authors declare that the research was conducted in the absence of any commercial or financial relationships that could be construed as a potential conflict of interest.

frontiers in Physiology

ORIGINAL RESEARCH
published: 10 June 2020
doi: 10.3389/fphys.2020.00525

Embracing Their Prey at That Dark Hour: Common Cuttlefish *(Sepia officinalis)* Can Hunt in Nighttime Light Conditions

Melanie Brauckhoff[1,2], Magnus Wahlberg[1], Jens Ådne Rekkedal Haga[3], Hans Erik Karlsen[3] and Maria Wilson[1,3,4]*

[1] Department of Biology, University of Southern Denmark, Odense, Denmark, [2] The Fisheries and Maritime Museum, Esbjerg, Denmark, [3] Department of Biosciences, Faculty of Mathematics and Natural Sciences, University of Oslo, Oslo, Norway, [4] NIRAS A/S, Aarhus, Denmark

Cuttlefish are highly efficient predators, which strongly rely on their anterior binocular visual field for hunting and prey capture. Their complex eyes possess adaptations for low light conditions. Recently, it was discovered that they display camouflaging behavior at night, perhaps to avoid detection by predators, or to increase their nighttime hunting success. This raises the question whether cuttlefish are capable of foraging during nighttime. In the present study, prey capture of the common cuttlefish (*Sepia officinalis*) was filmed with a high-speed video camera in different light conditions. Experiments were performed in daylight and with near-infrared light sources in two simulated nightlight conditions, as well as in darkness. The body of the common cuttlefish maintained a velocity of less than 0.1 m/s during prey capture, while the tentacles during the seizing phase reached velocities of up to 2.5 m/s and accelerations reached more than 450 m/s^2 for single individuals. There was no significant difference between the day and nighttime trials, respectively. In complete darkness, the common cuttlefish was unable to catch any prey. Our results show that the common cuttlefish are capable of catching prey during day- and nighttime light conditions. The common cuttlefish employ similar sensory motor systems and prey capturing techniques during both day- and nighttime conditions.

Keywords: cephalopod vision, *Sepia officinalis*, cuttlefish, predatory behavior, low light vision

OPEN ACCESS

Edited by:
Daniel Osorio, University of Sussex, United Kingdom

Reviewed by:
Thomas Cronin, University of Maryland, Baltimore County, United States
Felix Christopher Mark, Alfred Wegener Institute Helmholtz (AWI), Germany

****Correspondence:***
Melanie Brauckhoff
melanie@biology.sdu.dk;
melanie_brauckhoff@outlook.com

Specialty section:
This article was submitted to Invertebrate Physiology, a section of the journal Frontiers in Physiology

Received: *16 November 2019*
Accepted: *29 April 2020*
Published: *10 June 2020*

Citation:
Brauckhoff M, Wahlberg M, Haga JÅR, Karlsen HE and Wilson M (2020) Embracing Their Prey at That Dark Hour: Common Cuttlefish (Sepia officinalis) Can Hunt in Nighttime Light Conditions. Front. Physiol. 11:525. doi: 10.3389/fphys.2020.00525

INTRODUCTION

Prey capture behavior of coleoid cephalopods have been described for several species (Wilson, 1946; Messenger, 1968; Hurley, 1976; Duval et al., 1984; Mendes et al., 2006). These studies suggest that decapodiform cephalopods employ similar visual hunting techniques, using either their eight arms, and/or their two fast-extendable tentacles to seize the prey.

In the common cuttlefish (*Sepia officinalis*) hunting can normally be divided into three distinct phases (Messenger, 1968): attention, positioning, and striking. The attention phase occurs when the common cuttlefish first becomes aware of a prey item. The eyes then fixate on the prey, and the body slowly turn such that arms and head are oriented toward the prey. During the positioning phase,

it slowly moves closer to the prey until the predator-prey distance is approximately one mantle length (see Hanlon and Messenger, 2018). During this phase, the tentacles slowly extrude toward the prey. The movement of the tentacles remains under full motor control, and the orientation of the tentacles adjust to prey movements. The positive feedback from visual input and motor control is continuous during this "aiming" phase until the common cuttlefish enters the seizure phase. This phase is defined by the abrupt action when the tentacles shoot out with extreme speed in an *all-or-none* fashion (Messenger, 1968; Duval et al., 1984). Once the seizure phase has been initiated, the common cuttlefish loses any motor-control of the tentacles, and has no further ability to re-adjust their aim or speed (Messenger, 1968; Duval et al., 1984).

This rather "stereotypic" three-phase hunting strategy has been observed in all species of squid and cuttlefish where prey capture behavior has been studied (Messenger, 1968; Hurley, 1976; Duval et al., 1984; Mather and Scheel, 2014; Sykes et al., 2014). However, details of the hunting strategy may vary depending on prey type and agility (Duval et al., 1984). Fast-moving prey (e.g., shrimps or fish) are typically captured by a rapid final extrusion of the flexible tentacles. Slow-moving prey (like crabs) on the other hand, is largely caught by a final "jumping" method, where the cuttlefish seize the prey using their 8 arms (Duval et al., 1984; Villanueva et al., 2017). Zoratto et al. (2018) have in addition shown that intraspecific variations in hunting behaviors can be linked to "personality" differences between individual cuttlefish.

Decapodiform cephalopods in general have well developed eyes (Muntz, 1977; Hanlon and Messenger, 2018), and they are highly dependent on their vision during hunting (Young, 1963; Messenger, 1968; Hurley, 1976; Talbot and Marshall, 2011; York et al., 2016; Hanlon and Messenger, 2018). Interference with their visual system reduces hunting accuracy and success rate (Messenger, 1968; Chichery and Chichery, 1987). Since most cephalopods have just one visual pigment and thus one class of photoreceptors, they are considered to lack color vision (Hanlon and Messenger, 2018). However, they are highly sensitive to polarized light, and may use such cues during hunting (Messenger, 1981, 1991; Shashar et al., 2000; Pignatelli et al., 2011). The common cuttlefish have large and highly developed camera-type eyes which are capable of adapting to varying light levels. Common cuttlefish can rapidly adjust their pupil size in the range 100–3% of the maximal area (Douglas et al., 2005). Additional light/dark adaptation mechanisms documented in octopods, but so far, not specifically described in cuttlefish, include screening pigment migration, photoreceptor size modulation, and specialized foveas (see Hanke and Kelber, 2020).

The common cuttlefish lives from subtidal waters down to about 200 m, but are most abundant in the upper 100 m of the water column (Reid et al., 2005). Light conditions consequently vary a lot, ranging from high intensities near the surface on a sunny summer day (equivalent to terrestrial type conditions), to very dim light at deeper waters on a cloudy winter night. Natural illuminance at nighttime ranges from 0.0001 lux on a moonless overcast (starlight) night sky to around 0.002 lux on a moonless clear night sky with airglow (Schlyter, 2017), while a full moon on a clear night ranges from 0.05 to 0.3 lux (Kyba et al., 2017). These light intensities gradually diminish by depth in the ocean. In clear oceanic water, light drops by a factor of about 2.2% per meter (Curcio and Petty, 1951). Observations from the Atlantic Ocean have found light depletion of 3–7% per meter (Clarke and Wertheim, 1953), and in coastal waters with suspended particles such as: plankton, runoff from rivers and other impurities, and the light reduction can be even higher.

The common cuttlefish are known to be active during both day and night (Watanuki et al., 2000), and some of their physiological processes undergo circadian cycles in a way suggesting that physical activity may actually increase at night (Jaeckel et al., 2007). A study of the closely related giant Australian cuttlefish (*Sepia apama*) at their spawning grounds found that they ceased sexual signaling and reproductive behavior at dusk, and settled to the bottom to camouflage themselves against the background (Hanlon et al., 2007). Furthermore, similar observations of the common cuttlefish in the laboratory revealed that they do not only camouflage themselves at dusk, but also adapt their camouflage patterns to their surroundings at night (Allen et al., 2010). It has been proposed that common cuttlefish use this behavior to avoid predators with excellent night vision, and/or to increase their own hunting success at night (Allen et al., 2010). The fact that common cuttlefish can camouflage themselves successfully during night may reflect highly developed nighttime visual abilities (Warrant, 2007; Allen et al., 2010). However, to our knowledge, the kinematics of the rapid tentacular hunting technique of decapod cephalopods have only been described in daylight conditions. Therefore, it is currently unclear whether common cuttlefish readily hunt during nighttime conditions, and if so, whether they use the typical three-phase hunting strategy.

The tentacle seizure phase of squid and cuttlefish predatory behavior is too fast to be studied in any detail by the naked eye. Kier and Leeuwen (1997) therefore employed a high-speed film camera in order to describe the kinematics of this phase in *Loligo pealei*, and documented tentacle seizures reaching accelerations as high as 250 m/s^2. Additional studies confirmed the tentacle striking to be quite stereotypic (Kier and Leeuwen, 1997). The high-speed frame-capture methodology introduced by Kier and Leeuwen is invaluable for fine-detail insights into the fast tentacle strikes in cephalopods.

Accordingly, in the present study, we used high-speed video recordings to evaluate the prey capturing techniques in individuals of common cuttlefish at different light levels. The examined light levels were day- and two nighttime conditions, as well as complete darkness. The purpose was to elucidate whether high versus low light conditions influenced the hunting technique and tentacle fast-seizure characteristics of common cuttlefish.

MATERIALS AND METHODS

Experimental Animals

Five juvenile common cuttlefish with mantle lengths of 78 ± 7.6 mm (standard deviation) were used in the experiment. They were provided by Øresund Aquarium, University of

Copenhagen, and kept in 70 l holding glass aquariums with a closed seawater system (salinity 33–35‰ and temperature 18–20°C). The common cuttlefish were fed mysids (*Praunus flexuosus*) and shrimps (*Crangon crangon, Palaemon adspersus,* and *P. elegans*) two times daily.

Experimental Setup and Protocol

The experiment was carried out at Drøbak Marine Biological Station, University of Oslo, Norway. Common cuttlefish were tested in a transparent plexiglas aquarium (dimensions: 20 × 40 cm) with a water depth of 10 cm. Prey capture attempts were recorded under four light conditions, which we broadly refer to as daylight, moonlight, starlight night, and darkness below. We measured these light conditions in three ways. We used an Ocean Optics QE65000 spectrometer to describe the spectral distribution of the light sources, a Thorlabs PM100A Power meter to measure the gross flux of light over all wavelengths combined of the light sources and an Extech EA30 to make readings in lux. Lux is a standard measurement for light as perceived by the human eye. The spectral sensitivity of the human eye and eye of the common cuttlefish predominantly overlap, but common cuttlefish have a somewhat higher sensitivity for shorter wavelengths compared to human photopic vision, more similar to human scotopic spectral sensitivity. Conversions from irradiance to illuminance are only possible if the spectral distribution of the cuttlefish eye is compensated for. For the purposes in this study, spectral distributions of the light sources are biased toward longer wavelengths within the cuttlefish visual spectrum. We therefore argue that this bias will not produce any false positive results, since the vision of common cuttlefish peaks at shorter wavelengths and therefore will receive less light than actually reported in the different test conditions here. Experiments in daylight were conducted during the daytime, while testing in the other three light regimes were performed during the night to not disrupt the diel cycle of the test animals.

The test aquarium was shielded by a non-translucent box with a removable top. For daylight experiments, the top of the box was open, while it was closed during the three other light regimes. Three near-infrared lamps (model 995JH) provided sufficient light inside the box for high speed filming. Two of the IR-lamps were placed at one side of the aquarium and one at the opposite side.

The daylight experiments were conducted with natural light entering the experimental room through several large windows and with fluorescent ceiling lights (3000 K) turned on. Light intensities at the site of the experimental animal, i.e., inside the test aquarium and shielding box, and were approximately 200 lux. Even though natural sunlight was the main light source in the daylight experiments, the shielding box provided a distinctive reduction of the intensity, thus causing the relatively low daylight intensity of 200 lux. The lower light level, obtained by the shielding box, was deliberately chosen in order to reduce the stress of the animals and reduce the risk of affecting their eyes in ways that could potentially reduce their capacity to hunt in dimmer light conditions later.

Moonlight experiments were conducted with the laboratory ceiling lights off and with the experimental room shielded from ambient light. The three IR-lamps did not produce an even distribution of light in the test aquarium. The highest value, 0.3 lux, was obtained when the light sensor was directly facing the center of the IR-lamp at the typical "mysid –IR-lamp" distance of 35 cm during experiments. At other positions, the illuminance was around the Extech EA30 detection limit of 0.01 lux. We also measured the IR-lamps using the Thorlabs PM100A Power meter and the Ocean Optics QE65000 spectrometer. The light intensity peaked at 850 nm, in the infrared part of the spectrum, thus not detectable for humans and common cuttlefish. Low intensities, from approximately 0.5–1% of the entire energy spectrum, was found to be from 700–765 nm, which are partly within the cuttlefish visible spectrum (**Figure 1**). The three IR-lamps provided an irradiance of 3 W/m^2, or less than 0.003 lux at the spectral range of the common cuttlefish. This corresponds to moonlight intensities in the cuttlefish visual spectrum from 380–740 nm.

Starlight experiments were performed similarly to the experiments in moonlight but adding a custom-made filter to the IR-lamps. The filters reduced the visual light to the extent that it was not possible to measure directly at relevant experimental distances (35 cm). Measurements very close to the IR-lamp revealed that the filter reduced the visual light by more than three orders of magnitude to an estimated 10^{-6} lux during the experiments at relevant distances.

For the experiments in darkness, the experimental set up was identical to the experiments in starlight with the only exception that the LED lamps were turned off and the only source of illumination was a near-IR laser (Olng 300 L). This laser was equipped with a custom-made filter to spread the laser beam. The laser has a very narrow spectral band (peak 810 nm) and very little stray light compared to the LED lamps. As common cuttlefish are not known to detect IR light, this experiment was performed in complete darkness from the common cuttlefish' point of view.

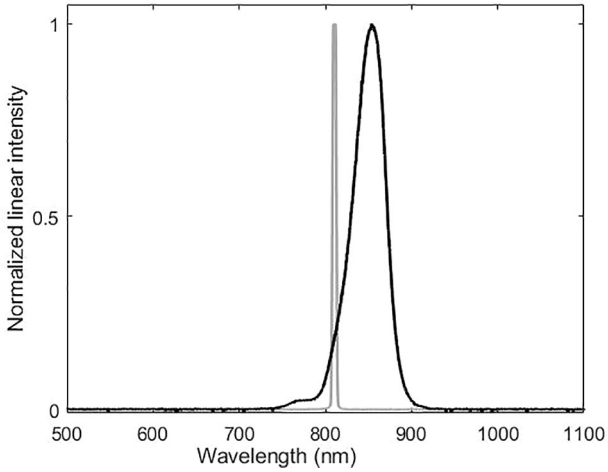

FIGURE 1 | Spectral analysis of the near-infrared lamps used in the trials. Gray line is laser and black line LED. Peak intensity of the LED lamp is at around 850 nm. Approximately 1% of the intensity is between 700–765 nm.

The video camera was placed one meter above the aquarium providing a two-dimensional top view of the prey-capture sequence. Video recordings were performed using an IR-sensitive Mikrotron EoSens MC1362 camera and Inspecta-5 PCI-X frame grabber card. For day- and moonlight experiments we used 1,000 frames per second (fps), and for starlight and darkness 25 fps due to the limited available light. The lower frame rate during experiments in starlight and darkness did not allow for detailed, kinematic analyses. Monitoring of the test animal during experiments was done on a monitor connected to the high-speed camera.

Prey items (mysids, approximately 20 mm in length) were introduced into the aquarium through a small gate in the box. Prey were introduced with at least 15 min between each session. Test continued until the cuttlefish showed no more interest in the prey. Animals were used in only one trial sequence, and were kept in the experimental setup for a maximum of 24 h. The three different light settings were chosen in a random order in consecutive trials.

A total of 33 day-, 40 moon-, and 12 starlight prey capture events were recorded. In addition, 2 darkness trials were conducted. For the present study, 8 prey-capture sequences from daylight (with three different cuttlefish, $n = 3$), and 11 from moonlight experiments (with four different cuttlefish, $n = 4$) were selected for analysis using the following criteria: (1) Neither cuttlefish nor mysid were in touch with the side walls of the test tank; (2) Cuttlefish and mysid were at the same depth (near the bottom), assessed from visual inspection of the eye position of the cuttlefish; and (3) Cuttlefish tentacles were clearly visible during the entire prey capture sequence.

In addition, control trials were conducted to ensure that the cuttlefish did not rely on other sensory abilities than eyesight while hunting for prey under low light conditions. A live mysid was placed in a glass jar and sealed with a lid before it was placed in the test aquarium. In control trials, the cuttlefish was able to see the mysid, but all olfactory and mechanical/vibrational cues were eliminated. These controls were conducted during day- ($n = 1$) and moonlight ($n = 1$) conditions.

Video Analysis

Video sequences were tracked in ImageJ (1.47) using the MTrackJ plugin (Meijering et al., 2012). Movements of the cuttlefish body, arms, and tentacles and the movement of the mysid were tracked on each video sequence in steps of 4 ms. During tentacle striking, tracking time steps were reduced to 1 ms in order to capture the very rapid tentacle movements during this phase. Tracking started 100 ms prior to the strike, and continued until 12 ms after the tentacles had made contact with the mysid.

The ImageJ tracking program provided raw numerical data for kinematic analysis. The distance between two tracking points was given by a basic distance formula. From the distances between tracking points, the velocity was calculated and smoothed over 5 consecutive measurements. Acceleration was calculated from the smoothed velocity data.

Statistical analysis was performed using GraphPad Prism version 8.0.2. Data from daylight and moonlight conditions were compared using a nested *t*-test, with the measurements from trials made with the same individual cuttlefish nested under each specimen.

RESULTS

Prey Capturing Phases

Every selected hunting sequence in day-, moon-, and starlight conditions roughly followed the same pattern in the way the cuttlefish changed its attention, positioning and finally seized the moving prey (**Figures 2**, **3**).

The day- and moonlight trials showed no significant difference in all three phases of predatory behavior. During the attention phase (**Figure 2A**) the cuttlefish detected and fixated on the prey while the body moved to a position where the tip of the 10 arms faced the prey. During the positioning phase (**Figure 2B**), the cuttlefish slowly approached the prey while slowly extruding the tentacles with an average velocity of 0.13 m/s (SD $\pm$ 0.05, 19 video sequences from four cuttlefish; $n = 4$). The tentacles were kept closely together during the initial phase of the fast extension but opened in front to expose the suckers in the final phase when the tentacles made contact with the prey (**Figure 2C**). The outermost part of the tentacle tip stayed together (as visibly in **Figure 2C** frame 1). The split between the tentacles extended backwards toward the animal and was total when retraction of the prey began (**Figure 2C**).

During the experiments in starlight, the cuttlefish still readily performed typical three stage hunting and prey capture behaviors as illustrated in **Figures 3A–C**. Even though conditions of observations were significantly worse in these trials (due to the low light conditions and low frame rate), it was clear that fast tentacle seizure behavior involved an attention phase (**Figure 3A**) with the cuttlefish orienting toward the prey. Notably, all mysids were in their normal head up and tail down orientation, and thereby still in a visual behavior mode (see darkness section below). The attention phase in the cuttlefish was followed by a positioning phase (**Figure 3B**) and a tentacle seizure phase (**Figure 3C**). Overall, tentacle seizures in the starlight trials appeared very close to the day- and moonlight tentacle seizures, but reliable seizure velocity and acceleration values were not possible to obtain due the low frame rate.

In the darkness experiments, cuttlefish responded to the very low light levels with a complete inhibition of prey searching behavior and prey capture. Instead, they started to express a state of "panic-like" confusion by swimming uncontrolled around the aquarium. In addition, during these trials the mysid showed a clear change in their behavior by changing from the upright body position to a near horizontal body orientation and active swimming around the test tank. This was a behavior never seen in the day-, moon- and starlight trials. Thus, both the cuttlefish and the mysid shrimp showed distinctly changed behaviors when deprived of all visual light in the laboratory.

Experimental Control Trials

Control trials contained a living mysid in a sealed glass jar. Both in day- and moonlight conditions, the cuttlefish were attacking

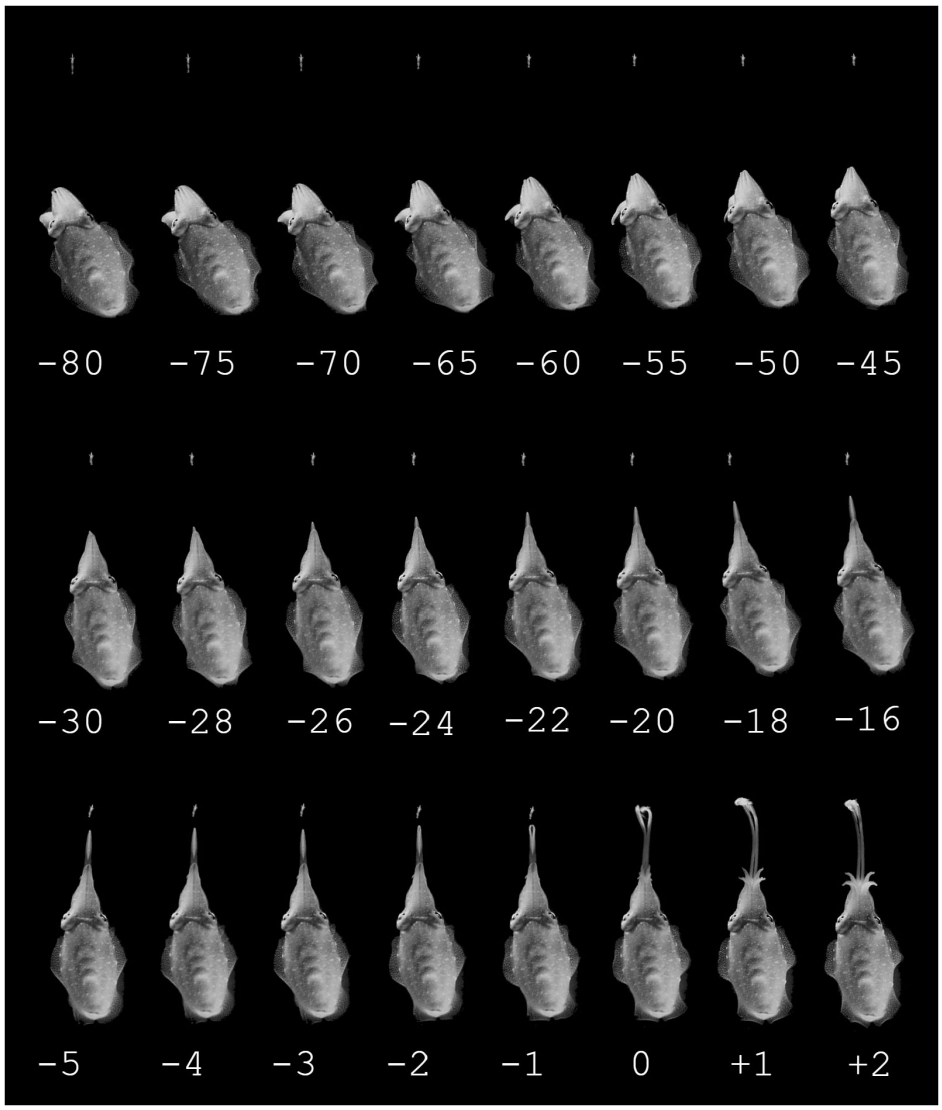

FIGURE 2 | Example of a prey capture sequence of a cuttlefish hunting during moonlight conditions, the time in ms is stated below the pictures. Top row: Attention phase, starting by the cuttlefish detecting the prey and ending by having aligned the body axis in the direction of the prey. There are intervals of 5 ms between the pictures. Middle row: Positioning phase, starting with the cuttlefish slowly moving to the preferred distance to the prey, slowly ejecting the tentacles. There are intervals of 2 ms between the pictures. Bottom row: Seizure phase. The tentacles are ejected very rapidly in an all or nothing fashion. There is 1 ms between every picture.

the mysid in a similar way as when the mysid was swimming freely (**Figure 4**).

Kinematics of Capturing Sequences

The detailed movements of cuttlefish and prey were very similar in day- and moonlight trials (**Figure 5**). **Figure 5A** shows the distance between the tip of the cuttlefish tentacle and the body of the prey during the positioning and seizure phases. The timing of the sequences is synchronized so that the instant when the tentacles touch the mysid is 0. The tentacular seizure occurred after an average of 88.0 ± 0.5 ms (8 video sequences from three cuttlefish, $n = 3$) in daylight, and 90 ± 1.6 ms (11 video sequences from four cuttlefish, $n = 4$) in moonlight trials. The distance between the tip of the tentacles and the prey (seizure distance) was 22.96 ± 3.3 mm (8 video sequences, $n = 3$) for seizures in daylight and 17.87 ± 4.0 mm (11 video sequences, $n = 4$) in moonlight. There was no significant difference between the mean time or distance upon tentacle seizure (nested t-test, P value = 0.08, df = 5, $t = 1.8$ and $p = 0.13$).

Before the tentacle made contact with the mysid, the velocity of the prey remained constant at 0.04 ± 0.01 m/s in both day- and moonlight trials. After contact, the mysid velocity increased rapidly to 0.9 ± 0.4 m/s (**Figure 5B**). Throughout the entire capturing sequence, the velocity of the cuttlefish body was approximately 0.13 ± 0.04 m/s (19 video sequences, $n = 4$) for both day-, and moonlight trials (**Figure 5C**).

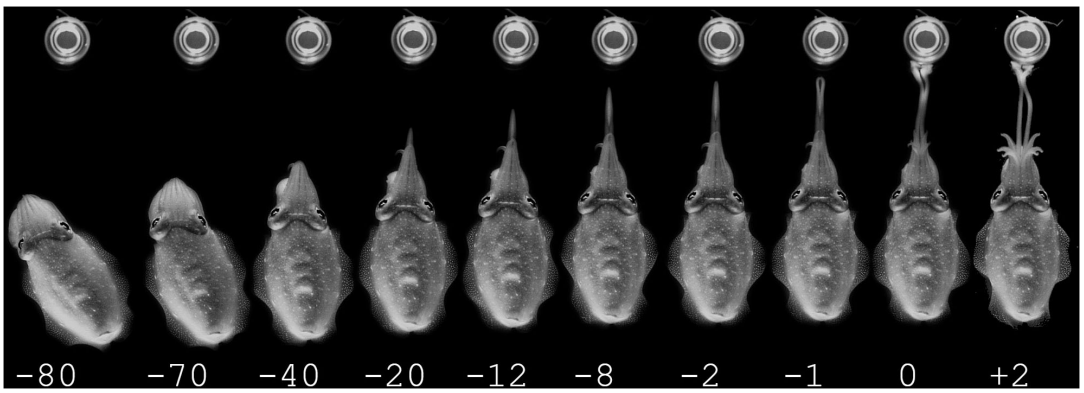

FIGURE 3 | Prey capture experiments of cuttlefish with prey enclosed in a jar in moonlight conditions. The cuttlefish displays the same stereotypic behavior as when hunting free-swimming animals. The time in ms is stated below the pictures.

When tentacle seizures were initiated, tentacle velocities and accelerations increased rapidly. The maximum velocity was 2.34 ± 0.27 m/s (8 video sequences, n = 3) in daylight and 2.03 ± 0.11 m/s (11 video sequences, n = 4) in moonlight (**Figure 5C**). The mean velocities were significantly different (Nested t-test, P value = 0.07, df = 5 and t = 2.3). The corresponding mean maximum accelerations were 418.3 ± 33 m/s^2 (8 video sequences, n = 3) in daylight and 366.3 ± 18.5 m/s^2 (11 video sequences, n = 4) in moonlight. The mean accelerations were significantly different (Nested t-test, P value = 0.03, df = 5 and t = 3.0).

DISCUSSION

The experiments showed that common cuttlefish prey capture behavior are not restricted by low light levels. The common cuttlefish successfully captured mysids during the three different simulated light levels; daylight, moonlight and starlight (**Figures 2**, **3**, and **5**), with very little difference in the common cuttlefish prey capture behavior between daylight and moonlight. The unchanged behavior during the starlight trial (**Figure 4**), combined with no successful prey captures and drastically changed behavior during the trials in complete darkness, indicate the importance of visual cues during predatory behavior.

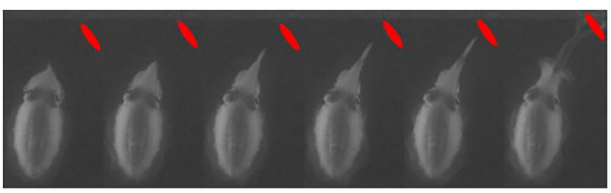

FIGURE 4 | Cuttlefish catching an alive and free-swimming mysid during starlight conditions. The quality of the video is significantly reduced due to the very low light intensities. The location of the mysid is marked with a red dot. The cuttlefish displayed the same stereotypic hunting behavior as it did in day- and moonlight conditions.

Besides vision, cephalopods have very complex sensory systems, e.g., the sense of touch (Kier and Leeuwen, 1997; Hanlon and Shashar, 2003), and an olfactory organ (Polese et al., 2016). Earlier experiments indicate that common cuttlefish rely on mainly visual cues when hunting, since physically blinding cuttlefish resulted in a significant drop of attack rates (Messenger, 1968). It is unclear, however, to what extent Messenger's (1968) results were confounded by behavioral changes in the blinded common cuttlefish, due to the rather brute-force method used. Still, our darkness experiments corroborates Messenger's (1968) conclusions: When the common cuttlefish was deprived of any visual cues, they were not able to forage even though all other sensory cues were available.

During the daylight tests, common cuttlefish readily attacked the mysid shrimp employing the typical three-phase hunting strategy previously described in all other studied species of cuttlefish and many other species of decapodiform cephalopods (**Figure 2**; for an extensive review see Hanlon and Messenger, 2018). The maximum tentacle strike accelerations were similar, albeit sometimes higher, than the ones measured in *L. pealei* (see Kier and Leeuwen, 1997). The higher tentacle acceleration in common cuttlefish may indicate that this species is capable of catching faster moving prey than *L. pealei*, but this hypothesis needs to be validated in further experimentation. The tentacle velocity and acceleration were significant higher during day- than moonlight trials (**Figure 5**). Thus, even though the common cuttlefish performed similar hunting behaviors, there were some differences in the prey capturing techniques for our simulated day- and nighttime light levels.

Our results indicate that common cuttlefish might be able to navigate and forage at nighttime and in low-light environments. This strongly supports the notion that cuttlefish may perform advanced behaviors, including foraging and actively camouflaging themselves during nighttime (Watanuki et al., 2000). When all light cues were eliminated, the behavior of the common cuttlefish changed drastically, and did not seem to be able to catch any prey. We believe that a sensation of complete darkness in combination with a rather "sterile" aquarium, with no

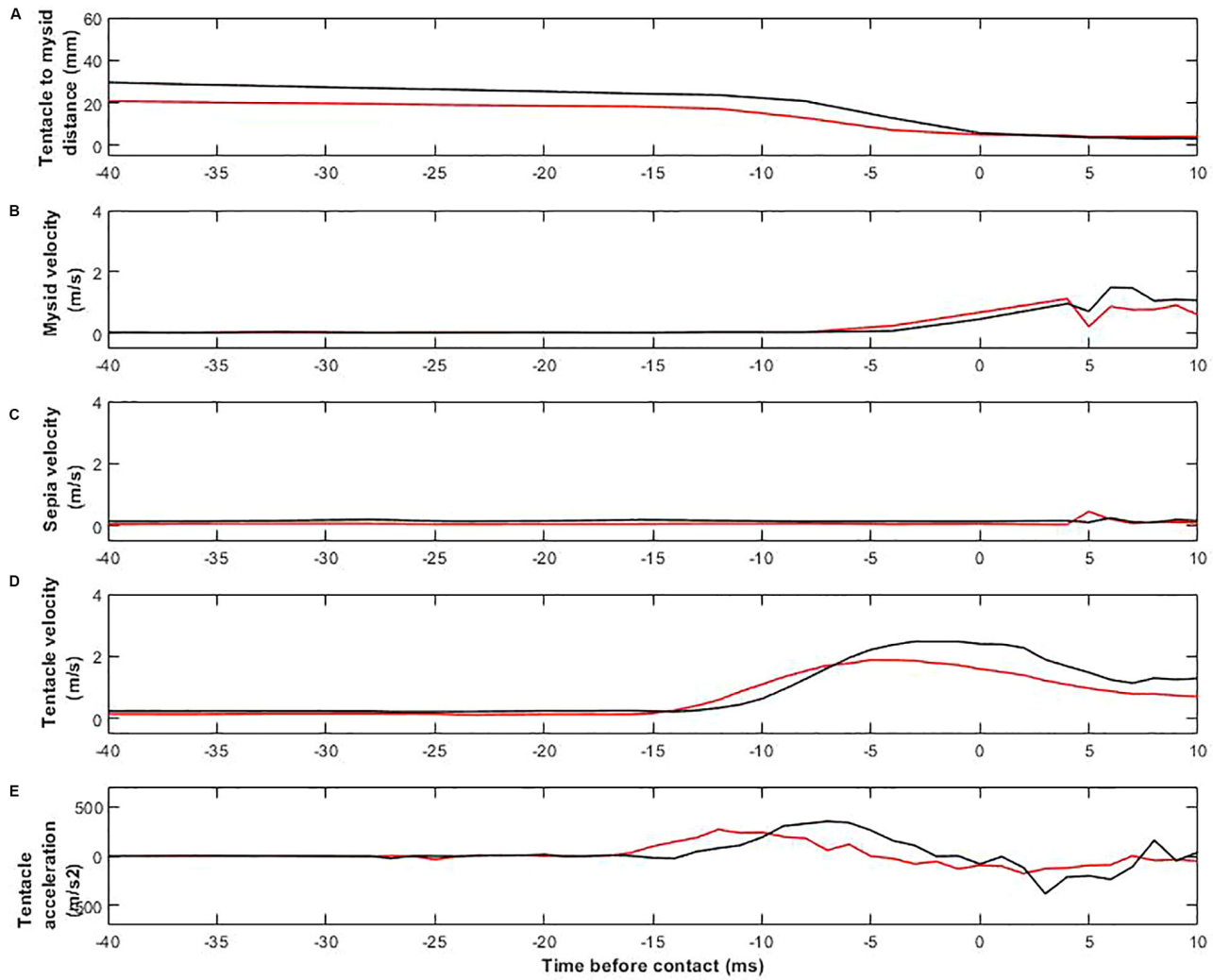

FIGURE 5 | Plots of kinematics of prey capture strikes. Black lines represent daylight, red moonlight conditions. Time, $t = 0$, is defined as the video frame where the tentacle reaches the prey. **(A)** Distance between the tip of the cuttlefish's tentacles and the prey's head. **(B)** Velocity of the prey. **(C)** Velocity of the cuttlefish body. **(D)** Velocity of the tip of the tentacle. **(E)** Acceleration of the tip of the tentacle.

hiding places, might have been discomforting to the test animals, and that this was the cause of their altered behavior.

The behavior of the prey was similar in all trials, regardless of lighting. This implies that the movement of the prey did not affect the common cuttlefish approach during different light conditions. The body of the cuttlefish did not seem to alter its velocity throughout the entire attack sequence (**Figure 5B**). This might also indicate the stereotypic nature of the common cuttlefish's hunting strategy. While the tentacles were slowly extruded toward the mysid, the rest of the cuttlefish body stayed motionless. The reason why this strategy is so efficient may be due to the prey keeping its attention on the cuttlefish body, missing the fact that the almost see-through tentacles are slowly approaching the prey.

The high catching performance of common cuttlefish in the low-light levels tested here strongly indicates that common cuttlefish can forage during very limited light conditions. The most important sensory stimulus used during foraging behavior are visual cues, even during very limited light conditions. Common cuttlefish may therefore be more active at night than what has previously been assumed. This may also explain why common cuttlefish actively adjust their camouflage during nighttime (Watanuki et al., 2000). We encourage studies in the wild, without the use of artificial light sources in the visible spectrum, to verify that even at that Dark Hour, tiny marine creatures might be both embracing death and being embraced – by our heroes: the true knights in the dwindling lights of the ocean nights (Shakespeare, 1626).

DATA AVAILABILITY STATEMENT

The datasets generated for this study are available on request to the corresponding author.

ETHICS STATEMENT

All studies were conducted in accordance with the Norwegian Animal Welfare Act of 2018, the Regulation of Animal Experimentation of 2017 and approved as field studies at the Marine Biological Station Drøbak by the University of Oslo, Animal Welfare Unit (ref. 155 UiO – Department of Biosciences). All animals used in this study were treated according to the guidelines provided by the European Directive in Directive 86/609/EEC and Directive 2010/63/EU.

AUTHOR CONTRIBUTIONS

Experimental trials were conducted by MWi, JH, and HK. Data were analyzed by MB. Figures were made by MB and MWa. All authors contributed to the editoral work of this manuscript.

FUNDING

This work was funded by grants from the Danish Council for Independent Research, Natural Sciences and the Carlsberg Foundation (Carlsbergfondet: CF14-0444), both to MWi, and Finn Jørgen Walvigs Foundation.

ACKNOWLEDGMENTS

We thank Kristian Vedel and Michael Hansen at the Øresund Aquarium, Denmark for providing *S. officinalis* and guidance on cuttlefish husbandry, and Espen Grønlie at the University of Oslo for fruitful discussions. We thank the technical staff at the Marine Biological Station Drøbak and René Lynge Eriksen, University of Southern Denmark, for the help with measuring and calibrating the light sources. We thank Adam Smith, postdoctoral researcher at the Marine Biological Research Centre, University of Southern Denmark for proofreading this manuscript.

REFERENCES

Allen, J. J., Mäthger, L. M., Buresch, K. C., Fetchko, T., Gardner, M., and Hanlon, R. T. (2010). Night vision by cuttlefish enables changeable camouflage. *J. Exp. Biol.* 213, 3953–3960. doi: 10.1242/jeb.044750

Chichery, M. P., and Chichery, R. (1987). The anterior basal lobe and control of prey-capture in the cuttlefish (*Sepia officinalis*). *Physiol. Behav.* 40, 329–336. doi: 10.1016/0031-9384(87)90055-2

Clarke, G. L., and Wertheim, G. K. (1953). Measurements of illumination at great depths and at night in the Atlantic Ocean by means of a new bathyphotometer 3. *Deep Sea Res.* 8, 189–205. doi: 10.1016/0146-6313(56)90003-X

Curcio, J. A., and Petty, C. C. (1951). Optical absorption of water. *J. Opt. Soc. Am.* 41, 302–304.

Douglas, R. H., Williamson, R., and Wagner, H.-J. (2005). The pupillary response of cephalopods. *J. Exp. Biol.* 208, 261–265. doi: 10.1242/jeb.01395

Duval, P., Chichery, M., and Chichery, R. (1984). Prey capture by the cuttlefish (*Sepia officinalis* L): an experimental study of two strategies. *Behav. Process.* 9, 13–21. doi: 10.1016/0376-6357(84)90004-4

Hanke, F. D., and Kelber, A. (2020). The eye of the common *Octopus* (*Octopus vulgaris*). *Front. Physiol.* 10:1637. doi: 10.3389/fphys.2019.01637

Hanlon, R., and Messenger, J. (2018). *Cephalopod Behaviour*. Cambridge, MA: Cambridge University Press.

Hanlon, R., and Shashar, N. (2003). "Aspects of the sensory ecology of cephalopods," in *Sensory Processing in Aquatic Environments*, eds S. P. Collin, and N. J. Marshall (New York, NY: Springer), 226–282.

Hanlon, R. T., Naud, M.-J., Forsythe, J. W., Hall, K., Watson, A. C., and McKechnie, J. (2007). Adaptable night camouflage by cuttlefish. *Am. Nat.* 169, 543–551. doi: 10.1086/512106

Hurley, A. (1976). Feeding behavior, food consumption, growth, and respiration of the squid Loligo opalescens raised in the laboratory. *Fish. Bull. Natl. Ocean. Atmos. Admin.* 74, 176–182.

Jaeckel, G., Mark, F., Gutowska, M., Oellermann, M., Ellington, C., and Pörtner, H. (2007). Analysis of diurnal activity patterns and related changes in metabolism in the cephalopod *Sepia officinalis*. *Comp. Biochem. Physiol.* 146A:S83. doi: 10.1016/j.cbpa.2007.01.109

Kier, W., and Leeuwen, J. (1997). A kinematic analysis of tentacle extension in the squid *Loligo pealei*. *J. Exp. Biol.* 200:41.

Kyba, C. C. M., Mohar, A., and Posch, T. (2017). How bright is moonlight? *Astron. Geophys.* 58, 131–132. doi: 10.1093/astrogeo/atx025

Mather, J., and Scheel, D. (2014). "Behavior," in *Cephalopod Culture*, eds J. Iglesias, L. Fuentes, and R. Villanueva (Dordrecht: Springer), 17–39.

Meijering, E., Dzyubachyk, O., and Smal, I. (2012). Methods for cell and particle tracking. *Methods Enzymol.* 504, 183–200. doi: 10.1016/B978-0-12-391857-4.00009-4

Mendes, A. D., Cristo, M., Senão, J., and Borges, T. (2006). Diet of the cuttlefish *Sepia officinalis* (Cephalopoda: Sepiidae) off the south coast of Portugal (eastern Algarve). *J. Mar. Biol. Assoc. U.K.* 86, 429–436. doi: 10.1017/S0025315406013312

Messenger, J. B. (1968). The visual attack of the cuttlefish, *Sepia officinalis*. *Anim. Behav.* 16, 342–357. doi: 10.1016/0003-3472(68)90020-1

Messenger, J. B. (1981). "Comparative physiology of vision in molluscs," in *Handbook of Sensory Physiology, Vol. VII/6C, Comparative Physiology and Evolution of Vision in Invertebrates*, ed. H. Autrum (Berling: Springer-Verlag), 3–200.

Messenger, J. B. (1991). "Photoreception and vision in Molluscs," in *Evolution of the Eye and the Visual System*, eds J. R. Cronly-Dillon, and R. L. Gregory (London: Macmillan), 364–397.

Muntz, W. R. A. (1977). "Pupillary responses of cephalopods," in *Symposium on the Biology of Cephalopods*, eds M. Nixon, and J. B. Messenger (London: Symposia of the Zoological Society), 277–285.

Pignatelli, V., Temple, S. E., Chiou, T. H., Roberts, N. W., Collin, S. P., and Marshall, N. J. (2011). Behavioral relevance of polarization sensitivity as a target detection mechanism in cephalopods and fishes. *Philos. Trans. R. Soc. Lond. B Biol. Sci.* 366, 734–741. doi: 10.1098/rstb.2010.0204

Polese, G., Bertapelle, C., and Cosmo, A. D. (2016). Olfactory organ of *Octopus vulgaris*: morphology, plasticity, turnover and sensory characterization. *Biol. Open* 5, 611–619. doi: 10.1242/bio.017764

Reid, A., Jereb, P., and Roper, C. F. E. (2005). "Family Sepiidae," in *Cephalopods of the World. An Annotated and Illustrated Catalogue of Species known to Date. Volume 1. Chambered Nautiluses and Sepioids (Nautilidae, Sepiidae, Sepiolidae, Sepiadariidae, Idiosepiidae and Spirulidae)*, eds P. Jereb, and C. F. E. Roper (Rome: FAO), 57–152.

Schlyter, P. (2017). *Radiometry and Photometry in Astronomy*. Available at: https://stjarnhimlen.se/comp/radfaq.html#10 (accessed March 16, 2020).

Shakespeare, W. (1626). *Macbeth. Braunmuller, A.R. (Ed.) 1997*. Cambridge, MA: Cambridge University Press.

Shashar, N., Hagan, R., Boal, J. G., and Hanlon, R. T. (2000). Cuttlefish use polarization sensitivity in predation on silvery fish. *Vis. Res.* 40, 71–75. doi: 10.1016/s0042-6989(99)00158-3

Sykes, A. V., Domingues, P., and Andrade, J. P. (2014). "*Sepia officinalis*," in *Cephalopod Culture*, eds J. Iglesias, L. Fuentes, and R. Villanueva (Dordrecht: Springer), 175–204.

Talbot, C. M., and Marshall, J. N. (2011). The retinal topography of three species of coleoid cephalopod: significance for perception of polarized light. *Philos. Trans. Biol. Sci.* 366, 724–733. doi: 10.1098/rstb.2010.0254

Villanueva, R., Perricone, V., and Fiorito, G. (2017). Cephalopods as predators: a short journey among behavioral flexibilities, adaptions, and feeding habits. *Front. Physiol.* 8:598. doi: 10.3389/fphys.2017.00598

Warrant, E. J. (2007). Visual ecology: hiding in the dark. *Curr. Biol.* 17, R209–R211. doi: 10.1016/j.cub.2007.01.043

Watanuki, N., Kawamura, G., Kaneuchi, S., and Iwashita, T. (2000). Role of vision in behavior, visual field, and visual aucuity of cuttlefish *Sepia esculenta*. *Fish. Sci.* 66, 417–423. doi: 10.1046/j.1444-2906.2000.00068.x

Wilson, D. P. (1946). A note on the capture of prey by *Sepia officinalis* L. *J. Mar. Biol. Assoc. U.K.* 26, 421–425. doi: 10.1017/S0025315400012248

York, C. A., Bartol, I. K., and Krueger, P. S. (2016). Multiple sensory modalities used by squid in successful predator evasion throughout ontogeny. *J. Exp. Biol.* 219:2870. doi: 10.1242/jeb.140780

Young, J. Z. (1963). Light-and dark-adaptation in the eyes of some cephalopods. *Proc. Zool. Soc. Lond.* 140, 255–270. doi: 10.1111/j.1469-7998.1963.tb01863.x

Zoratto, F., Cordeschi, G., Grignani, G., Bonanni, R., Alleva, E., Nascetti, G., et al. (2018). Variability in the "stereotyped" prey capture sequence of male cuttlefish (*Sepia officinalis*) could relate to personality differences. *Anim. Cogn.* 21, 773–785. doi: 10.1007/s10071-018-1209-8

Conflict of Interest: The authors declare that the research was conducted in the absence of any commercial or financial relationships that could be construed as a potential conflict of interest.

frontiers in Physiology

ORIGINAL RESEARCH
published: 18 June 2020
doi: 10.3389/fphys.2020.00648

Visual Attack on the Moving Prey by Cuttlefish

*José Jiun-Shian Wu[1], Arthur Hung[1,2], Yen-Chen Lin[1,3] and Chuan-Chin Chiao[1,4]**

[1] Institute of Systems Neuroscience, National Tsing Hua University, Hsinchu, Taiwan, [2] Interdisciplinary Program of Sciences, National Tsing Hua University, Hsinchu, Taiwan, [3] Interdisciplinary Program of Engineering, National Tsing Hua University, Hsinchu, Taiwan, [4] Department of Life Science, National Tsing Hua University, Hsinchu, Taiwan

Visual attack for prey capture in cuttlefish involves three well characterized sequential stages: attention, positioning, and seizure. This visually guided behavior requires accurate sensorimotor integration of information on the target's direction and tentacular strike control. While the behavior of cuttlefish visual attack on a stationary prey has been described qualitatively, the kinematics of visual attack on a moving target has not been analyzed quantitatively. A servomotor system controlling the movement of a shrimp prey and a high resolution imaging system recording the behavior of the cuttlefish predator, together with the newly developed DeepLabCut image processing system, were used to examine the tactics used by cuttlefish during a visual attack on moving prey. The results showed that cuttlefish visually tracked a moving prey target using mainly body movement, and that they maintained a similar speed to that of the moving prey right before making their tentacular strike. When cuttlefish shot out their tentacles for prey capture, they were able to either predict the target location based on the prey's speed and compensate for the inherent sensorimotor delay or adjust the trajectory of their tentacular strike according to the prey's direction of movement in order to account for any changes in prey position. These observations suggest that cuttlefish use the various visual tactics available to them flexibly in order to capture moving prey, and that they are able to extract direction and speed information from moving prey in order to allow an accurate visual attack.

Keywords: tentacular strike, sensorimotor integration, visual prediction, DeepLabCut, *Sepia pharaonis*

OPEN ACCESS

Edited by:
Graziano Fiorito, Stazione Zoologica Anton Dohrn, Italy

Reviewed by:
Noam Josef, Ben-Gurion University of the Negev, Israel
David B. Edelman, Dartmouth College, United States

***Correspondence:**
Chuan-Chin Chiao
ccchiao@life.nthu.edu.tw

Specialty section:
This article was submitted to Invertebrate Physiology, a section of the journal Frontiers in Physiology

Received: *05 November 2019*
Accepted: *20 May 2020*
Published: *18 June 2020*

Citation:
Wu JJ-S, Hung A, Lin Y-C and Chiao C-C (2020) Visual Attack on the Moving Prey by Cuttlefish. Front. Physiol. 11:648. doi: 10.3389/fphys.2020.00648

INTRODUCTION

Cephalopods (octopuses, cuttlefish, and squids) are highly visual animals, and most of their behaviors are visually driven (Hanlon and Messenger, 2018). During hunting behavior, unlike octopuses, which predominately use monocular vision and arms to grab their prey (Maldonado, 1964; Messenger, 1967) cuttlefish and squids use binocular vision and a tentacular strike to capture small fast-moving prey with great accuracy (Messenger, 1968; Kier and Leeuwen, 1997). This visually guided behavior is akin to amphibian prey capture during which the tongue is projected ballistically in order to seize the prey (Roth, 1976).

The predatory behavior of cuttlefish with respect to prawns has been described previously (Holmes, 1940; Sanders and Young, 1940; Wilson, 1946; Boulet, 1958; Wells, 1958). However, Messenger (1968) was the first to systematically examine the visual attack of cuttlefish and characterize the sequence of preying behavior into attention, positioning, and seizure. In the

attention phase, the whole animal turns to face the prey and aligns its anterior-posterior body axis with the prey via convergent eye movement, a form of stereopsis (Feord et al., 2020). During the positioning phase, the cuttlefish swims toward or away from the prey until it is roughly one mantle length away from it. In the seizure phase, the animal shoots out tentacles quickly to capture the prey with its suckers and then retracts the tentacles to bring the prey to the arms and mouth. From existing evidence, it has been suggested that the seizure phase is under open-loop control without visual feedback (Messenger, 1968). While cuttlefish usually track moving prey visually and attack the prey when it has stopped, they are also able to capture continuously moving prey. This demands a faculty for visual prediction that can compensate for the animal's inherent sensorimotor delay in relation to the visual attack (Borghuis and Leonardo, 2015). Alternatively, cuttlefish may correct the trajectory of the tentacular strike whilst carrying out the attack, and this may require a closed-loop control system with sensory feedback. Furthermore, it is well known that the prey capture tentacles of squid and cuttlefish lack rigid skeletal elements; rather they consist of a three-dimensional array of muscle fibers called a muscular hydrostat. This hydrostat allows the tentacular strike to be actively controlled and maneuvered (Kier, 2016). The foregoing suggest that cuttlefish are ideal animals for the study of sensorimotor integration during dynamic prey capture behavior.

To systematically assess the visual attack of cuttlefish on moving prey and characterize the kinematics of their preying behavior, we designed a programmable servomotor system to control the movement of a shrimp target and linked this to an imaging system with infrared sensitivity that is able to record the animal's behavior. Using DeepLabCut (Mathis et al., 2018; Nath et al., 2019), a markerless pose estimation system that integrates deep learning, we were able to quantitatively analyze the visual attack of cuttlefish on moving prey and showed that cuttlefish use a number of different tactics when capturing a moving target and that the nature of their tentacular strike is sufficiently flexible that it is able to take into account and adjust for movement by the prey.

MATERIALS AND METHODS

Animals

Sub-adult pharaoh cuttlefish *Sepia pharaonis* (mantle length, 6–10 cm) were reared from eggs collected at I-Lan, Taiwan. These cuttlefish were transported to the National Tsing Hua University and maintained in the laboratory using two close-circulation aquarium systems (700 l each; water temperature, 23∼25°C). The animals were housed individually in plastic containers (45 cm × 23 cm × 24 cm) inside the aquarium with water exchange. They were fed live post-larval white shrimp, *Litopenaeus vannamei,* or, alternatively, freshwater shrimp, *Neocaridina denticulate,* at least three times per day. The photoperiod of the aquaculture system was a 12/12 h light/dark cycle that used six ceiling full spectrum LED lights (7.5 W each; see the website for LED spectrum[1]). In total, 22 cuttlefish were used during the course of the present study, but only 10 animals expressed attention to the moving prey. Among them, five cuttlefish made successful tentacular strikes against moving targets during the experiments, and the other two cuttlefish initiated tentacular strikes but failed to seize the prey. All animals showed attention to the moving prey were summarized in **Table 1**. Although the reason that the rest of 12 cuttlefish did not respond to the moving prey was not known, it may be a result of stress in a confined environment during the experiment. As a consequence, the animal/repetition number was relatively low in the present study, given the difficulty of maintaining healthy cuttlefish in the lab for a long period of time and constraining the animal in a small tank during the experiment. Nevertheless, these focal observations provide key features of cuttlefish's visual attack on the moving prey. This research was approved by the Institutional Animal Care and Use Committee of the National Tsing Hua University (Protocol # 108047).

Experimental Setup

The configuration of the imaging system is shown in **Figure 1A**. The whole system was placed on a shockproof table to stabilize the image during data acquisition. To enhance image contrast and to reduce ambient light intensity, infrared illumination invisible to the cuttlefish was provided from below to create a cuttlefish silhouette against a lighted background. The experimental tank was made of thick acrylic (35 cm × 38 cm × 12 cm). The bottom of the tank had a sheet

[1]https://philips.to/2FYU8Cx

TABLE 1 | Summary of all cuttlefish used in the present study.

Animal	Trial	Strike attempt	Strike success	Attention time (s) in each episode	Figure	Supplementary Movie
A	1	Yes	Yes	2.6*	**6**	**1**
B	1	Yes	Yes	5.7*		**2**
C	1	Yes	Yes	3.9*		**3**
D	1	Yes	Yes	34.7, 7.3*	**8**	**4**
	2	Yes	Yes	13.7*	**3**	**5**
	3	Yes	Yes	5.3*	**7**	**6**
	4	Yes	Yes	24.3, 35.3, 12.5, 33.0*		**7**
E	1	Yes	Yes	8.5, 3.6*		**8**
F	1	Yes	No	24.8*, 12.9		**9**
G	1	Yes	No	17.7*, 23.3		**10**
	2	No	No	18.2, 42.0, 12.5		
	3	No	No	19.0		
H	1	No	No	12.1, 6.7, 5.1		
	2	No	No	31.7, 13.8		
I	1	No	No	6.9		
J	1	No	No	11.6, 5.7		

Attention followed with a strike attempt.

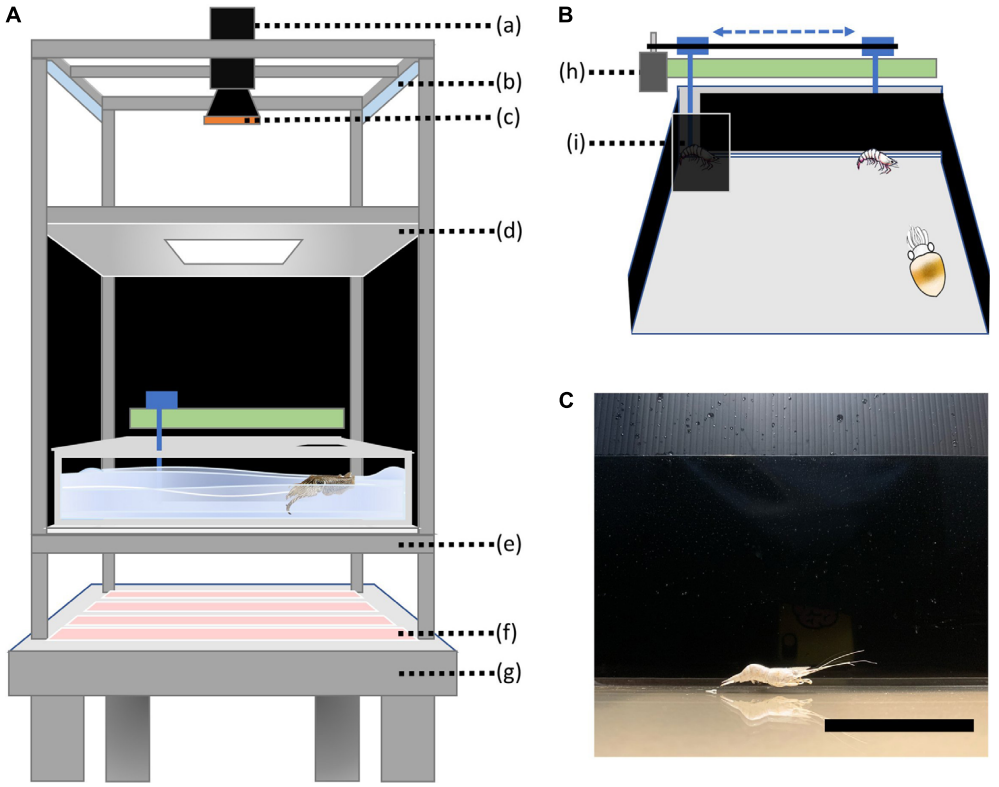

FIGURE 1 | The experiment setup. **(A)** The tank and imaging system for recording cuttlefish predatory behavior. The specific components included: (a) a high speed camera, (b) white light LEDs, (c) an adjustable neutral density filter, (d) a light diffuser screen, (e) a diffuser plate, (f) infrared LEDs, and (g) a shockproof table. **(B)** The motor system for controlling prey movement consisted of: (h) a servomotor and (i) a prey-starting area. The shrimp was attached to a steel rod via a hook, and the back-and-forth movement was programmed via Arduino to control the sliding rail driven by the servomotor. The prey-starting area was covered by a black screen to prevent cuttlefish from seeing and accessing the shrimp in this area. **(C)** The live view of the hooked shrimp from the perspective of the cuttlefish in the experimental tank. Note that the servomotor control system and the steel bar are completely invisible behind the black wall, and only the shrimp is visible to the cuttlefish. Scale bar, 5 cm.

of a brown paper and a semi-transparent film attached from the outside as a diffuser, and the inside walls of the tank were covered with a matted surface film to reduce light reflection. A set of white LED lights (15 W) with a plastic diffuser was used to provide an even illumination of the animal from above. A high-speed monochromatic 10GigE camera (HT-4000-N, Emergent Vision Technologies, Canada) with a 35 mm lens (HF-3514V-2, Myutron Inc., Japan) was fixed on the top using a rack that included a two-axis manual translation stage (ThorLabs, Newton, NJ, United States); this allowed flexible maneuvering of the camera. In addition, an adjustable neutral density filter, which was made up of two circular polarizers, was placed in front of the lens to reduce the light intensity within the visible range; this also removed ripples and reflections from the water surface, which improved the image quality significantly. The whole system was enclosed within a black tent to eliminate any human disturbance during the experiment. The camera was connected to a specialized 10G adapter board (Myricom, Arcadia, CA, United States) that was part of an Intel based PC computer; this computer had a high-speed solid state drive (v-NAND SSD 970 Pro NVMe M.2, 1Tb, Samsung, South Korea) for image storage and a high performance graphics card (Geforce RTX 2070s, ASUS, Taiwan). This PC was thus suitable for deep layer artificial neural network training.

The motor control system, which provided programmable one-dimensional horizontal movement of a prey target, is shown in **Figure 1B**. The system consisted of a servomotor (WLC stepping motor, Taiwan) and a sliding rail that was connected to a steel rod with a hook at one end for attaching the prey. The servomotor was connected to a programmable Arduino board (UNO, Somerville, MA, United States) and this allowed the prey to move back and forth at two constant speeds. Specifically, the prey was moved slowly (ca. 25 mm/s) in one direction, and suddenly reversed and moved fast (ca. 75 mm/s) in the opposite direction. To prevent any vibration produced by the servomotor from affecting the stability of image acquisition, the motor control system was placed on a separate table next to the shockproof table used for the imaging system. In addition, to prevent the cuttlefish from seeing the steel rod and the sliding rail, the motor control system was covered by black cloth and only the prey was visible to the cuttlefish in the experimental tank (**Figure 1C**).

The images were acquired using high-speed digital video recording software (StreamPix 7.0; NorPix, Canada) with an

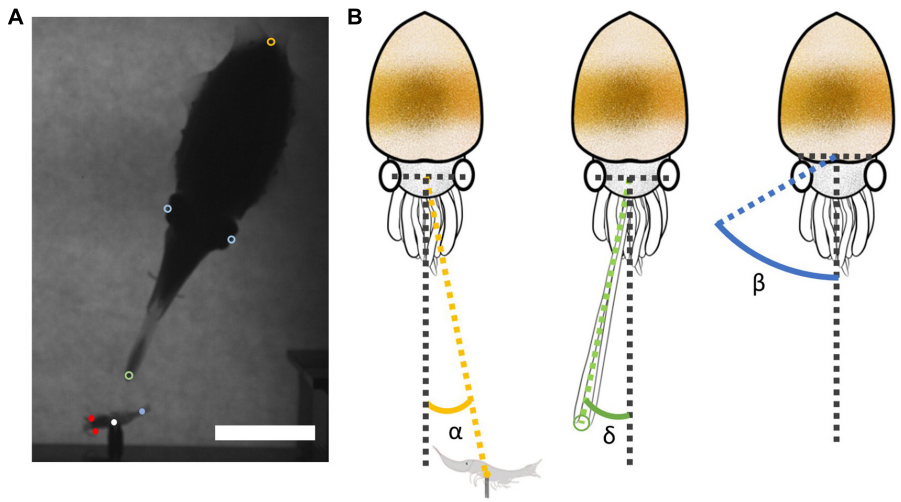

FIGURE 2 | Labeling for DeepLabCut training and angular parameters for data analysis. **(A)** The labeled body parts of the cuttlefish during the DeepLabCut training were the left and right eyes (blue circles), the left and right tentacle club tips (green circles), and the dorsal mantle end (yellow circle). Similarly, the labeled body parts of the shrimp prey during training were the left and right eyes (red dots), the hook site (white dot), and the tail (blue dot). Scale bar, 5 cm. **(B)** The angular parameters used in the image analysis. The visual attack angle α was the difference between the prey direction (yellow dashed line) and the cuttlefish anterior-posterior axis (gray dashed line). The tentacular strike angle δ was the difference between the tentacle direction (green dashed line) and the cuttlefish anterior-posterior axis. The eye angle β was the difference between the ocular axis (blue dashed line) and the cuttlefish anterior-posterior axis.

image size of 2048 × 2048 pixels at a speed of 90 frame per second. The images were recorded in TIFF format on the high-speed SSD hard drive. Image preview was carried out using ImageJ (1.52a; National Institute of Health, United States) and further processing was done using MATLAB (Mathworks, Natick, MA, United States).

Experimental Procedure

To motivate cuttlefish to prey on the moving prey, the animals were starved for 8–16 h before experimentation. Each cuttlefish was put in the experimental tank and allowed for acclimation at least 30 min. After the cuttlefish was settled down, judged by reduced ventilation rate and fin movement, the moving prey was appeared and started the back and forth movement pattern. The response of cuttlefish to the presence of the moving prey was recorded for the entire session (120 s) or until the cuttlefish captured the prey. If the cuttlefish did not respond to the moving prey in three consecutive sessions, the trial was aborted for the day. If the cuttlefish made a successful tentacular strike on the moving prey, it was allowed to rest for at least 10 min before starting a new trial (e.g., Animal D in **Table 1**). During the experiment, fresh seawater was slowly flowing into the tank and replaced some of seawater to ensure the oxygen and temperature levels constant.

Image Analysis

To quantitatively analyze the visual attack behavior of cuttlefish efficiently, DeepLabCut, a markerless pose estimation system based on transfer learning with deep neural networks using the Python programming environment (Mathis et al., 2018; Nath et al., 2019) was used to track the various body parts of both the cuttlefish and its prey, frame by frame. The successful tentacular strike videos with sufficient number of frames (typically 500 frames) that showed the full breadth of cuttlefish and prey behavior were critical to the training dataset. In the present study, the video images of four trials from one cuttlefish (Animal D in **Table 1**) were used for the DeepLabCut training. The labeled body parts of the cuttlefish during training included the dorsal mantle end, the left eye, the right eye, the left tentacle club tip, and the right tentacle club tip (**Figure 2A**). Similarly, the labeled body parts of the shrimp prey during training included the left eye, the right eye, the hook site, and the tail (**Figure 2A**). All the labeling was done manually. Training typically proceeded for more 500,000 iterations in order to reach each individual loss plateau. Analysis of the performance was evaluated by computing the mean average error (MAE; which is proportional to the average root mean square error) between the manual labels and the ones predicted by DeepLabCut. This allowed for the exclusion of any occluded body parts from the probabilistic output of the score map that reported whether a body part was visible in each frame. The trained network was then used to analyze all experimental videos that included successful tentacular strikes (see the **Supplementary Movies 1–8**), failed attempts (see the **Supplementary Movies 9, 10**), and attention but no strike ones (**Table 1**). The output was a data sheet that contained the x and y pixel coordinates of each labeled body part of each cuttlefish and shrimp in all frames of the video image. For unknown reasons, there were some mislabeled points on the cuttlefish in a small number of the image frames analyzed by DeepLabCut. In these instances, the x–y coordinates were corrected by linear interpolation. The above dataset was then used to compute the distance and angularity between the cuttlefish and the shrimp as well as cuttlefish's horizontal speeds and angular parameters during each strike. Specifically, the visual attack angle α, the

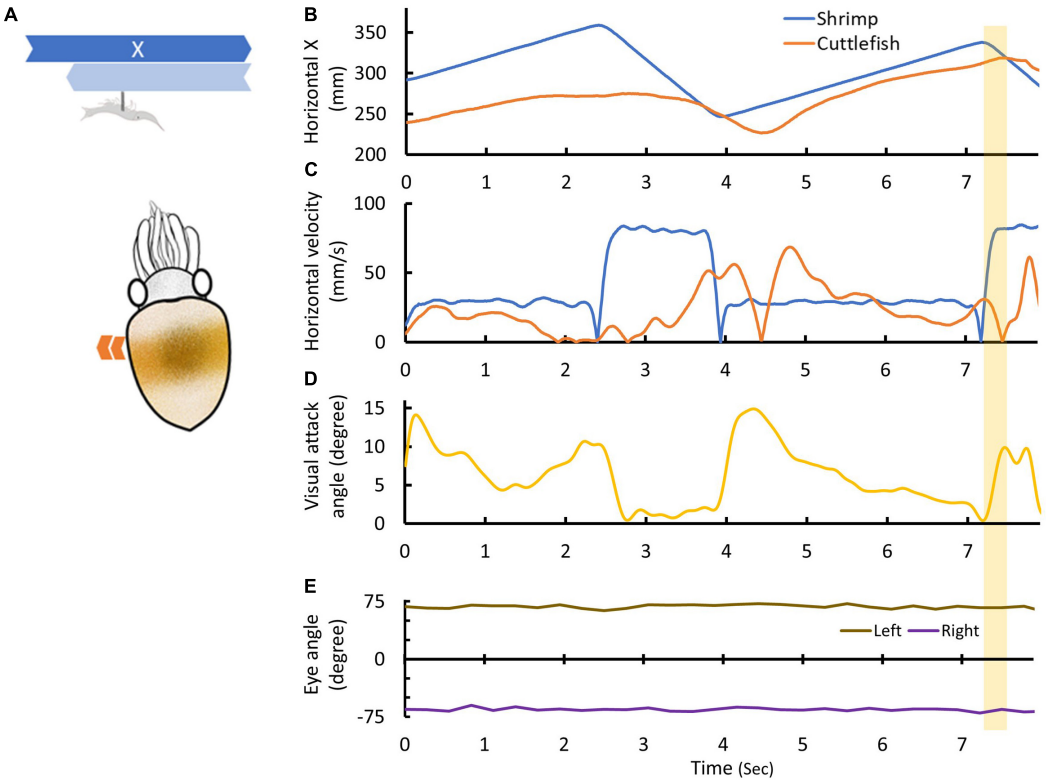

FIGURE 3 | Cuttlefish track the moving prey before initiating the tentacular strike. **(A)** The shrimp was moved back-and-forth continuously with a faster rightward movement (dark blue arrow) and a slower leftward movement (light blue arrow). The cuttlefish usually followed the movement of the shrimp before making the tentacular strike. **(B)** The horizontal distance covered by the shrimp (blue line) and the cuttlefish (orange line) as a function of time. The cuttlefish moved close to the shrimp and then made the strike on it. The yellow shaded area indicates the period of the tentacular strike. **(C)** The horizontal movement speed of the shrimp (blue line) and the cuttlefish (orange line) as a function of time. The cuttlefish moved relatively slowly before making the strike. **(D)** The visual attack angle α of the cuttlefish as a function of time. The cuttlefish reduced the visual attack angle before making the strike. **(E)** The eye angles β of left and right eyes (brown and purple lines) as a function of time. The cuttlefish maintained relatively constant eye angles throughout visual attack. See **Supplementary Movie 5** for details.

tentacular strike angle δ, and the eye angle β were derived from the data (**Figure 2B**).

Statistics

The Wilcoxon matched-pairs signed rank test was used to compare the cuttlefish moving velocity at two different prey movement speeds. The Mann–Whitney U test was used to assess the difference between the attention time of cuttlefish with and without tentacular strikes. It was also used to evaluate the data spread of cuttlefish's visual attack distance and body axis angle relative to the prey, as well as the extent of left and right eye angle changes Δβ during the visual attack. All statistics were conducted in MATLAB.

RESULTS

Cuttlefish Visually Track Moving Prey With Body Movement Before the Tentacular Strike

To capture a moving prey, cuttlefish have to constantly re-position themselves relative to the prey location before initiating the tentacular strike. It is apparent from our analysis that cuttlefish often moved laterally via fin movement and thus were able to maintain a speed that is similar to that of the prey when it moved slowly (**Figures 3A,C**; see also **Supplementary Movies 1–8**). Furthermore, cuttlefish specifically moved close to the shrimp before making their strike on the prey (**Figure 3B**). It was also observed that the cuttlefish reduced the visual attack angle α before making their tentacular strike (**Figure 3D**). This maneuver involved coordinated body movement, and this allowed the cuttlefish to visually track the moving prey while at the same time keeping the prey aligned with their anterior-posterior body axes. Interestingly, there was less eye movement observed when the cuttlefish actively tracked the moving prey, as the eye angle β was kept relatively steady throughout the visual attack (**Figure 3E**). This behavior is equivalent to the attention and positioning phases that cuttlefish deploy during a visual attack on a stationary prey target (Messenger, 1968).

Despite the cuttlefish attempted to keep up with the prey movement when it moved slowly, they were not able to follow the moving prey when it moved fast (**Figures 3C**, **4A**). The horizontal speed of cuttlefish movement was actually decreased,

rather than increased, when the prey moved fast during the attention phase; and this difference was statistically significant (p = 0.0038; **Figure 4A**). This finding suggests that cuttlefish attempt to keep up with the prey speed only when the prey moves slowly. Interestingly, it was also found that the attention time before initiating the tentacular strike varied a lot, ranging from 2.6 to 33.0 s, and it was not significantly different from the attention time of the episodes without the attempt of tentacular strikes (p = 0.0985; **Figure 4B**). This finding suggests that the duration of the attention phase is independent of the decision of the tentacular strike. Although we only observed two attempts of tentacular strike without successful capture of the prey (**Table 1**; see **Supplementary Movies 9, 10**), the attention time before making the strike seemed relatively longer (24.8 and 17.7 s; red dots in **Figure 4B**).

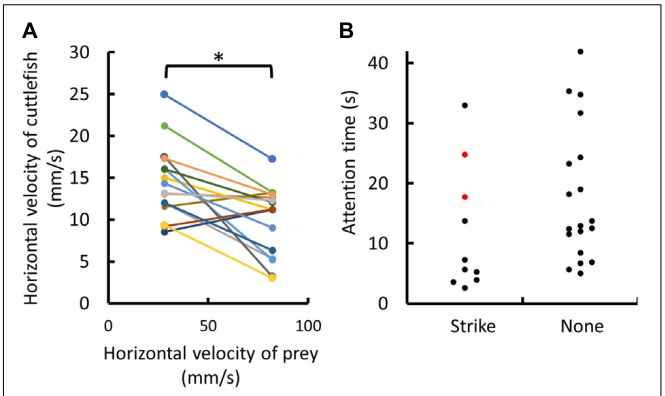

FIGURE 4 | Cuttlefish attempt to keep up with the prey speed only when the prey moves slowly, and the time of the attention phase with or without initiating a tentacular strike varies among individuals. **(A)** Average horizontal velocities of individual cuttlefish during the attention phase at both slow and fast prey-moving speeds. Cuttlefish maintained relatively similar speed when the prey moved slowly, but reduced the body movement when the prey moved fast. All 16 trials listed in **Table 1** were used in the analysis. **(B)** The attention time of individual cuttlefish with or without an attempt of the tentacular strike. All 29 attention episodes listed in **Table 1** were used in the analysis. Note that the attention time of two strike attempts without successful capture of the prey was marked by red dots.

Cuttlefish Initiate the Tentacular Strike at Different Angles and Distances From the Moving Prey

Mobile prey are able to move in different directions at various speeds and with different temporal patterns. In the stationary prey condition, after the attention and positioning phases, cuttlefish typically keep themselves in front of the prey, and roughly one mantle length away from it, before initiating the tentacular strike (Messenger, 1968). However, under moving prey conditions, cuttlefish were found to make a visual attack at a variety of angles and distances from the prey location (**Figure 5A**), and the spread of data was not significantly different from the norms (p = 1.0, one mantle length of the prey in **Figure 5B**; p = 1.0, perpendicular to the prey moving direction in **Figure 5C**). This suggests that cuttlefish are able to freely use various different tactics when capturing a moving prey. Furthermore, the extent of left and right eye angle changes Δβ during the visual attack was significantly smaller when compared with Δβ observed immediately after the presence of the prey (**Figure 5D**; left eye Δβ 17.3 degree, p = 0.0444; right eye Δβ 16.7 degree, p = 0.0444). This suggests that cuttlefish use less eye movement when tracking the moving target during the visual attack. Interestingly, it was observed that cuttlefish did not always initiate their tentacular strike when the prey was moving slowly; they were also able to strike prey when it was moving at a fast speed, though it only occurred one out of eight trials in the present study (**Figure 5E**). This finding further supports the idea that flexible tactics are used by cuttlefish during the visual capture of moving prey.

Cuttlefish Visually Predict the Location of Moving Prey Before Initiating Their Tentacular Strike

To successfully seize a moving prey, the predator must be able to compensate for any inherent sensorimotor delay before initiating the visual attack. In other words, the predator must anticipate the trajectory of the moving prey and accordingly strike the prey at a predicted future position. Cuttlefish appeared to be able to predict the location of their prey based on binocular visual information that was obtained from their visual system and then initiated the tentacular strike ballistically so that the tentacles were able to land on the target with great accuracy (**Figure 6**). This visual prediction seemed to occur when cuttlefish were making a tentacular strike on a slow-moving target.

Cuttlefish Wiggle Their Tentacle Clubs in Order to Track a Fast-Moving Prey Before the Seizure Phase

When prey are moving at faster speeds, cuttlefish would not normally make a tentacular strike and they tend to wait until the prey slows down before initiating their strike. However, cuttlefish sometimes were found to wiggle their tentacle clubs when tracking a fast-moving prey before the seizure phase (**Figure 7**). This behavior may be involved in helping cuttlefish to obtain information about the direction of prey movement, thus increasing the probability of prey capture.

Cuttlefish Adjust the Trajectory of Their Tentacular Strike During the Later Stage of the Seizure Phase

In addition to visual prediction and tentacle wiggling, cuttlefish were observed to adjust the trajectory of their tentacular strike during the seizure phase. This was achieved by changing the tentacle club angle θ at the last instant of the seizure phase (**Figure 8**). This observation suggests that cuttlefish are able to use sensory information during the seizure phase and that there is feedback control during their tentacular strike. Without this adaptive maneuver, cuttlefish would be much more likely to miss strikes on moving prey.

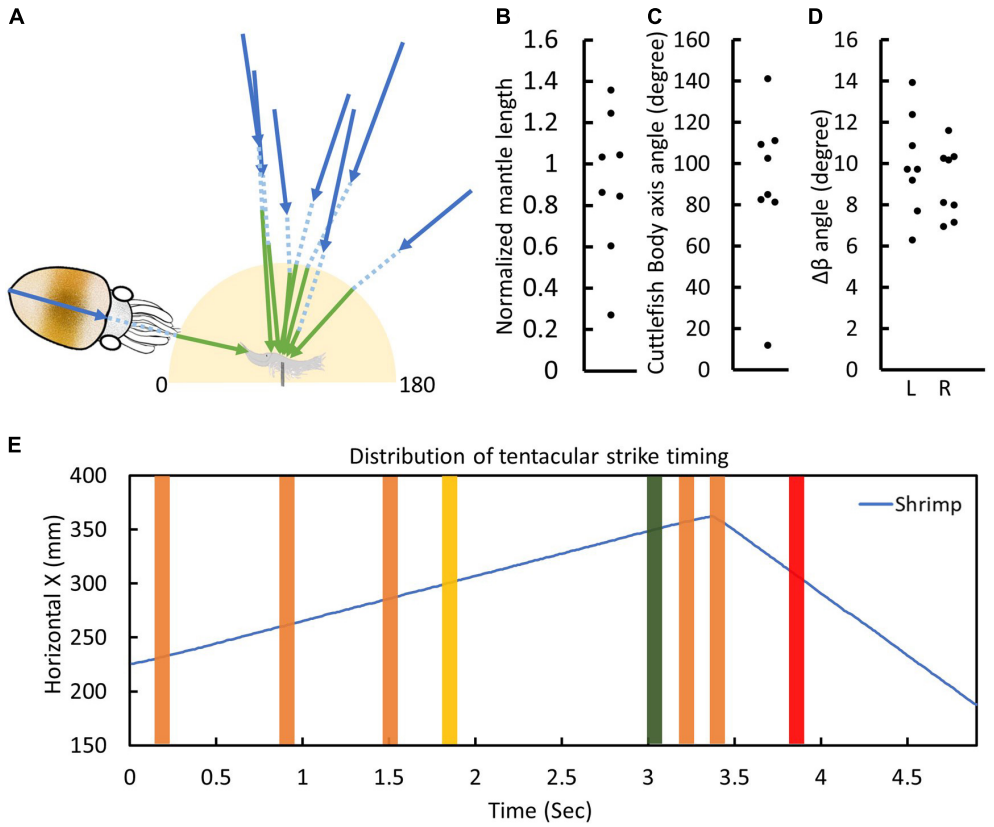

FIGURE 5 | Cuttlefish attack the moving prey from different directions, distances, and speeds. **(A)** A schematic representation of all recorded cuttlefish visual attacks captured during the present study. The blue arrow depicts the cuttlefish anterior-posterior axis and mantle length, whereas the green arrow indicates the tentacular strike direction and length during the seizure phase. The yellow shaded area shows the tentacular strike zone. **(B)** The distribution of tentacular strike lengths normalized to one mantle length. **(C)** The distribution of cuttlefish body axis angles relative to the moving prey. **(D)** The distribution of left and right eye angle changes $\Delta\beta$ during the visual attack. **(E)** The distribution of tentacular strike timing relative to the moving prey. The horizontal movement distance of the shrimp as a function of time (blue line). The green, red, and yellow lines represent the visual strikes shown in **Figures 6**, **7**, and **8**, respectively.

DISCUSSION

Cuttlefish Use Flexible Tactics to Capture Moving Prey

In the present study, the various types of preying tactics used by cuttlefish to capture a moving target were revealed by systematically controlling the speed and direction of moving shrimp. In a manner different than those employed during visual attack of a stationary prawn, in which the attention and positioning phases of cuttlefish are sequential (Messenger, 1968) visual attack on a moving prey requires cuttlefish to constantly track the target, and in the process there is dynamic alternation of the attention and positioning phases in order to prepare for the final phase of prey seizure (**Figure 3**). Cuttlefish typically use convergent eye movement and saccadic body movement to align the moving prey with their body axis (Helmer et al., 2017) and thus allow for accurate estimation of target distance. However, it has been found that there was no significant eye movement during the visual attack in the present study (**Figures 3E**, **5D**), and this suggests that both horizontal and rotational body movements were the main maneuver used by cuttlefish to visually track the moving prey. Interestingly, although cuttlefish could maintain a similar speed when the prey moved slowly, they decreased or even ceased movement when the prey moved fast (**Figures 3C**, **4A**, **7B**). This observation suggests that cuttlefish's body movement is not adapted to track a fast-moving target, thus visual attack is most successful at stationary or slow-moving prey.

Previous studies have shown that cuttlefish rely on several mechanisms to extract distance/depth information (Schaeffel et al., 1999; Mathger et al., 2013; Josef et al., 2014; Helmer et al., 2017). A recent study using the "anaglyph" glasses paradigm to examine cuttlefish's stereopsis demonstrated that they could extract depth information from the disparity between left and right visual fields, akin to the stereopsis mechanism found in vertebrates (Feord et al., 2020). However, estimating the distance of a moving target accurately whilst the cuttlefish itself is moving is not an easy task. As a consequence, cuttlefish did not always initiate their tentacular strike when a moving prey is one mantle length away (**Figure 5B**), as is usually the case when visually attacking a stationary prey (Messenger, 1968). In addition, by choosing different visual attack angles with respect

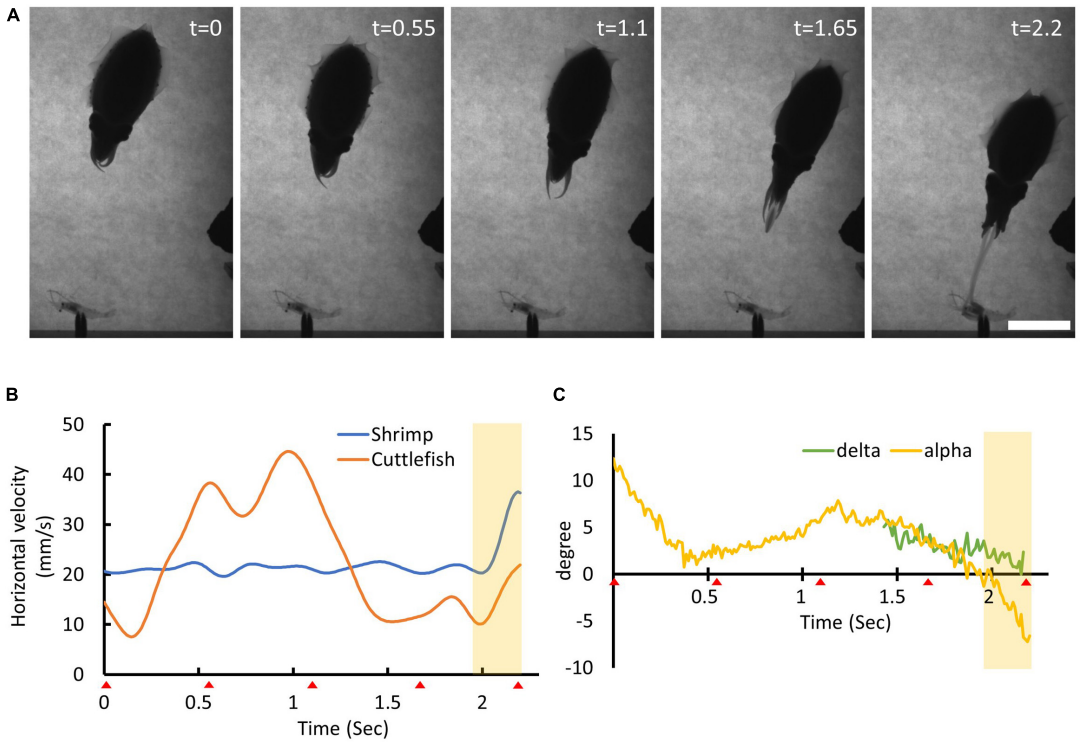

FIGURE 6 | Cuttlefish predict the moving prey location before making their visual attack. **(A)** The sequence of the cuttlefish's visual attack behavior. The time stamp on the top-right represents the recording time of each frame image in seconds. Scale bar, 5 cm. **(B)** The horizontal moving speed of the shrimp (blue line) and the cuttlefish (orange line) as a function of time. The red triangles at the bottom of the *x*-axis indicate the recording time of each frame image. The yellow shaded area depicts the period of the tentacular strike. **(C)** The visual attack angle α (yellow line) and the tentacular strike angle δ (green line) of the cuttlefish as a function of time. See **Supplementary Movie 1** for details.

to the trajectory of the prey, cuttlefish may be able to reduce the need for accurate target distance estimation. In the present study, cuttlefish sometimes struck at the target shrimp from an oblique angle (**Figure 5C**), a tactic that increased the probability of capturing a moving prey.

Finally, although cuttlefish frequently made their visual attack when the shrimp was moving at a slower speed, they were also able to initiate a tentacular strike when the shrimp was moving at a faster speed or when the shrimp was near the instant when the direction of movement was reversed (**Figure 5E**). This observation suggests that cuttlefish are able to adaptively adjust their target distance estimation, thus making them adept at capturing a fast-moving prey. Taken together, these results show that cuttlefish are able to freely choose from a variety of visual attack tactics when attempting to capture a moving prey. In future studies, it will be important to examine whether prior experience and learning influence their choice of tactics and whether such learning helps to maximize prey capture success.

Visual Prediction and Sensory Feedback Facilitate Accurate Visual Attack on Moving Prey by Cuttlefish

In contrast to visual attack on a stationary prawn by cuttlefish during which the seizure phase has been suggested to involve open-loop control without visual feedback (Messenger, 1968) visual attack on a moving prey requires cuttlefish to compensate for the sensorimotor delay using one or more predictive mechanisms before making their tentacular strike or, alternatively, they may need to use feedback mechanisms during prey seizure. To take prey movement into account, cuttlefish must be able to predict the position of their prey at the instant of tentacle club contact. In the present study, we found that some cuttlefish visually aim for the shrimp at a future location before initiating their tentacular strike (**Figure 6**). In a similar approach, it has been suggested that tongue-projecting salamanders use a mechanism involving motion extrapolation to predict the position of walking prey (Borghuis and Leonardo, 2015). In invertebrates, it has also been reported that the dragonfly and fruit fly use visually guided motor planning in order to predict a future event, such as prey interception or escape response (Card and Dickinson, 2008; Mischiati et al., 2015). Based on these previous studies, it seems likely that cuttlefish use similar internal models to compensate for the sensorimotor delay that is present during visual attack behavior. Although the neural mechanisms underlying visual prediction are currently unknown, a previous lesion study has shown that the anterior basal lobe – previously implicated in orientation and positioning of the head, arms, and eyes (Boycott, 1961) – is responsible for the control of prey capture in cuttlefish (Chichery and Chichery, 1987). In

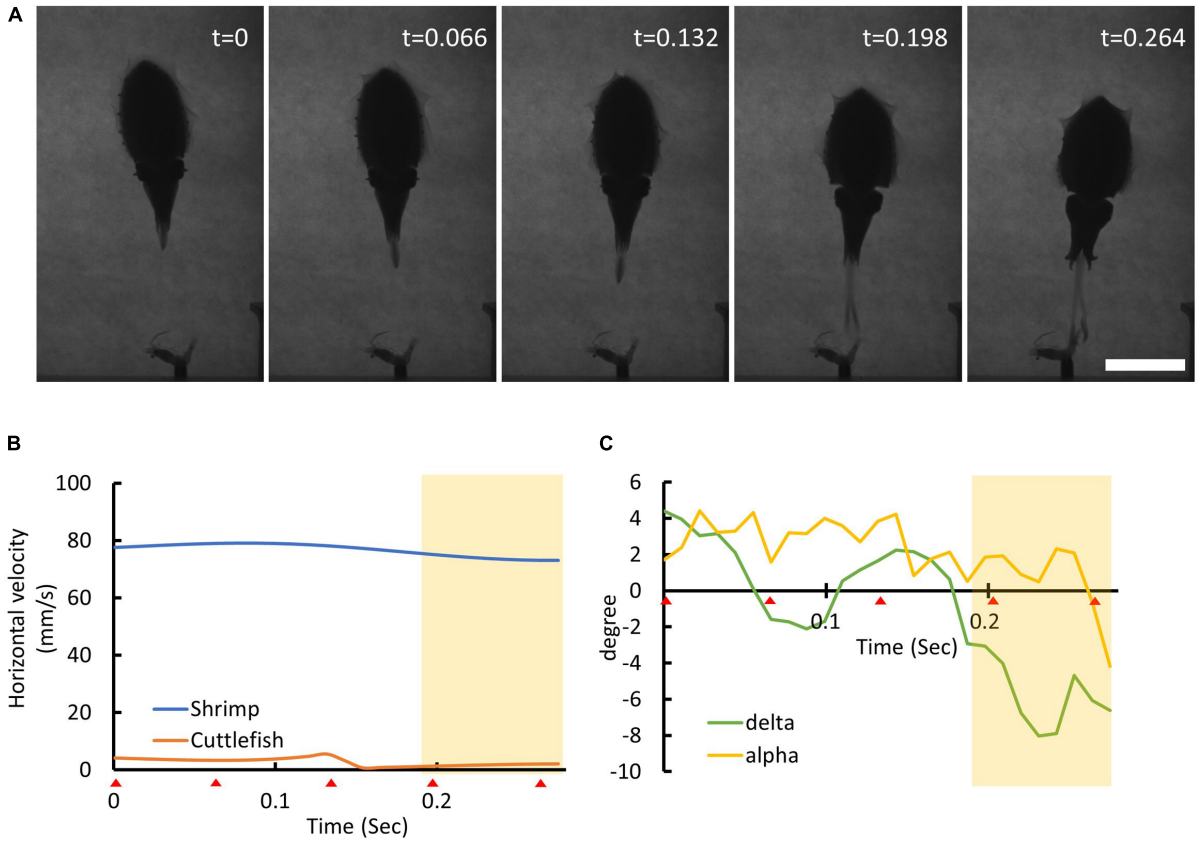

FIGURE 7 | Cuttlefish wiggle their tentacle clubs and this may help them estimate the location of the moving prey. **(A)** The sequence of cuttlefish visual attack behavior. The time stamp on the top-right represents the recording time of each frame image in seconds. Scale bar, 5 cm. **(B)** The horizontal movement speed of the shrimp (blue line) and the cuttlefish (orange line) as a function of time. The red triangles at the bottom of the *x*-axis indicate the recording time of each frame image. The yellow shaded area depicts the period of the tentacular strike. Note that the cuttlefish remained relatively motionless while the shrimp was moving fast. **(C)** The visual attack angle α (yellow line) and the tentacular strike angle δ (green line) of the cuttlefish as a function of time. Note that the tentacular strike angle δ alternated before and during the seizure phase. See **Supplementary Movie 6** for details.

future studies, it will be important to elucidate the brain area(s), neural circuitry, and computational model(s) involved in this predictive behavior.

When cuttlefish attempted to capture a fast moving prey, we observed an interesting tentacle maneuver before the seizure phase. This involved the wiggling of the cuttlefish's tentacle clubs left and right before initiating a ballistic strike to capture the shrimp (**Figure 7**). This behavior has not been reported before, and its function is currently unknown. We hypothesize that the wiggling of tentacles might generate a flow of water and that this enables the cuttlefish initiate mechanosensory detection of surrounding objects. This behavior may help to keep the attacking cuttlefish updated as to the position of a moving prey, which would increase the success rate of prey capture. This is akin to the lateral line system in fish which enables them to perceive surrounding objects by sensing changes in the flow fields generated around their bodies as they swim through the water (Coombs et al., 1989).

In addition to visual prediction, it has been observed that cuttlefish were able to correct the trajectory of their tentacular strike at the last instant of the seizure phase and thus take into account any prediction error (**Figure 8**). This finding implies that cuttlefish are able to continuously monitor the position of moving prey and that they are able to use sensory feedback and a closed-loop control system to change their motor output during their strikes. While the precise sensory information used for this feedback control remains unknown, it is likely that this is a mechanical cue rather than a visual one, due to the extremely short response time involved. In future studies, it will be important to identify the mechanosensory system that is responsible for this feedback control during visual attack by cuttlefish.

DeepLabCut as a Tool for the Kinematic Analysis of Locomotion by Soft Body Animals

The training carried out by DeepLabCut was vital to the success of the present study. However, it was not without issues. DeepLabCut was originally developed to track the locomotion of jointed and rigid animals, such as mice and flies (Mathis et al., 2018; Nath et al., 2019). Cuttlefish are soft-bodied animals.

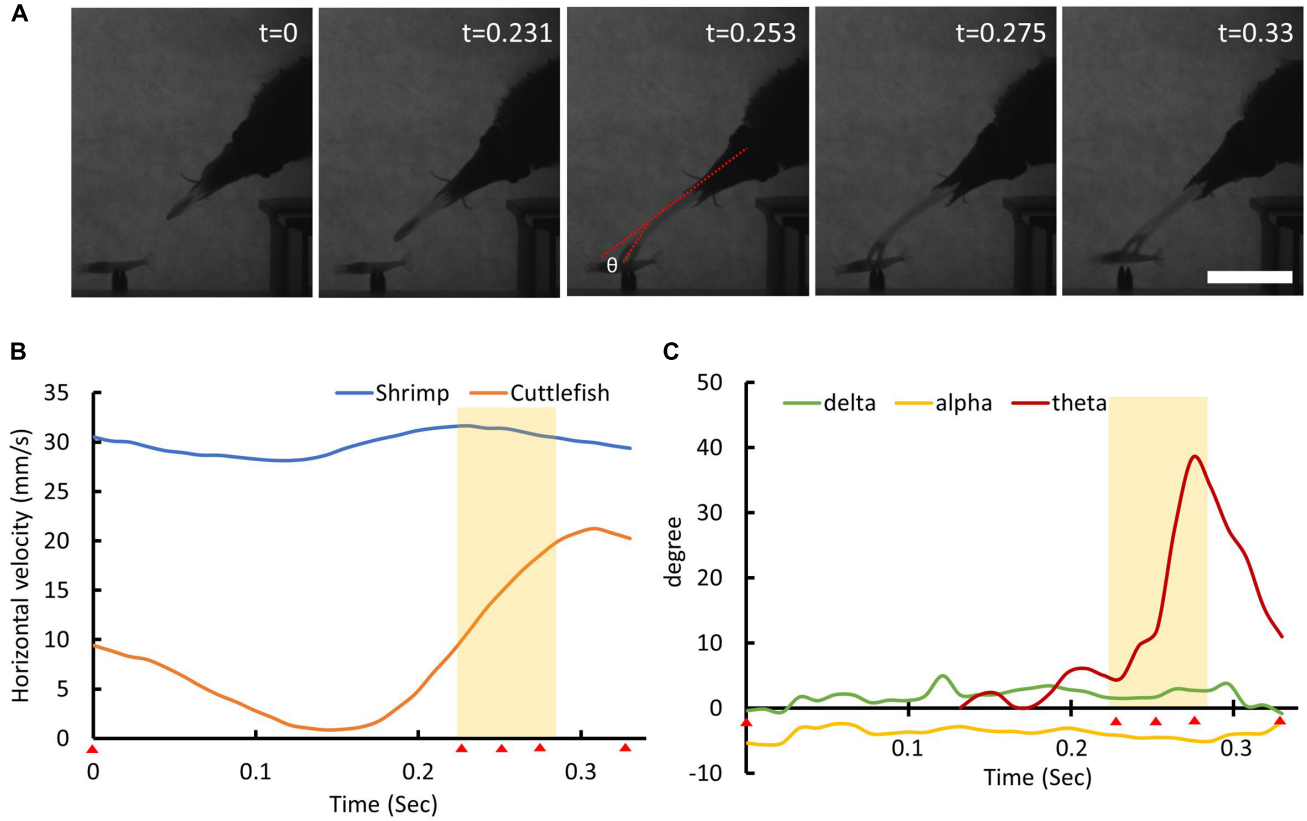

FIGURE 8 | Cuttlefish change their tentacle club direction at the last instant of the seizure phase. **(A)** The sequence of cuttlefish's visual attack behavior. The time stamp on the top-right represents the recording time of each frame image in seconds. The red dashed lines show the tentacle club angle θ relative to the tentacle axis. Scale bar, 5 cm. **(B)** The horizontal movement speed of the shrimp (blue line) and the cuttlefish (orange line) as a function of time. The red triangles at the bottom of the *x*-axis indicate the recording time of each frame image. The yellow shaded area depicts the period of the tentacular strike. **(C)** The visual attack angle α (yellow line), the tentacular strike angle δ (green line), and the tentacle club angle θ (red line) of the cuttlefish as a function of time. Note that the tentacle club angle θ altered significantly during the final stage of the seizure phase. See **Supplementary Movie 4** for details.

Although they have cuttlebones that constrain the body form to some extent, cuttlefish are able to change their body shape during predatory behavior. This makes transfer learning somewhat more difficult and means that there is a requirement for more image frames within the training data. Furthermore, while key features during the seizure phase, such as a pair of tentacle trajectories, are important for the kinematic analysis of visual attack by cuttlefish, image frames of tentacular strike are relatively scarce compared to the ones obtained during the attention and positioning phases. This highlights the necessity of acquiring more image frames during the seizure phase. In addition, the locomotion of cuttlefish during the seizure phase sometimes generated ripples on the water surface and these distorted the quality of the images captured. In future, such artifacts could be reduced by placing a transparent plate on the water surface to eliminate the wave effect caused by the cuttlefish movement.

DATA AVAILABILITY STATEMENT

All datasets generated for this study are included in the article/**Supplementary Material**.

ETHICS STATEMENT

The animal study was reviewed and approved by the Institutional Animal Care and Use Committee of the National Tsing Hua University (Protocol # 108047).

AUTHOR CONTRIBUTIONS

JW designed and performed the experiment and wrote the draft manuscript. AH helped in data analysis and interpretation. Y-CL helped in instrumentation and experimental design. C-CC designed the experiment and wrote the manuscript.

FUNDING

The initial study was sponsored by the Pilot Overseas Internship Program from the Ministry of Education in Taiwan (to AH and C-CC). This project was also supported by a research grant from

the Ministry of Science and Technology in Taiwan MOST-106-2311-B-007-010-MY3 (to C-CC).

ACKNOWLEDGMENTS

We thank Chien-Yi Chen, Wang-Ning Li, and Li-Hao Wang for helping to develop the DeepLabCut program, for their assistance when labeling the cuttlefish and shrimp for the network training, and for their help with automating the data analysis. This project was conceptualized initially by Donovan Ventimiglia with grant support and input from Stephanie Palmer and Roger Hanlon at the Marine Biological Laboratory, Woods Hole, United States. A pilot study at MBL performed on *Sepia officinalis* by Donovan Ventimiglia and Arthur Hung helped develop the methodology for this experiment and we are highly grateful to all parties for their ideas and support.

SUPPLEMENTARY MATERIAL

The Supplementary Material for this article can be found online at: https://www.frontiersin.org/articles/10.3389/fphys.2020.00648/full#supplementary-material

REFERENCES

Borghuis, B. G., and Leonardo, A. (2015). The role of motion extrapolation in amphibian prey capture. *J. Neurosci.* 35, 15430–15441. doi: 10.1523/jneurosci.3189-15.2015

Boulet, P. C. (1958). *La Perception Visuelle du Mouvement Chez la Perche et la Seiche*. Paris: Les Editions du Muséum.

Boycott, B. B. (1961). Functional organization of brain of cuttlefish *Sepia officinalis*. *Proc. R. Soc. Ser, B Bio* 153, 503–534. doi: 10.1098/rspb.1961.0015

Card, G., and Dickinson, M. H. (2008). Visually mediated motor planning in the escape response of Drosophila. *Curr. Biol.* 18, 1300–1307. doi: 10.1016/j.cub.2008.07.094

Chichery, M. P., and Chichery, R. (1987). The anterior basal lobe and control of prey-capture in the cuttlefish (*Sepia officinalis*). *Physiol. Behav.* 40, 329–336. doi: 10.1016/0031-9384(87)90055-2

Coombs, S., Gorner, P., and Munz, H. (1989). *The Mechanosensory Lateral Line: Neurobiology and Evolution*. New York, NY: Springer-Verlag.

Feord, R. C., Sumner, M. E., Pusdekar, S., Kalra, L., Gonzalez-Bellido, P. T., and Wardill, T. J. (2020). Cuttlefish use stereopsis to strike at prey. *Sci. Adv.* 6:eaay6036. doi: 10.1126/sciadv.aay6036

Hanlon, R. T., and Messenger, J. B. (2018). *Cephalopod Behaviour*, 2nd Edn. Cambridge: Cambridge University Press.

Helmer, D., Geurten, B. R. H., Dehnhardt, G., and Hanke, F. D. (2017). Saccadic movement strategy in common cuttlefish (*Sepia officinalis*). *Front. Physiol.* 7:660. doi: 10.3389/fphys.2016.00660

Holmes, W. (1940). The colour changes and colour patterns of *Sepia officinalis* L. *Proc. Zool. Soc. A* 110, 17–35. doi: 10.1111/j.1469-7998.1940.tb08457.x

Josef, N., Mann, O., Sykes, A. V., Fiorito, G., Reis, J., Maccusker, S., et al. (2014). Depth perception: cuttlefish (*Sepia officinalis*) respond to visual texture density gradients. *Anim. Cogn.* 17, 1393–1400. doi: 10.1007/s10071-014-0774-8

Kier, W., and Leeuwen, J. (1997). A kinematic analysis of tentacle extension in the squid Loligo pealei. *J. Exp. Biol.* 200, 41–53.

Kier, W. M. (2016). The musculature of coleoid cephalopod arms and tentacles. *Front. Cell Dev. Biol.* 4:410. doi: 10.3389/fcell.2016.00010

Maldonado, H. (1964). The control of attack by octopus. *Z. Vergleich. Physiol.* 47, 656–674. doi: 10.1007/bf00303314

Mathger, L. M., Hanlon, R. T., Hakansson, J., and Nilsson, D. E. (2013). The W-shaped pupil in cuttlefish (*Sepia officinalis*): functions for improving horizontal vision. *Vis. Res.* 83, 19–24. doi: 10.1016/j.visres.2013.02.016

Mathis, A., Mamidanna, P., Cury, K. M., Abe, T., Murthy, V. N., Mathis, M. W., et al. (2018). DeepLabCut: markerless pose estimation of user-defined body parts with deep learning. *Nat. Neurosci.* 21, 1281–1289. doi: 10.1038/s41593-018-0209-y

Messenger, J. B. (1967). The effects on locomotion of lesions to the visuo-motor system in octopus. *Proc. R. Soc. Lond. B. Biol. Sci.* 167, 252–281. doi: 10.1098/rspb.1967.0026

Messenger, J. B. (1968). The visual attack of the cuttlefish. *Sepia officinalis*. *Anim. Behav.* 16, 342–357. doi: 10.1016/0003-3472(68)90020-1

Mischiati, M., Lin, H. T., Herold, P., Imler, E., Olberg, R., and Leonardo, A. (2015). Internal models direct dragonfly interception steering. *Nature* 517, 333–338. doi: 10.1038/nature14045

Nath, T., Mathis, A., Chen, A. C., Patel, A., Bethge, M., and Mathis, M. W. (2019). Using DeepLabCut for 3D markerless pose estimation across species and behaviors. *Nat. Protoc.* 14, 2152–2176. doi: 10.1038/s41596-019-0176-0

Roth, G. (1976). Experimental-analysis of prey catching behavior of hydromantes italicus dunn (*Amphibia*, *Plethodontidae*). *J. Comp. Physiol.* 109, 47–58. doi: 10.1007/bf00663434

Sanders, F. K., and Young, J. Z. (1940). Learning and other functions of the higher nervous centres of sepia. *J. Neurophysiol.* 3, 501–526. doi: 10.1152/jn.1940.3.6.501

Schaeffel, F., Murphy, C. J., and Howland, H. C. (1999). Accommodation in the cuttlefish (*Sepia officinalis*). *J. Exp. Biol.* 202, 3127–3134.

Wells, M. J. (1958). Factors affecting reactions to mysis by newly hatched sepia. *Behaviour* 13, 96–111. doi: 10.1163/156853958x00055

Wilson, D. P. (1946). A note on the capture of prey by *Sepia officinalis* L. *J. Mar. Biol. Assoc. U. K.* 26, 421–425. doi: 10.1017/s0025315400012248

Conflict of Interest: The authors declare that the research was conducted in the absence of any commercial or financial relationships that could be construed as a potential conflict of interest.

frontiers in Physiology

ORIGINAL RESEARCH
published: 07 August 2020
doi: 10.3389/fphys.2020.00845

Dynamic Courtship Signals and Mate Preferences in *Sepia plangon*

Alejandra López Galán, Wen-Sung Chung* and N. Justin Marshall*

Sensory Neurobiology Group, Queensland Brain Institute, The University of Queensland, St Lucia, QLD, Australia

Communication in cuttlefish includes rapid changes in skin coloration and texture, body posture and movements, and potentially polarized signals. The dynamic displays are fundamental for mate choice and agonistic behavior. We analyzed the reproductive behavior of the mourning cuttlefish *Sepia plangon* in the laboratory. Mate preference was analyzed via choice assays ($n = 33$) under three sex ratios, 1 male (M): 1 female (F), 2M:1F, and 1M:2F. We evaluated the effect of modifying polarized light from the arms stripes and ambient light with polarized and unpolarized barriers between the cuttlefish. Additionally, to assess whether a particular trait was a determinant for mating, we used 3D printed cuttlefish dummies. The dummies had different sets of visual signals: two sizes (60 or 90 mm mantle length), raised or dropped arms, high or low contrast body coloration, and polarized or unpolarized filters to simulate the arms stripes. Frequency and duration (s) of courtship displays, mating, and agonistic behaviors were analyzed with GLM and ANOVAs. The behaviors, body patterns, and their components were integrated into an ethogram to describe the reproductive behavior of *S. plangon*. We identified 18 body patterns, 57 body patterns components, and three reproductive behaviors (mating, courtship, and mate guarding). Only sex ratio had a significant effect on courtship frequency, and the male courtship success rate was 80%. Five small (ML $<$ 80 mm) males showed the dual-lateral display to access mates while avoiding fights with large males; this behavior is characteristic of male "sneaker" cuttlefish. Winner males showed up to 17 body patterns and 33 components, whereas loser males only showed 12 patterns and 24 components. We identified 32 combinations of body patterns and components that tended to occur in a specific order and were relevant for mating success in males. Cuttlefish were visually aware of the 3D-printed dummies; however, they did not start mating or agonistic behavior toward the dummies. Our findings suggest that in *S. plangon,* the dynamic courtship displays with specific sequences of visual signals, and the sex ratio are critical for mate choice and mating success.

Keywords: cephalopods, reproductive behavior, female choice, ethogram, male competition, body pattern

OPEN ACCESS

Edited by:
Chuan-Chin Chiao,
National Tsing Hua University, Taiwan

Reviewed by:
Yoko Iwata,
The University of Tokyo, Japan
Christine Huffard,
Monterey Bay Aquarium Research Institute (MBARI), United States
José E. A. R. Marian,
University of São Paulo, Brazil

****Correspondence:***
Alejandra López Galán
a.lopezgalan@uq.edu.au
Wen-Sung Chung
w.chung1@uq.edu.au

Specialty section:
This article was submitted to Invertebrate Physiology, a section of the journal Frontiers in Physiology

Received: *21 December 2019*
Accepted: *24 June 2020*
Published: *07 August 2020*

Citation:
López Galán A, Chung W-S and Marshall NJ (2020) Dynamic Courtship Signals and Mate Preferences in Sepia plangon. *Front. Physiol. 11:845. doi: 10.3389/fphys.2020.00845*

1. INTRODUCTION

Animal communication is a complex mechanism to transfer information between signalers and perceivers (Scott-Phillips, 2008). Communication involves a signaller using specialized morphology or behaviors to influence the current or future behaviors of another individual (Owren et al., 2010). Animals communicate in response to different tasks, including alarm calls, allocation of food, courtship, and mating (Searcy and Nowicki, 2010). Courtship signaling is essential for

mate recognition and is frequently multimodal. Animals can use chemical signals (pheromones), vocalizations, color patterns, and movements during courtship displays (Mendelson and Shaw, 2012; Higham and Hebets, 2013). Courtship allows females and males to ensure that they are mating with an animal of the same species, and present information about their quality as a potential mate (Breed and Moore, 2012). There is a growing interest in studying mating signals with bright-colored patterns and intricate courtship displays in both terrestrial and aquatic organisms, such as those in peacock spiders (Girard et al., 2011, 2018; Taylor and McGraw, 2013), birds of paradise (Scholes, 2008; Scholes et al., 2017; Ligon et al., 2018), and siamese fighting fish (Ma, 1995). Cephalopods are renowned for their dynamic displays for courtship and agonistic competitions for potential mates (Hall and Hanlon, 2002; Naud et al., 2004; Allen et al., 2017; Lin et al., 2017; Lin and Chiao, 2018). The development of these elaborate displays is often driven by intense sexual selection, providing an excellent system to study behavior and sexual selection in mating systems (Andersson, 1994).

Most coastal coleoid cephalopods (e.g., octopus, cuttlefish, and squids) have a short life span of one or two years and die shortly after spawning (Jereb and Roper, 2005, 2010; Jereb et al., 2013; Lu and Chung, 2017). Cephalopods also have the most complicated central nervous system of all invertebrates at both anatomical and functional levels (Boycott, 1961; Nixon and Young, 2003; Shigeno et al., 2018), and possess unique colorblind camouflage, mimicry, and communication abilities (Hanlon and Messenger, 2018). Cephalopod dynamic body patterns are directly controlled by their brain and continuously adapt to match the visual perception of the environment, communicate with mates, and solve different tasks (Boycott, 1961; Darmaillacq et al., 2014; Liu and Chiao, 2017; Gonzalez-Bellido et al., 2018; Hanlon and Messenger, 2018). These dynamic body patterns are composed of multiple chromatic, textural, locomotor, and postural components simultaneously expressed (Packard and Hochberg, 1977). For example, the Intense Zebra pattern of the mature male *Sepia officinalis* has white and black zebra bands on the mantle, white and dark fin spots, dilated pupils (chromatic components), smooth skin (textural components), dropping arms and extended fourth arm (postural components), and hovering display (locomotor components). This pattern is displayed by mature males cuttlefish, and it is used for sex recognition and agonistic behavior (Hanlon and Messenger, 1988).

Coleoid cephalopods have evolved several reproductive strategies in response to sexual selection. For instance, the hectocotylus, ligula, and calamus in males are morphological adaptations to transfer the sperm to the females (Voight, 1991, 2002; Thompson and Voight, 2003). Alternative mating tactics in squids and cuttlefish enhance the mating opportunities of small males by avoiding male competitions (Hanlon et al., 2002; Wada et al., 2005; Zeidberg, 2009; Brown et al., 2012; Lin and Chiao, 2018; Marian et al., 2019). Male octopus mate "at a distance" to escape and avoid sexual cannibalism (Hanlon and Forsythe, 2008; Huffard and Bartick, 2015). Promiscuity, mating aggregations, and sperm competition are also behavioral adaptations related to sexual selection in cephalopods (Hall and Hanlon, 2002; Jantzen and Havenhand, 2003; Naud et al., 2004; Morse and Huffard, 2019). For instance, several investigations have shown that multiple paternity occurs in some species, such as *Octopus minor* (Bo et al., 2016), *Octopus vulgaris* (Quinteiro et al., 2011), and the cuttlefish *Sepiella japonica* (Liu et al., 2019). Other studies in squids have found a sequence of pattern-based signals associated with determining dominance in reproductive battles (Lin et al., 2017; Lin and Chiao, 2018).

Current knowledge of cuttlefish reproductive interactions and visual signals is based primarily on four large-sized species [Mantle length (ML) of mature individuals > 300 mm]: (1) *Sepia apama* (Hall and Hanlon, 2002; Zylinski et al., 2011; Schnell et al., 2015a,b, 2019), (2) *Sepia latimanus* (Roper and Hochberg, 1988; Adamo and Hanlon, 1996; How et al., 2017; Hanlon and Messenger, 2018) (3) *Sepia officinalis* (Hanlon and Messenger, 1988; Adamo and Hanlon, 1996; Boal, 1997; Hanlon et al., 1999; Chiao et al., 2005; Mäthger et al., 2009), and (4) *Sepia pharaonis* (Lee et al., 2016; Nakajima and Ikeda, 2017). Over the past 30 years, additional pattern, textural, postural and locomotor components have been documented in these species. Each has species-specific body patterns, but they also share a high degree of similarity in some courtship body patterns common across many day-active shallow-water cephalopods. For example, the male zebra pattern (white and dark zebra bands across the mantle, arms and/or fins), and the passing cloud display characterized by coordinated waves of expanded chromatophores flowing as dark bands over the body (Hanlon and Messenger, 1988; How et al., 2017). Another iconic cuttlefish species is the small (ML < 110 mm) flamboyant cuttlefish, *Metasepia pfefferi*, which possesses over 100 display components (Roper and Hochberg, 1988; Thomas and MacDonald, 2016). *Metasepia pfefferi* is capable of showing elaborate body patterns, with three pairs of large and flap-like papillae in the dorsal mantle, long papillae over eyes, and passing clouds running in several directions simultaneously (Roper and Hochberg, 1988; Jereb and Roper, 2005; Laan et al., 2014; Thomas and MacDonald, 2016). Although many studies have demonstrated the complexity of cuttlefish visual signaling, the temporal structure of the multiple behavioral displays associated with reproduction is poorly-known. To date, only one study has analyzed the temporal order of the body pattern components expressed by the squid *Sepioteuthis lessoniana* during reproductive interactions (Lin et al., 2017).

Here we selected a relatively small-sized cuttlefish, *Sepia plangon*, which inhabits seagrass beds around Australian coastal waters (living depth < 85 m) (Jereb and Roper, 2005). Brown et al. (2012) reported the mating behavior of this species in the wild and in captivity. Unlike other large cuttlefish species (Dunn, 1999; Hall and Hanlon, 2002; Naud et al., 2004), *S. plangon* apparently does not form large aggregations for mating. As Brown et al. (2012) reported, this species forms small groups on the spawning grounds. Male-only assemblages (32.50%), male-female pairs (1M:1F, 25.00%), and groups of two males with one female (2M:1F, 12.50%) were the most frequent. Interestingly, five small males (ML < 80.00 mm) displayed a deceptive body pattern in the presence of a female and a larger male. This dual-lateral display consisted of two simultaneous body patterns, one on each half of the mantle. Males showed the typical male coloration

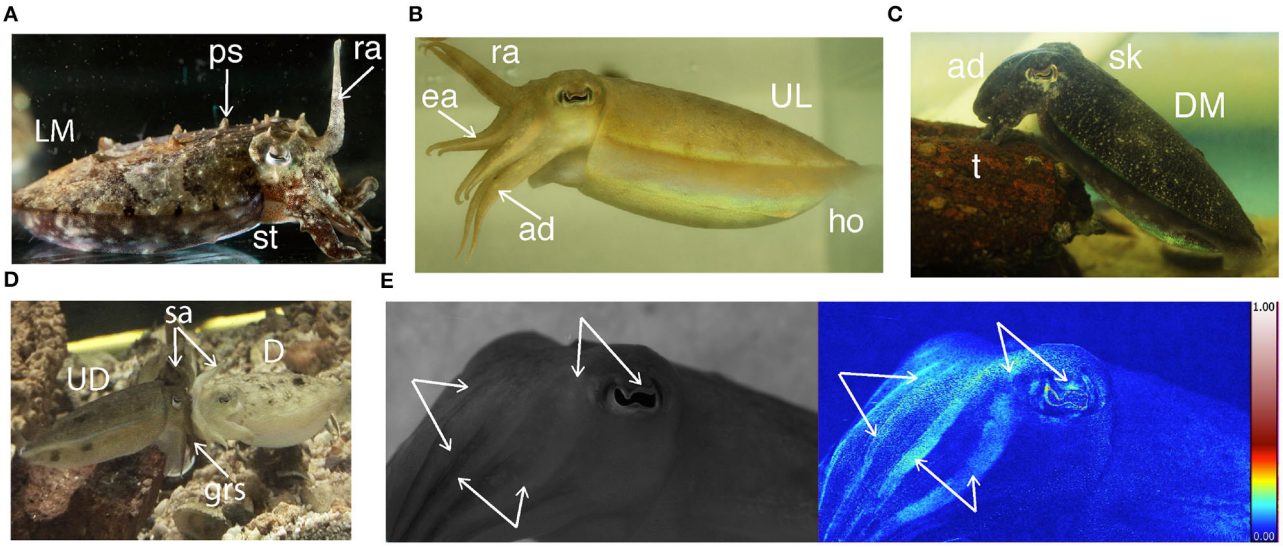

FIGURE 1 | Some of the body patterns of *S. plangon*. **(A)** Male with raised arms (ra), papillate skin (ps), sitting (st), and light mottle (LM). **(B)** Female. Hovering (ho), raised I arms (ra), extended II and III arms (ea), dropped arm (ad), and uniform light (UL) pattern. **(C)** Female in tripod posture (t), dropped arms (ad), smooth skin (sk), and dark mottle pattern. **(D)** Female and male in head-to-head mating position with splayed arms (sa), male grasping (grs), uniform darkening (UD), and deimatic pattern (D). **(E)** Male cuttlefish. The white arrows refer to polarized arm stripes and polarized eye sclera. The blue-red scale bar represents the percentage of polarization from 0 (blue) to 1 (white) through (red) which is typical for polarization in nature.

toward their counterparts but displayed the female appearance to a larger male to avoid fighting (Brown et al., 2012). In addition to the repertoire of visual signals, *S. plangon* spawns multiple times (Beasley et al., 2017), making this species suitable for observation of repeated mating behavior.

S. plangon has a single type of visual pigment (λmax 499 nm), suggesting that this species, like other cuttlefish species (Marshall and Messenger, 1996), is unable to detect or respond to colors through their retina (Chung and Marshall, 2016). *Sepia plangon* does possess orthogonally-arranged photoreceptors enabling sensitivity to polarized (PL) signals. This species may discriminate 1^0 e-vector difference, the highest PL resolution in animals with PL vision studied to date (Talbot and Marshall, 2010a,b; Temple et al., 2012). Additionally, *S. plangon* reflects PL light via iridophores located under the skin, forming strong PL signals on arms, the frontal area of the head, and around eyes (**Figure 1**). These signals are similar to those of *S. officinalis* (Shashar and Cronin, 1996; Shashar et al., 1996, 2002; Boal et al., 2004; Chiou et al., 2007; Mäthger and Hanlon, 2007; Mäthger et al., 2009; Cartron et al., 2013a,b,c). Several studies have proposed that PL vision enables a covert communication channel in cephalopods as many other animals are unable to detect the PL signals (Moody and Parriss, 1961; Jander et al., 1963; Tasaki and Karita, 1966; Saidel et al., 1983, 2005; Shashar and Cronin, 1996; Shashar et al., 1996, 2000, 2002; Boal et al., 2004; Talbot and Marshall, 2010b; Cartron et al., 2013a,b,c; Marshall et al., 2019). However, despite decades of study, the evidence is inconclusive and no behavioral function has been attributed to these signals.

To understand whether ambient light conditions affect mate choice, and which visual signals may influence the outcome of mating competitions, we selected *S. plangon* which can be reared in captivity and tested under different light conditions. First, we investigated the courtship and mate choice under different sex ratios. We evaluated whether the presence of polarized (POL) vs. unpolarized (UNPOL) barriers would affect the reproductive behavior of *S. plangon*, from courtship to mating. For example, we tested whether *S. plangon* started courtship and attempted to mate regardless of a barrier limiting physical contact between them (UNPOL), and regardless of a polarized filter (POL). Then, we used 3D resin-printed cuttlefish dummies with one static component of specific body patterns (e.g., large vs. small body size; PL vs. non-PL arm stripes, uniform light, dark uniform, weak zebra, strong zebra). We aimed to test if each component alone could trigger a response related to mating behavior, to ultimately understand the effect of each separate component in the complex courtship behavior of *S. plangon*.

2. METHODS

2.1. Animal Collection and Care

We collected 34 mature females and 32 males using seine nets in Dunwich, North Stradbroke Island, Queensland, Australia, between April-July 2016, August-October 2017, and Feb-May 2018. Our study was carried out following the permits by The University of Queensland - Animal Ethics Committee (permit number QBI/304/16), Queensland Government - Department of National Parks, Sports and Racing (Moreton Bay Marine Park Permit QS2018/CVL625), and Queensland Government - Department of Primary Industries and Fisheries (General Fisheries Permit 180731). Cuttlefish were placed individually in housing tanks of (610 × 600 × 450 mm) with running

seawater, which was monitored continuously using a filtered re-circulating water system (water temperature 20–24°C, salinity 35–36 psu, light-dark cycle 12–12 h) at Moreton Bay Research Station (MBRS). All tanks contained sand, rocks, and PVC tubes as substrates, and the cuttlefish were fed daily with live prey (e.g., glass shrimps and purple shore crabs *Hemigrapsus*) *ad libitum*. The animals were kept in housing tanks for at least a week before starting the behavioral experiments.

2.2. Pre-copulatory, Mating, and Postcopulatory Behavior

To analyze the effect of sex ratio in courtship behavior, a pair (a female and a male 1M:1F), or three cuttlefish (two males and a female 2M:1F, or one male and two females 1M:2F) were placed in a tank with a black acrylic divider to limit the visual contact for an hour prior to the start of each experiment (**Figures 2A–C**). Next, we removed the dividers between the tanks and recorded the cuttlefish interactions with four underwater cameras for at least an hour, or until animals stop interacting (1.5 h max) (**Figures 2I–K**).

Then using BORIS 7.7.4® Friard and Gamba (2016) to analyse the videos, we created a catalog of reproductive behaviors, agonistic fights, courtship, mating, mate guarding, and body patterns of *S. plangon*. The textural (skin texture), chromatic (body color), postural (body position), locomotor (body movement), and polarization components of the body patterns of *S. plangon* were also identified. We followed the body pattern descriptions by Hanlon and Messenger (1988), Borrelli et al. (2005), Schnell et al. (2015b), Thomas and MacDonald (2016), How et al. (2017) and Nakajima and Ikeda (2017) (**Table 1**). The body patterns were categorized into two groups: (1) Acute pattern (body patterns displayed for less than 5 min); (2) Chronic patterns (those lasting over 5 min) (**Table 1**). Furthermore, we classified the components of these body patterns in two categories: (1) Point events with a duration of 5 s or less, and (2) State events, which were visible for more than 5 s (**Table 1**).

2.3. Polarized vs. Non-polarized Barriers

Next, to study the effect of light conditions on the reproductive behavior of *S. plangon*, we put polarized (POL) or unpolarized (UNPOL) neutral density barriers between the cuttlefish and recorded the behavioral interactions in the three sex ratios mentioned above (1M:1F, 2M:1F, and 1M:2F, **Figures 2D–H**). Due to the small number of males collected for our study, 2M:1F - POL trials were not conducted, (see **Supplementary Material** for more details). The polariser filter was a 42.00% Transmission Neutral Gray Acrylic Laminated Linear Polarizer (AP27-024T, American Polarizers Inc., USA). The filter was horizontally aligned and attached to a frame made of PVC tubes. A sheet of a white diffuser (PTFE sheet, Dotmar EPP Pty Ltd, Australia) was attached to the light source (Arlec 2x20W LED Work light, Arlec Australia Pty Ltd) placed above the tank. A piece of 0.3 soft neutral density filters (Lee Filters, UK) were glued to a float glass window on both sides to make the unpolarized barrier. Using the same video analysis method, we identified the chromatic, textural, postural, and locomotor components of the body patterns that *S. plangon* used for reproductive behavior under different light conditions. POL filters modified the polarization signals from arm stripes and body of *S. plangon*; therefore, a cuttlefish could barely see the polarized signals from a mate placed at the other side of the filter.

2.4. Statistical Analysis

We analyzed the frequency and duration (in seconds, sec) of the courtship, mating, agonistic fights, and mate guarding. Due to a large number of zeros from our frequency data (animals that did not start courtship or mate), we used generalized linear models (GLM) with negative binomial (NB) distribution. The duration was analyzed with two-way factorial ANOVAs, using sex ratio as one factor of 3 levels—1M:1F, 1M:2F, 2M:1F, and type of barrier as the second factor of two levels—Polarized (POL) or Unpolarized (UNPOL). Cuttlefish like other cephalopods use their body patterns for communication; therefore, to demonstrate that a specific sequence of signals is determinant for mate choice in *S. plangon*, we transformed each body pattern and component to alphabetic codes of one to five letters (**Table 1**). Consecutively, we analyzed the data using text mining methods (Silge and Robinson, 2016) to estimate the frequency and the association of body patterns, such as radar charts and correlations with Bonferroni correction for multiple comparisons. All the analyses were conducted in (RStudio Team, 2015) v1.2.1335® (RStudio Team, 2015) using the packages FactoMineR v1.42 (Lê et al., 2008), tidyverse v1.2.1 (Wickham et al., 2019a), tidytext v0.2.2 (Silge and Robinson, 2016), dplyr v0.8.3 (Wickham et al., 2019b), widyr v0.1.2 (Robinson, 2019), tokenizers v0.2.1 (Mullen et al., 2018), quanteda v1.5.1 (Benoit et al., 2018) and igraph v1.2.4.1 (Csardi and Nepusz, 2006).

2.5. 3D Printed Cuttlefish Models

We selected five body pattern components from those observed in successful mating (see the details in results, and **Table 1**) for further tests using 3D printed resin cuttlefish. We downloaded the 3D models from CGTrader (https://www.cgtrader.com, see **Appendix** for more details). Then, we edited them using the software Blender® version 2.79. The models were printed using Stereolithography to 0.1 mm layer thickness, using a Form2 (Formolabs®) 3D printer at the Australian National Fabrication Facility, Queensland Node (ANFF-Q), and The University of Queensland Library 3D-printing facilities. Dummies (DUM) of two sizes (60 or 90 mm ML) were compared to analyze the effect of body size in mating choice. We measured the importance of body posture using dummies with arms extended or dropped. The models were painted with acrylic paints to simulate four body patterns, such as uniform light (UL) and dark mottle (DM) for females, or intense zebra (IZ) and weak zebra (WZ) for males. We attached stripes of polaroid or neutral-density filter to the arms of the dummies to simulate polarized and unpolarized arm stripes, respectively. All dummies were attached to a thin fishing line to place them into the testing tank. For this experiment, we counted a successful mate choice if a cuttlefish showed interest in the dummy, either by initiating courtship or attempting to mate. Negative

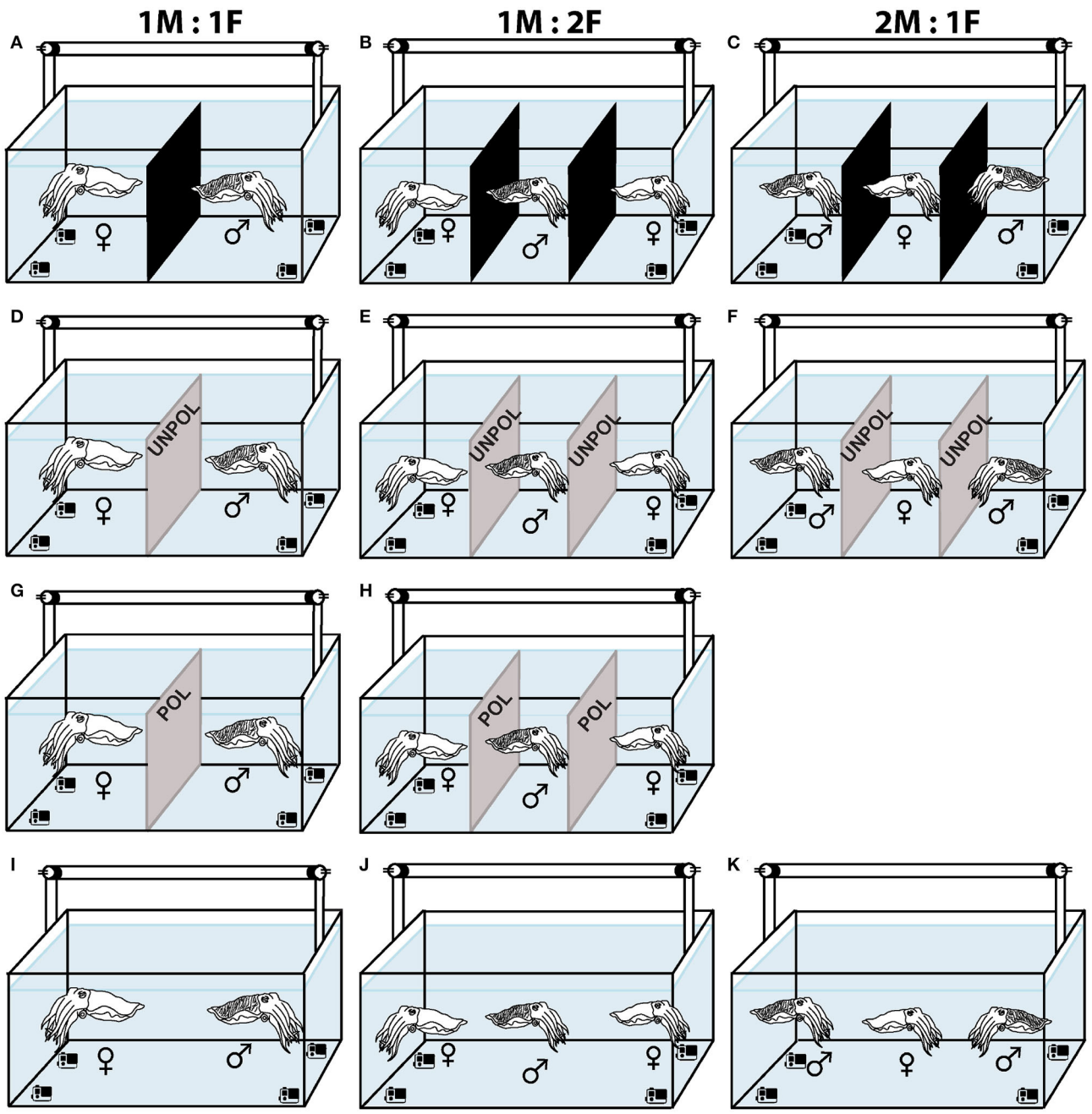

FIGURE 2 | Schematic representation of the experimental design for mate choice. ♀ = Females. ♂ = Males. **(A)** One pair and three cuttlefish **(B,C)** with black dividers to limit visual contact before the start of the experiments. **(D)** Two cuttlefish with an unpolarized (UNPOL) barrier between them. **(E,F)** Three cuttlefish with unpolarized barrier in the tank. **(G)** A male and a female with a polarized (POL) barrier between them. **(H)** Three cuttlefish with polarized barrier in the tank. **(I–K)** Two or three cuttlefish in control (DIRECT) condition. **(A,D,G,I)** Sex ratio = 1M:1F. **(B,E,H,J)** = 1M:2F. **(C,F,K)** = 2M:1F.

results were assigned if cuttlefish ignored, showed aggressive behavior, or remained distant from the dummies. We considered agonistic behavior as a negative result because we used the dummies to test whether the static body pattern could trigger courtship and mating behavior, as all these trials were intersexual experiments (male dummy for females, and female dummies for males).

3. RESULTS

We collected 34 mature females and 32 males. Females were larger than males, with mantle length (ML) (mean ± SD) = 74.92 ± 13.02 mm, and total length (TL) = 103.55 ± 21.23 mm. Males ML was 65.62 ± 10.15 mm, and TL = 90.41 ± 13.66 mm. We analyzed the behavior of *S. plangon* during 41h of video

TABLE 1 | Body patterns and their components of *S. plangon* and the alphabetic code used in this study.

Components - Body patterns	Code				
REPRODUCTIVE BEHAVIORS (3)					
Courtship display Ω	C	Mate Guarding Ω	MG	Mating Δ	M
BODY PATTERNS (18)					
Chromatic Pulse Π	CP	Dark Mottle Π	DM	Deimatic Π	D
Dual-Lateral Display Π	DLD	Dynamic Polarization SignalsΠ	DPS	Flamboyant Π	F
Intense Zebra Π	IZ	Lateral Display Π	LD	Light Mottle Ψ	LM
Multidirectional Passing Wave Display Π	MDPWD	Shovel Display Π	SHD	Strong Disruptive Π	STD
Stipple Π	ST	Uniform Blanching Π	UB	Uniform Darkening Π	UD
Uniform Light Ψ	UL	Weak Disruptive Ψ	WD	Weak Zebra Ψ	WZ
CHROMATIC COMPONENTS (28)					
Anterior Head Bar Δ	ahb	Anterior Mantle Bar Δ	amb	Anterior Transverse Mantle Line Δ	atml
Dark Arms Δ	da	Dark Arm Stripes Δ	das	Dark Eye Ring Δ	der
Dark Fin Spots Δ	dfs	Dark Zebra Bands Δ	dzb	Dilated Pupil Δ	dp
Large White Mantle Spots Δ	lwms	Latero-Ventral Patches Δ	lvp	Mantle Margin Scalloping Δ	mmsc
Mantle Margin Stripe Δ	mmst	Median Mantle Stripe Δ	mms	Paired of Mantle Spots Δ	pms
Posterior Head Bar Δ	phb	Posterior Mantle Bar Δ	pmb	Posterior Transverse Mantle Line Δ	ptml
White Arm Spots Δ	was	White Fin Spots Δ	was	White Head Bar Δ	whb
White Major Lateral Papillae Δ	whb	White Mantle Band Δ	wmb	White Neck Spots Δ	wns
White Posterior Triangle Δ	wpt	White Splotches Δ	ws	White Square Δ	wsq
White Zebra Bands Δ	wzb				
POSTURAL COMPONENTS (14)					
Arms Dropped Δ	ad	Bipod Δ	bi	Buried Δ	b
Elongated body Δ	eb	Extended II, III Arms Δ	ea	Extended IV Arms Δ	eaf
Flanged Fin Δ	ff	Flattened Body Δ	fb	Fully Extended I - IV Arms Δ	fe
Raised I, II Arms Δ	ra	Raised Head Δ	rh	Sitting Ω	st
Splayed Arms Δ	sa	Tripod Ω	t		
LOCOMOTOR COMPONENTS (12)					
Ambling Ω	a	Flee Δ	f	Forward Rush Δ	fr
Grappling Ω	grp	Grasping Ω	grs	Hiding Ω	h
Hovering Ω	ho	Inking Δ	i	Swimming Ω	sw
Turning toward a Mate Δ	ttm	Water Jetting Δ	wj	Waving arms Ω	wa
IRIDISCENT COMPONENTS (6)					
Iridescent Eye Sclera Δ	is	Iridescent Green/Blue Arm Stripes Δ	igas	Iridescent Green/Blue Mantle Margin Stripe Δ	igmm
Iridescent Pink/Orange Arm Stripes Δ	ipas	Iridescent Pink/Orange Mantle Margin Stripe Δ	ipmm	Iridescent Ventral Mantle Δ	ivm
TEXTURAL COMPONENTS (3)					
Coarse Skin Δ	cs	Papillate Skin Δ	ps	Smooth Skin Ω	sk

State component = Ω, Point component = Δ, Acute pattern = Ψ, Chronic pattern = Π.

analysis. The data were collected from 17 control experiments (no barrier between cuttlefish), four POL trials, four UNPOL observations, and eight DUM experiments ($n = 33$). Nine males were allocated to 1M:1F trials, nine more to 1M:2F condition, and 14 males in 2M:1F tests. Twenty-one males initiated courtship displays (65.63% from the total), and 17 males mated at least once, representing 80.95% success rate of courtship displays. On the other hand, nine females were tested in 1M:1F trials, 18 females in 1M:2F, and seven more in 2M:1F observations, but only 16 females mated (47.06% from the total).

3.1. Body Patterns and Courtship Display of *Sepia plangon*

We identified a total of 18 body patterns in *S. plangon* (**Table 1**, **Figures 1**, **3**). Males exhibited all 18 patterns, whereas females only showed 12. Following the general classification of cephalopods' body patterns, we classified them into two categories, Acute and Chronic (**Table 1**).

3.1.1. Acute Body Patterns

Eleven body patterns with a brief duration fell under this category. Acute patterns had a duration from seconds (sec) to a few minutes.

- 1. Chromatic pulse (CP, mean duration ± standard deviation = 50.75 ± 34.36 sec) (How et al., 2017), also known as "passing clouds" (Hanlon and Messenger, 1988), was a dynamic expansion and contraction of chromatophores to produce bands running in a single direction across the body.
- 2. Deimatic pattern (D, 28.48 ± 25.89 sec) (Hanlon and Messenger, 1988) was characterized by paling

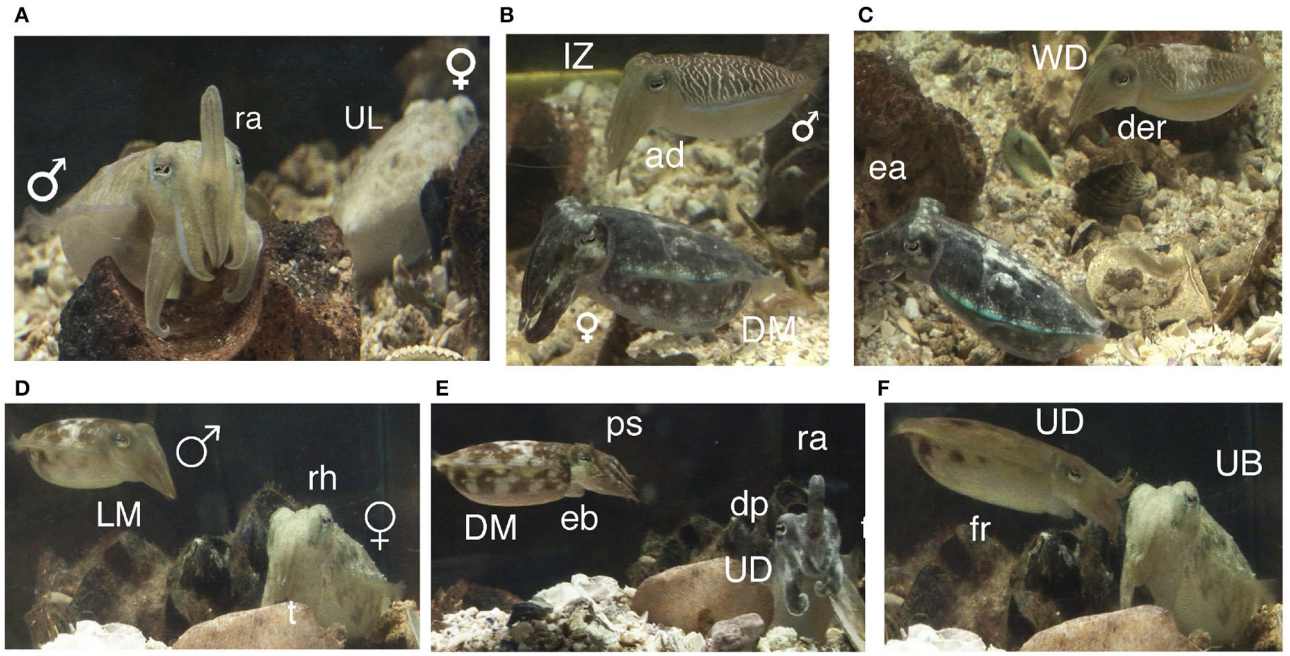

FIGURE 3 | Signals and body patterns of *Sepia plangon* during courtship. The images were from the same pair during the same interaction. **(A)** Before courtship, a male with raised arms (ra) and female with uniform light pattern (UL). **(B)** Male began the courtship with Intense Zebra pattern (IZ) and arms dropped (ad), whereas female showed Dark Mottle pattern (DM). **(C)** Male transitioning to Weak Disruptive (WD) and dark eye ring (der). Female maintained rejection signal (Dark mottle) and extended arms (ea). **(D)** Male with light mottle (LM). Female in tripod posture (t) and raised head (rh). **(E)** Male with elongated Body (eb), DM, and papillate skin (ps). Female showed Uniform Darkening (UD), dilated pupils (dp) and ra. **(F)** Female switched to uniform blanching pattern (UB) while male with UD coloration rushed forwards (fr) to touch the female's head.

and flattening of the body, a pair mantle spots (pms), dark eye rings (der), dilated pupils (dp), and smooth skin (SK).

– 3. Dual-lateral display (DLD, 141.35 ± 252.70 sec) (Brown et al., 2012) was characteristic of small males during agonistic contests. This pattern incorporated two patterns simultaneously. Males mimicked female coloration by showing light or dark mottle pattern in one half of the mantle. This strategy was used to avoid fighting with rivals. However, in the other half of the mantle, "sneaker males" showed the typical male coloration (intense or weak zebra) to the female.

– 4. Dynamic polarization signals (DPS, 191.10 ± 353.20 sec) (**Supplementary Video 3**): this hitherto undescribed pattern involved dynamic expansion and contraction of chromatophores only in areas where cuttlefish reflects polarized light (e.g., around the eyes, and in the arm stripes), producing bands running in a single direction in these regions. This pattern was expressed exclusively during courtship by males.

– 5. Flamboyant (F, 43.69 ± 43.68 sec) (Hanlon and Messenger, 1988) included papillate skin (ps), splayed arms (sa), dark mottle (DM) coloration, and latero-ventral patches (lvp). *Sepia plangon* displayed flamboyant primarily in the context of defense, but the males also showed this pattern if the females rejected any mating attempt by dropping the arms or moving away from the male.

– 6. Intense zebra (IZ,930.14 ± 1144.17 sec) (Hanlon and Messenger, 1988) was exclusive to males, and it included dark and white zebra bands (dzb, wzb) on the mantle, dark eye rings, smooth skin, and extended IV arms toward another male (eaf).

– 7. Lateral display (LD, 36.26 ± 49.15 sec) (Schnell et al., 2015a) was an agonistic signal from males characterized by light and dark moving bands over the mantle (chromatic pulse in the present study), with the body-oriented laterally to rivals and dark arms or face.

– 8. Multidirectional passing wave display (MDPWD, 214.86 ± 221.81 sec) (How et al., 2017) was similar to chromatic pulse; however, the bands moved in different directions across the body. We observed that small males exhibited this coloration when the females rejected them during courtship.

– 9. Shovel Display (SHD, 190.38 ± 290.26 sec) (Schnell et al., 2015a) incorporated the mantle raised, and rigid arms extended in a shovel-like shape. Large male *S. plangon* produced this pattern as an aggressive signal at the beginning of every male contest (See **Supplementary Figure 1**).

– 10. Uniform Blanching (UB, 59.16 ± 25.39 sec) (Hanlon and Messenger, 1988) was characterized by a fast retraction of all chromatophores creating a pale appearance.

– 11. Uniform Darkening (UD, 83.57 ± 20.89 sec) (Hanlon and Messenger, 1988) was a quick expansion of all chromatophores seen as an instant darkening of the body.

3.1.2. Chronic Body Patterns

The duration of these displays extends to several minutes. This category encompassed seven body patterns.

- 1. Strong Disruptive (STD, 231.00 ± 323.33 sec) (Hanlon and Messenger, 1988) comprised bold transverse and longitudinal components, both light and dark.
- 2. Weak Disruptive (WD, 578.76 ± 673.95 sec) (Hanlon and Messenger, 1988) is similar to strong Disruptive, but the contrast between dark and light components is less vivid. Both STD and WD had a maximum duration of 846.49 sec.
- 3. Dark Mottle (DM, 953.54 ± 1068.44 sec) (Hanlon and Messenger, 1988) had white and dark dots distributed in the arms, head, and dorsal mantle.
- 4. Light Mottle (LM, 781.52 ± 765.29 sec) (Hanlon and Messenger, 1988) made the overall body tone pale with some of the dark chromatophores expressed as spots or splotches.
- 5. Uniform Light (UL, 263.18 ± 326.51 sec) (Hanlon and Messenger, 1988) had a body coloration similar to white, as the expansion of chromatophores was minimum.
- 6. Stipple (ST, 64.71 ± 61.15 sec) (Hanlon and Messenger, 1988) included light body coloration with small dark spots due to the partial expansion of some chromatophores and papillate skin.
- 7. Weak Zebra (WZ, 673.51 ± 710.70 sec) (Hanlon and Messenger, 1988) was a low-contrast zebra patterning, with white and black zebra bands covering the mantle. Males showed this body color throughout courtship displays.

3.2. Courtship, Agonistic, and Mating Behavior

Before courtship, cuttlefish often camouflaged with light mottle, weak disruptive, or stipple patterns to match with the background of the testing tank. After 1–32 min, males turned toward one female and initiated a courtship display (C) in 20 trials (60.61%). Mating was observed at least once in 17 of 33 experiments (courtship success = 85.00%). *Sepia plangon* had multiple matings (**Figure 4**), and all the males that mated showed at least one courtship display to the female. Mating was not observed without prior courtship display.

The courtship started when a male showed quick changes of body patterns to the female, and it lasted until both cuttlefish adopted the mating position (head-to-head). Courtship excluded agonistic encounters between males and mating. Courtship latency was then the time before males showed any courtship behavior, and it had a duration of 60.00 to 1923.50 sec. Males initiated courtship displays with the repetitive sequence of seven fast changes of body patterns (**Figure 3**). The courtship display was formed with an orderly sequence of body patterns starting with light mottle, followed by intense zebra, weak zebra, dark mottle, uniform blanching, uniform darkening, and dark mottle (**Figure 3**). Intense zebra was continuously observed in 2M:1F trials, but males in 1M:1F and 1M:2F trials showed intense zebra pattern only at the beginning of courtship display. The components of the body patterns during courtship quickly changed from smooth to papillate skin, elongated body (eb), raised arms (ra), flattened body (fb), fully extended I - IV arms (fe), and forward rush (fr) (**Figures 3E,F**).

Agonistic signals between males encompassed intense zebra display with dark eye rings, extended IV arms to push competitors away from the female, lateral display, raised head, and shovel display. Escalation to agonistic fights was observed only during one trial, (2M:1F with no barrier between cuttlefish) where two males engaged in three aggressive fights. The ML difference between males that showed only agonistic signals was 13.64±9.33 mm. On the other hand, males that initiated agonistic contests had a size difference in ML of 6.48 mm. The average size of winner males was 64.13 ± 11.67 mm of ML, whereas, loser males had 65.49 ± 9.09 mm of ML.

Similar to other cuttlefish, *S. plangon* mated in head-to-head position (**Figure 1D**). Eight females (23.53% from all females) and eight males (25.00% from all males) coupled only once, five females (14.71%) and seven males (21.88%) mated twice, one female (2.94%) and a male (3.13%) had three copulations, and two females (5.88%) and a male (3.13%) had four.

3.2.1. Sex Ratio

In 1M:2F experiments, the males first chose a female to court but also approached and courted the other female if rejected by the first mate. Rejection signals by the females consisted of dark mottle coloration, dark eye rings, dropped arms, and moving away from the male.

In 2M:1F observations, the males established dominance using agonistic signals. Agonistic signals between males encompassed intense zebra display with dark eye rings, extended IV arms to push competitors away from the female, shovel, and lateral display. Cuttlefish presented these agonistic signals only in six control experiments (2M:1F), where cuttlefish had no barrier between them. Escalation to physical fights included animals grappling (grp) their opponent and inking (See **Supplementary Figure 1**). We observed male-male fight only in one trial; hence, male dominance was established primarily by agonistic visual signals. The dominant male remained close to the female and was the first to start the courtship display. Furthermore, the dominant males were the first to mate with the female. Five "sneaker" males (see **Supplementary Figure 1**) avoided fights by simulating female coloration in five control trails (2M:1F), and this strategy led to successful matings by four males (80.00% success rate). Dominant males guarded the female (Mating Guarding, MG) before, during, and after copulation. MG consisted of males with Intense Zebra coloration, or dark mottle, hovering close to the females while extending the IV arms toward competitors. Small males also guarded the paired female, but only in the absence of another competitor.

3.2.2. Polarized / Unpolarized Barriers

POL and UNPOL barriers did not prevent cuttlefish from attempting to mate (See **Supplementary Figure 1**), as we observed five females and males attempting to mate while they were separated by the POL ($n = 2$) and UNPOL ($n = 3$) barriers (See **Supplementary Figure 1**). Similar body patterns and behaviors were observed in these trials to those seen in experiments without a barrier, such as courtship display by males (including forward rush trying to push the barrier), females raising the first pair of arms, and both the female and male adopting the head-to-head mating position with spread arms.

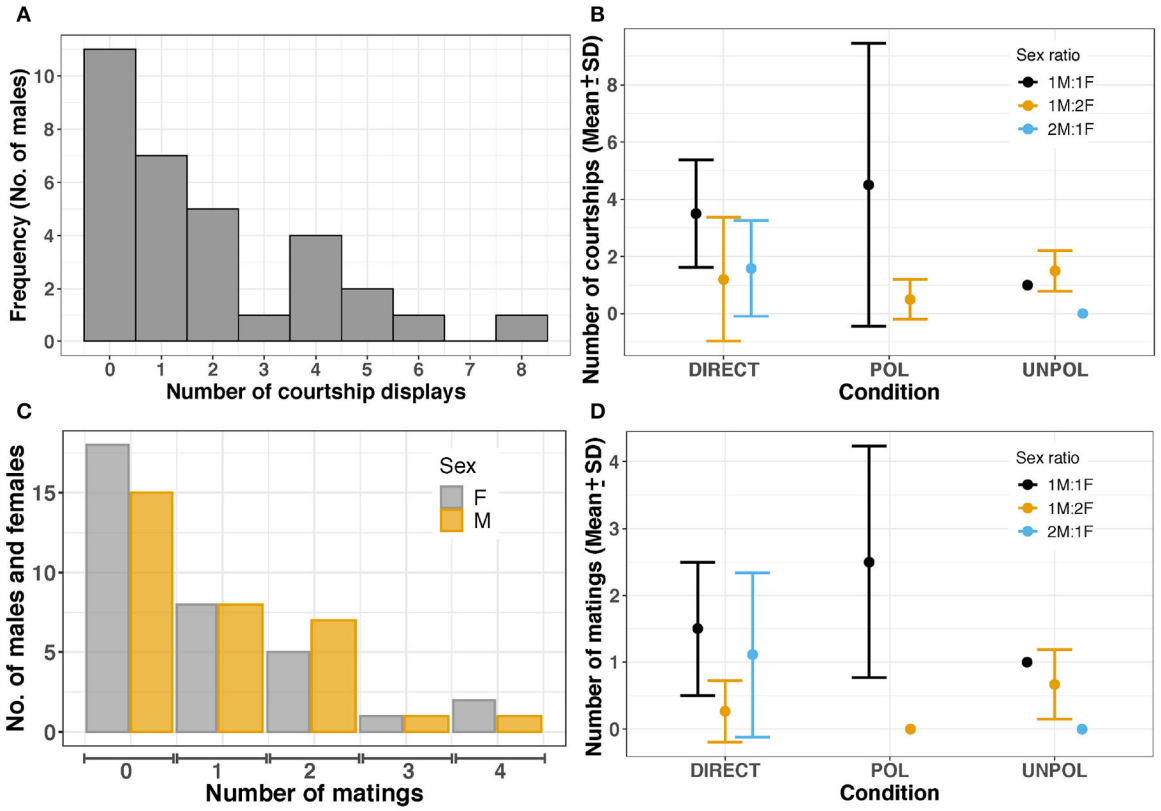

FIGURE 4 | (A) Total frequency of courtship displays by males **(B)** Frequency of courtship displays. Large dots and bars represent the mean and standard deviation, respectively. DIRECT, control (no barrier); POL, polarized barrier; UNPOL, unpolarized barrier. Sex ratio = 1M:1F in black, 1M:2F in yellow, 2M:1F in blue. **(C)** Mating frequency in females and males. **(D)** Mean and standard deviation of mating frequency in both males and females. No courtships were observed in 2M:1F - UNPOL experiments. In 1M:2F - POL trials ($n = 2$), only one male started courtship. No matings were observed in 1M:2F - POL and 2M:1F - UNPOL trials.

Mating duration in POL and UNPOL observations was measured from the moment when both cuttlefish attempted to mate. Cuttlefish spread their arms and moved toward each other to adopt the head-to-head mating position despite of the barrier between them. We considered the end of a mating attempt when both cuttlefish moved apart. We observed males and females pushing the barrier trying to reach each other during the matting attempts.

3.3. Frequency of Courtship Displays, Male Competitions, and Copulations

3.3.1. Frequency

Sepia plangon males males had an average of 1.88±2.11 courtship displays. The maximum number of courtship displays was eight in a 1:1 - POL experiment. Males courted females in all 1M:1F trials, five of nine 1M:2F experiments, and all 2M:1F trials (**Figure 4**). Cuttlefish in 1:1 - POL condition showed more courtship displays than cuttlefish in the other conditions tested (4.50 ± 4.95). However, the negative binomial GLM suggested that sex ratio was the only variable with a significant effect on courtship frequency, as it was more likely that any male initiated courtship in 2M:1F condition (b=−1.017, p=0.034) than 1M:2F (b=−1.017, p=0.034). Four male cuttlefish started courtship displays in 1M:1F, but they were unable to attract females for successful mating. The courtship frequency of the four loser males was 2.25±1.97, whereas in winner males it was 2.94 ± 1.98.

The most frequent agonistic signal was dark eye ring with a maximum of 73 counts (19.90 ± 19.91), followed by intense zebra (max frequency = 16, 3.78 ± 4.27), extended IV arms (max frequency = 32, 1.16 ± 5.66), raised head (max = 5, 0.56 ± 1.22), shovel display (max = 8, 0.38 ± 1.43), mate guarding (max = 2, 0.16 ± 0.45), and lateral display (max = 2, 0.09 ± 0.39). Furthermore, winner males showed agonistic signals more frequently than losers, particularly dark eye rings and intense zebra pattern.

Overall, the mating frequency was 0.86 ± 1.11, but the highest number of copulation attempts (due to the physical limitation by a barrier) was observed in POL - 1:1 condition (2.50 ± 1.73) (**Figure 4D**); however, GLM did not find any effect by Sex ratio or POL condition on mating frequency ($p > 0.05$).

3.3.2. Duration

Courtship duration was highly variable as males exhibited courtship displays between one to eight times (**Figure 4A**). The shortest courtship was 11.75 sec, and the longest was 1867.35 sec,

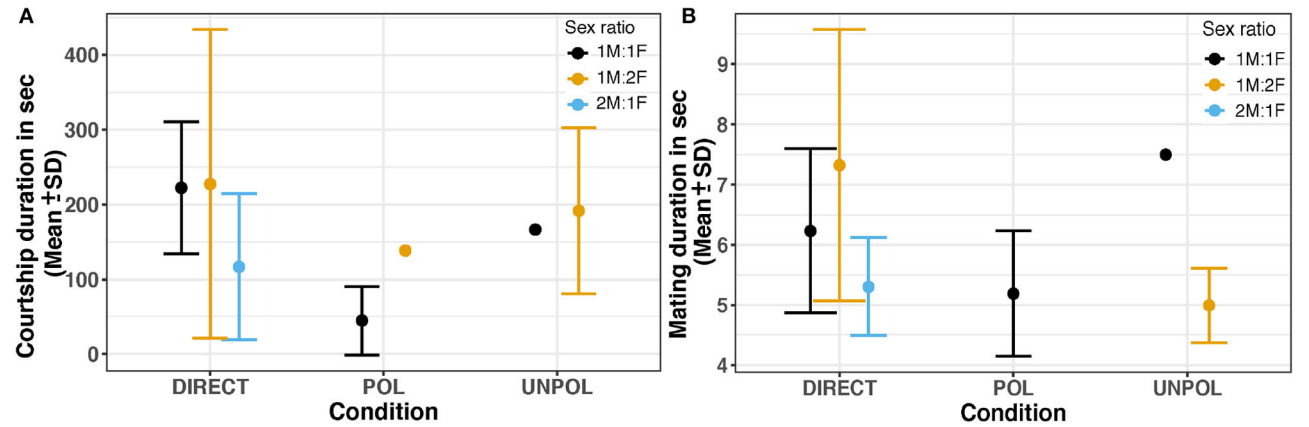

FIGURE 5 | (A) Courtship duration in second. **(B)** Mating duration (s). Large dots and bars represent the mean and standard deviation, respectively. DIRECT, Control (no barrier); POL, Polarized Barrier; UNPOL, Unpolarized barrier. Sex ratio = 1M:1F in black, 1M:2F in yellow, 2M:1F in blue.

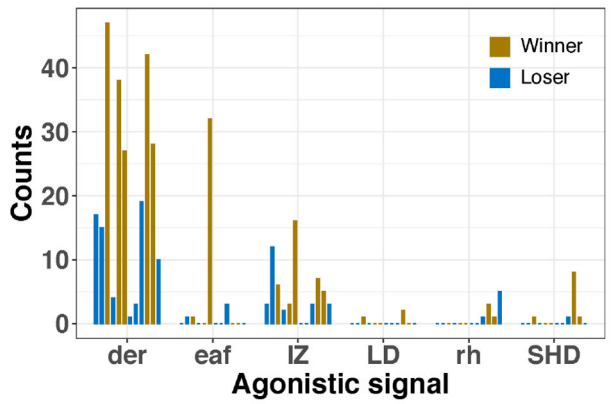

FIGURE 6 | Frequency of each agonistic signal by every male during male competitions. Dark eye ring (der), extended arm IV (eaf), Intense Zebra pattern (IZ), lateral display (LD), raised head (rh), and shovel display (SHD). Each bar represents a male and the number of times each signal was observed. Winners in yellow and losers in blue.

with a mean of 161.22 ± 106.82 sec. We analyzed courtship duration with Factorial ANOVAs using transformed data (as the relative percentage from total duration (%), and also z-scores); however, the sex ratio and types of barriers did not have a significant effect on courtship duration ($p > 0.05$) (**Figure 5A**).

We described the DPS as a new pattern (see **Supplementary Video 1**), which was observed in three 1M:1F - control tests, one 1M:2F - control experiment, and one 2M:1F - unpolarized test. The duration of DPS was 191.101 ± 353.20 sec. Males displaying DPS pattern had a high success rate of mating, as four males mated using this particular display (80.00%).

The agonistic signal with intense zebra coloration had a duration of 930.14 ± 1144.17 sec. This pattern was present in 19 control experiments (57.58%), one POL (3.03%), and three UNPOL observations (9.09% from all the trials). Cuttlefish exhibited shovel displays only in six control trials and had duration 190.38 ± 290.26 sec. Only two cuttlefish showed the lateral display pattern, with a duration of 36.255 ± 49.15 sec in two observations (2M:1F - control). Four cuttlefish showed mate-guarding behavior with duration 289.07 ± 288.04 sec in 2M:1F control experiments.

The cumulative mating duration was between 4.35 and 24.826 sec, with a mean of 10.31 ± 0.66 sec. Statistical analysis did not reveal any significant differences in mating duration ($p > 0.05$) among the sex ratios and polarized conditions tested in our study (**Figure 5B**).

3.4. Differences in Type and Sequence of Body Patterns Between Successful and Non-successful Courtships

Cuttlefish displayed up to 17 body patterns during courtship, agonistic fights, mate guarding, and copulation. Males showed a specific sequence of body patterns for courtship display (**Figure 3**), including light mottle, intense zebra, weak zebra, dark mottle, uniform blanching, uniform darkening, and dark mottle. Rapid changes between smooth and papillate skin, elongated and flattened body, extended arms, forward rush, dark eye rings, and turning toward the female were also part of courtship displays. Males that mated at least once displayed up to 17 body patterns and 33 body pattern components (**Figures 6**, **7B**, **8B,C**, **9A,C**); whereas loser males exhibited a maximum of 12 body patterns, and 24 components (**Figures 7C**, **9B–D**). The most frequent signals amongst winner males were dark eye ring, elongated body, forward rush, raised arms, and papillate skin, dark mottle, light mottle, uniform blanching, and uniform light (**Figures 9A,C**).

We identified 32 sequences of components and body patterns that were relevant for successful mating. Males showed these sequences for at least five times throughout courtship displays. These sequences were made of combinations between one textural component (ps), a locomotor component (fr), two postures (eaf, ra), one chromatic component (der), and four

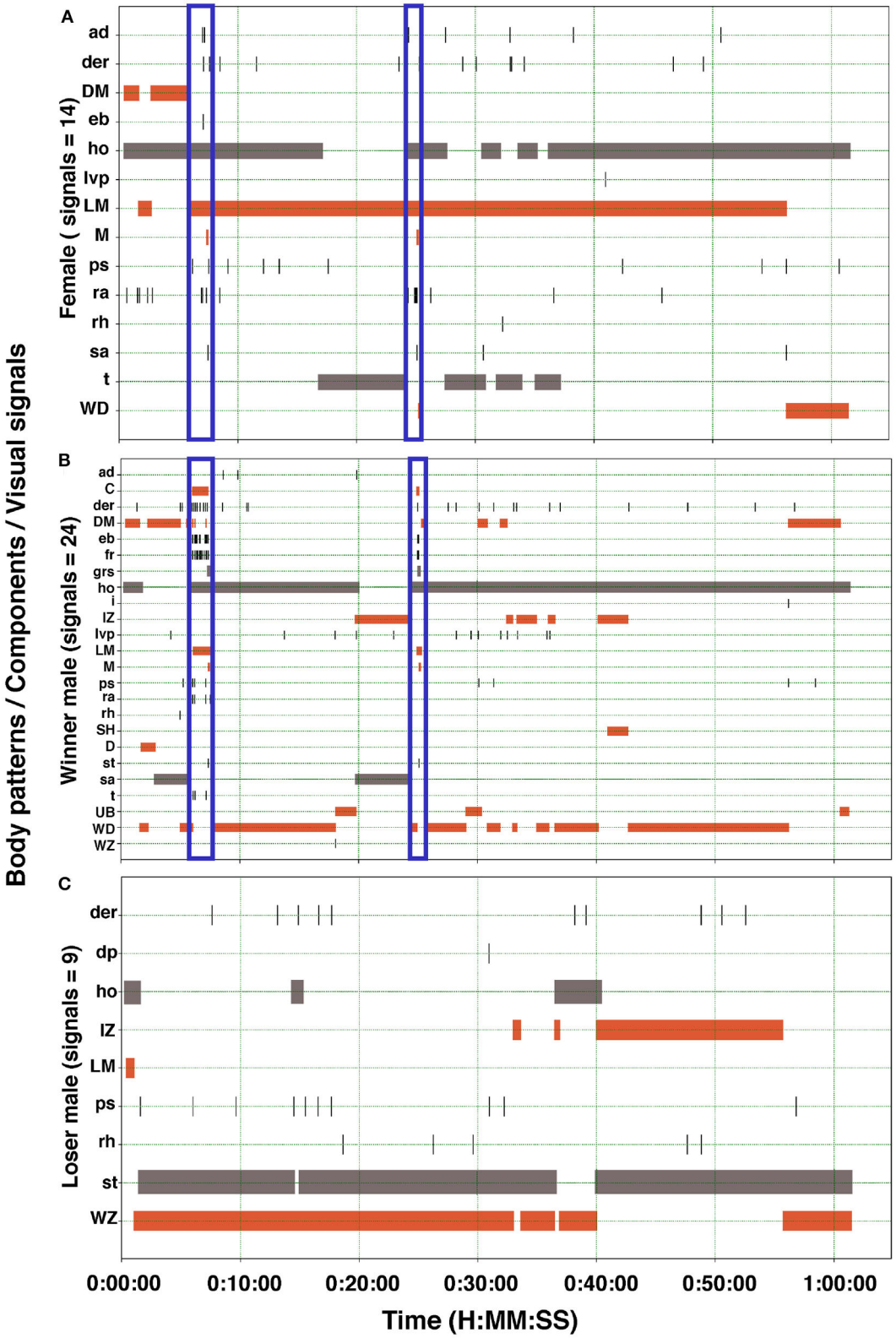

FIGURE 7 | Ethogram of the body patterns and behaviors of two males and a female *S. plangon* showed for courtship and mating. The orange horizontal bars represent duration of the chronic patterns. Gray bars denote state events. Black vertical lines correspond to point events and acute patterns. Blue vertical rectangles encompass signals during courtship and mating. **(A)** In this observation, the female displayed 14 visual signals (Body patterns and components). **(B)** Winner male displayed up to 24 signals, whereas the loser male **(C)** showed only nine. See **Table 1** for the codes' abbreviations.

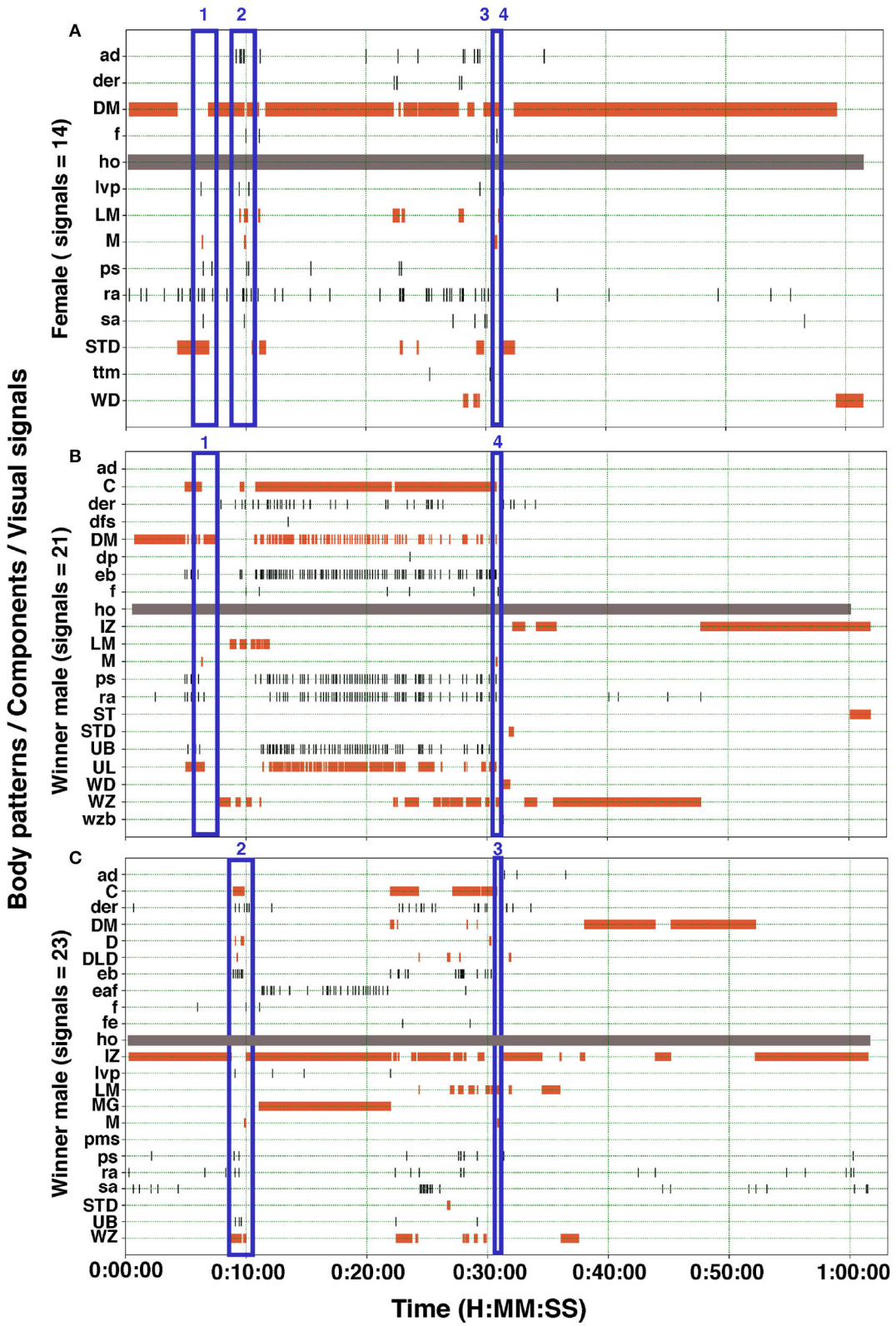

FIGURE 8 | Ethogram of the body patterns and reproductive behaviors of two males and a female *S. plangon*. In this experiment, the female **(A)** mated twice with each male **(B,C)**. The orange horizontal bars represent duration of the chronic patterns. Gray bars denote state events. Black vertical lines correspond to point events and acute patterns. Blue rectangles encompass signals during courtship and mating. The numbers above the blue rectangles represent the mating events. Mating 3 and 4 occurred very near to each other. See **Table 1** for the codes' abbreviations.

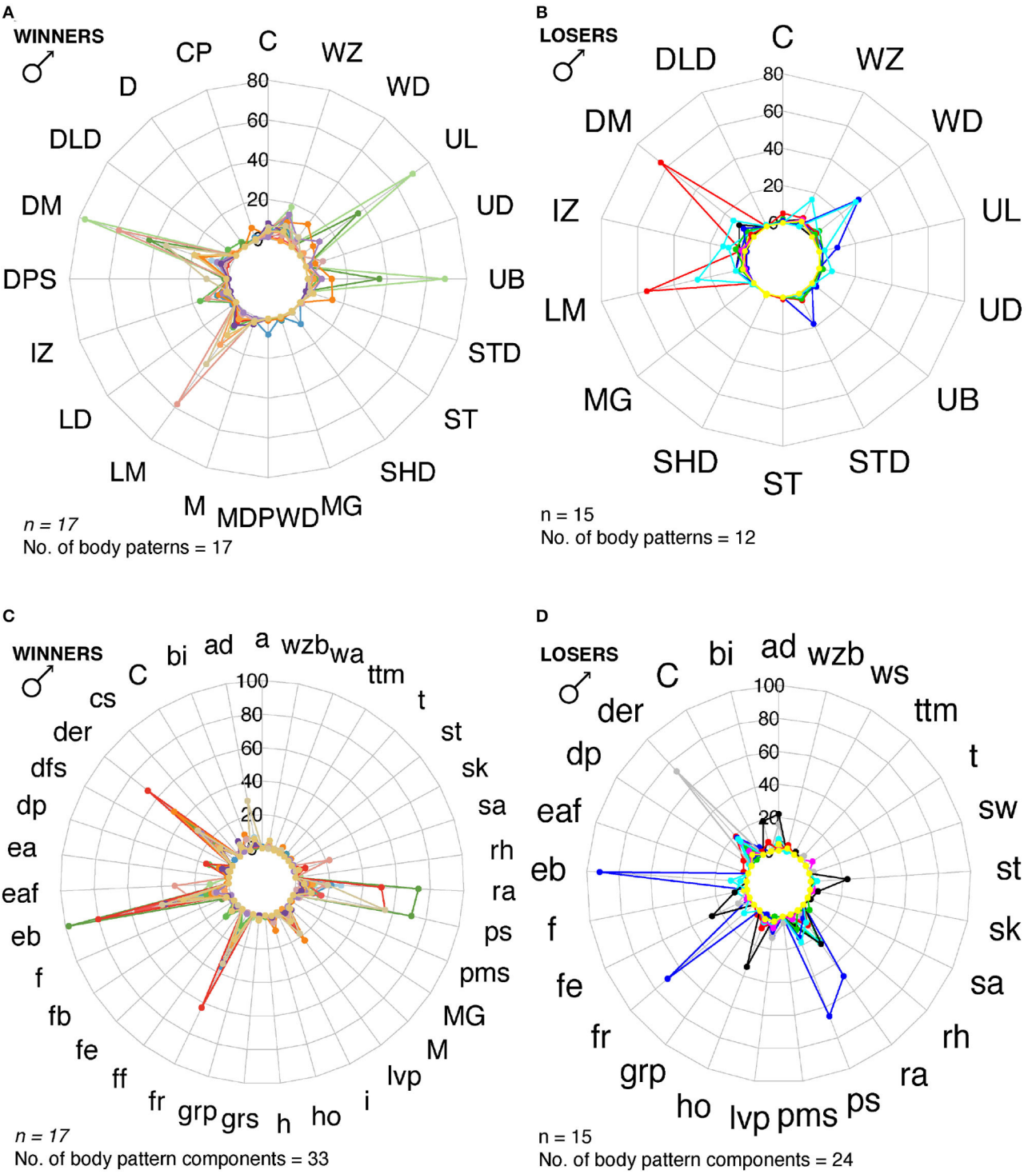

FIGURE 9 | Radar charts representing the number of body patterns and components that winner and loser males used for reproductive behavior. Each colored line corresponds to a different individual. **(A)** Winner males ($n = 17$) showed a max of 17 body patterns. **(B)** Winner males showed 33 body pattern components. **(C)** Loser males ($n = 15$) displayed a max of 12 body patterns, and 24 body pattern components **(D)**. M, Mating; MG, Mate Guarding; C, Courtship. See **Table 1** for the codes' abbreviations.

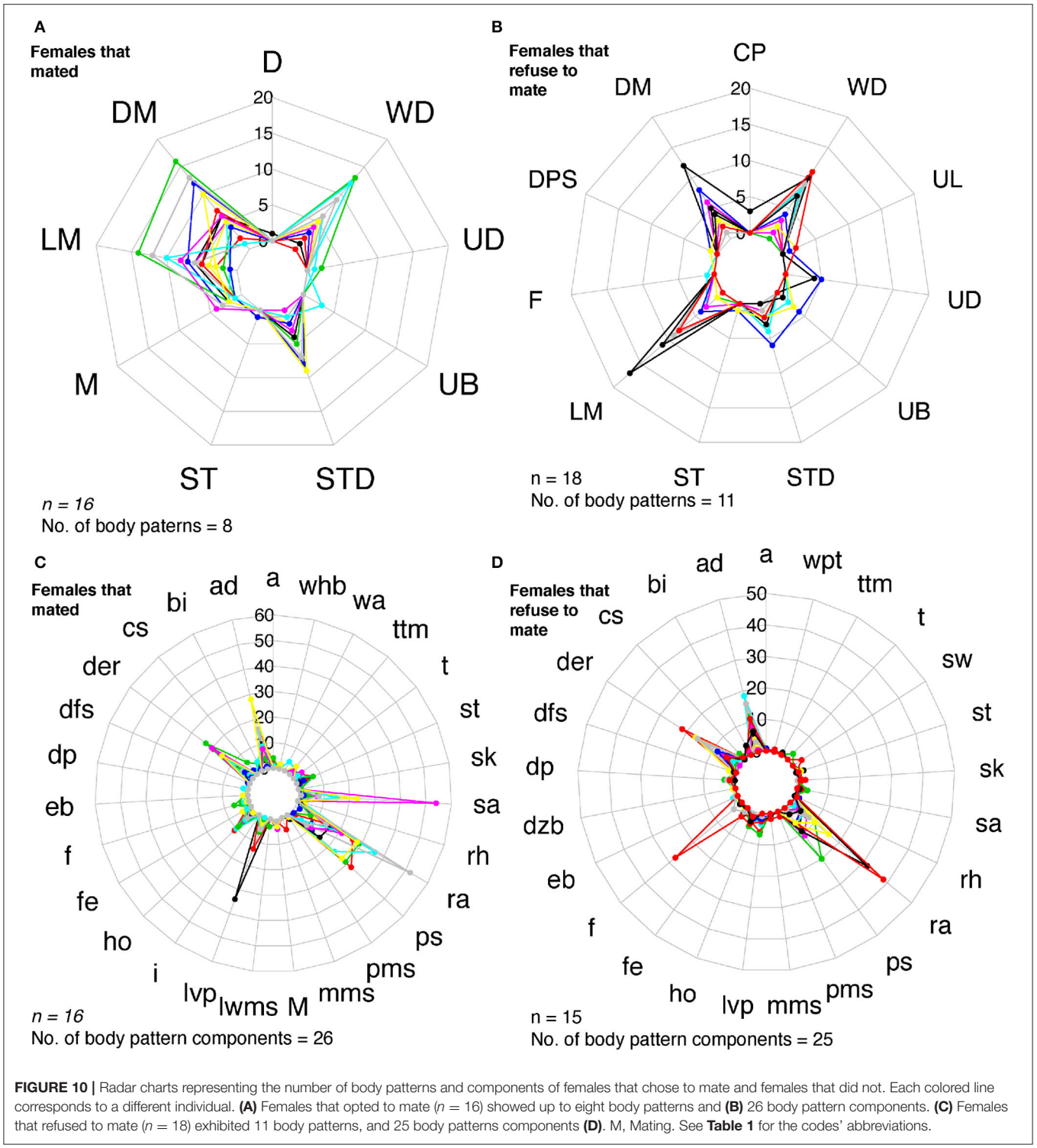

FIGURE 10 | Radar charts representing the number of body patterns and components of females that chose to mate and females that did not. Each colored line corresponds to a different individual. **(A)** Females that opted to mate ($n = 16$) showed up to eight body patterns and **(B)** 26 body pattern components. **(C)** Females that refused to mate ($n = 18$) exhibited 11 body patterns, and 25 body patterns components **(D)**. M, Mating. See **Table 1** for the codes' abbreviations.

patterns (DM, UB, UL, and LM) in an orderly fashion (**Figure 11A**). Losers showed a similar sequence of body patterns and components; however, the frequency of these signals was much lower than those displayed by winner males (**Figure 6**). On the other hand, females showed 43 visual signal sequences before mating. One textural component (ps), one locomotor (a), three postural (ad, ra, sa), two chromatic (der, lvp), and five patterns (DM, LM, UB, WD, STD) encompassed the sequences in females for mating (**Figures 10A,C**, **11B**). On the other hand, females that refused to mate kept the arms dropped, dark eye rings, fled and

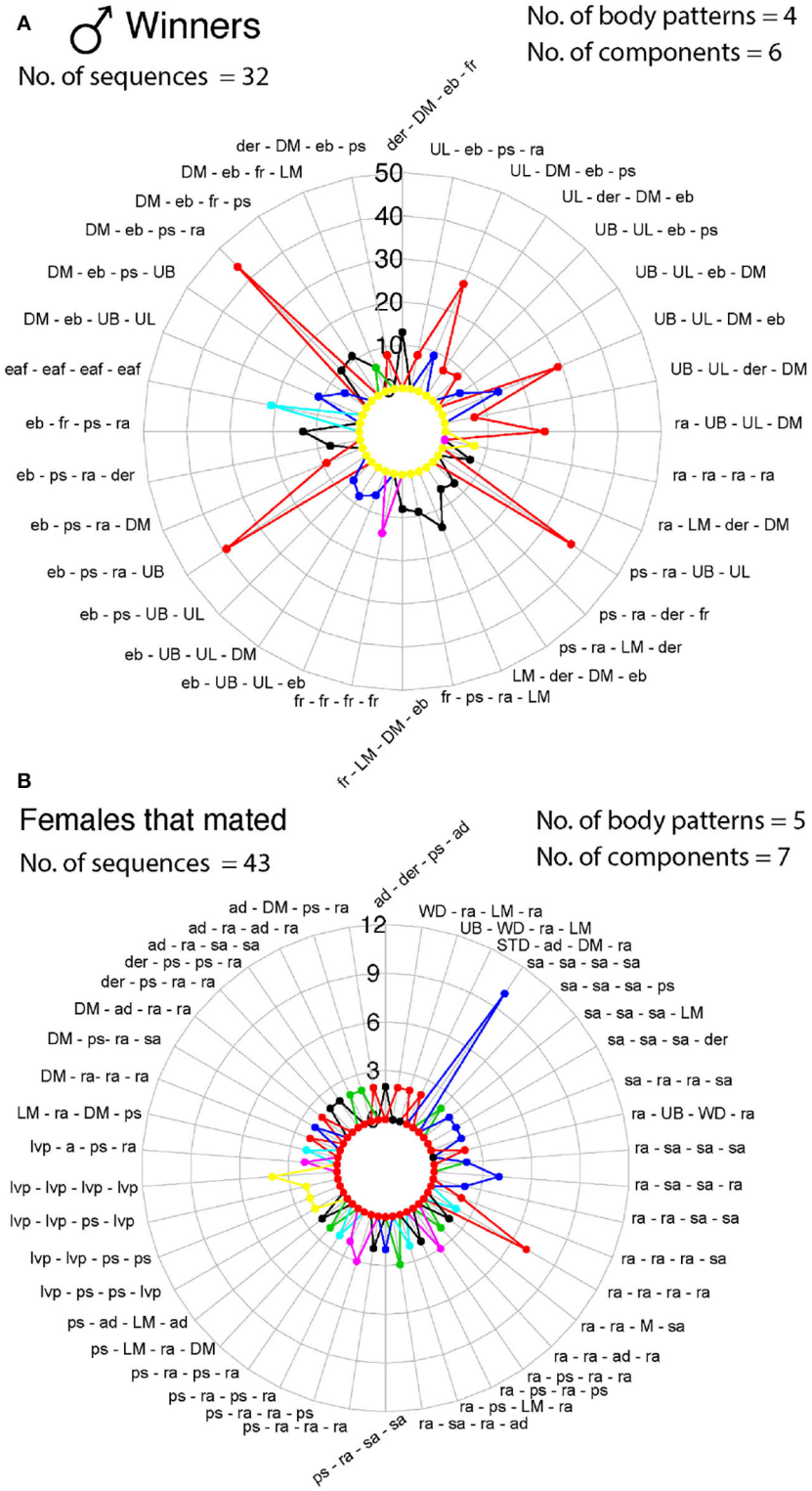

FIGURE 11 | Radar charts representing the sequence of signals (body patterns and components) that *S. plangon* used for mating. Each colored lined represents a cuttlefish. Each sequence was observed more than twice in all cuttlefish. **(A)** Winner males. A total of 32 sequences were observed in males that successfully mated. Combinations of four body patterns (DM, LM, UB, and UL) and six components (der, eb, ps, fr, eaf, and ra) were observed in all sequences. **(B)** Females that were inclined to mate exhibited up to 43 sequences; however, the frequency of these signals was lower than those in males. Five body patterns (DM, LM, UB, WD, and STD), and seven components (a, ad, der, ps, ra, sa, lvp) were showed by the females for these sequences. See **Table 1** for the codes' abbreviations.

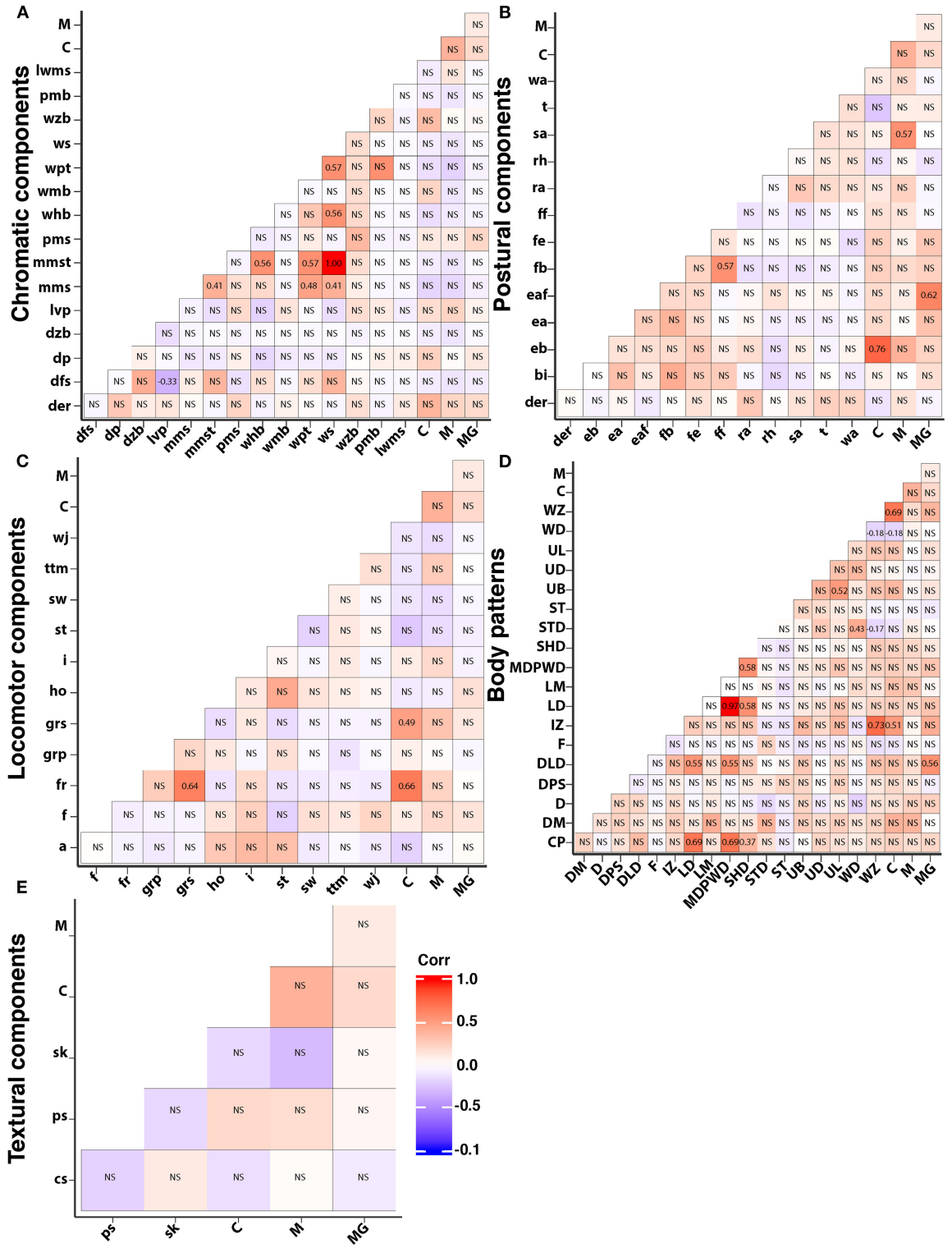

FIGURE 12 | Heatmap with pairwise correlations between all the body patterns, components, and courtship (C), mating (M), mate guarding (MG) of *S. plangon*. Red squares are positive correlations and blue are negative. Non significant *p* values are marked with NS. **(A)** Chromatic components. **(B)** Postural components. In this case, the only component correlated to courtship was elongated body. Similarly, splayed arms was significantly correlated to mating, and extended IV arm to mate guarding. **(C)** Locomotor components. Courtship was significantly correlated to forward rush and grasping. **(D)** Intense zebra, weak disruptive, and weak zebra were significantly correlated to courtship. **(E)** All Skin texture components were non-significant. See **Table 1** for all the codes' abbreviations. Significant *p*-values were marked with their corresponding coefficients of determination (r^2) in black numbers.

showed papillate skin as response to the courtship displays of the males (**Figures 10B,D**).

We integrated the data from all subjects into a matrix with the frequency of each behavior, body pattern, and component to analyze the correlation between them (**Figure 12**). We found that courtship was significantly correlated to forward rush (r^2=0.66, $p < 0.01$), grasping (r^2=0.49, $p < 0.01$), elongated body (r^2=0.66, $p < 0.01$), Intense Zebra pattern (r^2=0.51, p=0.01), Weak Disruptive (r^2=−0.183, p=0.042), and Weak Zebra pattern (r^2=0.69, $p < 0.01$). Mating was significantly correlated to splayed arms only (r^2=0.57, $p < 0.01$); while extended IV arms (r^2=0.62, $p < 0.01$) and Dual-Lateral Display (r^2=0.56, $p < 0.01$) were significantly correlated to mate guarding.

3.5. 3D Printed Cuttlefish

We analyzed the behavioral responses of the cuttlefish in the presence of one or two dummies (number of experiments, $n = 8$). However, cuttlefish did not attempt to mate with the dummies. *Sepia plangon* displayed defense signals, such as deimatic, dark mottle, strong disruptive, weak zebra, flee, hiding, inking, dilated pupils, and papillate skin toward the dummies, or remained away from them. No agonistic behavior was observed in these experiments.

4. DISCUSSION

This study is the first to describe in detail the mating behavior of *S. plangon* under different light conditions and sex ratios in captivity. The intricate mating system of *S. plangon* comprises male agonistic behavior and signaling, alternative reproductive tactics, female mate choice, and multiple matings. Furthermore, the temporal order of component and body pattern expression is critical to winning mating competitions, similar to the communication system in the reef squid (Lin et al., 2017).

In the spawning season, *S. plangon* showed strong sexual dimorphism as mature females were larger than males. Similar results were previously reported by Beasley et al. (2017). Larger females are relatively common in other cephalopod species, for example, in the squid *Dosidicus gigas* (Nigmatullin et al., 2001), the octopus *Eledone cirrhosa* (Regueira et al., 2013), and *Haliphron atlanticus* (Lu and Chung, 2017). On the other hand, *S. plangon* male size might be a critical factor that lead to the development of male alternative mating strategies similar to those in squids (Wada et al., 2005; Lin and Chiao, 2018), and octopus (Huffard et al., 2008). For instance, smaller males can use different mating behavior (e.g., male-upturned and sneaking) to avoid male competition and mate. In this study, we observed small *S. plangon* males using the dual-lateral display to avoid male competitions and mate with large females. Similar results were previously reported by Brown et al. (2012).

In our study, we observed that males *S. plangon* were smaller than females; therefore, it is likely that the body size does not determine male dominance in this species while in others such as *S.apama* it does (Hall and Hanlon, 2002). The number and variety of displays potentially act as signals to communicate male fitness, which could influence *S. plangon* female choice. Other investigations have shown that larger females generally have higher fecundity and produce larger offspring in mammals (Kilanowski and Koprowski, 2016), insects, and arthropods (Honěk, 1993; Fox and Czesak, 2000; Stillwell et al., 2010). Additionally, intersexual selection may drive the evolution of small male size in *S. plangon*, for example, small body size could be beneficial to males that show dynamic or acrobatic courtship (Székely et al., 2004).

4.1. Courtship Behavior, Agonistic Signals, and Mating

Sexually selected signals fall into two categories, signals used in inter-sexual displays (e.g., courtship), or signals used in intra-sexual displays (agonistic signals) as proposed by Andersson (1994). Courtship includes one or more sensory modalities (visual, olfactory, auditory, tactile, and some others), and often leads to the evolution of traits through sexual selection (Owren et al., 2010). Precopulatory processes occur in both females and males, such as male-male competitions, female and male mate choice (Kuester and Paul, 1996; Johannesson et al., 2008; Edward and Chapman, 2011; Hamel et al., 2015; Gwynne, 2016; Roberts and Mendelson, 2017). Postcopulatory mechanisms are sperm competition in males (Simmons, 2014), cryptic female choice (CFC), and cryptic male choice (CMC). CFC occurs when females use specific traits or mechanisms to influence the probability that males fertilize their eggs, whereas CMC is any male behavior that allows males to bias their investment in matings toward certain females (Eberhard, 1996; Reinhold et al., 2002; Arnqvist, 2014).

Previous literature has not found clear evidence of courtship displays in some cephalopods species, such as *S. apama* (Hall and Hanlon, 2002), *S. officinalis* (Boal, 1997; Adamo et al., 2000), *Idiosepius paradoxus* (Kasugai, 2000; Sato et al., 2010), and *Euprymna scolopes* (Hanlon et al., 1997). Nonetheless, intricate courtship displays have been described in *S. latimanus* (Corner and Moore, 1980; Hanlon and Messenger, 2018), and *S. sepioidea* (Moynihan and Rodaniche, 1982), and *Loligo pealei* (Hanlon, 1996). These patterns are characterized by quick changes in patterns and bright colorations (Hanlon and Messenger, 2018). It is notable in *S. plangon* that the chromatic changes described are in fact largely a-chromatic, that is black and white and most likely signaling in contrast, not color.

Males *S. plangon* potentially established dominance through the use of visual signals (**Figure 6**), such as intense zebra, extended IV arms, uniform blanching, dark eye rings, lateral display, uniform darkening, shovel display, and elongated body. Escalation to physical fights was only observed in one control experiment (2M:1F) and had a duration shorter than 6 s. Similar results were observed in the giant cuttlefish *S. apama* (Hall and Hanlon, 2002; Schnell et al., 2015b) and the squid *Loligo plei* (DiMarco and Hanlon, 1997), as males contest duration and frequency decreased by the presence of a female and whether temporary pairing had occurred. By contrast, smaller *S. plangon* males (ML < 80mm) showed the dual-lateral display (DLD) to sneak in and mate with females without fighting with a dominant male. Our results suggest that DLD is an efficient tactic that small cephalopod *S. plangon* use to avert a fight with larger rivals

and obtain opportunities to mate. Similar cases were reported in *S. plangon* by Brown et al. (2012), the squid *Sepioteuthis sepioidea* (Hanlon and Messenger, 2018), and *S. apama* (Hall and Hanlon, 2002; Naud et al., 2004; Hanlon et al., 2005). Males mimicking females are also commonly observed in birds, lizards, and crustaceans. For instance, male pied flycatchers use female mimicry as an advantage to choose when to initiate an attack, thus increasing the chances of winning male contests (Saetre and Slagsvold, 1996). Males Augrabies flat lizards often mimic female coloration to avoid the injuries and energetic cost associated with fighting other males; however, they still use male pheromones as an honest signal of their gender for mating (Whiting et al., 2009). Spider crabs (Laufer and Ahl, 1995), and isopods (Shuster, 1989; Shuster and Wade, 1991) also use female mimicry as an alternative mating tactic to access females and avoid male competitions.

In our study, we observed four male cuttlefish mate-guarding the females only in 2M:1F control experiments. The guarded females were large, fully mature, carrying eggs, and had ML between 73.00 and 90.00 mm. We did not determinate the number of eggs carried by the guarded females; however, this strategy could represent a cryptic male choice, as males could bias their mate-guarding efforts toward particular females (Aumon and Shuker, 2018). The bobtail squid *Sepiadarium austrinum* exhibited strategic male choice as their mating efforts were more substantial toward egg-carrying females (Wegener et al., 2013; Hooper et al., 2016). Similarly, large male *Abdopus aculeatus* copulate frequently in mate-guarding situations with large females Huffard et al. (2008). Several studies have reported temporary mate guarding in several species of cephalopods, such as *S. apama* (Hall and Hanlon, 2002; Naud et al., 2004), *S. officinalis* (Adamo and Hanlon, 1996; Hanlon and Messenger, 2018), and *Loligo pealeii* (Shashar and Hanlon, 2013). Precopulatory mate guarding might allow the male to monopolize the female until she is receptive, and postcopulatory mate guarding could prevent females from prematurely removing the sperm and ensure insemination.

We observed only one female mating with both males; however, fifteen females had multiple matings (**Figures 7A**, **8A**), and nineteen females did not mate once. Possibly, potential pre and postcopulatory CFC also occur in *S. plangon*, as some females rejected mating attempts, but others had multiple matings with several males. Potentially, females *S. plangon* could choose the sperm that fertilizes their eggs. Previous investigations have analyzed CFC in squids (Sato et al., 2013, 2014, 2016; Shashar and Hanlon, 2013; Mather, 2016; Lin and Chiao, 2018; Iwata et al., 2019), and octopus (Huffard et al., 2008; Morse et al., 2015; Morse and Huffard, 2019); however, CFC studies in cuttlefish are limited (Boal, 1997; Hall and Hanlon, 2002; Naud et al., 2005). Boal (1997) found that females *S. officinalis* prefer to mate with males that had copulated recently. According to Hall and Hanlon (2002), *S. apama* might possess a mechanism for postcopulatory CFC. Two sources of sperm were available to the female to fertilize the eggs: (1) spermatangia from the most recent matings around the buccal region, and (2) sperm stored internally in receptacles located around the beak. Similar results were reported by Naud et al. (2005) in *S. apama* using genetic analysis. They found evidence supporting the biased use of sperm from those sources mentioned above, which suggests a potential postcopulatory CFC in this species. We collected animals from the wild and did not control whether females had already mated, which could reduce mating likelihood in our experiments. Future studies should focus on both female and male cryptic choice, comparing the probability of mating with virgin cuttlefish, and analyze whether females choose the sperm to fertilize the eggs from one male or another (Iwata et al., 2019).

The sex ratio was the only factor affecting courtship frequency in *S. plangon* of the two factors tested in our experiments. On the other hand, the intensity and frequency of male competitions in *S. plangon* were not affected by sex ratio. Similar results were reported in flies (Leftwich et al., 2012), and fish (de Jong et al., 2009; Clark and Grant, 2010), as the sex ratio had a significant effect on the courtship behavior and duration. Lobsters (Debuse et al., 1999), fish (Mills and Reynolds, 2003), and arthropods (Enders, 1993; Waiho et al., 2015) change the reproductive behavior depending on the sex ratio. For instance, at high male density (more than three males) large European bitterling males ceased to be territorial and instead competed with groups of smaller males (Mills and Reynolds, 2003). It is likely that our test did not trigger frequent aggressive male fights because we only placed two males with one female as the highest sex ratio for males.

POL and UNPOL barriers did not have a significant effect on the frequency and duration of courtship, agonistic encounters, and mating. However, the POL barrier caused a large variation in courtship and mating frequency (**Figure 4**). Likely, GLM did not find any statistical significance because we have more observations in control experiments than POL-UNPOL tests; thus, statistical power could be a limitation in our study. Although POL and UNPOL barriers limited the physical contact between cuttlefish and modified the light conditions, males started their repetitive courtship display. Several studies have suggested that polarized light is used in cephalopods for communication and navigation (Shashar and Cronin, 1996; Shashar et al., 2000; Boal et al., 2004; Saidel et al., 2005; Chiou et al., 2007; Talbot and Marshall, 2010b; Cartron et al., 2013a; Marshall et al., 2019); however, to date, there is no conclusive evidence that shows the function of polarization signals in the reproductive context. This study showed that changes in polarized light did not affect mating behavior in *S. plangon*, and that the presentation and sequence of body patterns were decisive for mate choice.

4.2. Visual Signaling and Communication

The body patterns of *S. plangon* are similar to those of *Sepia officinalis* (Hanlon and Messenger, 1988), *Sepia pharaonis* (Nakajima and Ikeda, 2017), and *M. pfefferi* (Roper and Hochberg, 1988; Thomas and MacDonald, 2016). We identified 18 body patterns in mature male and female *S. plangon*, whereas *S. officinalis* and *S. pharaonis* have only 13 (Hanlon and Messenger, 1988; Nakajima and Ikeda, 2017). Our study used mature individuals, whereas the descriptions of *S. officinalis, S. pharaonis*, and *M. pfefferi* were based on juveniles. Additionally, our study revealed signals and body patterns used for reproductive behavior, such as multidirectional passing wave display, shovel display, lateral display, and dynamic polarization

signals which were not reported in the studies of Hanlon and Messenger (1988), Thomas and MacDonald (2016), and Nakajima and Ikeda (2017).

Two patterns in *S. plangon* are rare in other cephalopod species: the dual lateral display (DLD), and the dynamic polarization signals (DPL). DLD was previously described in males *S. plangon* by Brown et al. (2012), and we also identified this pattern in five small males (ML < 80.00 mm) that were between a larger rival and a female. DLD is a deceptive signal, and similar to *S. sepioidea* (Hanlon and Messenger, 2018), and *S. latimanus* (Corner and Moore, 1980), is often used as an alternative method to avoid competitions and find females to mate. This behavior is not particular to cephalopods; male cricket frogs change their dominant calls in the presence of an opponent to mimic the female calls (Wagner, 1992). Likewise, females dance fly can also use deceptive signals to prey on males seeking for mates (Funk and Tallamy, 2000). The evolutionary consequences of deceptive displays are hard to interpret as they depend on the costs and benefits of deception to both senders and receivers (Stuart-Fox, 2005). We reported 80.00% of mating success in males *S. plangon* that used DLD to avoid male competitions; possibly, DLD is a common and successful strategy in the mating system of *S. plangon* (Brown et al., 2012).

We reported DPL as a new pattern in our study. This display was exclusive to males and used during courtship, and involved running bands across areas where cuttlefish reflected strong PL signals; four of five males successfully mated after showing this pattern. This pattern is similar to the Passing cloud display of *S. officinalis* (Hanlon and Messenger, 1988). However, the passing cloud was only reported in juveniles, and it is a defense mechanism involving bands running across the entire body. In contrast, DPS has dark bands running horizontally across the arms stripes and around the eyes. It is possible that *S. plangon* might control the intensity of PL signals for courtship by controlling the expansion and retraction of chromatophores as dark bands over the arms stripes. Although the evidence supporting the direct control of PL signals for communication in cuttlefish is not definitive yet (Shashar et al., 1996, 2002; Mäthger et al., 2009; Marshall et al., 2019), Gonzalez-Bellido et al. (2014) reported that the expression of iridescence in squids was controlled by the brain but also changed in response to environmental luminance. Thus, the iridophores in cuttlefish reflect strong PL signals potentially controlled by the brain, and these signals could be used for communication with conspecifics (Shashar et al., 1996). In this study we did not find any effect by POL and UNPOL barriers; however, the perspective of the animal under natural conditions should be considered in the future to investigate polarized vision and communication (Marshall et al., 2019).

S. plangon body patterns differed between the winner and loser males. Winners showed up to 17 body patterns and 33 components, whereas losers only showed 12 patterns and 24 components. Conversely, females that did not mate showed more body patterns (18) than mating females (16) (**Figure 10**). The dynamic and repetitive nature of the courtship displays was similar between winners and losers; however, the number of times that winner showed each pattern and component of the courtship was higher than those in loser (**Figure 4**). Highly repetitive signals may have provided more information about mate quality by transmitting the same message (courtship display) multiple times. Therefore, females could assess more accurately one or more stimuli that are displayed repeatedly before choosing a mate (Mowles and Ord, 2012). We identified 32 sequences of visual signals displayed by males *S. plangon* that were crucial for successful mating. These sequences were composed of combinations of four body patterns (DM, LM, UB, and UL) and six components (der, eb, ps, fr, eaf, and ra) in a specific order (**Figure 11**). Similarly, females showed up to 43 sequences composed of five body patterns (DM, LM, STD, UB, and WD) and seven components (a, ad, der, lvp, ps, ra and sa). Therefore, it was not just the presentation of these body patterns that led to mating, but the sequence of specific body patterns. A similar study done by Lin et al. (2017) analyzed the visual signals and body patterns of the squid *S. lessoniana* for reproductive behavior. They reported that each behavior was composed of multiple chromatic components, and each component is often involved in multiple behaviors. Thus, the dynamic body patterning and expression of unique sets of components represents an efficient communication system in squids. Our results suggest that *S. plangon* also use specific set of signals (body pattern, chromatic, postural, locomotor, and textural components) to communicate efficiently for successful mating. In females, the most frequent postural components for mating involved the arms (e.g., arms dropped, raised arms, and splayed arms), which could be associated with the fact that male cuttlefish deposit the sperm in the female's buccal area (Hall and Hanlon, 2002; Naud et al., 2004; Hanlon and Messenger, 2018). Therefore, females exposing the buccal area to the male could be interpreted as a positive cue for mating.

The dummies used in this study did not trigger behavioral interactions with the cuttlefish, suggesting that a static body pattern component is not a strong stimulus to start courtship behavior. One suggestion for future studies would be to present videos of real animals to the cuttlefish and see whether the video of a real mate triggers courtship behavior. In fact, Pignatelli et al. (2011) and Temple et al. (2012) have previously shown that squids and cuttlefish react to computer-generated polarized looming stimuli. However, these investigations did not test the reaction to a PL video of a real cuttlefish displaying courtship patterns.

This study was the first to report in detail the reproductive behavior of *S. plangon* under different sex ratios and light conditions. Sex ratio was the only factor that had a significant effect on courtship frequency. Furthermore, we showed evidence that the size or presentation of a specific body pattern and posture is not sufficient to initiate courtship behavior in *S. plangon*, as 3D models did not trigger any mating. We found that the number and specific order of sequences of body patterns and components are determinant for successful matings, presented as dynamic courtship signals. We introduced *S. plangon* as an attractive animal model and very convenient for laboratory behavioral studies due to its small size.

DATA AVAILABILITY STATEMENT

The original contributions presented in the study are included in the article/supplementary files, further inquiries can be directed to the corresponding authors.

ETHICS STATEMENT

The animal study was reviewed and approved by the Animal Ethics Unit, Office of Research Ethics of the University of Queensland (Permit number QBI/304/16).

AUTHOR CONTRIBUTIONS

AL performed the experiments, analyzed the data, and drafted the manuscript. All authors contributed to the design of experiments, manuscript revision, and approved the final version.

FUNDING

JM and WC supported by the Australian Research Council (ARC Laureate Fellowship FL140100197) and the Asian Office of Aerospace Research and Development (AOARD-12-4063). AL supported by Consejo Nacional de Ciencia y Tecnologia de Mexico (CONACYT), The University of Queensland, and Moreton Bay Research Station-SIBELCO scholarships.

ACKNOWLEDGMENTS

We acknowledge the Quandamooka People, Traditional Custodians of the lands, winds, and waters of Minjerribah (North Stradbroke Island). We pay our respects to Quandamooka Elders past, present, and future. We would like to thank Moreton Bay Research Station staff (Martin Wynne, Cameron Cotterell, Lucy Trippet, Elisa Girola, and Sheridan Rabbit) for supporting animal care work. We appreciate the fieldwork support from Timothy Boudreau, Miriam Henze, Bert Koster, Martin Luehrmann, Gaia Marini, Gabriel Perrit, Alisa Pie, and Gabriella Scatta. We also acknowledge the reviewers for constructive comments on the manuscript.

SUPPLEMENTARY MATERIAL

The Supplementary Material for this article can be found online at: https://www.frontiersin.org/articles/10.3389/fphys.2020.00845/full#supplementary-material

Supplementary Video 1 | The flickering effect in the video represent the areas where *Sepia plangon* reflect polarized signals. The video was recorded with a modified Sony©HVR-Z1P video-camera. The camera had a nematic switch-plate polarizer attached. Alternate horizontal (H) and vertical (V) polarizing were fitted every other frame.

Supplementary Video 2 | Video from a polarization camera. Left: intensity (black and white image). Center: degree (%) polarization, scale 0–100%, blue to white with deep-red at approximately 45%. Right: angle or e-vector direction, the circular key shows orange/red as horizontal and cyan as vertical. Video from a mature female *Sepia plangon*.

Supplementary Video 3 | Two cuttlefish *Sepia plangon* during courtship behavior. Male (top) showing dynamic polarization signals (DPS) to the female (bottom). This pattern appeared as moving bands and flashes over the arms stripes and eye sclera, which are areas with strong polarized reflection (see **Supplementary Video 2**).

Supplementary Figure 1 | Patterns and behaviors observed during courtship, agonistic, and mating in *S. plangon*. **(A)** Two males and a female. To the right, male showing shovel display (SHD) as agonistic signal to the other male. **(B)** Two males fighting for the female. Males showed Intense Zebra, or Dark Mottle coloration, dark eye rings, and extended Arms to push the competitor. Meanwhile, the female hold a dark mottle coloration. **(C)** A large male with intense zebra pattern pushing a small male away from the female. The small male showed light mottle pattern. **(D)** Close view of a male showing DLD, two patterns simultaneously (intense zebra and dark mottle). **(E)** "Sneaker" male showing dark mottle pattern to the other male, and intense zebra to the female. **(F)** A male and a female adopting the mating position in a experiment with a polarized barrier between cuttlefish. The barrier was attached to PVC pipes.

Supplementary Figure 2 | (A) Mantle length (ML) and **(B)** Total length (TL) of mature females (gray boxplot, $n = 34$) and males (yellow boxplot, $n = 32$) *S. plangon*.

REFERENCES

Adamo, S. A., Brown, W. M., King, A. J., Mather, L. D., Mather, J. A., Shoemaker, K. L., et al. (2000). Agonistic and reproductive behaviours of *Sepia officinalis* in a semi-natural environment. *J. Molluscan Stud.* 66, 417–419. doi: 10.1093/mollus/66.3.417

Adamo, S. A., and Hanlon, R. T. (1996). Do cuttlefish (Cephalopoda) signal their intentions to conspecifics during agonistic encounters? *Anim. Behav.* 52, 73–81. doi: 10.1006/anbe.1996.0153

Allen, J. J., Akkaynak, D., Schnell, A. K., and Hanlo, R. T. (2017). Dramatic fighting by male cuttlefish for a female mate. *Am. Natural.* 190, 144–151. doi: 10.1086/692009

Andersson, M. (1994). *Sexual Selection*. Chichester: Princenton University Press. doi: 10.1515/9780691207278

Arnqvist, G. (2014). "Cryptic female choice," in *The Evolution of Insect Mating Systems,* eds D. Shuker and L. W. Simmons (Oxford: Oxford Scholarship Online), 204–220. doi: 10.1093/acprof:oso/9780199678020.003.0011

Aumon, C., and Shuker, D. M. (2018). Cryptic male choice. *Curr. Biol.* 28, R1177–R1179. doi: 10.1016/j.cub.2018.07.071

Beasley, A. L., Hall, K. C., Latella, C. I., Harrison, P. L., Morris, S. G., and Scott, A. (2017). Reproductive characteristics of three small-bodied cuttlefish in subtropical waters. *Mar. Freshw. Res.* 69, 403–417. doi: 10.1071/MF17169

Benoit, K., Watanabe, K., Wang, H., Nulty, P., Obeng, A., Muller, S., et al. (2018). quanteda: An R package for the quantitative analysis of textual data. *J. Open Sour. Softw.* 3:774. doi: 10.21105/joss.00774

Bo, Q.-K., Zheng, X.-D., Gao, X.-L., and Li, Q. (2016). Multiple paternity in the common long-armed octopus *Octopus minor* (Sasaki, 1920) (Cephalopoda: Octopoda) as revealed by microsatellite DNA analysis. *Mar. Ecol.* 37, 1073–1078. doi: 10.1111/maec.12364

Boal, J. G. (1997). Female choice of males in cuttlefish (Mollusca: Cephalopoda). *Behaviour* 134, 975–988. doi: 10.1163/156853997X00340

Boal, J. G., Shashar, N., Grable, M. M., Katrina, H. V., Loew, E. R., and Hanlon, R. T. (2004). Behavioral evidence for intraspecific signaling with achromatic and polarized light by cuttlefish (Mollusca: Cephalopoda). *Behaviour* 141, 837–861. doi: 10.1163/1568539042265662

Borrelli, L., Gherardi, F., and Fiorito, G. (2005). *A Catalogue of Body Patterning in Cephalopods*. Florence: Firenze University Press. doi: 10.36253/88-8453-376-7

Boycott, B. B. (1961). The functional organization of the brain of the cuttlefish *Sepia officinalis*. *Proc. R. Soc. Lond. B Biol. Sci*. 153, 503–534. doi: 10.1098/rspb.1961.0015

Breed, M. D., and Moore, J. (2012). *Animal Behavior, 2nd Edn*. San Diego, CA: Academic Press.

Brown, C., Garwood, M. P., and Williamson, J. E. (2012). It pays to cheat: tactical deception in a cephalopod social signalling system. *Biol. Lett*. 8, 729–732. doi: 10.1098/rsbl.2012.0435

Cartron, L., Dickel, L., Shashar, N., and Darmaillacq, A.-S. (2013a). Maturation of polarization and luminance contrast sensitivities in cuttlefish (*Sepia officinalis*). *J. Exp. Biol*. 216, 2039–2045. doi: 10.1242/jeb.080390

Cartron, L., Josef, N., Lerner, A., McCusker, S. D., Darmaillacq, A.-S., Dickel, L., et al. (2013b). Polarization vision can improve object detection in turbid waters by cuttlefish. *J. Exp. Mar. Biol. Ecol*. 447, 80–85. doi: 10.1016/j.jembe.2013.02.013

Cartron, L., Shashar, N., Dickel, L., and Darmaillacq, A.-S. (2013c). Effects of stimuli shape and polarization in evoking deimatic patterns in the European cuttlefish, *Sepia officinalis*, under varying turbidity conditions. *Invertebr. Neurosci*. 13, 19–26. doi: 10.1007/s10158-013-0148-y

Chiao, C.-C., Kelman, E. J., and Hanlon, R. T. (2005). Disruptive body patterning of cuttlefish (*Sepia officinalis*) requires visual information regarding edges and contrast of objects in natural substrate backgrounds. *Biol. Bull*. 208, 7–11. doi: 10.2307/3593095

Chiou, T.-H., Mäthger, L. M., Hanlon, R. T., and Cronin, T. W. (2007). Spectral and spatial properties of polarized light reflections from the arms of squid (*Loligo pealeii*) and cuttlefish (*Sepia officinalis* L.). *J. Exp. Biol*. 210, 3624–3635. doi: 10.1242/jeb.006932

Chung, W.-S., and Marshall, N. J. (2016). Comparative visual ecology of cephalopods from different habitats. *Proc. R. Soc. Lond. B Biol. Sci*. 283, 20161346. doi: 10.1098/rspb.2016.1346

Clark, L., and Grant, J. W. (2010). Intrasexual competition and courtship in female and male Japanese medaka, *Oryzias latipes*: effects of operational sex ratio and density. *Anim. Behav*. 80, 707–712. doi: 10.1016/j.anbehav.2010.07.007

Corner, B. D., and Moore, H. T. (1980). Field observations on the reproductive behavior of *Sepia latimanus*. *Micronesica* 16, 235–260.

Csardi, G., and Nepusz, T. (2006). The igraph software package for complex network research. *InterJ. Complex Syst*. 1695. doi: 10.5281/zenodo.3630268

Darmaillacq, A.-S., Dickel, L., and Mather, J. (eds.). (2014). *Cephalopod Cognition*. Cambridge: Cambridge University Press. doi: 10.1017/CBO9781139058964

de Jong, K., Wacker, S., Amundsen, T., and Forsgren, E. (2009). Do operational sex ratio and density affect mating behaviour? An experiment on the two-spotted goby. *Anim. Behav*. 78, 1229–1238. doi: 10.1016/j.anbehav.2009.08.006

Debuse, V. J., Addison, J. T., and D.Reynolds, J. (1999). The effects of sex ratio on sexual competition in the European lobster. *Anim. Behav*. 58, 973–981. doi: 10.1006/anbe.1999.1213

DiMarco, F. P., and Hanlon, R. T. (1997). Agonistic behavior in the squid *Loligo plei* (Loliginidae, Teuthoidea): Fighting tactics and the effects of size and resource value. *Ethology* 103, 89–108. doi: 10.1111/j.1439-0310.1997.tb00010.x

Dunn, M. (1999). Aspects of the stock dynamics and exploitation of cuttlefish, *Sepia officinalis* (Linnaeus, 1758), in the English Channel. *Fish. Res*. 40, 277–293. doi: 10.1016/S0165-7836(98)00223-9

Eberhard, W. G. (1996). *Female Control: Sexual Selection by Cryptic Female Choice*. Princeton, NJ: Princeton University Press. doi: 10.1515/9780691207209

Edward, D. A., and Chapman, T. (2011). The evolution and significance of male mate choice. *Trends Ecol. Evol*. 26, 647–654. doi: 10.1016/j.tree.2011.07.012

Enders, M. M. (1993). The effect of male size and operational sex ratio on male mating success in the common spider mite, *Tetranychus urticae koch* (Acari: Tetranychidae). *Anim. Behav*. 46, 835–846. doi: 10.1006/anbe.1993.1269

Fox, C. W., and Czesak, M. E. (2000). Evolutionary ecology of progeny size in arthropods. *Annu. Rev. Entomol*. 45, 341–369. doi: 10.1146/annurev.ento.45.1.341

Friard, O., and Gamba, M. (2016). Boris: a free, versatile open-source event-logging software for video/audio coding and live observations. *Methods Ecol. Evol*. 7, 1325–1330. doi: 10.1111/2041-210X.12584

Funk, D. H., and Tallamy, D. W. (2000). Courtship role reversal and deceptive signals in the long-tailed dance fly, *Rhamphomyia longicauda*. *Anim. Behav*. 59, 411–421. doi: 10.1006/anbe.1999.1310

Girard, M. B., Kasumovic, M. M., and Elias, D. O. (2011). Multi-modal courtship in the peacock spider, *Maratus volans* (O.P.-Cambridge, 1874). *PLoS ONE* 6:e25390. doi: 10.1371/journal.pone.0025390

Girard, M. B., Kasumovic, M. M., and Elias, D. O. (2018). The role of red coloration and song in peacock spider courtship: insights into complex signaling systems. *Behav. Ecol*. 29, 1234–1244. doi: 10.1093/beheco/ary128

Gonzalez-Bellido, P. T., Scaros, A. T., Hanlon, R. T., and Wardill, T. J. (2018). Neural control of dynamic 3-dimensional skin papillae for cuttlefish camouflage. *iScience* 1, 24–34. doi: 10.1016/j.isci.2018.01.001

Gonzalez-Bellido, P. T., Wardill, T., Buresch, K., Ulmer, K., and Hanlon, R. (2014). Expression of squid iridescence depends on environmental luminance and peripheral ganglion control. *J. Exp. Biol*. 217, 850–858. doi: 10.1242/jeb.091884

Gwynne, D. (2016). Sexual selection: roles evolving. *Curr. Biol*. 26, R935–R936. doi: 10.1016/j.cub.2016.08.063

Hall, K., and Hanlon, R. (2002). Principal features of the mating system of a large spawning aggregation of the giant australian cuttlefish *Sepia apama* (Mollusca: Cephalopoda). *Mar. Biol*. 140, 533–545. doi: 10.1007/s00227-001-0718-0

Hamel, J. A., Nease, S. A., and Miller, C. W. (2015). Male mate choice and female receptivity lead to reproductive interference. *Behav. Ecol. Sociobiol*. 69, 951–956. doi: 10.1007/s00265-015-1907-z

Hanlon, R. T. (1996). Evolutionary games that squids play: fighting, courting, sneaking, and mating behaviors used for sexual selection in *Loligo pealei*. *Biol. Bull*. 191, 309–310. doi: 10.1086/BBLv191n2p309

Hanlon, R. T., Claes, M. F., Ashcraft, S. E., and Dunlap, P. V. (1997). Laboratory culture of the sepiolid squid *Euprymna scolopes*: a model system for bacteria-animal symbiosis. *Biol. Bull*. 192, 364–374. doi: 10.2307/1542746

Hanlon, R. T., and Forsythe, J. W. (2008). Sexual cannibalism by *Octopus cyanea* on a pacific coral reef. *Mar. Freshw. Behav. Physiol*. 41, 19–28. doi: 10.1080/10236240701661123

Hanlon, R. T., and Messenger, J. B. (1988). Adaptive coloration in young cuttlefish (*Sepia officinalis* L.): The morphology and development of body patterns and their relation to behaviour. *Philos. Trans. R. Soc. Lond. Ser. B Biol. Sci*. 320, 437–487. doi: 10.1098/rstb.1988.0087

Hanlon, R. T., and Messenger, J. B. (2018). *Cephalopod Behaviour*. Cambridge: Cambridge University Press. doi: 10.1017/9780511843600

Hanlon, R. T., Naud, M.-J., Shaw, P. W., and Havenhand, J. N. (2005). Transient sexual mimicry leads to fertilization. *Nature* 433, 212–212. doi: 10.1038/433212a

Hanlon, R. T., Smale, M. J., and Sauer, W. H. H. (2002). The mating system of the squid *Loligo vulgaris reynaudii* (Cephalopoda, Mollusca) off South Africa: fighting, guarding, sneaking, mating and egg laying behavior. *Bull. Mar. Sci*. 71, 331–345.

Hanlon, T. R., Ament, A. S., and Gabr, H. (1999). Behavioral aspects of sperm competition in cuttlefish, *Sepia officinalis* (Sepioidea: Cephalopoda). *Mar. Biol*. 134, 719–728. doi: 10.1007/s002270050588

Higham, J. P., and Hebets, E. A. (2013). An introduction to multimodal communication. *Behav. Ecol. Sociobiol*. 67, 1381–1388. doi: 10.1007/s00265-013-1590-x

Honěk, A. (1993). Intraspecific variation in body size and fecundity in insects: a general relationship. *Oikos* 66, 483–492. doi: 10.2307/3544943

Hooper, A. K., Wegener, B. J., and Wong, B. B. (2016). When should male squid prudently invest sperm? *Anim. Behav*. 112, 163–167. doi: 10.1016/j.anbehav.2015.12.005

How, M. J., Norman, M. D., Finn, J., Chung, W.-S., and Marshall, N. J. (2017). Dynamic skin patterns in cephalopods. *Front. Physiol*. 8:393. doi: 10.3389/fphys.2017.00393

Huffard, C. L., and Bartick, M. (2015). Wild *Wunderpus photogenicus* and *Octopus cyanea* employ asphyxiating "constricting" in interactions with other octopuses. *Molluscan Res*. 35, 12–16. doi: 10.1080/13235818.2014.909558

Huffard, C. L., Caldwell, R. L., and Boneka, F. (2008). Mating behavior of *Abdopus aculeatus* (d'Orbigny 1834) (Cephalopoda: Octopodidae) in the wild. *Mar. Biol*. 154, 353–362. doi: 10.1007/s00227-008-0930-2

Iwata, Y., Sato, N., Hirohashi, N., Kasugai, T., Watanabe, Y., and Fujiwara, E. (2019). How female squid inseminate their eggs with stored sperm. *Curr. Biol*. 29, R48–R49. doi: 10.1016/j.cub.2018.12.010

Jander, R., Daumer, K., and Waterman, T. H. (1963). Polarized light orientation by two Hawaiian decapod cephalopods. *Z. Physiol*. 46, 383–394. doi: 10.1007/BF00340466

Jantzen, T. M., and Havenhand, J. N. (2003). Reproductive behavior in the squid *Sepioteuthis australis* from south Australia: interactions on the spawning grounds. *Biol. Bull.* 204, 305–317. doi: 10.2307/1543601

Jereb, P., and Roper, C. F. E. (eds.). (2005). *Cephalopods of the World. An Annotated and Illustrated Catalogue of Cephalopod Species Known to Date, Volume 1. Chambered Nautiluses and Sepioids (Nautilidae, Sepiidae, Sepiolidae, Sepiadariidae, Idiosepiidae, and Spirulidae) of FAO Species Catalogue for Fishery Purposes*. Food and Agriculture Organization of the United Nations.

Jereb, P., and Roper, C. F. E. (eds.). (2010). *Cephalopods of the World. An Annotated and Illustrated Catalogue of Cephalopod Species Known to Date, volume 2. Myopsid and Oegopsid Squids of FAO Species Catalogue for Fishery Purposes*. Food and Agriculture Organization of the United Nations.

Jereb, P., Roper, C. F. E., Norman, M. D., and Finn, J. K. (eds.). (2013). *Cephalopods of the World. An Annotated and Illustrated Catalogue of Cephalopod Species Known to Date, volume 3. Octopds and Vampire Squids of FAO Species Catalogue for Fishery Purposes*. Food and Agriculture Organization of the United Nations.

Johannesson, K., Havenhand, J. N., Jonsson, P. R., Lindegarth, M., Sundin, A., and Hollander, J. (2008). Male discrimination of female mucous trails permits assortative mating in a marine snail species. *Evolution* 62, 3178–3184. doi: 10.1111/j.1558-5646.2008.00510.x

Kasugai, T. (2000). Reproductive behavior of the pygmy cuttlefish *Ideosepius paradoxus* in an aquarium. *Venus* 59, 37–44. doi: 10.18941/venusjjm.59.1_37

Kilanowski, A. L., and Koprowski, J. L. (2016). Female-biased sexual size dimorphism: ontogeny, seasonality, and fecundity of the cliff chipmunk (*Tamias dorsalis*). *J. Mammal.* 98, 204–210. doi: 10.1093/jmammal/gyw172

Kuester, J., and Paul, A. (1996). Female-female competition and male mate choice in barbary macaques (*Macaca sylvanus*). *Behaviour* 133, 763–790. doi: 10.1163/156853996X00468

Lê, S., Josse, J., and Husson, F. (2008). FactoMineR: An R package for multivariate analysis. *J. Stat. Softw.* 25, 1–18. doi: 10.18637/jss.v025.i01

Laan, A., Gutnick, T., Kuba, M., and Laurent, G. (2014). Behavioral analysis of cuttlefish traveling waves and its implications for neural control. *Curr. Biol.* 24, 1737–1742. doi: 10.1016/j.cub.2014.06.027

Laufer, H., and Ahl, J. S. (1995). Mating behavior and methyl farnesoate levels in male morphotypes of the spider crab, *Libinia emarginata* (leach). *J. Exp. Mar. Biol. Ecol.* 193, 15–20. doi: 10.1016/0022-0981(95)00107-7

Lee, M.-F., Lin, C.-Y., Chiao, C.-C., and Lu, C.-C. (2016). Reproductive behavior and embryonic development of the pharaoh cuttlefish, *Sepia pharaonis* (Cephalopoda: Sepiidae). *Zool. Stud.* 55, 1–16.

Leftwich, P. T., Edward, D. A., Alphey, L., Gage, M. J. G., and Chapman, T. (2012). Variation in adult sex ratio alters the association between courtship, mating frequency and paternity in the lek-forming fruitfly *Ceratitis capitata. J. Evol. Biol.* 25, 1732–1740. doi: 10.1111/j.1420-9101.2012.02556.x

Ligon, R. A., Diaz, C. D., Morano, J. L., Troscianko, J., Stevens, M., Moskeland, A., et al. (2018). Evolution of correlated complexity in the radically different courtship signals of birds-of-paradise. *PLoS Biol.* 16:e2006962. doi: 10.1371/journal.pbio.2006962

Lin, C.-Y., and Chiao, C.-C. (2018). Female choice leads to a switch in oval squid male mating tactics. *Biol. Bull.* 233, 219–226. doi: 10.1086/695718

Lin, C.-Y., Tsai, Y.-C., and Chiao, C.-C. (2017). Quantitative analysis of dynamic body patterning reveals the grammar of visual signals during the reproductive behavior of the oval squid *Sepioteuthis lessoniana. Front. Ecol. Evol.* 5:30. doi: 10.3389/fevo.2017.00030

Liu, L., Zhang, Y., Hu, X., Lü, Z., Liu, B., Jiang, L. H., and Gong, L. (2019). Multiple paternity assessed in the cuttlefish *Sepiella japonica* (Mollusca, Cephalopoda) using microsatellite markers. *ZooKeys* 880, 33–42. doi: 10.3897/zookeys.880.33569

Liu, T.-H., and Chiao, C.-C. (2017). Mosaic organization of body pattern control in the optic lobe of squids. *J. Neurosci.* 37, 768–780. doi: 10.1523/JNEUROSCI.0768-16.2016

Lu, C.-C., and Chung, W.-S. (2017). *Guide to the Cephalopods of Taiwan*. National Museum of Natural Science.

Ma, P. M. (1995). On the agonistic display of the Siamese fighting fish. *Brain Behav. Evol.* 45, 301–131. doi: 10.1159/000113558

Marian, J. E., Apostólico, L. H., Chiao, C. C., Hanlon, R. T., Hirohashi, N., Iwata, Y., et al. (2019). Male alternative reproductive tactics and associated evolution of anatomical characteristics in loliginid squid. *Front. Physiol.* 10:1281. doi: 10.3389/fphys.2019.01281

Marshall, N. J., and Messenger, J. B. (1996). Colour-blind camouflage. *Nature* 382, 408–409. doi: 10.1038/382408b0

Marshall, N. J., Powell, S. B., Cronin, T. W., Caldwell, R. L., Johnsen, S., Gruev, V., et al. (2019). Polarisation signals: a new currency for communication. *J. Exp. Biol.* 222, jeb134213. doi: 10.1242/jeb.134213

Mather, J. (2016). Mating games squid play: Reproductive behaviour and sexual skin displays in Caribbean reef squid *Sepioteuthis sepioidea. Mar. Freshw. Behav. Physiol.* 49, 359–373. doi: 10.1080/10236244.2016.1253261

Mäthger, L. M., and Hanlon, R. T. (2007). Malleable skin coloration in cephalopods: selective reflectance, transmission and absorbance of light by chromatophores and iridophore. *Cell Tissue Res.* 329, 179–186. doi: 10.1007/s00441-007-0384-8

Mäthger, L. M., Shashar, N., and Hanlon, R. T. (2009). Do cephalopods communicate using polarized light reflections from their skin? *J. Exp. Biol.* 212, 2133–2140. doi: 10.1242/jeb.020800

Mendelson, T. C., and Shaw, K. L. (2012). The (mis)concept of species recognition. *Trends Ecol. Evol.* 27, 421–427. doi: 10.1016/j.tree.2012.04.001

Mills, S. C., and Reynolds, J. D. (2003). Operational sex ratio and alternative reproductive behaviours in the European bitterling, *Rhodeus sericeus. Behav. Ecol. Sociobiol.* 54, 98–104. doi: 10.1007/s00265-003-0616-1

Moody, M. F., and Parriss, J. R. (1961). The discrimination of polarized light by *Octopus*: a behavioural and morphological study. *Z. Physiol.* 44, 268–291. doi: 10.1007/BF00298356

Morse, P., and Huffard, C. L. (2019). Tactical tentacles: new insights on the processes of sexual selection among the cephalopoda. *Front. Physiol.* 10:1035. doi: 10.3389/fphys.2019.01035

Morse, P., Zenger, K. R., McCormick, M. I., Meekan, M. G., and Huffard, C. L. (2015). Nocturnal mating behaviour and dynamic male investment of copulation time in the southern blue-ringed octopus, *Hapalochlaena maculosa* (Cephalopoda: Octopodidae). *Behaviour* 152, 1883–1910. doi: 10.1163/1568539X-00003321

Mowles, S. L., and Ord, T. J. (2012). Repetitive signals and mate choice: insights from contest theory. *Anim. Behav.* 84, 295–304. doi: 10.1016/j.anbehav.2012.05.015

Moynihan, M., and Rodaniche, A. F. (1982). The behavior and natural history of the Caribbean reef squid *Sepioteuthis sepioidea*. with a consideration of social, signal and defensive patterns for difficult and dangerous environment. *Adv. Ethol.* 25, 1–150.

Mullen, L. A., Benoit, K., Keyes, O., Selivanov, D., and Arnold, J. (2018). Fast, consistent tokenization of natural language text. *J. Open Source Softw.* 3:655. doi: 10.21105/joss.00655

Nakajima, R., and Ikeda, Y. (2017). A catalog of the chromatic, postural, and locomotor behaviors of the pharaoh cuttlefish (*Sepia pharaonis*) from Okinawa Island, Japan. *Mar. Biodivers. Recent Adv. Knowl. Cephalopod Biodivers.* 47, 735–753. doi: 10.1007/s12526-017-0649-8

Naud, M.-J., Hanlon, R. T., Hall, K. C., Shaw, P. W., and Havenhand, J. N. (2004). Behavioural and genetic assessment of reproductive success in a spawning aggregation of the Australian giant cuttlefish, *Sepia apama. Anim. Behav.* 67, 1043–1050. doi: 10.1016/j.anbehav.2003.10.005

Naud, M.-J., Shaw, P. W., Hanlon, R. T., and Havenhand, J. N. (2005). Evidence for biased use of sperm sources in wild female giant cuttlefish (*Sepia apama*). *Proc. Biol. Sci.* 272, 1047–1051. doi: 10.1098/rspb.2004.3031

Nigmatullin, C., Nesis, K., and Arkhipkin, A. (2001). A review of the biology of the jumbo squid *Dosidicus gigas* (Cephalopoda: Ommastrephidae). *Fish. Res.* 54, 9–19. doi: 10.1016/S0165-7836(01)00371-X

Nixon, M., and Young, J. Z. (2003). *The Brains and Lives of Cephalopods*. Oxford: Oxford University Press.

Owren, M., Rendall, D., and Ryan, M. (2010). Redefining animal signaling: Influence versus information in communication. *Biol. Philos.* 25, 755–780. doi: 10.1007/s10539-010-9224-4

Packard, A., and Hochberg, F. G. (1977). "Skin patterning in *Octopus* and other genera," in *The Biology of Cephalopods*, eds M. Nixon and J. B. Messenger (London: The Zoological Society of London, Academic Press), 191–231.

Pignatelli, V., Temple, S. E., Chiou, T.-H., Roberts, N. W., Collin, S. P., and Marshall, N. J. Behavioural relevance of polarization sensitivity as a target detection mechanism in cephalopods and fishes. Philosophical

Transactions of the Royal Society B: Biological Sciences, 2011, 366, 734–741. doi: 10.1098/rstb.2010.0204

Quinteiro, J., Baibai, T., Oukhattar, L., Soukri, A., Seixas, P., and Rey-Méndez, M. (2011). Multiple paternity in the common octopus *Octopus vulgaris* (Cuvier, 1797), as revealed by microsatellite DNA analysis. *Molluscan Res*. 31, 15–20.

Regueira, M., González, A. F., Guerra, A., and Soares, A. (2013). Reproductive traits of horned octopus *Eledone cirrhosa* in Atlantic Iberian waters. *J. Mar. Biol. Assoc. U. K.* 93, 1641–1652. doi: 10.1017/S0025315413000118

Reinhold, K., Kurtz, J., and Engqvist, L. (2002). Cryptic male choice: sperm allocation strategies when female quality varies. *J. Evol. Biol.* 15, 201–209. doi: 10.1046/j.1420-9101.2002.00390.x

Roberts, N. S., and Mendelson, T. C. (2017). Male mate choice contributes to behavioural isolation in sexually dimorphic fish with traditional sex roles. *Anim. Behav.* 130, 1–7. doi: 10.1016/j.anbehav.2017.06.005

Robinson, D. (2019). *widyr: Widen, Process, Then Re-Tidy Data.* Available online at: https://CRAN.R-project.org/package=widyr

Roper, C. F. E., and Hochberg, F. G. (1988). Behavior and systematics of cephalopods from Lizard Island, Australia, based on color and body patterns. *Malacologia* 29, 153–193.

RStudio Team (2015). *RStudio: Integrated Development Environment for R*. RStudio, Inc., Boston, MA.

Saetre, G.-P., and Slagsvold, T. (1996). The significance of female mimicry in male contests. *Am. Natural.* 147, 981–995. doi: 10.1086/285889

Saidel, W. M., Lettvin, J. Y., and F, M. E. (1983). Processing of polarized light by squid photoreceptors. *Nature* 304, 53–536. doi: 10.1038/304534a0

Saidel, W. M., Shashar, N., Schmolesky, M. T., and Hanlon, R. T. (2005). Discriminative responses of squid (*Loligo pealeii*) photoreceptors to polarized light. *Comp. Biochem. Physiol. A Mol. Integr. Physiol.* 142, 340–346. doi: 10.1016/j.cbpa.2005.08.003

Sato, N., Kasugai, T., Ikeda, Y., and Munehara, H. (2010). Structure of the seminal receptacle and sperm storage in the Japanese pygmy squid. *J. Zool.* 282, 151–156. doi: 10.1111/j.1469-7998.2010.00733.x

Sato, N., Kasugai, T., and Munehara, H. (2013). Sperm transfer or spermatangia removal: Postcopulatory behaviour of picking up spermatangium by female Japanese pygmy squid. *Mar. Biol.* 160, 553–561. doi: 10.1007/s00227-012-2112-5

Sato, N., Kasugai, T., and Munehara, H. (2014). Female pygmy squid cryptically favour small males and fast copulation as observed by removal of spermatangia. *Evol. Biol.* 41, 221–228. doi: 10.1007/s11692-013-9261-4

Sato, N., Yoshida, M.-a., and Kasugai, T. (2016). Impact of cryptic female choice on insemination success: larger sized and longer copulating male squid ejaculate more, but females influence insemination success by removing spermatangia. *Evolution* 71, 111–120. doi: 10.1111/evo.13108

Schnell, A. K., Jozet-Alves, C., Hall, K. C., Radday, L., and Hanlon, R. T. (2019). Fighting and mating success in giant Australian cuttlefish is influenced by behavioural lateralization. *Proc. R. Soc. B Biol. Sci.* 286:20182507. doi: 10.1098/rspb.2018.2507

Schnell, A. K., Smith, Carolynn L. snf Hanlon, R. T., and Harcourt, R. (2015b). Giant Australian cuttlefish use mutual assessment to resolve male-male contests. *Anim. Behav.* 107, 31–40. doi: 10.1016/j.anbehav.2015.05.026

Schnell, A. K., Smith, C. L., Hanlon, R. T., and Harcourt, R. T. (2015a). Female receptivity, mating history, and familiarity influence the mating behavior of cuttlefish. *Behav. Ecol. Sociobiol.* 69, 283–292. doi: 10.1007/s00265-014-1841-5

Scholes, E. (2008). Evolution of the courtship phenotype in the bird of paradise genus Parotia (Aves: Paradisaeidae): homology, phylogeny, and modularity. *Biol. J. Linnean Soc.* 94, 491–504. doi: 10.1111/j.1095-8312.2008.01012.x

Scholes, E., Gillis, J. M., and Laman, T. G. (2017). Visual and acoustic components of courtship in the bird-of-paradise genus *Astrapia* (aves: Paradisaeidae). *PeerJ* 5:e3987. doi: 10.7717/peerj.3987

Scott-Phillips, T. (2008). Defining biological communication. *J. Evol. Biol.* 21, 387–395. doi: 10.1111/j.1420-9101.2007.01497.x

Searcy, W. A., and Nowicki, S. (2010). *The Evolution of Animal Communication: Reliability and Deception in Signaling Systems*. Princeton, NJ: Princeton University Press. doi: 10.1515/9781400835720

Shashar, N., and Cronin, T. W. (1996). Polarization contrast vision in *Octopus*. *J. Exp. Biol.* 199, 999–1004.

Shashar, N., Hagan, R., Boal, J. G., and Hanlon, R. T. (2000). Cuttlefish use polarization sensitivity in predation on silvery fish. *Vis. Res.* 40, 71–75. doi: 10.1016/S0042-6989(99)00158-3

Shashar, N., and Hanlon, R. T. (2013). Spawning behavior dynamics at communal egg beds in the squid *Doryteuthis (Loligo) pealeii*. *J. Exp. Mar. Biol. Ecol.* 447, 65–74. doi: 10.1016/j.jembe.2013.02.011

Shashar, N., Milbury, C., and Hanlon, R. (2002). Polarization vision in cephalopods: Neuroanatomical and behavioral features that illustrate aspects of form and function. *Mar. Freshw. Behav. Physiol.* 35, 57–68. doi: 10.1080/10236240290025617

Shashar, N., Rutledge, P., and Cronin, T. (1996). Polarization vision in cuttlefish-a concealed communication channel? *J. Exp. Biol.* 199, 2077–2084.

Shigeno, S., Andrews, P. L. R., Ponte, G., and Fiorito, G. (2018). Cephalopod brains: an overview of current knowledge to facilitate comparison with vertebrates. *Front. Physiol.* 9:952. doi: 10.3389/fphys.2018.00952

Shuster, S. M. (1989). Male alternative reproductive strategies in a marine isopod crustacean (*Paracerceis sculpta*): the use of genetic markers to measure differences in fertilization success among α–, β–, and ɤ-males. *Evolution* 43, 1683–1698. doi: 10.1111/j.1558-5646.1989.tb02618.x

Shuster, S. M., and Wade, M. J. (1991). Equal mating success among male reproductive strategies in a marine isopod. *Nature* 350, 608–610. doi: 10.1038/350608a0

Silge, J., and Robinson, D. (2016). tidytext: text mining and analysis using tidy data principles in R. *JOSS* 1, 37. doi: 10.21105/joss.00037

Simmons, L. W. (2014). "Sperm competition," in *The Evolution of Insect Mating Systems,* eds D. Shuker, and L. W. Simmons (Oxford: Oxford Scholarship Online), 181–203. doi: 10.1093/acprof:oso/9780199678020.003.0010

Stillwell, R. C., Blanckenhorn, W. U., Teder, T., Davidowitz, G., and Fox, C. W. (2010). Sex differences in phenotypic plasticity affect variation in sexual size dimorphism in insects: From physiology to evolution. *Annu. Rev. Entomol.* 55, 227–245. doi: 10.1146/annurev-ento-112408-085500

Stuart-Fox, D. (2005). Deception and the origin of honest signals. *Trends Ecol. Evol.* 201, 521–523. doi: 10.1016/j.tree.2005.08.004

Székely, T., Freckleton, R. P., and Reynolds, J. D. (2004). Sexual selection explains Rensch's rule of size dimorphism in shorebirds. *Proc. Natl. Acad. Sci. U.S.A.* 101, 12224–12227. doi: 10.1073/pnas.0404503101

Talbot, C. M., and Marshall, J. (2010a). Polarization sensitivity and retinal topography of the striped pyjama squid (*Sepioloidea lineolata*-Quoy/Gaimard 1832). *J. Exp. Biol.* 213, 3371–3377. doi: 10.1242/jeb.048165

Talbot, C. M., and Marshall, J. (2010b). Polarization sensitivity in two species of cuttlefish-*Sepia plangon* (Gray 1849) and *Sepia mestus* (Gray 1849) - demonstrated with polarized optomotor stimuli. *J. Exp. Biol.* 213, 3364–3370. doi: 10.1242/jeb.042937

Tasaki, K., and Karita, K. (1966). Discrimination of horizontal and vertical planes of polarized light by the cephalopod retina. *Jpn. J. Physiol.* 16, 205–216. doi: 10.2170/jjphysiol.16.205

Taylor, L. A., and McGraw, K. J. (2013). Male ornamental coloration improves courtship success in a jumping spider, but only in the sun. *Behav. Ecol.* 24, 955–967. doi: 10.1093/beheco/art011

Temple, S. E., Pignatelli, V., Cook, T., How, M. J., Chiou, T.-H., Roberts, N. W., et al. (2012). High-resolution polarisation vision in a cuttlefish. *Curr. Biol.* 22, R121–R122. doi: 10.1016/j.cub.2012.01.010

Thomas, A., and MacDonald, C. (2016). Investigating body patterning in aquarium-raised flamboyant cuttlefish (*Metasepia pfefferi*). *PeerJ* 4:e2035. doi: 10.7717/peerj.2035

Thompson, J. T., and Voight, J. R. (2003). Erectile tissue in an invertebrate animal: the *Octopus* copulatory organ. *J. Zool.* 261, 101–108. doi: 10.1017/S0952836903003996

Voight, J. R. (1991). Ligula length and courtship in *Octopus digueti*: a potential mechanism of mate choice. *Evolution* 45, 1726–1730. doi: 10.1111/j.1558-5646.1991.tb02680.x

Voight, J. R. (2002). Morphometric analysis of male reproductive features of octopodids (Mollusca: Cephalopoda). *Biol. Bull.* 202, 148–155. doi: 10.2307/1543651

Wada, T., Takegaki, T., Mori, T., and Natsukari, Y. (2005). Alternative male mating behaviors dependent on relative body size in captive oval squid *Sepioteuthis lessoniana* (Cephalopoda, Loliginidae). *Zool. Sci.* 22, 645–651. doi: 10.2108/zsj.22.645

Wagner, W. E. (1992). Deceptive or honest signalling of fighting ability? A test of alternative hypotheses for the function of changes in call dominant frequency by male cricket frogs. *Anim. Behav.* 44, 449–462. doi: 10.1016/0003-3472(92)90055-E

Waiho, K., Mustaqim, M., Fazhan, H., Norfaizza, W. I. W., Megat, F. H., and Ikhwanuddin, M. (2015). Mating behaviour of the orange mud crab, *Scylla olivacea*: the effect of sex ratio and stocking density on mating success. *Aquacult. Rep.* 2, 50–57. doi: 10.1016/j.aqrep.2015.08.004

Wegener, B. J., Stuart-Fox, D. M., Norman, M. D., and Wong, B. B. (2013). Strategic male mate choice minimizes ejaculate consumption. *Behav. Ecol.* 24, 668–671. doi: 10.1093/beheco/ars216

Whiting, M. J., Webb, J. K., and Keogh, J. S. (2009). Flat lizard female mimics use sexual deception in visual but not chemical signals. *Proc. R. Soc. B Biol. Sci.* 276, 1585–1591. doi: 10.1098/rspb.2008.1822

Wickham, H., Averick, M., Bryan, J., Chang, W., D'Agostino McGowan, L., François, R., et al. (2019a). Welcome to the tidyverse. *J. Open Source Softw.* 4:1686. doi: 10.21105/joss.01686

Wickham, H., Francois, R., Henry, L., and Muller, K. (2019b). *dplyr: A Grammar of Data Manipulation*. R package version 0.8.3. Available online at: https://CRAN.R-project.org/package=dplyr

Zeidberg, L. D. (2009). First observations of "sneaker mating" in the California market squid, *Doryteuthis opalescens*, (Cephalopoda: Myopsida). *Mar. Biodivers. Rec.* 2:e6. doi: 10.1017/S1755267208000067

Zylinski, S., How, M. J., Osorio, D., Hanlon, R. T., and Marshall, N. J. (2011). To be seen or to hide: visual characteristics of body patterns for camouflage and communication in the Australian giant cuttlefish *Sepia apama*. *Am. Natural.* 5, 681–690. doi: 10.1086/659626

Conflict of Interest: The authors declare that the research was conducted in the absence of any commercial or financial relationships that could be construed as a potential conflict of interest.

APPENDIX

Material Methods

Sample Size

TABLE A1 | Sample size (n = number of experiments) for each condition tested in this study.

	1M:1F-DIRECT	1M:1F-POL	1M:1F-UNPOL	1M:2F-DIRECT	1M:2F-POL	1M:2F-UNPOL	2M:1F-DIRECT	2M:1F-UNPOL
n	6	2	1	5	2	2	6	1

3D Printed Cuttlefish Models

- CGTrader model 1: https://www.cgtrader.com/3d-models/animals/fish/cuttlefish-e0177629-4eba-4166-b54c-a2b06c9e011c
- CGTrader model 2: https://www.cgtrader.com/3d-models/animals/fish/low-poly-cuttle-fish-animated-game-ready
- CGTrader model 3: https://www.cgtrader.com/3d-models/animals/fish/cuttlefish-19d89111-3607-4770-8303-59f5a98c2dde.

frontiers in Physiology

ORIGINAL RESEARCH
published: 18 September 2020
doi: 10.3389/fphys.2020.01112

The Pupillary Response of the Common Octopus (*Octopus vulgaris*)

*Cecilia Soto[1], Almut Kelber[2] and Frederike D. Hanke[2,3]**

[1] Sensory and Cognitive Ecology, Institute for Biosciences, University of Rostock, Rostock, Germany, [2] Vision Group, Department of Biology, Lund University, Lund, Sweden, [3] Neuroethology, Institute for Biosciences, University of Rostock, Rostock, Germany

Cephalopods have very conspicuous eyes that are often compared to fish eyes. However, in contrast to many fish, the eyes of cephalopods possess mobile pupils. To increase the knowledge of pupillary and thus visual function in cephalopods, the dynamics of the pupil of one of the model species among cephalopods, the common octopus *(Octopus vulgaris)*, was determined in this study. We measured pupillary area as a function of ambient luminance to document the light and dark reaction of the octopus eye. The results show that weak light (<1 cd/m^2) is enough to cause a pupil constriction in octopus, and that the pupil reacts fast to changing light conditions. The t_{50}-value defined as the time required for achieving half-maximum constriction ranged from 0.45 to 1.29 s and maximal constriction from 10 to 20% of the fully dilated pupil area, depending on the experimental condition. Axial light had a stronger influence on pupil shape than light from above, which hints at a shadow effect of the horizontal slit pupil. We observed substantial variation of the pupil area under all light conditions indicating that light-independent factors such as arousal or the need to camouflage the eye affect pupil dilation/constriction. In conclusion, the documentation of pupil dynamics provides evidence that the pupil of octopus is adapted to low ambient light levels. Nevertheless it can quickly adapt to and thus function under brighter illumination and in a very inhomogeneous light environment, an ability mediated by the dynamic pupil in combination with previously described additional processes of light/dark adaptation in octopus.

Keywords: pupil, vision, pupil light reaction, pupil dark reaction, shadow effect

OPEN ACCESS

Edited by:
Graziano Fiorito, University of Naples Federico II, Italy

Reviewed by:
Rhanor Gillette, University of Illinois at Urbana-Champaign, United States
Primož Pirih, University of Ljubljana, Slovenia

****Correspondence:***
Frederike D. Hanke
frederike.hanke@uni-rostock.de

Specialty section:
This article was submitted to Invertebrate Physiology, a section of the journal Frontiers in Physiology

Received: *19 December 2019*
Accepted: *11 August 2020*
Published: *18 September 2020*

Citation:
Soto C, Kelber A and Hanke FD (2020) The Pupillary Response of the Common Octopus (Octopus vulgaris). Front. Physiol. 11:1112. doi: 10.3389/fphys.2020.01112

INTRODUCTION

The cephalopods are a molluscan class that differs from other members of the phylum by a number of characters such as the anatomy of the body and the organization of the nervous system. One of the most prominent characteristics of cephalopods are their eyes (for review see Packard, 1972; Messenger, 1979; Land, 1984; Budelmann, 1994, 1996). They are large and often actively scanning the animal's surrounding. To some extent, cephalopod eyes resemble vertebrate camera-type eyes. A conspicuous feature of the cephalopod eye is its pupil, which is peculiarly shaped in some species. Pupil shape varies from horizontal to U- or W-shaped in bright light depending

on species (see **Figure 1** and photos within for example Douglas, 2018). A number of studies have already tried to assess the function of these specific pupillary shapes (Hanlon and Messenger, 1988; Schaeffel et al., 1999; Mäthger et al., 2013; Stubbs and Stubbs, 2016) or provided descriptions of the anatomy of the iris as well as of pupillary dynamics in some species (Beer, 1897; Magnus, 1902; Wiley, 1902; Hess, 1910; Heidermanns, 1928; Weel and Thore, 1936; Froesch, 1973; Muntz, 1977; Hurley et al., 1978; Muntz and Ray, 1984; Douglas et al., 2005; Bozzano et al., 2009; McCormick and Cohen, 2012; Matsui et al., 2016).

A dynamic pupil, as present in cephalopods, generally helps (1) to balance sensitivity and resolution of an eye (Douglas, 2018), and (2) to adapt the eye to different light conditions thereby avoiding the saturation of the photoreceptors and increasing the probability of light detection. Besides pupillary changes, adaptation to light can involve the migration of screening pigment – separating the two rhabdoms of a photoreceptor and separating the distal segments of the photoreceptors, or changes in the photoreceptor length in cephalopods (Babuchin, 1864; Rawitz, 1891; Hesse, 1900; Hess, 1905; Glockauer, 1915;

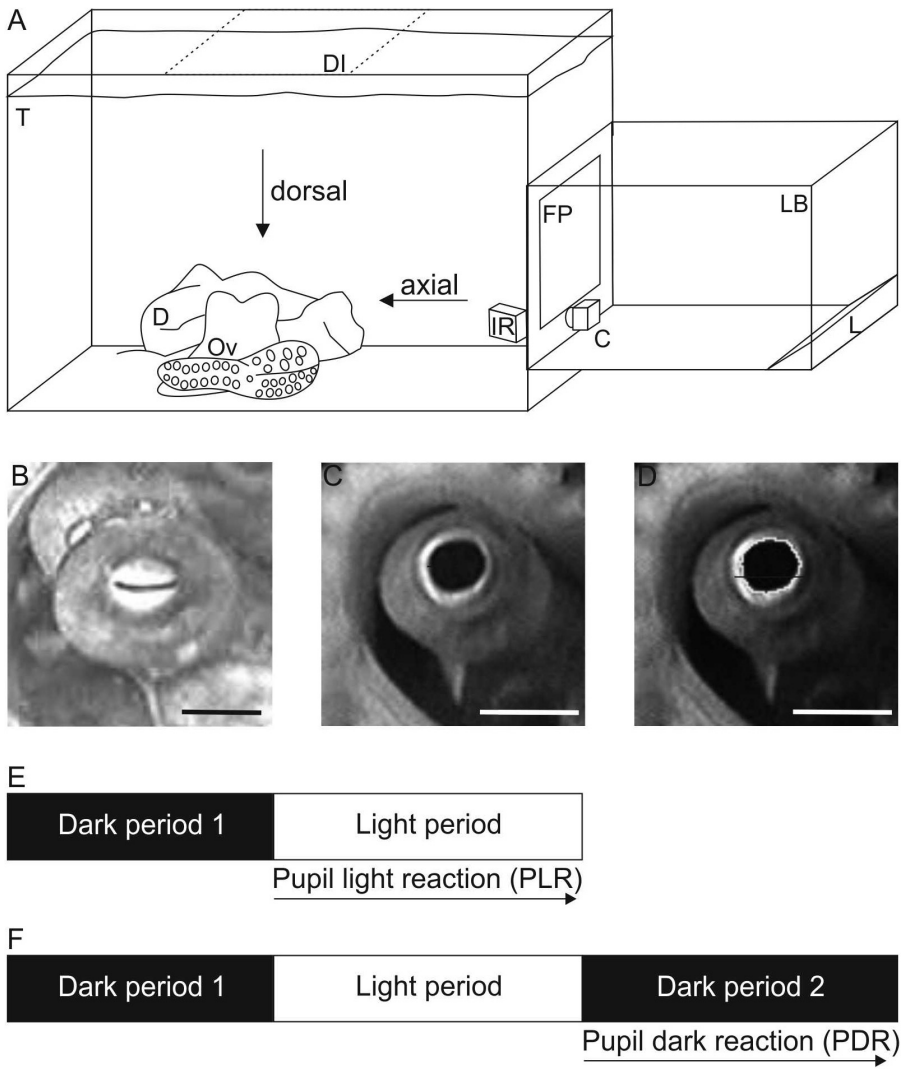

FIGURE 1 | Experimental setup and procedure. **(A)** Sketch of the experimental setup to record pupillary responses. During measurements, the animal (Ov) was hiding in its den (D) in its holding tank (T). The scene was either illuminated axially with the light box (LB) and camera C as shown or from dorsal (position of light box shaded, DI; camera remains in position as during axial illumination). Within the light box, light of three reflector light bulbs (L) was reflected numerous times by aluminum foil lining the inside of the box before it indirectly hit the semitransparent front plate (FP). The scene was additionally illuminated by infrared light (IR) allowing to document the pupil in darkness/dim light conditions. Not drawn to scale. **(B–D)** Pupil of *Octopus vulgaris*. B Constricted pupil when the scene was illuminated with 170.3 cd/m^2 axially. Absolute pupil area was 4 mm^2 on this frame. C Dilated pupil measured in darkness under IR-light before the light was switched on. Absolute pupil area was determined as 33 mm^2 on this frame. **(D)** Image of the dilated pupil showing how the pupil was encircled in ImageJ to determine the pupil area. Scale 10 mm. **(E,F)** Sketch of the experimental procedure to document **(E)** the pupil light reaction (PLR) and **(F)** the pupil dark reaction (PDR). For both pupil reactions, the animal was first kept in darkness (dark period 1) followed by a light period. During this light period with a specific light level set up, the pupil light reaction was documented. The pupil dark reaction was recorded in a subsequent dark period (dark period 2).

Hagins and Liebman, 1962; Young, 1963; Daw and Pearlman, 1974; Suzuki et al., 1985; Suzuki and Takahashi, 1988; Gleadall et al., 1993; Bozzano et al., 2009). Cellular processes within the photoreceptors might additionally adapt the eye.

The pupillary reflex is usually considered to be a fast mechanism of adaptation. A fast pupil response is indeed characteristic for the eyes of some cephalopod species (**Table 1**). It takes the pupils of *Lolliguncula brevis* (McCormick and Cohen, 2012), *Sepia officinalis*, and *Eledone cirrhosa* (Douglas et al., 2005), *Todarodes pacificus* (Matsui et al., 2016) as well as *Sepioloidea lineolate* (Douglas, 2018) only 1–3 s to constrict; the t_{50}-values, defined as the time required to achieve 50% pupil constriction, were assessed as 0.3–1.5 s in these species. In contrast, the pupils of *Japetella diaphana* and *Nautilus pompilius* react more slowly to changes in light condition (**Table 1**; Hurley et al., 1978; Douglas, 2018). Previous studies described that diffuse light is sufficient to cause constriction of the cephalopod pupil (Beer, 1897; Weel and Thore, 1936). Most cephalopods seem to lack a consensual pupil response (Beer, 1897; Magnus, 1902; Weel and Thore, 1936; Douglas et al., 2005; McCormick and Cohen, 2012), thus if one eye is illuminated, only the pupil of this eye constricts but not the pupil of the non-illuminated eye. Nautilus (*Nautilus pompilius*), on the other hand, has a consensual pupil response (Hurley et al., 1978), meaning that both pupils constrict even if only one eye is illuminated. In the Atlantic brief squid (*Lolliguncula brevis*), the pupil of the unstimulated eye also contracts, but less so than the pupil of the stimulated eye (McCormick and Cohen, 2012).

In this study, the pupil light and dark reaction of the common octopus, *Octopus vulgaris*, was analyzed; throughout the text, we will refer to the common octopus as octopus for simplicity. The pupil of octopus is circular when the eye is in darkness and constricted to a horizontal slit in bright light (**Figures 1B,C**). Previous researchers have already described some aspects of the pupil/iris of octopus such as the brain centers, nerves, and muscles controlling pupillary function (Magnus, 1902; Weel and Thore, 1936; Budelmann and Young, 1984), the histological fine structure of the iris (Froesch, 1973), and the fact that the octopus always keeps its slit-shaped pupil horizontal irrespective of body position (Wells, 1960). In a similar way as in other animals (Douglas, 2018), the pupil size of octopus is not only depending on the ambient illumination but also on other factors such as arousal (Weel and Thore, 1936). According to Weel and Thore (1936), the octopus has a non-consensual pupil response thus the pupil is only constricting when the respective eye is illuminated by light but not when the contralateral eye is illuminated. This observation is consistent with the octopus often looking at objects with one of its laterally placed eyes only (Heidermanns, 1928; Muntz, 1963; Byrne et al., 2002) and showing asymmetry in eye use (Byrne et al., 2002).

Pupillary dynamics in *Octopus vulgaris,* which, according to our knowledge, have not been quantified before, were of interest as one tessera of the mosaic of vision and the visual abilities in octopus. The rate of pupillary constriction and dilation reflects the rate of light changes experienced by the animal in its daily life, and the light range within which the pupil dilates or constricts differentially is informative regarding the animal's light environment. Besides the documentation of the pupillary dynamics, the aim of this study was to compare the pupil light and dark reaction when the eye is illuminated axially or from above (called dorsal illumination hereafter). Observations made by ourselves and others (Hess, 1909, 1910; Douglas et al., 2005; McCormick and Cohen, 2012; Mäthger et al., 2013) suggested that the horizontal and probably even more the W- or U-shaped pupils of cephalopods serve to protect the eyes from down-welling light. Consequently, dorsal compared to axial illumination should affect the octopus pupil less; a hypothesis tested in the study at hand.

MATERIALS AND METHODS

Experimental Animal

Pupillary reactions were documented in one wild-caught (Tuscan Archipelago of the Mediterranean Sea), female adult common octopus, *Octopus vulgaris*, with a mantle length of 6.5 cm. At the Marine Science Center Rostock, Germany, it was housed solitarily in a compartment (130 × 85 × 78 cm) of a 3,000 l seawater aquarium with a substrate composed of small stones and small pieces of corals. Large stones as well as shells were provided to allow the animal to hide underneath or to construct a den. In the aquarium, salinity was kept at 32–33 g/kg, temperature was

TABLE 1 | Overview of the results obtained in previous studies on pupillary reactions in cephalopods including the t_{50}-value, the time interval after light onset, at which half-maximum constriction is reached (in s), the maximal constriction of the pupil (in % of the fully dilated pupil before light onset), the pupillary parameter (either pupil area or pupil diameter) measured during the study, and the reference.

Species	t_{50} (s)	Maximal constriction (%)	Measure of pupillary opening	References
Eledone cirrhosa	0.65	<3	Area	Douglas et al., 2005
Japetella diaphana	6.2	8	Area	Douglas, 2018; (Figure 20)
Sepia officinalis	0.32	<3	Area	Douglas et al., 2005
Sepioloidea lineolate	0.4	2	Area	Douglas, 2018 (Figure 19)
Loliguncula brevis	0.49-1.2	24	Area	McCormick and Cohen, 2012
Todarodes pacificus	1-1.5	<20	Diameter	Matsui et al., 2016 (Figure 5)
Nautilus pompilius	39	20	Vertical diameter	Hurley et al., 1978 (Figure 1A)
		40	Horizontal diameter	Hurley et al., 1978 (Figure 1B)

adjusted to 21–23°C, and water quality was regularly checked. After transport, the animal was adapted to the salinity and temperature of the aquarium by adding water from the holding tank dropwise to the container the animal was residing in and that contained natural ocean water from the point of capture. During the phase of adaptation, lasting several hours, the animal was continuously monitored.

A day and night cycle with 9 h daylight, 1 h dusk and dawn, and 13 h night was achieved with the help of artificial illumination (Aqua Medic Ocean Lights, Reef blue, 2× 150 W and T52×54 W, Bissendorf, Deutschland; Starlicht KOS Cut-Case 1×13L White, Herzebrock-Clarholz, Deutschland).

During the study with an experimental phase of 2 months, the octopus was fed with a mixture of northern prawn *(Pandulus borealis)*, petan fish *(Osmerus eperlanus*), and saltwater mussles *(Mytilidae* sp.) 6–7 days a week *ad libitum*.

Maintenance, care, and welfare followed published recommendations (Smith et al., 2013; Fiorito et al., 2014, 2015). This study was conducted in accordance with the directive 2010/63/EU, and maintenance and the measurements (Permit No. 6712GH00113, Staatliches Amt für Umwelt und Natur Rostock, Landesamt für Landwirtschaft, Lebensmittelsicherheit und Fischerei, Mecklenburg-Vorpommern) as well as the transport (EG Verordnung 1/2005, Reg.-Nr. 082120000714) were approved by local authorities. The ARRIVE guidelines (Kilkenny et al., 2010) checklist was the basis for the preparation of this manuscript.

Experimental Setup

The pupillary reactions of the octopus were documented with the animal residing in its home tank (**Figure 1A**). For the documentation of the pupil light and dark response (PLR, PDR), the octopus eye was illuminated with light emitted from a light box that was directly attached to the aquarium from outside. The light box was installed either on the side of the aquarium to illuminate the eye axially or placed on top of the aquarium to illuminate the eye from above.

The front plate of the light box was a square acrylic plate with 25 cm side length. It allowed 92% of the light to be transmitted. This plate was indirectly illuminated by the light of three 20 W lamps (mirror reflector bulb, CIL FTD/A 20W/12 V, diameter 77 mm) reflected by aluminum foil lining the inside of the box. The position of the lamps was adjusted to achieve a homogenous illumination of the front plate varying only by ± 12% across the surface on average. The light box emitted light of wavelengths between 400 and 860 nm (measured with Ocean Optics spectrometer USB 2000). Additional infrared light at 850 nm was always illuminating the scene allowing the documentation of the pupil responses with an infrared-sensitive camera even at the lowest light intensities.

The light emitted from the light box could be dimmed with a dimmer (REV Ritter GmbH, 40–300W, 230V, Typ EMD 200). Nine different light intensities ranging from 0.7 ± 0.4 cd/m^2 to 186.1 ± 18.7 cd/m^2 were chosen to document the pupil responses (**Table 2**). The luminance of the light box was measured with a luminance meter (Minolta Luminance Meter LS-110, Japan) from the distance at which the eye of the octopus had been within the aquarium during measurements, at five points on the front plate after every measurement/light period. Final luminance values (**Table 2**) represent averages of all measurements per light level (axial illumination N = 45, dorsal illumination N = 40). Additionally we assessed t_{50}-values of the light unit for three luminances: 0.29 ± 0.017 s for 1 cd/m^2, 0.25 ± 0.000 s for 60 cd/m^2, and 0.142 ± 0.003 s for 150 cd/m^2; the t_{50} value indicates the time needed to reach half maximum luminance.

The pupil responses were recorded with a camera (DSP CCD Camera XC229SR) at 30 fps, which was always filming the octopus eye axially (**Figures 1B,C**).

Experimental Procedure

The octopus was filmed when sitting in its den with only its eyes protruding. Before each experimental session, the room was completed darkened, and the octopus was kept in darkness for a minimum of 3 min during which time the pupil dilated fully (**Figure 1C**). After this initial dark period (dark period 1, **Figure 1E**), the light source was switched on with the lowest luminance (light period with light level 1, **Figure 2E** and **Table 2**). The PLR was recorded during this light period that lasted 15–600 s depending on the experimental phase. Immediately after the recordings were finished, the

TABLE 2 | Light levels used to elicit a pupil response of *Octopus vulgaris* during axial and dorsal illumination average luminance as well as log (luminance) in cd/m^2 ± SD) as well as the t_{50}-values (in s) determined during the respective pupillary light reaction with the number of measurements (N) performed to determine the t_{50}-value.

Axial illumination				Dorsal illumination			
Luminance (cd/m^2)	Log (Luminance) (cd/m^2)	t_{50} (s)	N	Luminance (cd/m^2)	Log (Luminance) (cd/m^2)	t_{50} (s)	N
0.7 ± 0.4	−0.15 ± 0.40	0.83	6	1.0 ± 0.3	0 ± 0.52	1.29	5
2.2 ± 0.8	0.34 ± 0.10	0.57	7	2.4 ± 0.6	0.38 ± 0.22	1.06	7
17.6 ± 3.9	1.2 ± 0.59	0.45	9	18.3 ± 3.3	1.26 ± 0.51	0.66	8
24.3 ± 5.0	1.39 ± 0.70	0.50	9	26.4 ± 4.7	1.42 ± 0.67	0.60	8
50.9 ± 8.1	1.71 ± 0.91	0.54	9	59.7 ± 8.1	1.78 ± 0.91	0.61	8
66.1 ± 11.8	1.82 ± 1.07	0.50	9	74.0 ± 9.3	1.87 ± 0.97	0.56	8
104.5 ± 14.5	2.02 ± 1.16	0.52	9	115.9 ± 10.4	2.06 ± 1.02	0.54	8
125.8 ± 18.2	2.10 ± 1.26	0.52	9	142.3 ± 14.6	2.15 ± 1.16	0.59	8
170.3 ± 21.6	2.23 ± 1.33	0.49	9	186.1 ± 18.7	2.27 ± 1.27	0.59	8

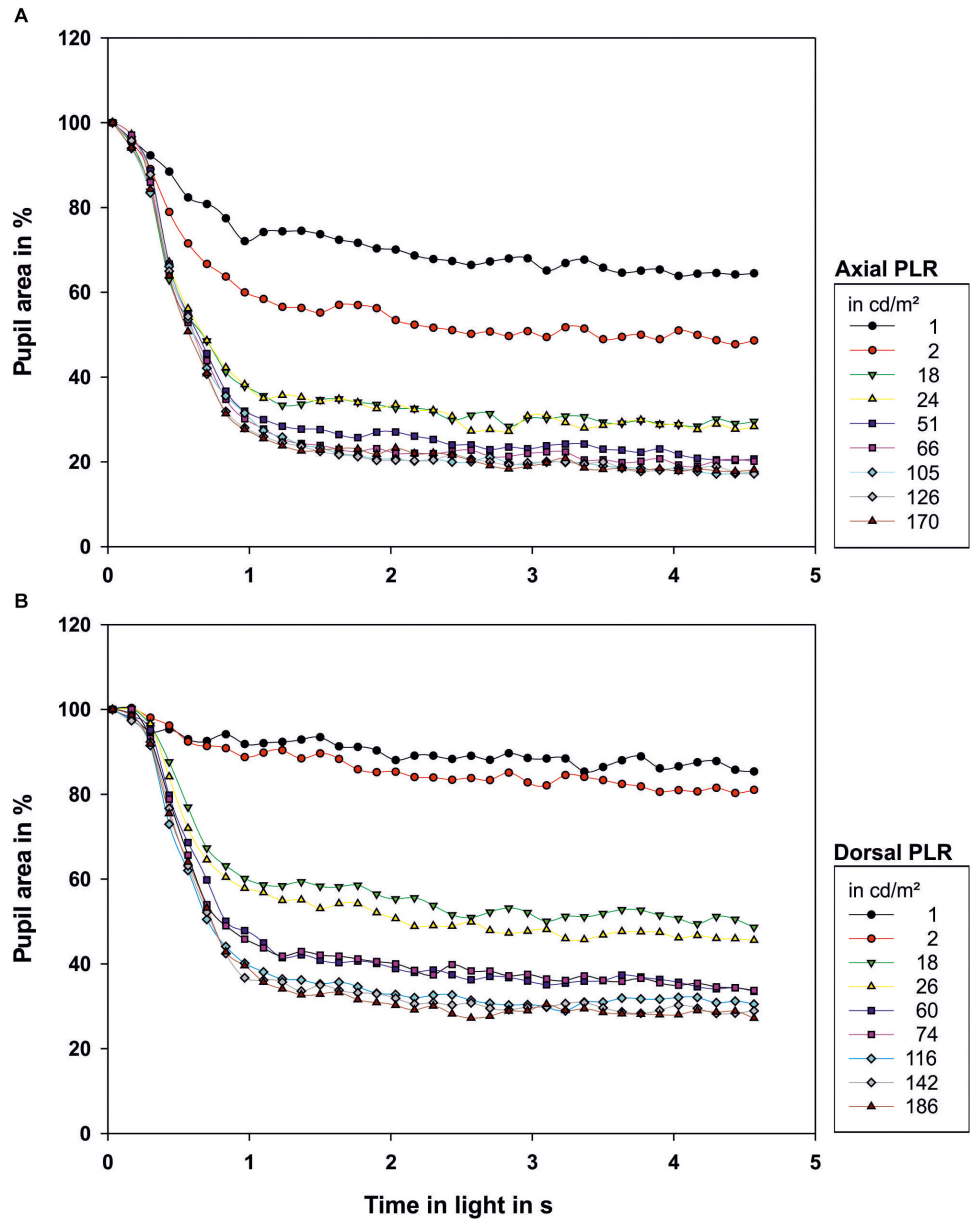

FIGURE 2 | Light reaction of the octopus pupil when **(A)** illuminated axially or **(B)** from dorsal. The area of the pupil is depicted as percentage of the area of the maximally dilated pupil at light onset. Each data point represents the mean value of the pupillary area of 3–9 measurements. The luminance of the light source in cd/m^2 measured from the distance at which the eye of the octopus had been during measurement is indicated in the legend. Light onset is zero on the time axis.

luminance of the front plate was measured. Before the next measurement, the animal was again in darkness for at least 3 min, ensuring that the pupil was fully dilated before the animal was exposed to the next light level. This way the luminance was increased stepwise from light level 1 to light level 9 (**Table 2**).

To assess the PDR, the octopus was first exposed to a dark period (dark period 1, **Figure 1F**), and second to a light period (**Figure 1F**) as during the documentation of the PLR. After this light period, during which a specific light level was set up (**Table 2**), the light was switched off, and the camera recorded the response of the pupil to sudden darkness over time (dark period 2, **Figure 1F**).

Data Analysis

For every PLR measurement, 140 frames (4.6 s) during the light period with the first frame at light onset were analyzed in ImageJ (Wayne Rasband). For the documentation of the PDR, 140 frames (4.6 s) during the dark period with the first frame at light turn-off were taken for the analysis, respectively. Thus the PLR and the PDR

were assessed over a time interval of 4.6 s with time steps of 0.125 s.

Pupillary area (**Figure 1D**) was measured with ImageJ (Wayne Rasband, W.S., ImageJ, U. S. National Institutes of Health, Bethesda, MD, United States, 1997–2018[1]) on all selected frames. A few frames could not be analyzed as

(1) the frame was blurred, mainly due to movements of the animal, or
(2) the pupil was fully or partially occluded, for example by an arm of the octopus.

To present the PLR and PDR, the pupil area was expressed as percent of the fully dilated pupil area measured on the first frame of the corresponding light period (Douglas et al., 1998, 2005; McCormick and Cohen, 2012).

The following aspects were analyzed:

(1) Pupil light reaction (PLR) – analysis of the pupil over time as a reaction to axial and dorsal light.
    a. t_{50}-value defined as the time after the onset of the light phase to achieve 50% maximum pupil constriction, derived from the minimal and the maximal pupil area measured.
    b. the PLR over a prolonged time period of 10 min as exemplary measurements
    c. maximum pupil constriction, defined as the minimal pupil area occurring during a measurement
(2) Pupil dark reaction (PDR) – analysis of the pupil area over time as reaction to darkness after axial and dorsal illumination in the light period.
    a. the PDR over a prolonged time period of 10 min as exemplary measurements
    b. maximum pupil dilation relative to maximal pupil area assessed right at the onset of the light period.

The data were statistically analyzed in R [R Core Team (2017) R: A language and environment for statistical computing. R Foundation for Statistical Computing, Vienna, Austria[2]].

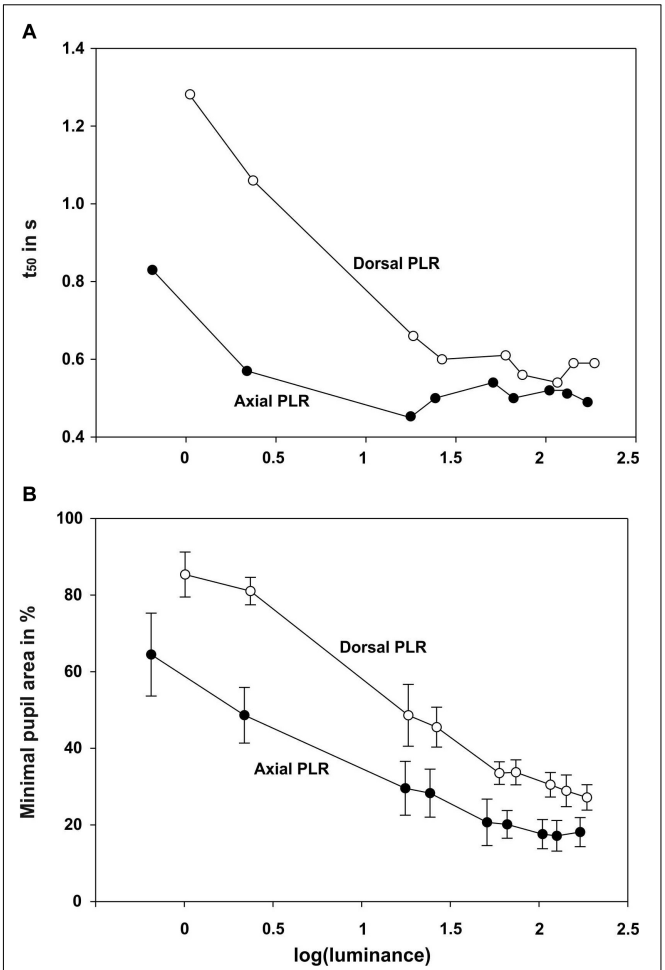

FIGURE 3 | Summary graphs showing for the pupillary light reaction with dorsal and axial illumination **A** the t_{50} value (in s) and **B** minimal pupil area (in % of the maximum pupil area at light onset) as a function of log (luminance).

RESULTS

After light onset, the pupil constricted within less than 1 s (**Figure 2**; all measurements can be found in **Supplementary Figure 1** and **Figure 3**). The t_{50}-values ranged from 0.45 to 0.83 s for axial illumination and from 0.54 to 1.29 s for dorsal illumination (**Table 2**). The pupil response was significantly faster to axial illumination than to dorsal illumination for low luminance values up to 2.4 cd/m^2 (general linear model with comparison of means, $p < 0.01$; **Figure 3A**). For higher luminance values, pupil reaction was not significantly faster during axial illumination in comparison to dorsal illumination ($p > 0.05$).

With luminance values up to 17.6 cd/m^2 for axial illumination (general linear model with comparison of means, $p < 0.001$) and to 26.4 cd/m^2 for dorsal illumination (general linear model with comparison of means, $p < 0.05$), the pupil only closed partially (**Figures 2**, **3B**). Higher ambient luminance values did not result in a significantly different pupil reaction.

Single measurements over a time period of 10 min revealed that the pupil finally re-dilated in light up to 86.4% of its maximal area for axial illumination (**Figure 4**). For dorsal illumination, the pupil even dilated completely with the pupil area reaching values above 100% of its initial maximal area at the onset of the light period.

The pupil area at maximum constriction of 10.3% of the dilated pupil area for axial illumination and 18.1% for dorsal illumination was reached after 4.3 and 3.5 s, respectively. For every light level, the pupil area was smaller during axial than during dorsal illumination (general linear model with comparison of means, $p < 0.05$).

[1]https://imagej.nih.gov/ij/
[2]https;//www.R-project.org/

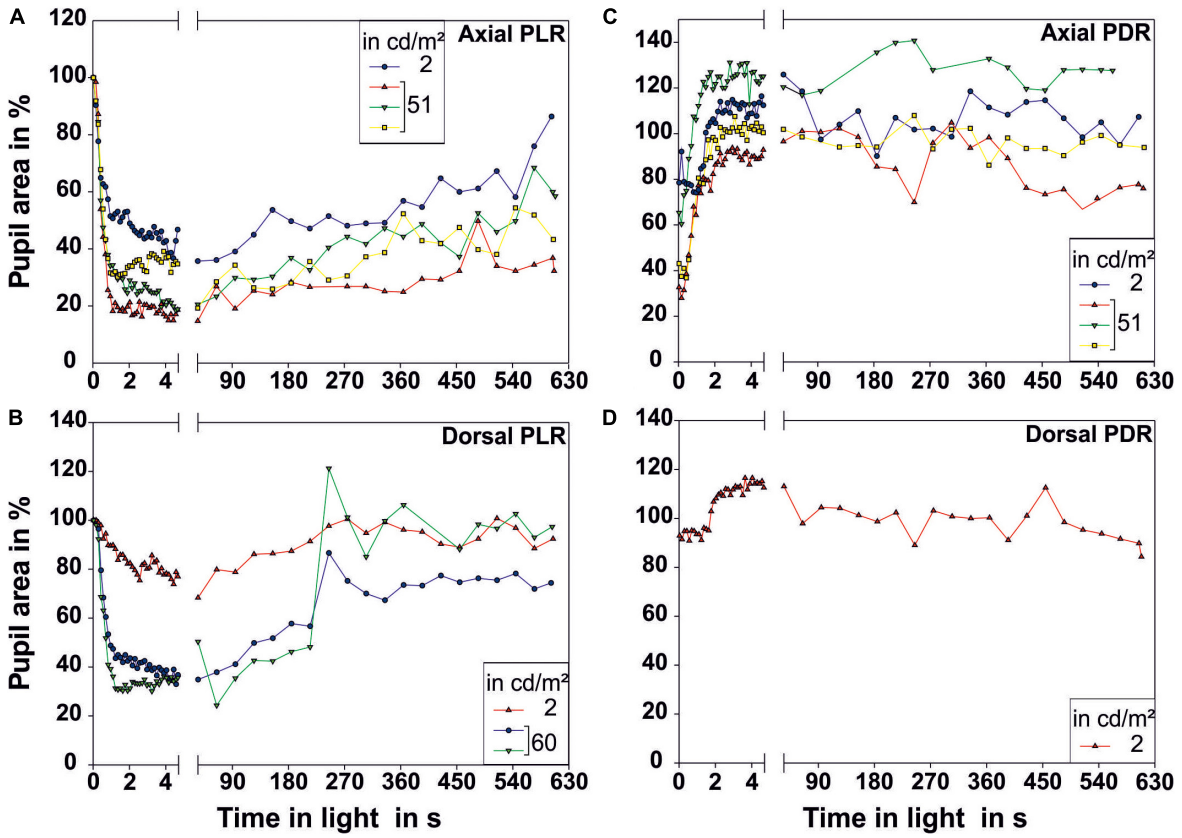

FIGURE 4 | Pupillary reactions measured over a prolonged time period of 10 min. **(A,B)** Illustrate the pupillary light reaction (PLR) for **(A)** axial (N = 4) and **(B)** dorsal illumination (N = 3). **(C,D)** Illustrate the pupillary dark reaction (PDR) for **(C)** axial (N = 4) and **(D)** dorsal illumination (N = 1). Only one low and one higher luminance were chosen for these long-term recordings. All measurements performed are plotted in this figure. The pupil size on the first frame of the light period was taken as 100% pupillary area. Each data point represents one measurement of pupillary area. The luminance of the light source in cd/m^2 measured from the distance at which the eye of the octopus had been during measurement is indicated in the legend. Light onset is zero on the time axis.

During the PDR, full pupillary dilation (**Figure 5**; all measurements can be found in **Supplementary Figure 2** and **Figure 4**) took slightly longer than 1 s especially when the eye was illuminated axially. Under this condition, there was more variation in the final pupil area than under dorsal illumination, and low light levels experienced before the documentation of the PDR caused the pupil to dilate to a larger area than the pupil area measured on the first frame of the light period. Prolonged measurements in darkness revealed that pupillary area varied drastically even in darkness with the pupil sometimes constricting even down to 66.9% for previous axial illumination and 84.3% for previous dorsal illumination (**Figure 3**).

DISCUSSION

In this study, we documented the course of the pupil light and dark reaction of one common octopus, *Octopus vulgaris*. This octopus showed vivid pupillary responses, and the resulting data are similar to pupillary reactions documented for other animals including other cephalopods (Douglas, 2018). Furthermore the reproducibility of our measurements is high. Thus we are confident that our measurements are reliable for this individual. Future measurements could help to clarify whether our results are representative for the species by measuring pupillary responses in other octopus individuals that will allow us to document their pupillary response without restrain. At the same time, the non-consensual pupillary response of the octopus described by Weel and Thore (1936) could be quantified in these future experiments.

Only weak light of <1 cd/m^2 was necessary to cause the pupil of *Octopus vulgaris* to constrict, similar to observations by previous researchers (Beer, 1897; Weel and Thore, 1936). A pupil constriction upon experiencing low ambient light is generally found in animals that are active under low light conditions (Douglas, 2018). The octopus experiences low light intensities for example in its den or when being active at night (Woods, 1965; Altman, 1966; Kayes, 1974) or during dusk or dawn (Mather, 1988). Thus a pupillary response adapted to operate under dim light conditions fits the ecology of the common octopus.

After the light was switched on, the octopus pupil closed within approximately 1 s. It needs to be mentioned that, in this study, we might have slightly overestimated the t_{50} value as the light was not instantaneously on; in the future, the pupillary responses could be re-determined and compared with

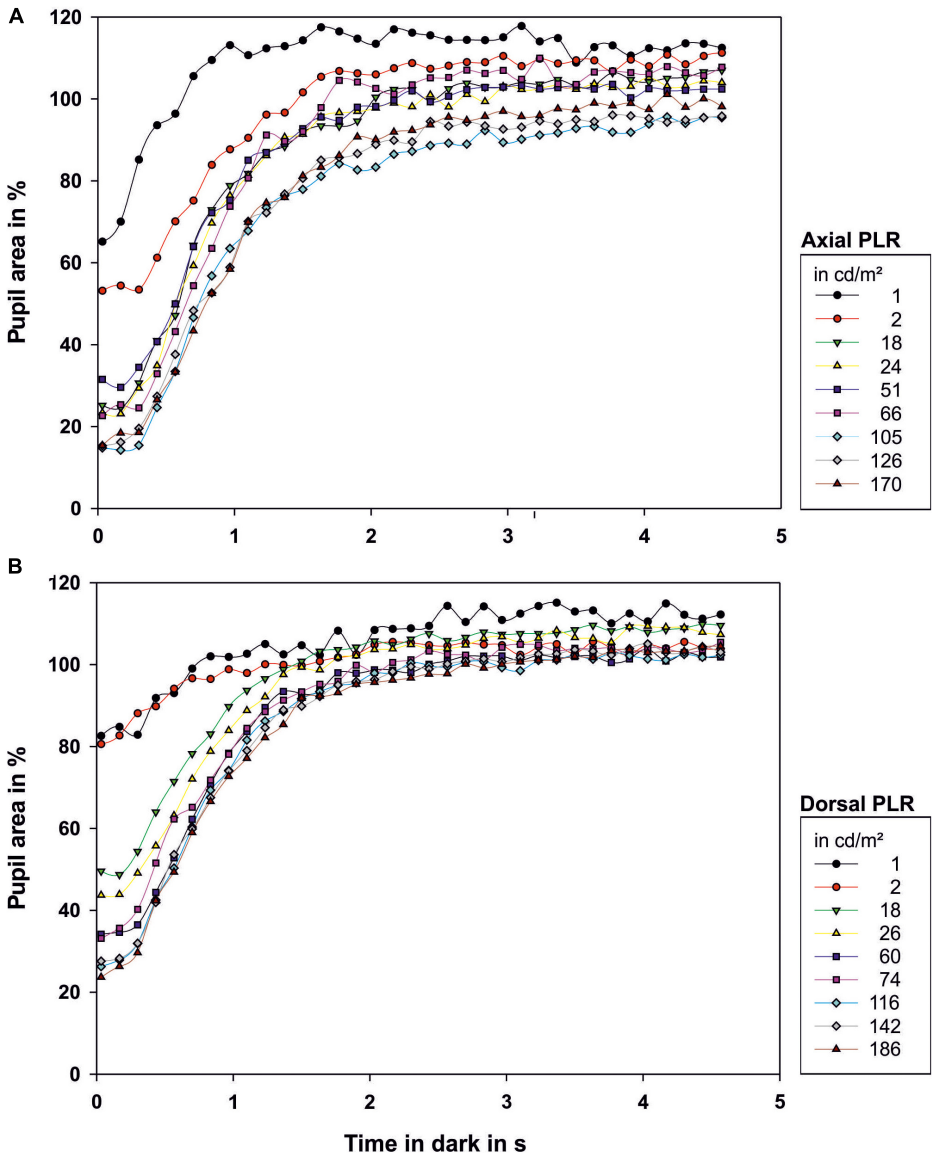

FIGURE 5 | Dark reaction of the octopus pupil when **(A)** illuminated axially or **(B)** from dorsal. The pupil size on the first frame of the light period was taken as 100% pupillary area. Therefore values above 100% occur. Zero on the time axis indicates when the light was switched off. Each data point represents the mean value of the pupillary area of 3–9 measurements. The luminance of the light source in cd/m^2 in the light period preceding the respective dark phase 2 is indicated in the legend.

new data obtained with a different light source that can be switched on instantaneously. The PLR of octopus as currently determined was slower than that of birds, but similar to that of humans or teleost fish (for overview see Douglas, 2018). Time for pupil closure was also in the same range as for many previously examined cephalopods (**Table 1**; Douglas et al., 2005; McCormick and Cohen, 2012; Matsui et al., 2016; Douglas, 2018). Most likely, the PLR is fast in these cephalopods as they experience rapid changes in ambient illumination in their natural habitat. *Octopus vulgaris* that can show diurnal activity (Meisel et al., 2003, 2006), might experience a fast and large increase of light intensity when leaving its dark den in shallow water during daytime. In this or similar situations, light incidence into the eye is regulated rapidly by the pupil, avoiding photon overload. However, under these circumstances, the pupil alone is not sufficient to adapt the eye; it has to be accompanied by other mechanisms (Douglas et al., 2005) such as pigment migration and/or changes in the length of the photoreceptors as mentioned in the introduction.

During our measurements, light caused the pupil to maximally constrict to approximately 10% of the dark-adapted pupil area. This maximal value is similar to previous results obtained in cephalopods (**Table 1**). However, we never observed the octopus pupil to constrict even further allowing light to only penetrate the eye at the two corners of the pupil as described for *Octopus vulgaris* by Weel and Thore (1936) and by

Heidermanns (1928). It remains to be determined whether the pupil of other *Octopus vulgaris* individuals would constrict to less than 10% of the dark-adapted pupil area. A constriction down to 10% fits to the octopus being a shallow-water species (Jereb et al., 2014; Sanchez et al., 2015). By contrast, many species diving fast and deep can close the pupil to much smaller areas (see for example data obtained in seals Levenson and Schusterman, 1997), which prepares the eyes for the darkness encountered at depth.

Under dorsal illumination, light had less effect on pupil area, compared to axial illumination; higher light intensities were required to cause pupillary constriction, and maximal constriction was 18%, thus less closed by almost a factor of two. In line with Jagger and Sands (1999) and Mäthger et al. (2013), we conclude that these effects were likely caused by the horizontal pupillary slit of octopus shielding light from above. Such a shadow effect is beneficial in the habitat of octopus (Jereb et al., 2014), in which light incidence is almost exclusively from above (see for example **Figure 5B** in Mäthger et al., 2013). As a consequence, a homogeneous illumination in the eye is most likely achieved (Jagger and Sands, 1999; Mäthger et al., 2013), and local adaptation of the retina will not be necessary. To support this consideration, a retinal illumination map would need to be computed for octopus the same way as was done in *Sepia officinalis* (Mäthger et al., 2013) and the octopus pupillary responses would need to be recorded with illumination from different sectors for comparison.

The PLR was slightly faster than the PDR in octopus as documented for humans (Mathôt, 2018) or insects (Stavenga, 1979; Stavenga et al., 1979). The fact that both reactions are fast, suggests that the eye of octopus possesses a dilator and a sphincter muscle. Froesch (1973) described a muscle layer within the iris of octopus, however, he could not distinguish between sphincters and dilators; an aspect that still awaits examination in a future project. Modeling the pupillary responses of *Octopus vulgaris* (see models for the human pupil such as Longtin and Milton, 1989; Pamplona et al., 2009; Fan and Yao, 2011; Johansson and Balkenius, 2017), another possible direction of current research, might additionally help to understand the underlying mechanisms.

We observed variations in pupil area under all experimental conditions. These variations can possibly be explained by pupil size serving additional functions besides the regulation of light incidence. First, if the lens suffers from longitudinal spherical aberration, a constricted pupil can result in an enhanced quality of the image, because light is restricted to the central part of the lens (Sivak, 1991; Douglas et al., 2005). Most likely the spherical lenses of *Octopus vulgaris* and other octopus species are corrected for longitudinal spherical aberration (Jagger and Sands, 1999). However, if some residual longitudinal spherical aberration was present as in other cephalopods (Sivak, 1982; Sroczynski and Muntz, 1985; Sroczynski and Muntz, 1987; Sivak, 1991; Sivak et al., 1994; Kröger and Gislen, 2004; Sweeney et al., 2007), closing the aperture of the eye would benefit image quality. Second, depth of focus is large in an eye with constricted pupil; being horizontally slit-shaped, depth of field is increased for horizontal contours (Banks et al., 2015). At specific times, it might be advantageous to have several objects in focus simultaneously eliminating the need for strong accommodation, even though *Octopus vulgaris* might be able to accommodate (Beer, 1897). Third, a constricted pupil could help to camouflage the eye. Cephalopods are masters of camouflage, however, camouflaging the eye is challenging especially if the pupil is dilated and can thus be seen as a large, dark, and regular spot. In contrast, a constricted pupil is less conspicuous than a dilated pupil as the dark area is smaller. Thus constricting the pupil, in combination with chromatophores and iridophores on the iris (Froesch, 1973), might conceal the eye for example in the presence of predators. In a benthic animal, predators might primarily approach from above, the direction which might be perfectly shielded by the horizontal arrangement of the pupil of octopus if the dorsal part of the eye lid indeed serves as a dorsal shield; an aspect that needs to be worked on in the future. An eye concealment function of the pupil has already been put forward for bottom-dwelling fish with mobile irises (Douglas, 2018; Youn et al., 2019) that stand in contrast to most teleost fish with immobile irises (Douglas, 2018). Lastly, a constricted and especially constricted off-axis pupil can increase chromatic blur of the optical system which monochromats might be able to use to obtain color information nevertheless (Stubbs and Stubbs, 2016).

While the previously mentioned functions relate to a constricted pupil, a dilated pupil can also fulfill additional functions; these might explain why we observed a strong re-dilation in light over time. The pupil might dilate due to arousal (Weel and Thore, 1936), or the dilated pupil could serve as an intraspecific signal (Packard, 1972). Additionally, if the pupil dilated when viewing close objects, defined as the near response, then the animal could use accommodation to judge its distance to an object (Wells, 1966). In general, pupil dilation can also be part of a deimatic display, as it possibly creates the illusion of being larger which could be essential when a predator suddenly appears (Wells, 1966; Hanlon and Messenger, 1988, 1996; Messenger, 2001).

CONCLUSION

In conclusion, the common octopus can rely on a mobile pupil to assist light and dark adaptation in its at times light-inhomogeneous environment.

DATA AVAILABILITY STATEMENT

All datasets generated for this study are included in the article/**Supplementary Material**.

ETHICS STATEMENT

The animal study was reviewed and approved by the Staatliches Amt für Umwelt und Natur Rostock, Landesamt für Landwirtschaft Lebensmittelsicherheit und Fischerei, Mecklenburg-Vorpommern.

AUTHOR CONTRIBUTIONS

CS and FH performed the measurements and analyzed the data. All authors conceived the experiment and contributed to and approved the final version of the manuscript.

FUNDING

This study was supported by a grant of the Deutsche Forschungsgemeinschaft to FH (HA 17891/2-1). We furthermore acknowledge the financial support of the Deutsche Forschungsgemeinschaft and the University Rostock/University medicine Rostock within the funding program Open Access Publishing.

SUPPLEMENTARY MATERIAL

The Supplementary Material for this article can be found online at: https://www.frontiersin.org/articles/10.3389/fphys.2020.01112/full#supplementary-material

REFERENCES

Altman, J. S. (1966). *The Behaviours of Octopus Vulgaris Lam. in its Natural Habitat: A Pilot Study*. Sliema: Underwater Association of Malta.

Babuchin, A. (1864). Vergleichend histologische Studien - übder den Bau der Cephalopodenretina. *Würzburger Naturwissenschaftliche Zeitschrift* 5, 127–140.

Banks, M. S., Sprague, W. W., Schmoll, J., Parnell, J. A. Q., and Love, G. D. (2015). Why do animal eyes have pupils of different shapes? *Sci. Adv.* 1:e1500391. doi: 10.1126/sciadv.1500391

Beer, T. (1897). Die Accommodation des kephalopodenauges. *Pflüger's Arch. Physiol.* 67, 541–587. doi: 10.1007/bf01661630

Bozzano, A., Pankhurst, P. M., Moltschaniwsky, N. A., and Villaneuva, R. (2009). Eye development in southern calamary, *Sepioteuthis australis*, embryos and hatchlings. *Mar. Biol.* 156, 1359–1373. doi: 10.1007/s00227-009-1177-2

Budelmann, B. U. (1994). Cephalopod sense organs, nerves and the brain: adaptations for high performance and lifestyle. *Mar. Freshw. Behav. Physiol.* 25, 13–33. doi: 10.1080/10236249409378905

Budelmann, B. U. (1996). Active marine predators: the sensory world of cephalopods. *Mar. Freshw. Behav. Physiol.* 27, 59–75. doi: 10.1080/10236249609378955

Budelmann, B. U., and Young, J. Z. (1984). The statocyst-oculomotor system of *Octopus vulgaris*: extraocular eye muscles, eye muscle nerves, statocyst nerves and the oculomotor centre in the central nervous system. *Philos. Trans. R. Soc. Biol. Charact.* 306, 159–189. doi: 10.1098/rstb.1984.0084

Byrne, R. A., Kuba, M., and Griebel, U. (2002). Lateral asymmetry of eye use in *Octopus vulgaris*. *Anim. Behav.* 64, 461–468. doi: 10.1006/anbe.2002.3089

Daw, N. W., and Pearlman, A. L. (1974). Pigment migration and adaptation in the eye of the squid, *Loligo pealei*. *J. Gen. Physiol.* 63, 22–36. doi: 10.1085/jgp.63.1.22

Douglas, R. H. (2018). The pupillary light response of animals; a review of their distribution, dynamics, mechanisms and functions. *Prog. Retin. Eye Res.* 66, 17–48. doi: 10.1016/j.preteyeres.2018.04.005

Douglas, R. H., Harper, R. D., and Case, J. F. (1998). The pupil of a teleost fish, *Porichthys notatus*: description and comparison to other species. *Vis. Res.* 38, 2697–2710. doi: 10.1016/s0042-6989(98)00021-2

Douglas, R. H., Williamson, R., and Wagner, H.-J. (2005). The pupillary response of cephalopods. *J. Exp. Biol.* 208, 261–265. doi: 10.1242/jeb.01395

Fan, X., and Yao, G. (2011). Modeling transient pupillary light reflex induced by a short light flash. *IEEE Trans. Biomed. Eng.* 58, 36–42. doi: 10.1109/tbme.2010.2080678

Fiorito, G., Affuso, A., Anderson, D. B., Basil, J. A., Bonnaud, L., Botta, G., et al. (2014). Cephalopods in neuroscience: regulations, research and the 3Rs. *Invertebr. Neurosci.* 14, 13–36. doi: 10.1007/s10158-013-0165-x

Fiorito, G., Affuso, A., Basil, J. A., Cole, A., de Girolamo, P., D'Angelo, L., et al. (2015). Guidelines for the care and welfare of cephalopods in research – a consensus based on an initiative by CephRes, FELASA and the Boyd Group. *Lab. Anim.* 49, 1–90. doi: 10.1177/0023677215580006

Froesch, D. (1973). On the fine structure of the *Octopus iris*. *Z. Zellforschung* 145, 119–129. doi: 10.1007/bf00307193

Gleadall, I. G., Ohtsu, K., Gleadall, E., and Tsukahara, Y. (1993). Screening pigment migration in the *Octopus* retina includes control by dopaminergic efferents. *J. Exp. Biol.* 185, 1–16.

Glockauer, A. (1915). Zur Anatomie und Histologie des Cephalopodenauges. *Z. Wissenschaftliche Zool.* 113, 325–360.

Hagins, W. A., and Liebman, P. A. (1962). Light-induced pigment migration in the squid retina. *Biol. Bull.* 123:498.

Hanlon, R. T., and Messenger, J. B. (1988). Adaptive coloration in young cuttlefish (*Sepia officinalis* L.): the morphology and development of body patterns and their relation to behaviour. *Philos. Trans. R. Soc. Biol. Charact.* 320, 437–487. doi: 10.1098/rstb.1988.0087

Hanlon, R. T., and Messenger, J. B. (1996). *Cephalopod Behaviour*. Cambridge: Cambridge University Press.

Heidermanns, C. (1928). Messende Untersuchungen über das Formensehen der Cephalopoden und ihre optische Orientierung im Raume. *Zool. Jahrbuecher Abteilung Allgemeine Zool. Physiol.* 45, 346–349.

Hess, C. (1905). Beiträge zur Physiologie und Anatomie des Cephalopodenauges. *Pflügers Arch. Gesamte Physiol.* 109, 393–439. doi: 10.1007/bf01677979

Hess, C. (1909). Die Accommodation der Cephalopoden. *Arch. Augenheilkunde* 64, 125–152.

Hess, C. (1910). Untersuchungen über den Lichtsinn bei wirbellosen Tieren. *Pflüger Arch. Gesamte Physiol.* 136, 282–367. doi: 10.1007/bf01681999

Hesse, R. (1900). Untersuchungen über die Organe der Lichtempfindung bei niederen Tieren. Die Retina der Cephalopoden. *Z. Wissenschaftliche Zool.* 68, 379–477. doi: 10.1007/bf00339022

Hurley, A. C., Lange, G. D., and Hartline, P. H. (1978). The adjustable "pinhole camera" eye of Nautilus. *J. Exp. Zool.* 205, 37–44. doi: 10.1002/jez.1402050106

Jagger, W. S., and Sands, P. J. (1999). A wide-angle gradient index optical model of the crystalline lens and eye of the *Octopus*. *Vis. Res.* 39, 2841–2852. doi: 10.1016/s0042-6989(99)00012-7

Jereb, P., Roper, C. F. E., Norman, M. D., and Finn, J. K. (2014). *Cephalopods of the World - An Annotated and Illustrated Catalogue of Cephalopod Species Known to Date. Volume 3. Octopods and Vampire Squids*. Rome: FAO.

Johansson, B., and Balkenius, C. (2017). A computational model of pupil dilation. *Connect. Sci.* 30, 1–15. doi: 10.1080/09540091.2016.1271401

Kayes, R. J. (1974). The daily activity pattern of *Octopus vulgaris* in a natural habitat. *Mar. Behav. Physiol.* 2, 337–343. doi: 10.1080/10236247309386935

Kilkenny, C., Browne, W. J., Cuthill, I. C., Emerson, W., and Altmann, D. G. (2010). Improving bioscience research reporting: the ARRIVE guidelines for reporting animal research. *PLoS Biol.* 8:e1000412. doi: 10.1371/journal.pbio.1000412

Kröger, R. H. H., and Gislen, A. (2004). Compensation for longitudinal chromatic aberration in the eye of the firefly squid, *Watasenia scintillans*. *Vis. Res.* 44, 2129–2134. doi: 10.1016/j.visres.2004.04.004

Land, M. F. (1984). "Molluscs," in *Photoreception and Vision in Invertebrates*, ed. M. A. Ali (New York, NY: Plenum Press), 699–725. doi: 10.1007/978-1-4613-2743-1_20

Levenson, D. H., and Schusterman, R. J. (1997). Pupillometry in seals and sea lions: ecological implications. *Can. J. Zool.* 75, 2050–2057. doi: 10.1139/z97-838

Longtin, A., and Milton, J. G. (1989). Modelling autonomous oscillations in the human pupil light reflex using non-linear delay-differential equations. *Bull. Math. Biol.* 51, 605–624. doi: 10.1016/s0092-8240(89)80103-x

Magnus, R. (1902). Die Pupillarreaction der Octopoden. *E. Pflüger Arch. Physiol.* 92, 623–643. doi: 10.1007/bf01790186

Mather, J. A. (1988). Daytime activity of juvenile *Octopus vulgaris* in Bermuda. *Malacologia* 29, 69–76.

Mäthger, L. M., Hanlon, R. T., Hakansson, J., and Nilsson, D.-E. (2013). The W-shaped pupil in cuttlefish (*Sepia officinalis*): functions for improving horizontal vision. *Vis. Res.* 83, 19–24. doi: 10.1016/j.visres.2013.02.016

Mathôt, S. (2018). Pupillometry:psychology, physiology, and function. *J. Cogn.* 1, 1–23. doi: 10.5334/joc.18

Matsui, H., Takayama, G., and Sakurai, Y. (2016). Physiological response of the eye to different colored light-emitting diodes in Japanese flying squid *Todarodes pacificus*. *Fish. Sci.* 82, 303–309. doi: 10.1007/s12562-015-0965-5

McCormick, L. R., and Cohen, J. H. (2012). Pupil light reflex in the Atlantic brief squid, *Lolliguncula brevis*. *J. Exp. Biol.* 215, 2677–2683. doi: 10.1242/jeb.068510

Meisel, D. V., Byrne, M., Kuba, M., Mather, J. A., Ploberger, W., and Reschenhofer, E. (2006). Contrasting activity patterns of two related *Octopus* species, *Octopus macropus* and *Octopus vulgaris*. *J. Comp. Psychol.* 120, 191–197. doi: 10.1037/0735-7036.120.3.191

Meisel, D. V., Byrne, R. A., Kuba, M., Griebel, U., and Mather, J. A. (2003). "Circadian rhythms in *Octopus vulgaris*," in *Coleoid Cephalopods Through Time*, eds K. Warnke, H. Keupp, and S. V. Boletzky (Berlin: Berlin Paläobiologische Abhandlung), 171–177.

Messenger, J. B. (1979). The eyes and skin of *Octopus*: compensating for sensory deficiencies. *Endeavour* 3, 92–98. doi: 10.1016/0160-9327(79)90096-6

Messenger, J. B. (2001). Cephalopod chromatophores: neurobiology and natural history. *Biol. Rev.* 76, 473–528. doi: 10.1017/s1464793101005772

Muntz, W. R. A. (1963). Intraretinal transfer and the function of the optic lobes in *Octopus*. *Q. J. Exp. Psychol.* 15, 116–124. doi: 10.1080/17470216308416562

Muntz, W. R. A. (1977). Pupillary response of cephalopods. *Symp. Zool. Soc. Lond.* 38, 277–285.

Muntz, W. R. A., and Ray, U. (1984). On the visual system of *Nautilus pompilius*. *J. Exp. Biol.* 109, 253–263.

Packard, A. (1972). Cephalopods and fish: the limits of convergence. *Biol. Rev.* 47, 241–307. doi: 10.1111/j.1469-185x.1972.tb00975.x

Pamplona, V. F., Oliveira, M. M., and Baranoski, G. G. (2009). Photorealtistic models for pupil light reflex and iridal pattern deformation. *ACM Trans. Graph.* 28, 106.101–106.112.

Rawitz, B. (1891). Zur Physiologie der Cephalopodenretina. *Arch. Anat. Physiol.* 5/6, 367–372.

Sanchez, P., Villanueva, R., Jereb, P., Guerra, A., Gonzalez, A. F., Sobrino, I., et al. (2015). "*Octopus*," in *Cephalopod biology and fisheries in Europe: II. Species accounts*, eds P. Jereb, L. Allcock, E. Lefkaditou, U. Piatkowski, L. C. Hastie, and G. J. Pierce (Copenhagen: ICES International Council for the Exploration of the Sea).

Schaeffel, F., Murphy, C. J., and Howland, H. C. (1999). Accommodation in the cuttlefish (*Sepia officinalis*). *J. Exp. Biol.* 202, 3127–3134.

Sivak, J. G. (1982). Optical properties of a cephalopod eye (the short finned squid, *Illex illecebrosus*). *J. Comp. Physiol. A* 147, 323–327. doi: 10.1007/bf00609666

Sivak, J. G. (1991). Shape and focal properties of the cephalopod ocular lens. *Can. J. Zool.* 69, 2501–2506. doi: 10.1139/z91-354

Sivak, J. G., West, J. A., and Campbell, M. C. (1994). Growth and optical development of the ocular lens of the squid (*Sepioteuthis lessoniana*). *Vis. Res.* 34, 2177–2187. doi: 10.1016/0042-6989(94)90100-7

Smith, J. A., Andrews, P. L. R., Hawkins, P., Louhimies, S., Ponte, G., and Dickel, L. (2013). Cephalopod research and EU Directive 2010/63/EU: requirements, impacts and ethical review. *J. Exp. Mar. Biol. Ecol.* 447, 31–45. doi: 10.1016/j.jembe.2013.02.009

Sroczynski, S., and Muntz, W. R. A. (1985). Image structure in *Eledone cirrhosa*, an *Octopus*. *Zool. Jahrbücher Abteilung Allgemeine Zool. Physiol.* 89, 157–168.

Sroczynski, S., and Muntz, W. R. A. (1987). The optics of oblique beams in the eye of *Eledone cirrhosa*, an *Octopus*. *Zool. Jahrbücher Abteilung Allgemeine Zool. Physiol.* 91, 419–446.

Stavenga, D. G. (1979). Visual pigment processes and prolonged pupillary responses in intact photoreceptor cells. *Biophys. Struct. Mech.* 5, 175–185. doi: 10.1007/bf00535446

Stavenga, D. G., Bernard, G. D., Chappell, R. L., and Wilson, M. (1979). Insect pupil mechanisms I. On the pigment migration in the retinula cells of Hymenoptera (suborder Apocrita). *J. Comp. Physiol.* 129, 199–205. doi: 10.1007/bf00657654

Stubbs, A. L., and Stubbs, C. W. (2016). Spectral discrimination in color blind animals via chromatic aberration and pupil shape. *PNAS* 113, 8206–8211. doi: 10.1073/pnas.1524578113

Suzuki, T., Inada, H., and Takahashi, H. (1985). Retinal adaptation of Japanese common squid (*Tedarodes pacificus* Steenstrup) to light changes. *Bull. Faculty Fish. Hokkaido Univ.* 36, 191–199.

Suzuki, T., and Takahashi, H. (1988). Responses of the retina of flying squid *Sthenotiuthis oualaniensis* (Lesson) to light changes. *Bull. Fac. Fish Hokkaido Univ.* 39, 21–26.

Sweeney, A. M., Des Marais, D. L., Ban, Y.-E. A., and Johnson, S. (2007). Evolution of graded refractive index in squid lenses. *J. R. Soc. Interface* 4, 685–698. doi: 10.1098/rsif.2006.0210

Weel, P. B., and Thore, S. (1936). Über die Pupillarreaktion von *Octopus vulgaris*. *Z. Vergleichende Physiol.* 23, 26–33.

Wells, M. J. (1960). Proprioception and visual discrimination of orientation in *Octopus*. *J. Exp. Biol.* 37, 489–499.

Wells, M. J. (1966). "Cephalopod sense organs," in *Physiology of Mollusca*, eds K. M. Wilbur and C. M. Yonge (New York, NY: Academic Press), 523–545. doi: 10.1016/b978-1-4832-3242-3.50020-3

Wiley, A. (1902). *Contribution to the Natural History of the Pearly Nautilus*. Cambridge, MA: Cambridge University Press.

Woods, J. (1965). *Octopus*-watching off Capri. *Animals* 7, 324–327.

Youn, S., Okinaka, C., and Mäthger, L. M. (2019). Elaborate pupils in skates may help camouflage the eye. *J. Exp. Biol.* 222:jeb195966. doi: 10.1242/jeb.195966

Young, J. Z. (1963). Light- and dark-adaptation in the eyes of some cephalopods. *Proc. Zool. Soc. Lond.* 140, 255–272. doi: 10.1111/j.1469-7998.1963.tb01863.x

Conflict of Interest: The authors declare that the research was conducted in the absence of any commercial or financial relationships that could be construed as a potential conflict of interest.

frontiers in Physiology

ORIGINAL RESEARCH
published: 29 September 2020
doi: 10.3389/fphys.2020.521989

Diversity of Light Sensing Molecules and Their Expression During the Embryogenesis of the Cuttlefish (*Sepia officinalis*)

Morgane Bonadè[1], Atsushi Ogura[2], Erwan Corre[3], Yann Bassaglia[1,4] and Laure Bonnaud-Ponticelli[1]*

[1] Laboratoire Biologie des Organismes et Ecosystèmes Aquatiques, Muséum National d'Histoire Naturelle, Sorbonne Université, Centre National de la Recherche Française (FRE2030), Université de Caen Normandie, Institut de Recherche pour le Développement (IRD 207), Université des Antilles, Paris, France, [2] Department of Computer Bioscience, Nagahama Institute of Bio-Science and Technology, Nagahama, Japan, [3] Station biologique de Roscoff, plateforme ABiMS, FR2424 CNRS-Sorbonne Université (UPMC), Roscoff, France, [4] Université Paris Est Créteil-Val de Marne (UPEC), Créteil, France

OPEN ACCESS

Edited by:
Chuan-Chin Chiao, National Tsing Hua University, Taiwan

Reviewed by:
Gabriella Mazzotta, University of Padua, Italy
Megan L. Porter, University of Hawaii, United States

***Correspondence:**
Morgane Bonadè
morgane.bonade@edu.mnhn.fr;
morgane.bonade@gmail.com

Specialty section:
This article was submitted to Invertebrate Physiology, a section of the journal Frontiers in Physiology

Received: *29 January 2020*
Accepted: *17 August 2020*
Published: *29 September 2020*

Citation:
Bonadè M, Ogura A, Corre E, Bassaglia Y and Bonnaud-Ponticelli L (2020) Diversity of Light Sensing Molecules and Their Expression During the Embryogenesis of the Cuttlefish (Sepia officinalis). Front. Physiol. 11:521989. doi: 10.3389/fphys.2020.521989

Eyes morphologies may differ but those differences are not reflected at the molecular level. Indeed, the ability to perceive light is thought to come from the same conserved gene families: opsins and cryptochromes. Even though cuttlefish (Cephalopoda) are known for their visually guided behaviors, there is a lack of data about the different opsins and cryptochromes orthologs represented in the genome and their expressions. Here we studied the evolutionary history of opsins, cryptochromes but also visual arrestins in molluscs with an emphasis on cephalopods. We identified 6 opsins, 2 cryptochromes and 1 visual arrestin in *Sepia officinalis* and we showed these families undergo several duplication events in Mollusca: one duplication in the arrestin family and two in the opsin family. In cuttlefish, we studied the temporal expression of these genes in the eyes of embryos from stage 23 to hatching and their expression in two extraocular tissues, skin and central nervous system (CNS = brain + optic lobes). We showed in embryos that some of these genes (Sof_CRY$_6$, Sof_reti-1, Sof_reti-2, Sof_r-opsin1 and Sof_v-arr) are expressed in the eyes and not in the skin or CNS. By looking at a juvenile and an adult *S. officinalis*, it seems that some of these genes (Sof_r-opsin1 and Sof_reti1) are used for light detection in these extraocular tissues but that they set-up later in development than in the eyes. We also showed that their expression (except for Sof_CRY$_6$) undergoes an increase in the eyes from stage 25 to 28 thus confirming their role in the ability of the cuttlefish embryos to perceive light through the egg capsule. This study raises the question of the role of Sof_CRY$_6$ in the developing eyes in cuttlefish embryos and the role and localization of xenopsins and r-opsin2. Consequently, the diversity of molecular actors involved in light detection both in the eyes and extraocular tissues is higher than previously known. These results open the way for studying new molecules such as those of the signal transduction cascade.

Keywords: opsin, cryptochrome, arrestin, eye, development, *Sepia officinalis*

INTRODUCTION

Eyes are specialized light-sensitive sensory structures, most of time involved in image forming vision. They can take a wide variety of shapes and the molluscan clade displays an amazing diversity of eye morphologies: pallial eyes in bivalves, cephalic eyes in gastropods, ocellus in chitons and camerular eyes in cephalopods. Cephalopods in general, and cuttlefish in particular, have been extensively studied for their visually guided behaviors. The visual system of coleoid cephalopods is mainly composed of two large spherical eyes with a lens, a vitreous cavity and an iris, known as camera (or camerular) eyes. They are linked to optic lobes through optic nerves. Optic lobes are located on each side, between the eye and the brain. They are involved in visual processing and visuomotor control and are essential for the transmission of light information to the brain (Boycott, 1961; Young, 1962, 1974). In *Sepia officinalis*, the two optic lobes represent about twice the size of the brain (Nixon and Young, 2003) and the eyes harbor rhabdomeric photoreceptor cells as in many protostomians. This visual system sets up during embryogenesis. This was described in *Sepiella japonica*: first the eyes vesicles are formed, then a light orange pigmentation starts to appear on the retina and darkens until reaching a dark brown color at the time of hatching. The photoreceptor cells appear from a differentiation of the retinal epithelium and are mature a little before hatching (Yamamoto, 1985). Furthermore, electrophysiological studies have shown that eyes of *S. japonica* embryos were already reacting to light before the final differentiation of the retina (Yamamoto et al., 1985). In *S. officinalis*, the macroscopic setting-up of the visual system is similar (**Figure 1**; Boletzky et al., 2016). Behavioural studies have shown that the embryo is able to answer a light stimulation as soon as the pigmentation starts to appear in the eyes (stage 25: Romagny et al., 2012). Indeed, this pigmentation is due to the presence of retinal in the rhabdomes: retinal is a chromophore that switches conformation when absorbing light, thus activating a light sensing molecule. Actually, at the molecular level, photoreceptor cells all contain light sensing molecules responsible of light detection. These light sensing molecules interact with a variety of other molecular actors, which either regulate their function or act as down-stream effectors to ensure the transduction of signals [depending on light sensing molecules reviewed in Yau and Hardie (2009) and Chaves et al. (2011)]. The transcription pathways of these molecules have just begun to be studied in cephalopods.

Most studies focusing on light sensing molecules in cephalopods have been done in adults whereas the embryos are able to perceive light suggesting the visual system is already functional in embryos (Romagny et al., 2012). Our work aims at identifying the light sensing molecules expressed in *S. officinalis* embryos in order to characterize the timeline and the putative correlation of the respective appearance of molecules and visual/photosensitive function. We focused on opsins and cryptochromes and we also study the "squid visual arrestin" (Yoshida et al., 2015) thought to be implicated in phototransduction in visual cells.

The opsin family is a multigenic family of G protein coupled receptors (GPCR) which can be found in most eumetazoans (Porter et al., 2011; Feuda et al., 2012; Ramirez et al., 2016). They bind retinal enabling light detection and have been studied in many taxa for their involvement in vision. Phylogenetic relationships of opsins are complex and a recent publication with large sampling across eumetazoans suggested at least 9 opsins paralogs in the ancestor of bilaterians (Ramirez et al., 2016). From these 9 groups of opsins, only 6 have been identified in molluscs (canonical r-opsins, non-canonical r-opsins, xenopsins, retinochromes, Go-opsins and neuropsins), 4 in cephalopods (canonical r-opsins, non-canonical r-opsins, xenopsins, retinochromes) but only 2 in *S. officinalis* (Ramirez et al., 2016). Most opsins are expressed in the eyes or in neural tissues, even if they may also be found in other tissues (Porter et al., 2011). In the pigmy squid (*Idiosepius paradoxus*), 5 sequences of opsins have been identified; all are expressed in the eyes but only r-opsin1 and retinochrome 1 (reti-1) seem eye-specific (Yoshida et al., 2015). The authors also documented a squid specific duplication of the retinochrome gene and identified for the first time a xenopsin in a cephalopod (firstly described as a c-opsin _ Yoshida et al., 2015; Ramirez et al., 2016). In adult *S. officinalis*, the spatial expression of the two known opsins has been studied: r-opsin1 (rhodopsin in the literature, Bellingham et al., 1998) and a retinochrome are expressed in the eyes and the skin (Mäthger et al., 2010; Kingston et al., 2015a). Indeed, r-opsins are known for their involvement in vision in many protostomians and retinochromes are thought to work together with them. Retinochromes have the ability to switch retinal back to its original conformation after its linkage with r-opsins thus allowing r-opsins to bind it and signal again. *In situ* hybridization also showed that r-opsin1 is expressed during late embryogenesis from stage 23 to hatching in the eye of *S. officinalis* embryos (Imarazene et al., 2017).

Cryptochromes belong to a family of molecules able to sense light in the blue and UV range. This family gathers photolyases and both animal and plant cryptochromes (which are not homologous). These flavoproteins are usually studied in the central nervous system (Benito et al., 2008). They have been detected in photoreceptor cells in the eyes of species far apart across the bilaterian phylogenetic tree (in amphibians: Zhu and Green, 2001; in insects: Yoshii et al., 2008; in mammals: Tosini et al., 2007; Nießner et al., 2016; in birds: Wiltschko and Wiltschko, 2014). They have been mainly studied for their involvement in non-visual light sensing roles such as control of circadian rhythm, compass navigation and maybe even magnetoreception [reviewed in Chaves et al. (2011)]. Recent studies in *Drosophila melanogaster* suggested that a cryptochrome could be able to interact with the phototransduction complex and that it would have an indirect role in vision by regulating the circadian plasticity of visual system sensitivity (Mazzotta et al., 2013; Mazzotta and Costa, 2016). Usually three families of animal cryptochromes are described: the Cry123 and the Cry45-Photolyase families which are found in all bilaterians and the Cry6 family which has only been described in

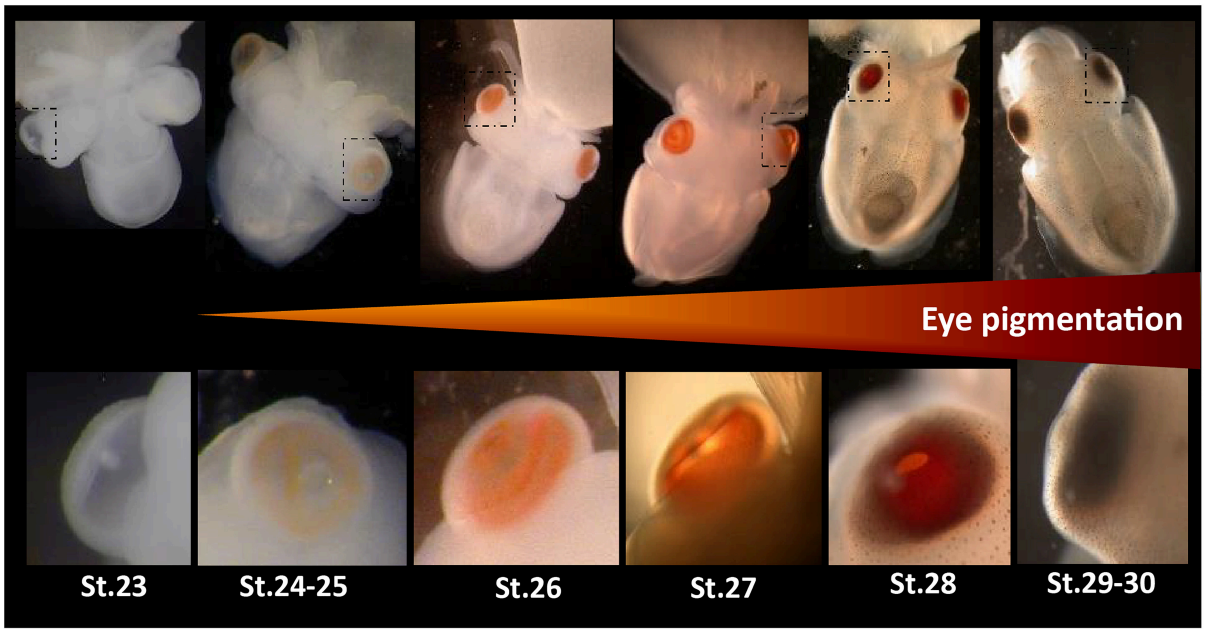

FIGURE 1 | Eye development in *Sepia* embryos. 30 developmental stages of *Sepia officinalis* are described (Boletzky et al., 2016). Top: full embryos, bottom: magnification of the eyes. Eye pigmentation starts at stage 24–25 (light orange) then darkens until reaching a dark brown color at the time of hatching.

protostomians (Oliveri et al., 2014; Haug et al., 2015). In molluscs, representatives of these three families have been described (Oliveri et al., 2014). Regarding cephalopods, the only published data focus on *Euprymna scolopes* (Heath-Heckman et al., 2013). In this species, two different cryptochromes (*escry1* and *escry2*) were identified with a daily cycling expression in the head for both of them.

The arrestin family is known for its ability to regulate signal transduction by interacting with GPCR. Several paralogs are known to be specifically expressed in the photoreceptor cells and to interact with visual opsins: S-Arrestin (or SAG) and Arrestin-C (or Arrestin-X) (Craft and Whitmore, 1995) in vertebrates and visual arrestins (also called phosrestines) in arthropods (Montell, 1999; Merrill et al., 2003). Recently a "squid visual arrestin", specifically expressed in the eyes, was identified in three Decabrachia cephalopods (Mayeenuddin and Mitchell, 2003; Yoshida et al., 2015).

In this study, we identified and phylogenetically characterized in *S. officinalis* the light-sensitive molecules, opsins and cryptochromes, and one associated molecule, visual arrestin. We localized transcripts of these molecules through different technics in embryos, a juvenile and adults. Expressions were found in the eyes but also in other tissues with photosensitive properties (skin and CNS). The dynamics were established in the developing eyes by looking at the temporal expression of these genes in several late embryonic stages. We found diverse photosensitive molecules and have a better understanding of their evolutionary history in molluscs and in cephalopods. Our results allowed us to try to link their expression to the acquisition of visual function and photosensitivity before and after hatching.

MATERIALS AND METHODS

Biological Samples, Dissection and Fixation

Embryos

S. officinalis eggs were all obtained from Roscoff marine station (CRB-Sorbonne Université-EMBRC, France) except the stage 30 embryo used for *in situ* hybridization (ISH), that comes from Caen (CREC station-Université Caen Normandie). The embryos used for RNA-seq were cultured in an open circulatory system with filtered sea water at 17°C and under natural light. The embryos used for RT-qPCR were kept in these same conditions except that the photoperiod was controlled with an alternating 12 h of light and 12 h darkness with a LED mimicking daylight. The embryo from Caen (for ISH) was kept for several weeks in a closed circulatory system, artificial sea water at 19°C and under natural light. Embryos were extracted from the chorion, in filtered seawater on ice in order to anesthetize the animals, the yolk was removed and they were staged (Boletzky et al., 2016). The fixation always took place from June to early August during day time (from 10 a.m. to 4 p.m.) under natural light.

For RT-qPCR experiment and RNA sequencing, the samples were immersed in RNA later and kept in RNA Later (SIGMA) at −20°C before being studied. Stages 23, 25, 28 and 30 were used for the RT-qPCR experiment and stages 24, 25, and 30 for the RNA sequencing. Prior to extraction, eyes were dissected and lens were removed, brain and optic lobes were dissected and samples of dorsal and ventral skin were taken.

For *in situ* hybridization, a late stage 30 embryo was fixed in 4% Paraformaldehyde (PAF-Formaldehyde- EMS, Hatfield) in PBS 1X at 4°C, 3 times 24 h. After being rinse in PBS 1X (3 times 10 min), it was dehydrated in 50% methanol/50% PBS 1X for 20 min, and in methanol 100% for 48 h at 4°C. The embryo was kept in methanol 100% at −20°C.

Juveniles

Eggs were obtained from Caen (CREC marine station-Université de Caen Normandie). They were maintained in a tank in a closed circulatory system of artificial seawater in controlled condition of temperature (19°C) until hatching. Hatchlings began to feed after 1 week, then juveniles were fed with alive or frozen preys until 1 month old in a tank equipped with structures adapted for animal welfare. They were placed on cold seawater with MgCl2 as an anesthetic. After several minutes, when no more reaction was observed, animals were immediately immersed in RNA later. Brain, eyes; skin, and other tissues were immediately taken and kept in RNA later.

Sub-Adults

Freshly fished specimens of *S. officinalis,* from Atlantic Ocean (Ile D'Yeu, France), that just died, were used. They were always kept on ice and were dissected on the boat: eyes, brains, optic lobes and skin were removed and placed in RNA Later. They were kept for 6 days at room temperature and maintained at −80°C until RNA extraction.

RNA Sequencing

RNA Extraction

Embryos

Eyes, skin and central nervous system (CNS = brain + optic lobes) of embryos from stage 24, stage 25 (only eyes and CNS) and stage 30 were used. For each organ, two embryos were used per stage (=2 biological duplicates). EZNA Mollusc RNA extraction kit (Omega bio-tek) was used with an on-membrane DNAse I (Qiagen) treatment and tissues were disrupted using lysis buffer from the kit and vortex alone. RNAs were eluted in RNAse-Free water at 65–70°C. Quantity and quality were assessed with Qubit 3 fluorometer (Invitrogen), Nanodrop^{TM} (ThermoScientific) and Bioanalyzer 2100 (Agilent). Finally, RNAs were stored at −80°C before use.

Juvenile

Brain, skin, eye for one specimen and overall body and shell sacs for three specimens were used. Tissue pieces were homogenized using needle in TriZol reagent (Life Technologies, Carlsbad, CA, United States) and the suspension was applied on Qiashredder column (Qiagen), and deproteinized with chloroform. Supernatant was applied on a gDNA eliminator column (Qiagen) to eliminate DNA, and RNAs were purified using Rneasy plus mini, midi or micro kit (Qiagen) depending on the weight of the tissue. RNAs were kept in water, the quality evaluated by Nanodrop^{TM} (ThermoScientific) and sent for sequencing.

Sequencing and Assembling

Embryos

RNAs were sequenced by BGI Inc., using Illumina HiSeq 2000 technology according to usual protocol. The 457.6 million clean short reads sequences obtained (ranging from 21.2 to 39.9 million/sample; Average Q20 = 96.4%) were pulled to one dataset and assembled *de novo* using Trinity (v2.8.4) (Grabherr et al., 2011) with quality trimming by Trimmomatic package (Bolger et al., 2014) forming 673645 contigs (N50 = 921). Expression frequencies were calculated after read remapping using bowtie2 (Langmead and Salzberg, 2012) on RSEM (v1.3.1) (Li and Dewey, 2011). Therefore normalized data representing the intensity of gene expression across samples (FPKM = fragments per kilobase per million reads) were obtained. The whole assembled sequences were also blasted using Diamond against NR and Uniprot in order to identify putative genes of interests. As we have duplicates, statistical analysis were done using Edger package in R with a FC threshold of 0.5 as recommended in literature for $n \leq 3$ (Schurch et al., 2016). We only considered results with a p-value < 0.01.

Juveniles

Synthesis of cDNA, library construction, Illumina sequencing and generation of FASTQ raw files were achieved by the sequencing platform of EUROFINS Genomics. Briefly, libraries were prepared using a HiSeq RNA sample preparation Kit (Illumina Inc., San Diego, CA, United States) according to the manufacturer's instruction. One lane was multiplexed for 12 samples and was sequenced as 125-bp paired-end reads using Illumina/Solexa technology (HiSeq 2500). For each library FASTQ file generation was performed by RTA v1.18.64.0 and CASAVA v1.8.2 software (Illumina). After quality assessment, trimming of adaptors, and filtering for low-quality reads (average QC < 30) with Trimmomatic v0.35, 230.2 million clean short reads sequences obtained (ranging from 14.85 to 25.92 million/sample; Q30 = 83.8 to 89.2%) were assembled with Trinity (v.2.2.1) leading to 586294 contigs (N50 = 594). After filtering transcripts weakly expressed (overall expression < 1 FPKM), a transcriptome with 93632 contigs was obtained (N50 = 748). Expression frequencies were calculated on RSEM (v1.3.1) (Li and Dewey, 2011) on the filtered transcriptome and were used for looking at the expression of our target genes in the skin, brain and eyes of the juvenile. A specific search on the unfiltered assembly for lowly expressed transcripts in brain, skin and eye libraries was done afterward. Reads mapping and expression analysis were conducted as previously described.

Transcriptome Blasts and Phylogenetic Analysis

In our transcriptomes of embryos, we found 10 sequences of interest: 6 blasting with opsins sequences, 2 with cryptochromes and 2 with arrestins (NCBI accession numbers MN788446-50, MN788452, MN788454-56 and MN788460 _ for some sequences, alternative isoforms were found with few to no differences in the amino acids sequences and were not included

in phylogenies). They were also retrieved from the juvenile transcriptome with 100% identity of the ORF nucleotide sequence (except 99.66% identity for r-opsin1 and only partial sequences for r-opsin2 (402nucl _ 100% id) and xeno2 (323 nucl. _ 99.66% id)). Two of the putative opsin sequences are partial (Sof_r-opsin2 and Sof_xeno2) but the corresponding full sequences could be retrieved from an already published transcriptome (Liscovitch-Brauer et al., 2017) and were used for the phylogenetic analysis. Using a p-blast algorithm in NCBI Blast putative homologous amino acids sequences in molluscs were retrieved. We used amino acids for the analysis as they are conserved because more constrained by their function. In order to confirm the orthology of these genes, sequences from taxa outside the molluscan clades (Annelida, Ecdysozoa, Deuterostomia) were added. We also blasted several genomes of cephalopods in NCBI (*Architeuthis dux* PRJNA534469, *Euprymna scolopes* PRJNA470951, *Octopus sinensis* PRJNA541812) and added data from transcriptomes of cephalopods (Liscovitch-Brauer et al., 2017). After a first alignment with MAFT (default parameters) implemented in JABAWS (Troshin et al., 2011) in the Jalview 2.11.0 software (Waterhouse et al., 2009) and manual trimming of sequences that were redundant or poorly aligned, datasets of 139 sequences (opsins), 50 sequences (cryptochromes) and 40 sequences (arrestins) were obtained (**Supplementary Figure S1**). For the opsin this was done by sub families and the results were then aligned all together using MAFT (L-INS-i and G-INS-i preset models). Finally the less conserved parts of the alignment were manually removed for all datasets and if necessary a last alignment with MAFT was done. It resulted on three alignments (**Supplementary Figure S2**) of, respectively, 311 aa (opsins), 402 aa (cryptochromes) and 325 aa (arrestins). ProtTest 3 (Guindon and Gascuel, 2003; Darriba et al., 2011) was used to define the better protein based evolution model to use for the phylogenetic analysis: respectively, LG + G + F (opsins), LG + G + I (cryptochromes) and LG + G + I (arrestins). A Bayesian inference tree was inferred using Mr. Bayes v3.2.7a (Ronquist et al., 2012) embedded in the CIPRES V 3.3 platform (2000000 generations, tree sampling frequency = 100, 4 Markov chains, 2 runs and burnin 25%). A maximum likelihood tree was also inferred (not shown) using RAxML-HPC v8.2.12 (Stamatakis, 2014) embedded in the CIPRES V 3.3 platform with similar results (Bootstrap values for conserved nodes are shown on the Bayesian phylogenetic trees _ 1000 bootstraps were performed).

Cryo-Sections and *in situ* Hybridization

Embryo in methanol was impregnated in 0.12M phosphate buffer pH 7.2 with 15% saccharose at 4°C for twice 24 h. Then, it was included in Neg-50^{TM} embedding medium (Richard-Allan Scientific^{TM}Thermo Scientific^{TM}) and blocks were frozen in 60 s at −80°C with PrestoCHILL (Milestone). Sections of 20 μm were performed using cryostat (HM560MV-Thermoscientific, France).

After 30 min at room temperature, the sections were rehydrated twice 15 min in PBS 1X followed by 15 min in SSC 5X. In a humid chamber, slides were prehybridated in hybridization solution (HS: 50% deionized formamide, 5X standard saline citrate, 40 μg/ml salmon sperm DNA, 5X Denhardt's, 10% dextran sulfate) for 2 h at 65°C before being incubated overnight with antisens probes (100 ng/mL) labeled with digoxigenin. Sense probes were also tested as negative controls. Sections were rinsed at 65°C: twice in SSC 2X for 30 min and 1 h and in SSC 0.1X. At room temperature, sections were treated with MABT (100 mM maleic acid, 150 mM NaCl, 1% tween20, pH 7.5) twice 15 min. Saturation was performed for 1 h in blocking solution (MABT, 4% blocking powder (Roche), 15% fetal bovine serum), followed by incubation for 1 h at 4°C with anti-digoxigenin antibodies (Roche) coupled to alkaline phosphatase (AP) and diluted at 1:500 in blocking solution (MABT, 1% blocking powder, 5% fetal bovine serum). Excess antibody was eliminated by 4 rinses in MABT (30 s, twice 45 min and overnight). Sections were impregnated for 20 min in AP solution (100 mM tris–HCL, 50 mM $MgCl_2$, 0.1% tween20) with 1 mM levamisole hydrochloride (Sigma). The revelation was conducted in the same solution containing 165 μg/ml BCIP (5-bromo-4-chloro-3'-indolyphosphate p-toluidine salt) and 330 μg/ml NBT (nitro-blue tetrazolium chloride) (Roche). The reaction was stopped by washing 2 times 20 min in PBS 1X. The slides were treated with DAPI (4',6-diamidino-2- phenylindole; 100 μg/L). Sections were mounted in Mowiol.

The labeled cryo-sections were observed under a Leica DMRB microscope. Several pictures per slices were taken with a camera color Canon EOS 60D. Images were assembled and treated for contrast and brightness using Adobe Photoshop CS6 (Adobe, CA, United States).

RT-qPCR

Extraction, DNase Treatment and Reverse Transcription

One embryo was used per biological sample. RNA was extracted using Nucleospin RNA mini kit (Macherey Nagel) with Type D Beads (Macherey Nagel) to disrupt tissues and on-membrane rDNAse treatment. RNA was eluted in RNAse-Free water at 65–70°C. Remaining gDNA was removed using Turbo Dnase (Ambion _ 2 UI/μL) at 37°C for 30 min and the solution was purified using RNA CleanUp kit (Macherey Nagel). Quantity and quality were assessed with Qubit 3 fluorometer (Invitrogen) and Bioanalyzer 2100 (Agilent). Finally, RNA was stored at −80°C before use.

Reverse transcription was done using Superscript III (Invitrogen) following the manufacturer's instructions with the same amount of RNA (215 ng) for each sample. cDNA was stored at −20°C.

RT-qPCR

Embryos

Primers were designed using Primer-BLAST on the NCBI website. Elongation factor 1 (Ef1) and β-actin were used as reference genes. Both genes have already been used as reference genes in cephalopods (Ef1 in *Octopus minor*: Xu and Zheng, 2018; [QSIImage]-actin in *Sepiella* sp.: Cao et al., 2016;

TABLE 1 | Primers for RT-qPCR experiment. Sof_β-actin and Sof_Ef1 (bold) were used as reference genes.

Abbreviation	Forward primer	Reverse primer	Amplicon size	Efficiency
Sof_β-actin	**GGTACCACCATGTTCCCTGG**	**GGACCGGACTCGTCATATTCC**	**197 nucl.**	**97%***
Sof_Ef1	**TGCCAGGTGACAATGTTGGT**	**CAATGTGTGCAGTGTGGCAA**	**198 nucl.**	**97%***
Sof_Cry_{123}	ATCTTGGGAGGATGGAATGAAGG	CAACAGGACAGTAGCAGTGGAA	134 nucl.	100%*
Sof_Cry_6	AGCTGTACTGTTTCCACGGAC	TTTCATCTCGCTCCTGCCAT	92 nucl.	103%
Sof_reti1	CAGTCACTTGGCGGGTCATA	AGTGCGGGCAGTAGCAATAA	91 nucl.	96%
Sof_reti2	TAGGTTGCTGTGTCTATGTCAGT	CAGCGATACAGGCCAAAAGA	117 nucl.	97%
Sof_r-opsin1	GAGTCCCTATGCTGTCGTGG	ACGGAGTAGATGAGTGGATTGTG	129 nucl.	100%
Sof_r-opsin2	CGTGCTCTTCTGTGCTGGAT	GTGACACACTTCGCCGCTAT	123 nucl.	N.A.
Sof_xeno1	TAAACGGAGCAATCGTCATCTTC	GCAATCAGAAAGTCGCACACA	100 nucl.	N.A.
Sof_xeno2	TTGGGCCTGACTTCCATCAC	GCGTACAATACACAACCGCC	134 nucl.	N.A.
Sof_β-arr	TATTGGGCCTCACCTTTCGC	CCTTGGAGCCTGGTTAGTGG	97 nucl.	N.A.
Sof_v-arr	CGCTAGGATTTGGATCTGGTGA	TTCCTTGGCTTCGGGTTTGA	98 nucl.	88%

**Indicates that the given efficiency is a mean of several experiments that were not done on the same plate. N.A. = Not Available.*

Song et al., 2017). The specificity of all primers used in this study was checked through a sequencing of a purified PCR product. Selected primers for each gene are given in **Table 1**. The RT-qPCR experiment was performed on an AriaMx Real-time PCR system (Agilent technology). The RT-qPCR mix includes 0.25 mM of both primers (20 mM each), 2 μl of Rnase Free water, 5 μl Brilliant II SybR© Green qPCR Master Mix (Agilent) and 2,5 μL of cDNA diluted at 1/20th in RNAse Free water per well. The PCR cycling program consisted of 10 min at 95°C, then 40 cycles of 30 s at 95°C, 30 s at 58°C and 30 s at 72°C and finally 30 s at 95°C, 30 s at 65°C and 30 s at 95°C before decreasing the temperature to room temperature. We used three different embryos per stage in order to have three independent biological replicates. For each embryo used, the two eyes were pulled together. Technical triplicates were systematically performed on all samples. The specificity of RT-qPCR was verified by looking at the melting curves and double-checked with an electrophoresis migration of the RT-qPCR product of at least 2 wells per genes. PCR primers efficiencies were evaluated through serial dilutions and ranged from 88% to 103%. The level of expression of Sof_xeno1, xeno2 and Sof_r-opsin2 was too low to calculate their primers efficiencies. The fold change for stages 25 to 30 where calculated using the mean Ct at stage 23 as a control. In order to normalize the results the geometric mean of reference genes was used for calculation of the fold change with the following formula (FC = Fold Change; E = Efficiency of considered target or reference gene; Target = target gene; Ref = reference gene):

$$FC = \frac{E^{\Delta Ct(Target)}}{Mean\ (E^{\Delta Ct(Ref)})}$$

Statistical analyses were performed with GraphPad Prism 8.0.1 Software (San Diego, CA, United States[1]). The normality of the distribution of Fold Changes was assessed through Shapiro-Wilk test, then one way ANOVA was performed with a Tukey's multiple comparisons test for each gene (significance: $p < 0.05$).

[1]www.graphpad.com

Adults

the tissues were obtained from different specimens, the skin came from a different sub-adult than the brain and optic lobes. Only one sample was tested for each organ. Technical triplicates were performed. We considered that there was a significant expression of the gene when the amplification took place before the 28th cycle of RT-qPCR (Cq < 28). Other results were regarded as non-significative and could indicate either a low expression or an absence of expression.

RESULTS

Identification and Characterization of Genes

Opsin Family

Besides the two opsins sequences already known in adult *S. officinalis*, we identified 4 new putative opsin sequences in transcripts from embryos. These 6 sequences all have features of GPCR. The presence of seven transmembrane domains was predicted using TMHMM server v.2.0 (Krogh et al., 2001; **Supplementary Figure S3**) for all sequences except r-opsin1. In this last sequence, the 7th transmembrane domain was not retrieved by the software but could be assumed due to amino-acids similarities (**Supplementary Figure S4**). All sequences have the two cysteines forming a disulphide bridge essential for GPCR stability (**Supplementary Figure S4**). Some other features of the rhodopsin family of GPCR were observed such as the chromophore/opsin predictive binding site which is a well-conserved lysine (K296 in the bovine rhodopsin sequence) and the E/DRY motif and NPXXY site both allowing interaction with G proteins (the latter is not conserved in all sequences) (**Supplementary Figure S4**). Sof_xeno1 and Sof_xeno2 sequences are divergent on the N-term of the amino acid chain (5 first transmembrane domains) but the C-terminal part is identical (last 2 transmembrane domains).

In our phylogenetic analyses (**Figures 2**, **3**) which included 7 groups of opsins (out of 9) and both dopamine receptors and melatonin receptors as outgroups we evidenced a monophyletic

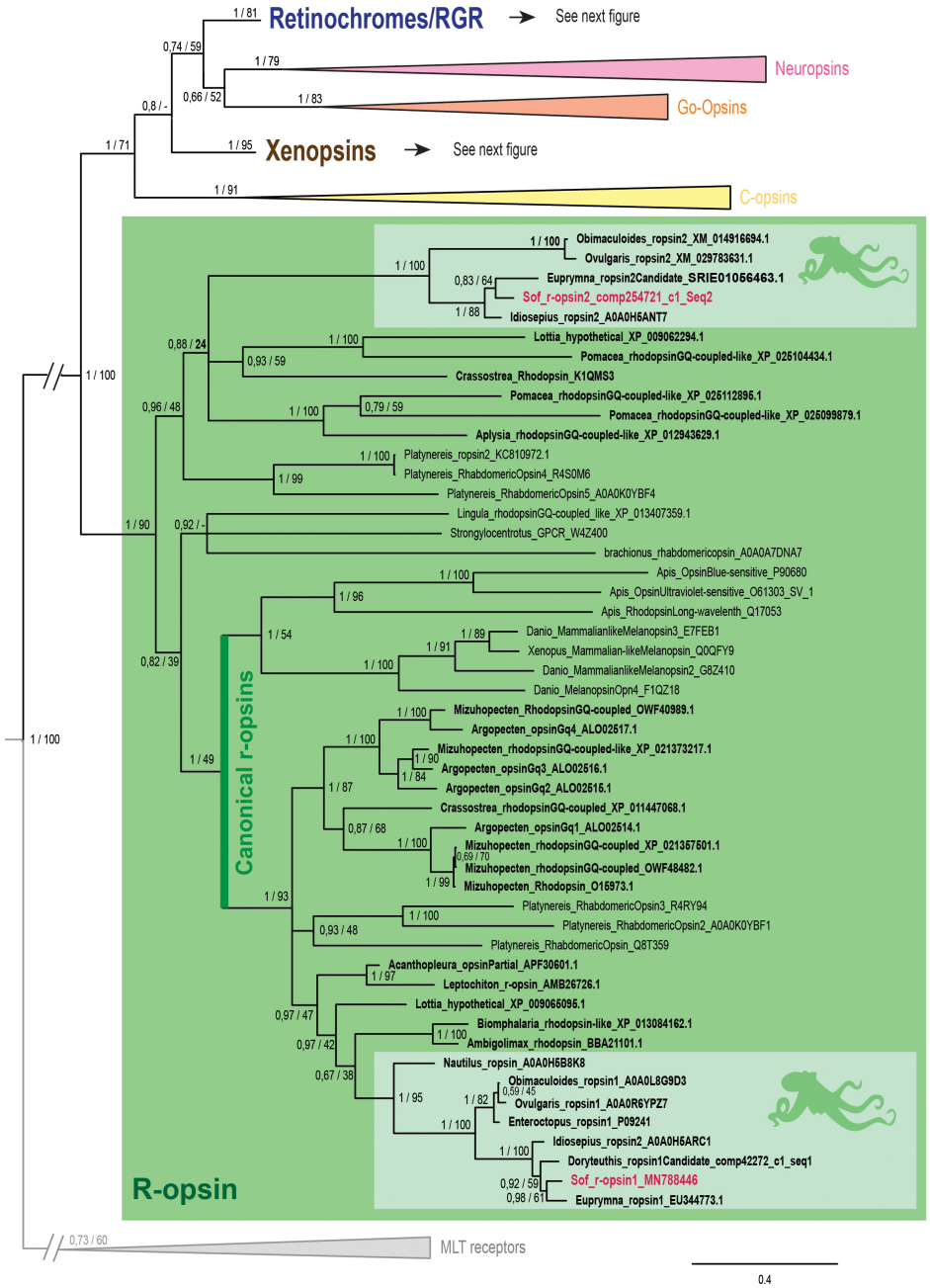

FIGURE 2 | Opsin phylogeny with a focus on r-opsins. Phylogenetic analysis of 139 sequences of 311 amino acids generated in Bayesian Inference (MrBayes v3.2.7a). 6 main groups of opsins are retrieved: retinochromes (blue), neuropsins (red), Go-opsins (orange), xenopsins (brown), c-opsins (yellow) and r-opsins (green). Sequences from *S. officinalis* are in red, sequences from other molluscs are in bold and outgroups (Melatonine receptors (MLT)) are in gray. Dopamine receptors used for rooting the tree are not shown on the figure. Nodes labels are posterior probabilities and bootstrap values (PP/BS). Lighter boxes with cephalopod silhouette [modified from Stöger et al. (2013)] represent groups of cephalopod sequences. The branch from the root to the ingroups and outgroups were shortened for more lisibility (//).

opsin family (Posterior Probabilities (PP) = 1/Bootstrap values (BS) = 100) thus confirming the identification of 6 opsins in *S. officinalis*. This opsin family was separated in 6 monophyletic groups (PP = 1 for all; BS between 79 and 95), three of which containing opsin sequences from *S. officinalis*. The general topology between the main families of opsins is not well-supported in this analysis.

The r-opsin clade (**Figure 2** _PP = 1; BS = 90) is divided in two monophyletic clades each containing a sequence from *S. officinalis*. The biggest r-opsin group has a good support in

the Bayesian inference tree (PP = 1; BS = 49). It is composed of a large lophotrochozoan r-opsin group (PP = 1; BS = 93) with both ecdysozoan r-opsins and deuterostomian melanopsins (PP = 1; BS = 54) as a sister-group thus characterizing it as a canonical r-opsin clade. Inside this group, the sequence from *S. officinalis* is included in a cephalopod r-opsins clade (PP = 1; BS = 95). The other cephalopod r-opsin group, which includes a second *S. officinalis* sequence, is well-supported in the Bayesian tree (PP = 1; BS = 100). It is included within a larger clade of lophotrochozoan sequences thus characterizing it as a second r-opsin ("non-canonical" r-opsin _ PP = 0.96; BS = 48). Therefore we chose to name these sequences Sof_r-opsin1 (former rhodopsin) and Sof_r-opsin2. This phylogenetic analysis allowed us to say that the division between these two paralogs was already there in the last common ancestor of all bilaterians. The bootstrap values are not as good as the posterior probabilities for the r-opsin1 and deuterostomian r-opsin clades, this might be due to some long branch attractions. In the literature, the "non-canonical r-opsin group" corresponding to our r-opsin2 group is sometimes paraphyletic (Ramirez et al., 2016).

Two other *S. officinalis* sequences (**Figure 3**) are grouped together with other cephalopod sequences (PP = 1; BS = 98) within a larger lophotrochozoan monophyletic group (PP = 1; BS = 99) and an even larger bilaterian group including annelids and deuterostomian retinochromes sequences (PP = 1; BS = 81). Therefore we named these two sequences Sof_reti1 and Sof_reti2. Thanks to the several sequences of cephalopods from various taxa (Nautiloidea, Coleoidea: Decabrachia and Octobrachia) included in our study, we evidenced that only decabrachian cephalopods have two retinochromes. All the reti1 sequences of Decabrachia were grouped together in a monophyletic group (PP = 1; BS = 100) and so are all the reti2 sequences of Decabrachia (PP = 1; BS = 100). These two groups seem to be sister-groups even though this clade is not well-supported (PP = 0.94; BS = 51). Furthermore only one monophyletic group of Octobrachia retinochrome sequences was found in our analysis (PP = 1; BS = 100) and it is the sister group of the clade formed by the two retinochromes groups thus suggesting the duplication event might have taken place after the splitting between Decabrachia and Octobrachia lineages.

Finally, the last two opsins sequences identified in *Sepia* are part of a lophotrochozoan-only group composed of molluscan and brachiopods sequences (**Figure 3** _ PP = 1; BS = 95). Most of them were recently identified as xenopsins (but some of them firstly described as c-opsins _ Yoshida et al., 2015). The sequences were therefore identified as Sof_xeno1 and Sof_xeno2. As for retinochromes, both the Decabrachia xenopsin 1 group and the Decabrachia xenopsin 2 group are monophyletic (PP = 1 for both; BS = 98 and 99). Furthermore there is a single clade gathering all the Octobrachia xenopsins sequences (PP = 1; BS = 100). This octobrachian clade is the sister-group of the decabrachian xenopsin clade. The support for this decabrachian clade, grouping both xenopsins 1 and xenopsins 2, is very low (PP = 0.8) and this topology is not found in the maximum likelihood tree. The duplication of the xenopsins took place in the Cephalopoda lineage but we cannot conclude when it precisely happened.

No sequence of *S. officinalis* or of any other cephalopod species was found in the three other clades of opsins (i.e., neuropsins, Go-opsins, and c-opsins).

Cryptochrome Family

We identified for the first time, two putative cryptochromes in the transcripts of *S. officinalis* embryos. They both carry the photolyase domain and the FAD binding domain which characterized animal cryptochromes (Chaves et al., 2011; **Supplementary Figure S4**) and were identified with the PFAM platform (El-Gebali et al., 2019).

In our phylogenetic analysis (**Figure 4**), we found three main monophyletic groups. One of the cryptochrome sequence of *S. officinalis* is grouped with other molluscan sequences, together with *Euprymna scolopes escry2* (Heath-Heckman et al., 2013) and the nudibranch *Melibe leonina* non-photoreceptive cryptochrome (Duback et al., 2018). This molluscan clade is part of a larger protostomian monophyletic group (PP = 1; BS = 89) and an even larger bilaterian monophyletic group (PP = 1; BS = 98) gathering all the CRY_1, CRY_2 and CRY_3 sequences of our analysis. Therefore the sequence from *S. officinalis* was identified as Sof_CRY_{123}. The second sequence from *S. officinalis* is found inside a well-supported lophotrochozoan monophyletic group (PP = 1; BS = 75). This group is part of a larger protostomian-only group including two arthropods CRY_6 sequences (PP = 0,96; BS = 71) therefore we identified our second sequence as Sof_Cry6. Finally, a monophyletic group gathering a few molluscan photolyase sequences with deuterostomian Cry4 and Cry5 sequences can be identified as the CRY_{45}/photolyase clade. No CRY_{45}/Photolyase sequence was retrieved from *S. officinalis* transcriptomes nor from any other cephalopod included in our analysis.

Arrestin Family

We found two sequences of arrestins in *S. officinalis* embryos. They both presented the canonical N- and C-arrestin domains identified through the PFAM platform (El-Gebali et al., 2019; data not shown). In our phylogenetic analysis, each of these sequences (**Figure 5**) is part of a distinct monophyletic group of coleoid cephalopod sequences. One of them gather only visual arrestins (PP = 1; BS = 100) and the other one only beta-arrestins (PP = 1; BS = 88). Relationships between these two groups and many sequences from other molluscs are not resolved. This politomy is part of a larger protostomian clade (PP = 1; BS = 100) including both arthropods beta arrestins and visual arrestins. All these sequences have deuterostomian arrestins as outgroups. Therefore our sequences derived from an ancestral β-arrestin. Visual arrestins sequences are only found in coleoid cephalopods and they are not orthologous to the visual arrestins of arthropods. From these results and present available databases, we cannot date the appearance of this duplication in molluscan history.

Expression of Target Genes

Qualitative Expression in a Stage 30 Embryo With Focus on the Eyes

By *in situ* hybridization, we evidenced expression of different photosensitive molecules (r-opsin1, both retinochromes, both

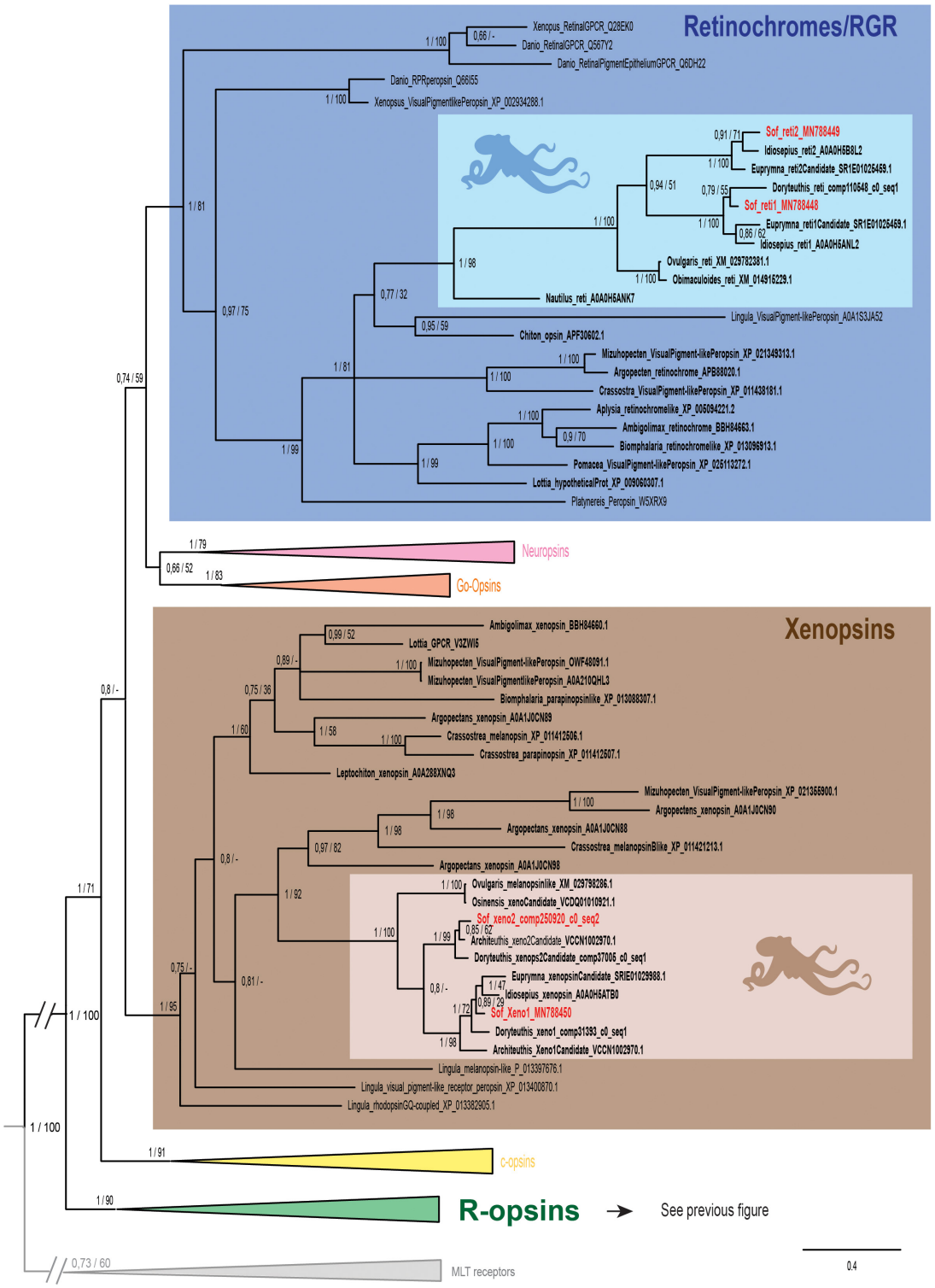

FIGURE 3 | Opsin phylogeny with a focus on retinochromes and xenopsins. Phylogenetic analysis of 139 sequences of 311 amino acids generated in Bayesian Inference (MrBayes v3.2.7a). 6 main groups of opsins are retrieved: retinochromes (blue), neuropsins (red), Go-opsins (orange), xenopsins (brown), c-opsins (yellow) and r-opsins (green). Sequences from *S. officinalis* are in red, sequences from other molluscs are in bold and outgroups [Melatonine receptors (MLT)] are in gray. Dopamine receptors used for rooting the tree are not shown on the figure. Nodes labels are posterior probabilities and bootstrap values (PP/BS). Lighter boxes with cephalopod silhouette [modified from Stöger et al. (2013)] represent groups of cephalopod sequences. The branch from the root to the ingroups and outgroups were shortened for more lisibility (//).

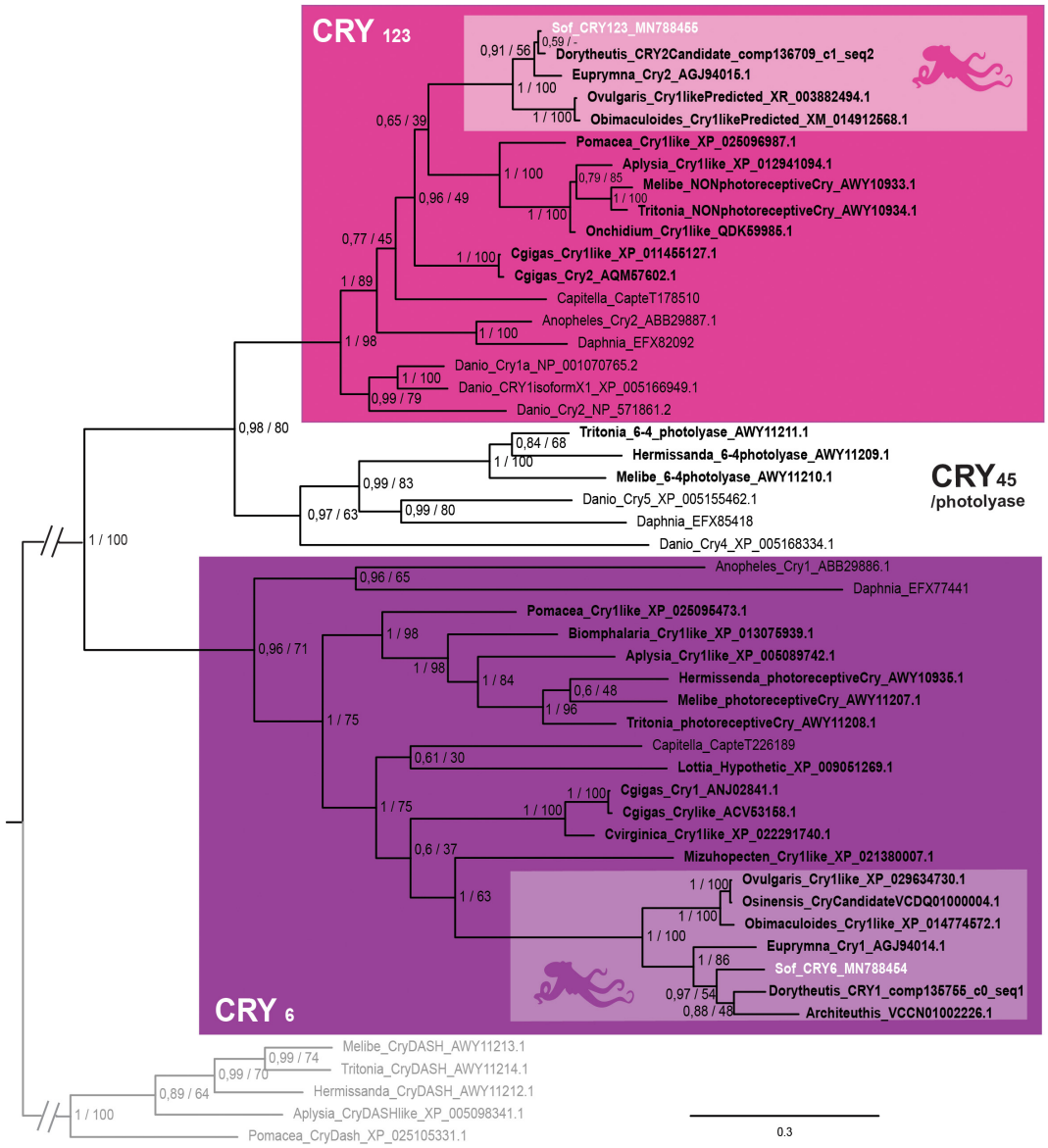

FIGURE 4 | Cryptochrome phylogeny. Phylogenetic analysis of 50 sequences of 402 amino acids generated in Bayesian Inference (Mr. Bayes v3.2.7a). Three main groups of animal cryptochromes are retrieved: CRY_{123}, CRY_{45}/Photolyase and CRY_6. Sequences from *S. officinalis* are in white, sequences from other molluscs are in bold font and outgroups used for rooting the tree (CRY-DASH) are in gray. Nodes labels are posterior probabilities and bootstrap values (PP/BS). Lighter boxes with cephalopod silhouette [modified from Stöger et al. (2013)] represent groups of cephalopod sequences. The branch from the root to the ingroups and outgroups were shortened for more lisibility (//).

cryptochromes _ **Figure 6**) in a late stage 30 embryo of *S. officinalis*: R-opsin1 mRNAs are found in all layers of the retina and in the periphery of the optic lobes (**Figures 6A,B**). No expression was evidenced in the brain as previously described (Imarazene et al., 2017). Both retinochromes mRNAs were found in the basal part of the inner layer of the retina where nucleus of the rhabdomeric photoreceptor cells is present (**Figures 6C–F**). CRY_{123} transcripts were widely present: mRNAs were found in the whole inner layer of the retina and in the whole central nervous system with a diffuse pattern in the optic lobes and in the brain (**Figures 6I–J**). CRY_6 mRNAs were mostly present in the basal part of the inner layer of the retina (**Figures 6G,H**). They also seemed to co-localize with CRY_{123} mRNAs in the CNS: a diffuse labeling (lighter than the one of Sof_CRY_{123}) was observed in some sections in the optic lobes and in the brain, long after the staining of the retina.

Semi-Quantitative Data in the Eyes (RNA-Seq)

In order to confirm the qualitative data, we looked at the expression of these genes with RNA-sequencing: at stage 24, three opsins were expressed in the eyes of *S. officinalis* embryos

according to our transcriptomic analysis (**Figure 7**): Sof_r-opsin1, Sof_reti1 and Sof_reti2. No significant expression of Sof_r-opsin2, Sof_xeno1 or Sof_xeno2 was observed (FPKM $\leq$ 1). Both Sof_CRY$_{123}$ and Sof_CRY$_6$ were expressed in this stage and so are Sof_v-arr and Sof_β-arr. For each of these genes the level of expression was similar in the two biological replicates. The expression of these genes ranged from FPKM$_{Sof_v-Arr}$ = 6.8 to FPKM$_{Sof_reti1}$ = 28. In stage 30 embryos, the same genes were expressed. The highest level of expression was found for Sof_r-opsin1 (mean FPKM = 3827) followed by Sof_reti1, Sof_reti2 and Sof_v-arr (respectively, mean FPKM = 352, 160 and 258). Both cryptochromes and β-arrestin had a lower level of expression than opsin genes (mean FPKM Sof_CRY$_{123}$ = 21;

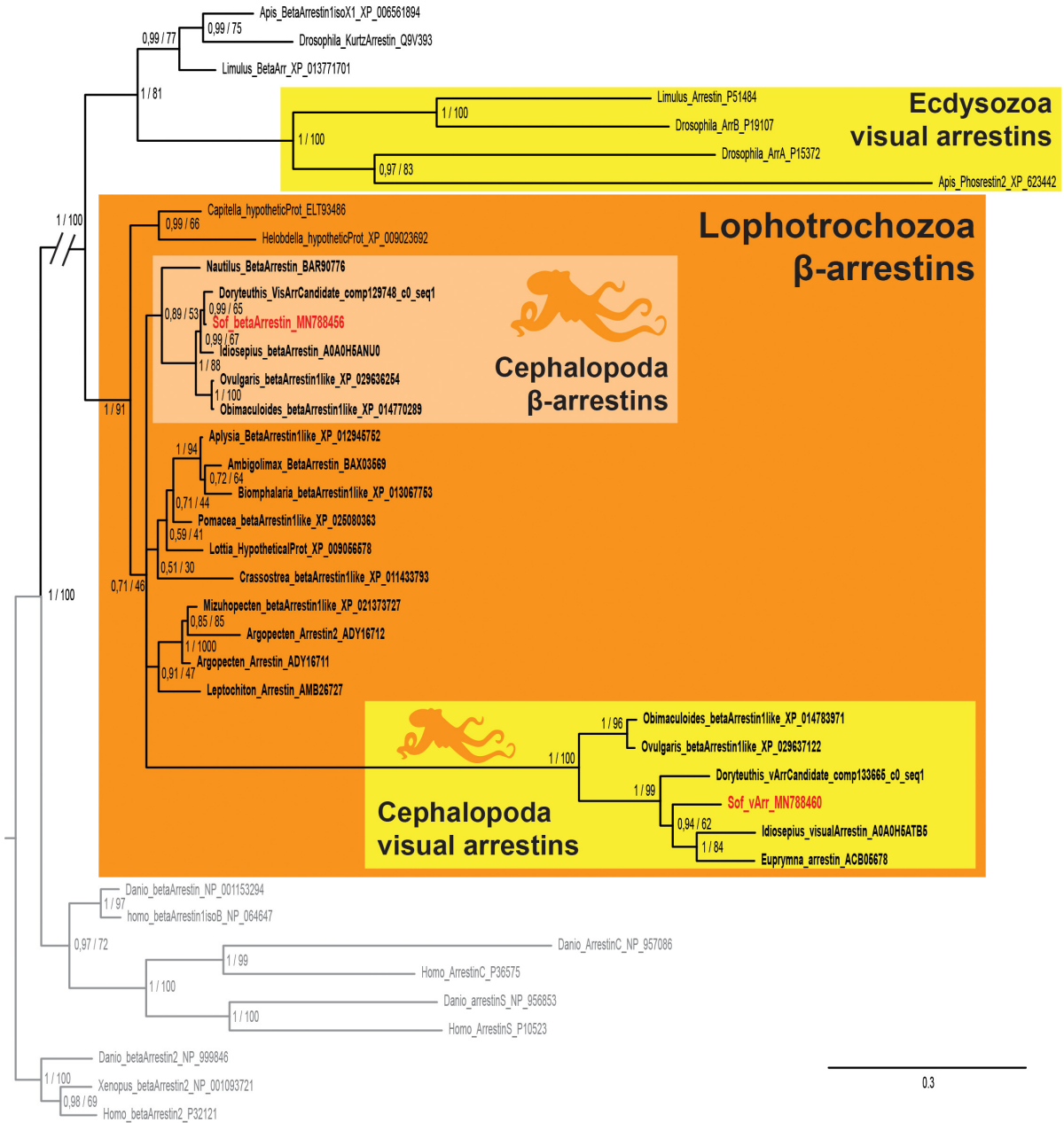

FIGURE 5 | Arrestin phylogeny. Phylogenetic analysis of 37 sequences of 325 amino acids generated in Bayesian Inference (Mr. Bayes v3.2.7a). Two groups of coleoid cephalopods arrestins are retrieved: visual arrestins (v-arr) in yellow and β-arrestins (β-arr) in light orange. Ecdysozoan visual arrestins (or phosrestines) sequences are highlited (yellow), sequences from *S. officinalis* are in red, sequences from other molluscs are in bold font and outgroups (vertebrates β-arrestins 2 for rooting and other deuterostomians arrestins) are in gray. Nodes labels are posterior probabilities and bootstrap values (PP/BS). Lighter boxes with cephalopod silhouette [modified from Stöger et al. (2013)] represent groups of cephalopod sequences. The branch from the root to the ingroups and outgroups were shortened for more lisibility (//).

Sof_CRY$_6$ = 12; Sof_β-arr = 12). Even though we have to be cautious when drawing conclusion due to small amount of replicates, a significant increase of Sof_r-opsin1, the two retinochromes and Sof_v-arr was found between stage 24 and 30.

Semi-Quantitative Expression in the Eyes, Through Developmental Stages (RT-qPCR)

RT-qPCR results (**Figure 8**) confirmed the increase of expression of Sof_r-opsin1, Sof_reti1, Sof_reti2 and Sof_v-arr and evidenced the increase of expression of the two cryptochromes. These expressions increased significantly between stage 25 and stage 30. Except for the cryptochromes, all the other genes had the biggest fold change between stages 25 and 28. Similar results were found between biological replicates for all the target genes. Sof_r-opsin1 ($\log_2FC_{23-30}$ = 7,46) and Sof_v-arr ($\log_2FC_{23-30}$ = 5,87) expressions underwent a drastic increase from stage 25 to stage 30. The increase was less important for both retinochromes ($\log_2FC_{23-30}$_Reti1 = 3,11; $\log_2FC_{23-30}$_Reti2 = 3,37) and both cryptochromes ($\log_2FC_{23-30}$_Cry$_{123}$ = 2,4; $\log_2FC_{23-30}$_Cry$_6$ = 1,54). R-opsin1 expression increased from stage to stage (**Figure 8A**) ($\log_2FC_{25-28}$ = 4,74; $\log_2FC_{28-30}$ = 1,57). Visual arrestin pattern of expression also increased from stage 25 to 30 ($\log_2FC_{25-28}$ = 3,78; $\log_2FC_{28-30}$ = 0,8). The expression of both retinochromes increased from stage 25 to 28 ($\log_2FC_{25-28}$_Reti1 = 2,47 and $\log_2FC_{25-28}$_Reti2 = 2,34), but not between stage 28 and 30.

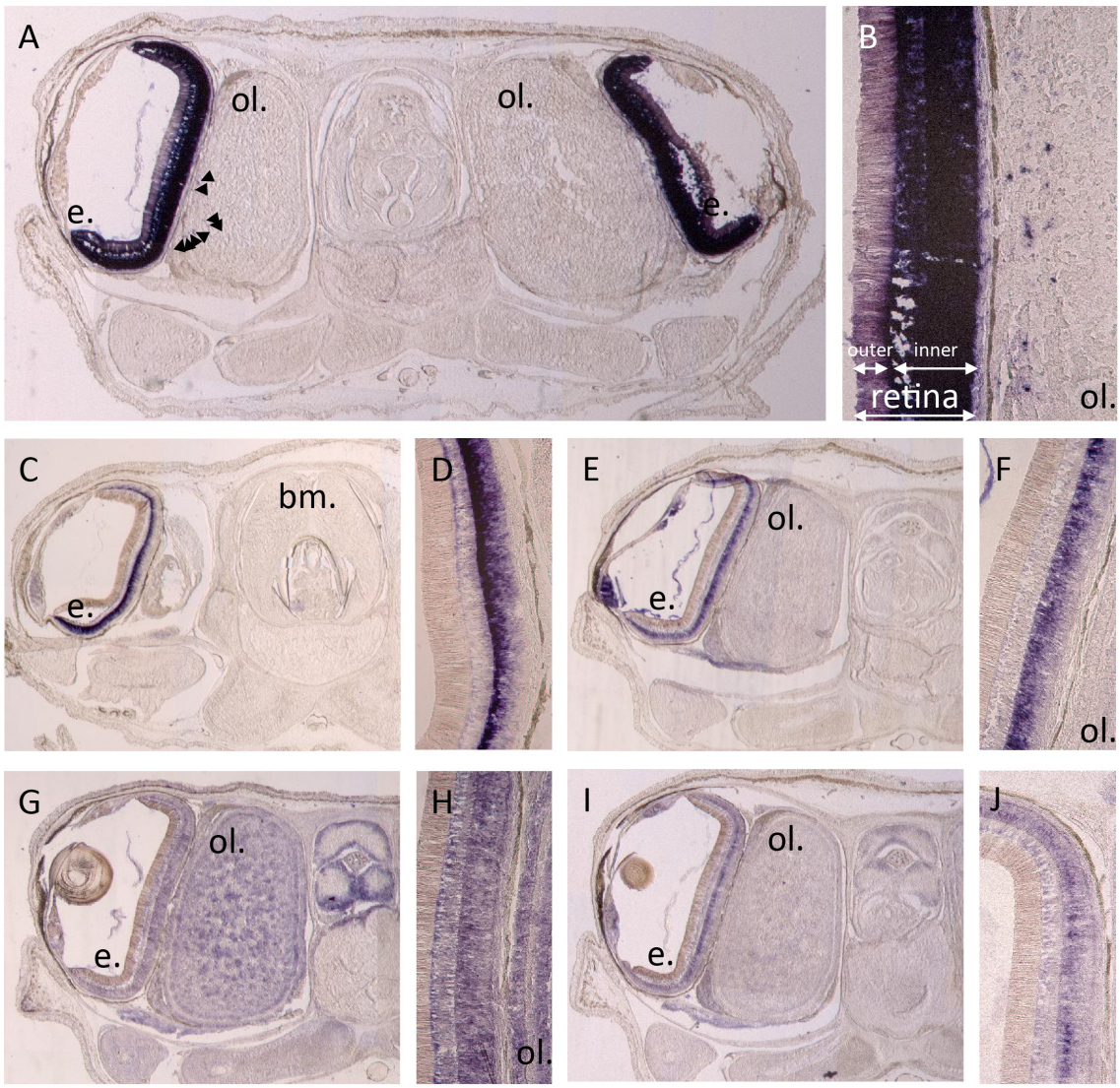

FIGURE 6 | *In situ* hybridization of r-opsin1 **(A,B)**, retinochrome 1 **(C,D)**, retinochrome 2 **(E,F)** and cryptochromes: CRY$_{123}$ **(G,H)** and CRY$_6$ **(I,J)**. Pictures **(A,C,E,G,I)** show a 20 μm section of an embryo head with brain (not on section **A,C**), optic lobes (not on section **C**) and eyes including retina and sometimes the lens. Pictures **(B,D,F,H,J)** are a magnification focused on the retina ± the side of the optic lobes. All pictures were taken after 11 h of revelation except CRY$_{123}$ pictures which were taken after 5h30. Arrows point some small stained spots. e. = eye, ol. = optic lobe, bm. = buccal mass.

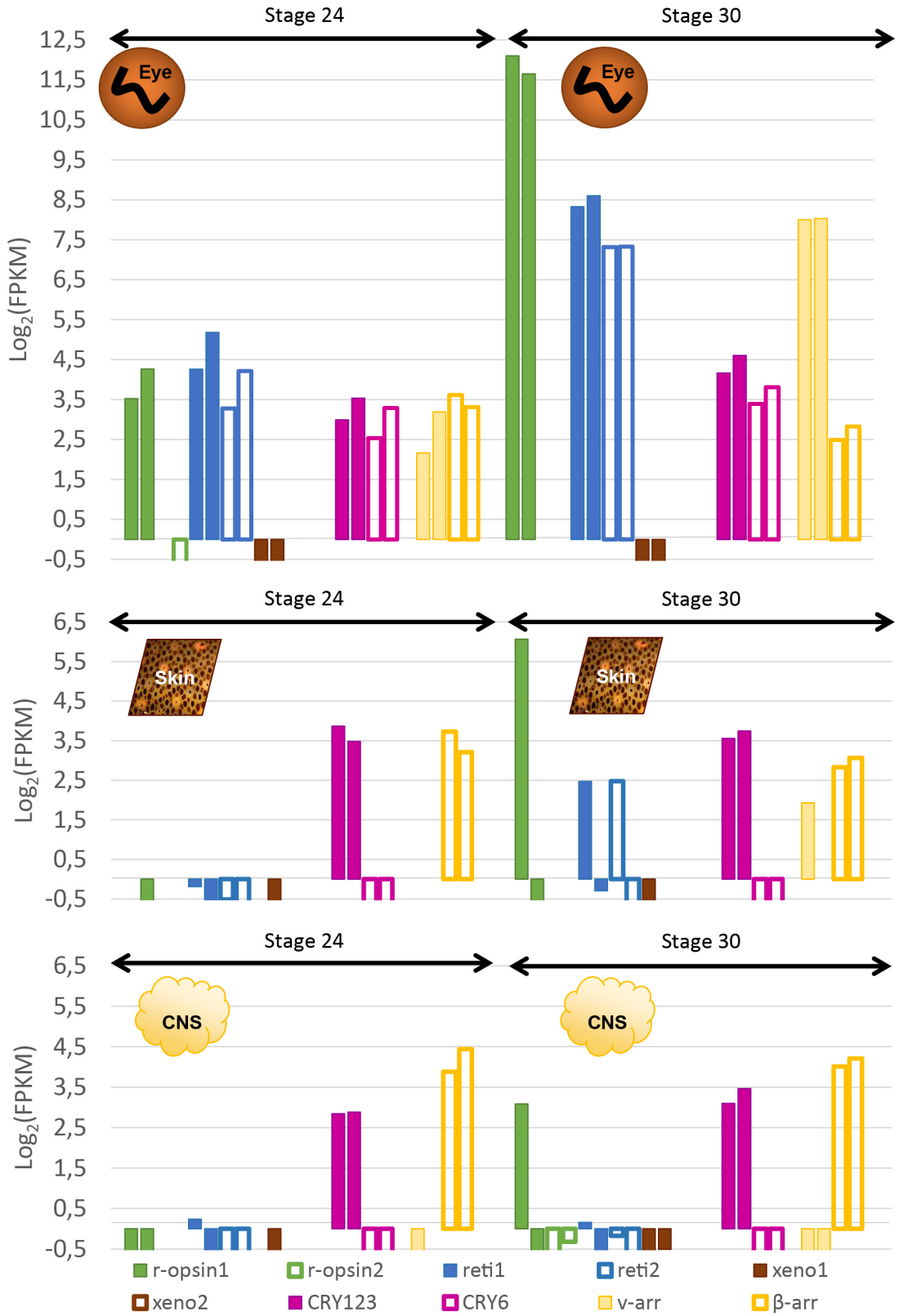

FIGURE 7 | Expression of light sensitive molecules in the eyes, skin and CNS of *Sepia* embryos. Expression is given in Log_2(FPKM) and are normalized with RSEM in order to compare between stage 24 and stage 30 in the eyes **(top)**, the skin **(middle)** and in the central nervous system (brain + OL _ **bottom**). For each gene, there are two bars each giving the expression in one of the two biological duplicates. The expression level of several isforms were summed up for some of the genes.

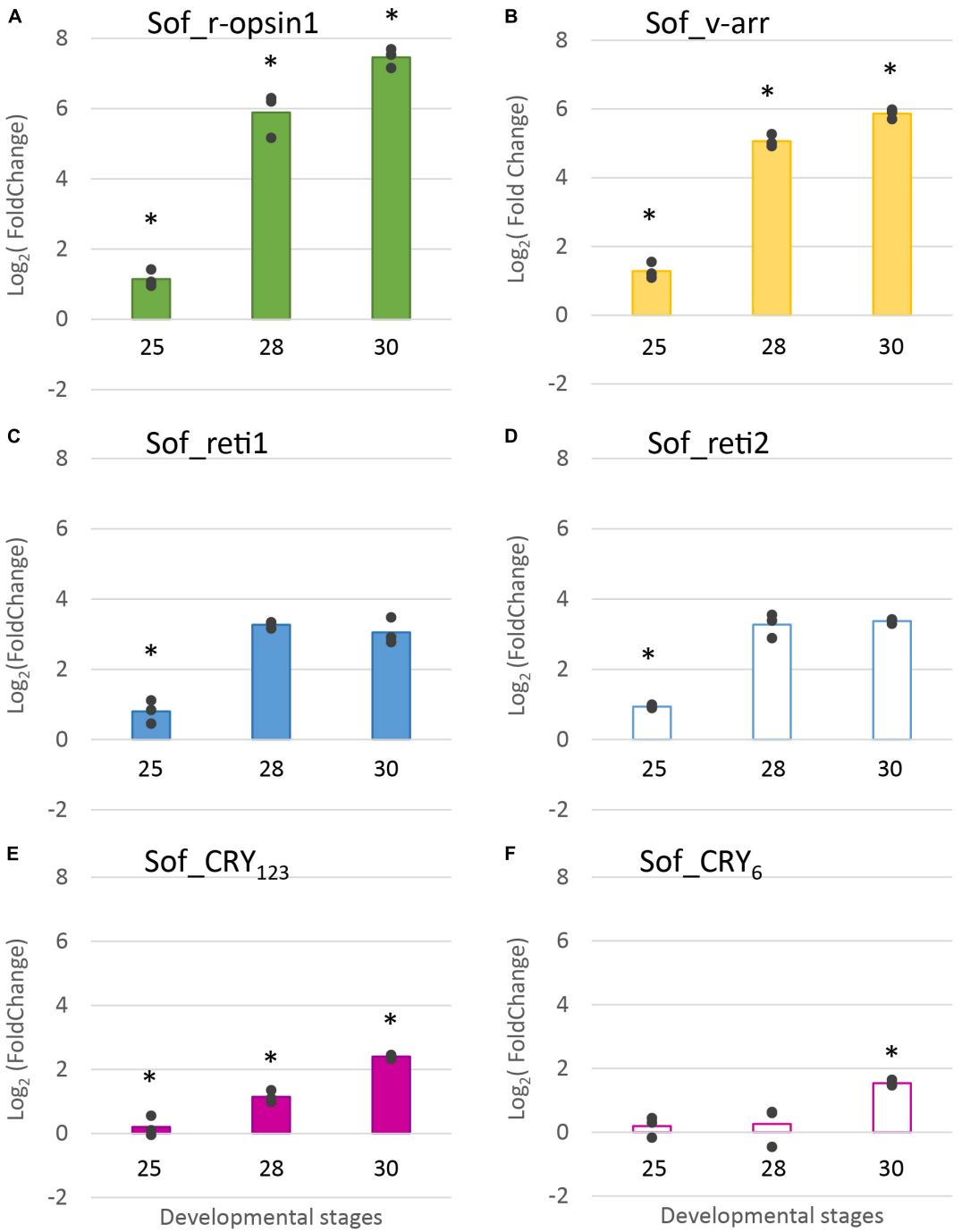

FIGURE 8 | Differential expression of light sensitive molecules at several embryogenic stages. Genes considered are: **(A)**. R-opsin1, **(B)**. visual arrestin **(C)**. retinochrome 1 **(D)**. retinochrome 2 **(E)**. CRY_{123} and **(F)**. CRY_6. The average log_2 Fold Change for the three developmental stages (stage 25, stage 28 and stage 30) is given in comparison to stage 23. In addition, all data points are plotted to show actual variability.* = results significantly different from the other ($p = 0.05$).

The expression of Sof_Cry_{123} increased gradually from stage to stage with the sharpest increase between stage 28 and 30 (log_2FC_{28-30} = 1,26) whereas Sof_Cry_6 expression seemed to be constant from stage 25 to 28 then increased between stage 28 and 30 (log_2FC_{28-30} = 1,28).

In summary, we showed that five light sensing molecules (3 opsins and 2 cryptochromes) and one visual arrestin were expressed in the eyes of *S. officinalis* embryos. All the photosensitive molecules studied in RT-qPCR had a significant increase of their expression between stage 25 and 30.

TABLE 2 | Expression of light sensitive molecules in a 1-month old juvenile.

	R-opsin1	R-opsin2	Reti1	Reti2	Xeno1	Xeno2	CRY_{123}	CRY_6	β-arr	V-arr
Eye	7572	Ø	362	59	Ø	Ø	10	6	6	344
Skin	10	Ø	1.3	0.2	Ø	Ø	7	0.5	9	0.1
Brain*	4	+	1.6	0.7	+	Ø	20	2	45	0.2

*Data are expressed in FPKM. * = Brain without optic lobes (in embryos and adult the full CNS was investigated). + = transcripts absent from the filtered version of the juvenile transcriptome but detected with weak expression (1 < FPKM < 2) in the brain libraries in the unfiltered transcriptomes.*

TABLE 3 | Expression of light sensitive molecules in sub-adults.

	R-opsin1	R-opsin2	Reti1	Reti2	Xeno1	Xeno2	CRY_{123}	CRY_6	β-arr	V-arr
Skin	N.S.	N.S.	+	N.S.	N.S.	N.S.	+	N.S.	+	N.S.
Brain	+	+	+	N.S.	N.S.	N.S.	+	+	+	N.S.
Optic lobes	+	+	+	N.S.	+	+	+	+	+	+

+ = presence of the gene (amplification before Cq < 28), N.S. = Non-significative results indicating either a small expression or an absence of expression.

Semi Quantitative Expression in Other Tissues With Photosensitive Properties (RNAseq)

Sof_CRY_{123} and Sof_β-arr seemed to have quite an ubiquitous expression as they are the only ones expressed at stage 24 in both the skin and the CNS (**Figure 7**). Their level of expression was not significantly different in stage 24 compared to stage 30 (CRY_{123}: $meanFPKM_{Skin24}$ = 12,86, $meanFPKM_{Skin30}$ = 12,57, $meanFPKM_{CNS24}$ = 7,27, $meanFPKM_{CNS30}$ = 9,8; β-arr: $meanFPKM_{Skin24}$ = 11,25, $meanFPKM_{Skin30}$ = 7,74, $meanFPKM_{CNS24}$ = 18,25, $meanFPKM_{CNS30}$ = 17,31). Sof_CRY_6 is not significantly expressed (FPKM ≥ 1) in these tissues at stage 24 and 30. R-opsin1, the two retinochromes and Sof_v-arr were expressed, only in one of the two stage 30 embryos in the skin. Moreover, in the central nervous system, r-opsin1 was also expressed in the same embryo and not in the other one. Because there are two samples, no conclusion can be drawn: either the differences are due to different steps in the stage 30, or to a cyclic expression during the day; or there is no biological significance and it corresponds to a random artifact. Neither Sof_xeno1 nor Sof_r-opsin2 were expressed at significant levels in any of the stages or tissues analyzed. Sof_xeno2 was not expressed in any stages except for one of the biological replicates at stage 25 (FPKM = 5.767).

Expression in the Juvenile (RNA-Seq)

In the eye of the juvenile (**Table 2**), three opsins (Sof_r-opsin1, Sof_reti1 and Sof_reti2), both cryptochromes and both arrestins are expressed, similarly to the observations in embryos from stage 23 to 30. In the skin, there is a small expression of Sof_CRY_{123} and Sof_β-arr as in the skin of the embryos. There is also an expression of Sof_r-opsin1 and a barely significant expression of Sof_reti1. In the brain, Sof_CRY123 and Sof_β-arr are the two genes mainly expressed in the brain of this juvenile as they were in the embryos, with the precision that there is no optic lobes studied in the juvenile (whereas CNS included both brain and optic lobes in embryos). There is a bare expression of Sof_r-opsin1, Sof_reti1, and Sof_CRY6 in the brain. As for sof_r-opsin2 and Sof_xeno1, these genes were absent from the filtered transcriptome but a weak expression was found when remapping the brain reads to the full assembly. These results need to be taken cautiously as they come from a single sample and cannot be compared to the other FPKM values of the filtered transcriptome.

Expression in the Adult (RT-qPCR)

In the sub-adult (**Table 3**), Sof_ β-arr, Sof_ CRY_{123} and Sof_reti1 were also significantly expressed in the skin. Sof_r-opsin1, Sof-r-opsin2, Sof_reti1, Sof_β-arr and both cryptochromes were expressed in the CNS (brain and optic lobes) of the sub-adult. A significant expression of Sof_v-arr and the two xenopsins was also attested in the optic lobes only. The fact that some of these genes are found expressed in the sub-adult and not in the juvenile might be due to an increase of expression later in life.

DISCUSSION

Localization of Expression

In our study we combined three different kind of data on the expression of light sensing molecules: qualitative *in situ* hybridization, semi-qualitative RT-qPCR and RNA-seq analyses. The results given by these different methods are mostly convergent. All methods found r-opsin1, two retinochromes, two cryptochromes and two arrestins expressed in the eyes of *S. officinalis* embryos and juvenile. This corroborates the *in situ* hybridization data on the expression of r-opsin1 in the retina of embryo (Imarazene et al., 2017) and the reported expression (RT-PCR) of both r-opsin1 and retinochrome1 in the retina of adult *S. officinalis* (Kingston et al., 2015b). Furthermore a personal communication from Maria Tosches confirmed the presence of Sof_r-opsin1, Sof_reti1 and Sof_reti2 in an unpublished transcriptome of the eyes of an adult *S. officinalis*. In the skin, only Sof_CRY_{123} and Sof_β-arrestins were expressed in the stage 24 embryo and one of the stage 30. These same genes were expressed together with Sof_r-opsin1 and Sof_reti1 in the other stage 30 embryo, the juvenile and the adult (only Sof_reti1 in the adult). In the CNS both RNA-seq and RT-qPCRs found Sof_CRY_{123} and Sof_β-arrestins as the two mainly expressed genes of our analysis

in embryos and the juvenile. More genes were expressed in the brain of the adult and even more in the optic lobes of the adult. Our comparative data did not show important variability from a biological duplicate to another except in the two stage 30 embryos of the RNA sequencing.

One main difference is the fact that CRY_6 is not expressed in the central nervous system of stage 30 embryos but was labeled in the *in situ* hybridization. As there is a small expression of Sof_CRY_6 in the brain of the juvenile this might mean that the expression start in very advanced stage 30 embryos as the one we used for *in situ* hybridization was very close to hatching. We cannot rule out the fact that this difference of expression might be due to a pattern of daily cycling of the gene as the expression of cryptochromes is known to oscillate during the day (in nudibranchs: Duback et al., 2018; in Crustacea: Biscontin et al., 2019).

Vision in Embryos and Adult

Two main opsin families have been well-studied for their involvement in image-forming vision: c-opsins and r-opsins. We did not find any c-opsins from our transcriptomes. This was expected as c-opsins are mostly restricted to deuterostomians and were not described in molluscs (Ramirez et al., 2016). We showed here for the first time that two r-opsins are expressed in *S. officinalis* but only Sof_r-opsin1 is expressed in the eyes. More precisely, r-opsin1 mRNAs could be found in all the retina but this is likely due to the fact that it is heavily translated in the nucleus of the rhabdomeric photoreceptor cells and then moved to the outer segment. Indeed in adult *D. pealeii,* the protein is localized only on the outer segment of the rhabomes (Kingston et al., 2015b). The expression of Sof_r-opsin1 increases significantly from stage 25 to 30. This strong increase of Sof_r-opsin1 mRNAs corroborates the qualitative *in situ* hybridization data already published about *S. officinalis* eye development (Imarazene et al., 2017) but also correlates with the appearance and darkening of pigmentation macroscopically visible in the eyes of the embryo (**Figure 1**). The biggest fold change value is found when comparing stages 25 and 28. This is convergent with the behavioral studies demonstrating an ability to perceive light as early as stage 25 in *S. officinalis* embryos (Romagny et al., 2012). Therefore, r-opsin1 is most likely the molecule responsible for this light detection. Moreover, r-opsin1 expression is still very high in juvenile and adult suggesting a "permanent" role in light detection/vision after hatching.

Our results support the hypothesis that cephalopods cannot see colors as only one opsin, i.e., r-opsin1, is expressed in their eyes. Nevertheless a color-based vision has been described in a butterfly expressing only one opsin with the involvement of filtering pigments (Zaccardi et al., 2006). This color vision may also exist in some cephalopods species as three different visual pigments with different λmax where identified in the retina of the deep-sea squid *Watasenia scintillans* (Matsui et al., 1988). To our knowledge, it is not the case in *S. officinalis* and in most cephalopod species and therefore the ability to see colors in cephalopods would be an exception rather than a rule. Recently some scientists have proposed that cephalopods (and maybe other marine animals) might rely on chromatic aberration and pupil shape in order to discriminate colors (Stubbs and Stubbs, 2016).

We have shown that the expression of Sof_CRY_6 in the developing eye of *S. officinalis* is eye-specific. For a very long time cryptochromes were discarded from a role in visual function; however, this vision is challenged by recent publication on *D. melanogaster* showing that cryptochrome is able to interact with elements of the phototransduction cascade and has an indirect role in vision by regulating the light sensitivity of opsins during the day (Mazzotta et al., 2013). Here, we showed that Sof_CRY_6 is expressed together with r-opsin1 only in the eye of *Sepia* embryos whereas in the juvenile and the adult it is also expressed in the CNS. This correlation is not enough to conclude but allows an interesting hypothesis regarding a role of CRY_6 in the phototransduction cascade in cephalopods. In the literature, an oscillating expression of period protein was evidenced in the eye of two different marine gastropods species (*Bulla* and *Aplysia*) indicating the likely existence of a Clock system within the eyes of these species (Siwick et al., 1989). In this context, Sof_CRY_6 expression could indicate that a clock system exists in the eyes of cephalopods and that it is already functioning in embryos.

Clock System

Our analysis shows the presence of two cryptochromes expressed in different tissues. CRY_{123} is expressed in all the tissues investigated in embryos and in the juvenile and adult. CRY_6 is expressed in the central nervous system only in the juvenile and the adult. The *in situ* hybridization shows a diffuse presence of CRY_{123} mRNAs in the retina and nervous tissues of the head of a stage 30 embryos and a lighter but similar pattern is found for CRY_6 mRNAs. The fact that both a photosensitive cryptochrome (i.e., CRY_6) and a non-photosensitive cryptochrome (CRY_{123}) could be co-expressed and work together to maintain a circadian rhythm is a recent discovery (Zhu et al., 2005). The mechanism of this Clock system has just been unraveled recently in ecdysozoans (Zhu et al., 2008; Biscontin et al., 2017). It is important to note that organs were collected in daylight. In order to go further on the involvement of the cryptochrome in the control of the circadian rhythm it would be interesting to compare the expression of cryptochromes and other genes involved in daily cycling in organs collected at different time of the night and day.

Retinochromes and Their Role

We identified two retinochromes expressed in the eyes of *S. officinalis* and we confirmed the hypothesis of a duplication limited to the Decabrachia clade (see results and Yoshida et al., 2015). For the first time we studied their expression during embryogenesis: the maximum fold change for retinochromes in *Sepia* embryos (between stage 25 and 28) correlates with the ones of Sof_r-opsin1 and Sof_v-arr. Furthermore both retinochromes mRNAs are found in inner layer of the retina, most likely in the cellular bodies of rhabdomeric photoreceptors cells as

it was already reported for the protein of retinochrome1 in *D. pealeii* (Kingston et al., 2015b). Retinochrome is thought to be involved in the recycling of the retinal photopigment back to its original state before its interaction with r-opsins in the rhabdomes (Terakita et al., 1989). In embryos, this correlation of expression and their co-localization suggest that both retinochromes are good candidates for playing this role. By contrast in the adult, they seem to be differentially expressed. Therefore it would be interesting to know if there is a functional differentiation of these two genes and look at their expression in more diverse tissues.

R-Opsin2 and Xenopsins

A partial sof_r-opsin2 sequence was found in our embryo transcriptomes but its expression was not detected at a significant level in any embryonic tissue studied. Thus we can hypothesized that it does not play an important role in light detection during the embryogenesis of *S. officinalis* (at least in studied tissues) even if we cannot exclude a high translation rate as the mRNA expression is not always correlated with protein synthesis. The presence of r-opsin2 was found in the brain and optic lobes of the adult and needs to be confirmed in the CNS of juveniles. This is convergent with previous knowledge as it was shown in *I. paradoxus* (Yoshida et al., 2015). A full sof_r-opsin2 sequences was retrieved from a transcriptome of adult *S. officinalis* including more nervous tissues (oesophageal ganglia and axial nerve cords): this might indicate that this gene is expressed in nervous tissues outside the CNS. It would be interesting to do a thorough investigation of the expression of r-opsin2 in more organs (including the peripheral ganglia and nerve cords) of adults *S. officinalis* in order to get some insight on its putative role.

To our knowledge, we described for the first time a duplication of a xenopsin gene in metazoans. Interestingly the C-terminal part of the protein is fully identical in both Sof_xeno1 and Sof_xeno2 suggesting a partial duplication likely coupled with an alternative splicing of the protein. We do not know if this duplication is linked to a functional differentiation of the two xenopsins. The xenopsin group is a recently described well-supported clade which includes a lot of gene formerly thought as c-opsins (Ramirez et al., 2016; Vöcking et al., 2017). But its phylogenetic position is currently under debate (Arendt, 2017) because it gathers only lophotrochozoan sequences and is found as a sister-group to cnidarian opsins. This suggests that xenopsin would have already been present in the ancestors of eumetazoans and would be lost in all major lineages except for lophotrochozoans and cnidarians. As for its role, not much is currently known. Xenopsins were found in the larval eyes of lophotrochozoans (brachiopod: Passamaneck et al., 2011 and flatworm: Rawlinson et al., 2019). They are co-expressed with a r-opsin in the photoreceptor of the eyes in two molluscs (*Leptochiton asellus*: Vöcking et al., 2017; *Limax valentianus:* Matsuo et al., 2019), leading to the conclusion that they most likely play a part in vision in these species. Our results show that no significant expression of xenopsin in early developing eyes is detected in *S. officinalis*. Thus it is unlikely that xenopsin plays a role in vision in *S. officinalis*. They most likely play a role in the optic lobes but their expression might be sporadic during development as the expression was not the same in the two stage 25 embryos. Xenopsins stay enigmatic for now and need to be further investigated.

An Eye Specific Visual Arrestin

In lophotrochozoans, we found the co-existence of both a visual arrestin and a β-arrestin in all the coleoid cephalopods we studied and not only in the decabrachian cephalopods as previously thought (Yoshida et al., 2015). Based on our phylogenetic analyses, we cannot conclude on the origin of this duplication: before or after the cephalopod lineage appearance. This might be due to the fact that arrestins rely on their conformation in order to function correctly: the evolution rate of β-arrestins is therefore low compared to the evolution rate of visual arrestins. This explains the long branch of the molluscan visual arrestin clade and maybe also the difficulty to resolve the relationships. Our phylogenetic analysis showed that cephalopod visual arrestins are more closely related to β-arrestin than to vertebrates or arthropods visual arrestins. Therefore these three families arose independently as it was previously reported for the vertebrates and arthropods visual arrestins (Gurevich and Gurevich, 2006). Furthermore, it has been shown in terrestrial gastropod that β-arrestin was co-expressed with r-opsin in the rhabdomes and could translocate in response to light (Matsuo et al., 2017). Two β-arrestins were also identified in the retina of a bivalve (*Argopecten irradians*) and an electrophysiological study showed that they were able to deactivate the photoresponse at the rhodopsin level (Gomez et al., 2011). This suggests that this "Mollusca/Coleoidea visual arrestin" could have arisen from β-arrestin gene duplication followed by a functional specialization. Our results showed that Sof_ β-arr is expressed in different tissues whereas Sof_v-arr is eye specific in embryos and correlates with r-opsin1 expression in the developing eyes. As visual arrestins are known to interact specifically with opsin receptors in order to quench phototransduction in both vertebrates (Gurevich et al., 1995) and arthropods (Montell, 1999) we assume a similar role in cephalopods.

Extraocular Light Detection

Our results suggest that extraocular photosensitive system in cephalopods (e.g., photosensitivity of CNS and the skin) most likely relies on r-opsin1 and sets-up latter than in the eyes. Indeed, widespread extraocular light detection using visual opsin and their putative phototransduction machinery was evidenced with immunostaining in the squid *D. pealeii* (Kingston et al., 2015b).

Previous work has shown that the skin of cephalopods is light sensitive suggesting a local role of r-opsin1 in the dynamic change in skin color. This takes place both in the chromatophores themselves and on sparse sensitive neurons in the epidermis. Moreover it has been linked to the expression of a r-opsin1 in several cephalopod species (*S. officinalis*: Mäthger et al., 2010; *O. bimaculoides*: Ramirez and Oakley,

2015) and also to the expression of the retinochrome in adult *D. pealeii* (Kingston et al., 2015a,b). Maybe due to the fact that we sampled the whole skin and not only chromatophores, we did not find r-opsin1 significantly expressed in the sub-adult and the expression of reti1 in the skin of the juvenile was barely significant. Despite that, our results seem to indicate that the "autonomous" photosensitivity of the skin would appear later than the ability to detect light in the eyes, around hatching or maybe even later, under direct environmental light.

We identified a very low expression of Sof_r-opsin1 and Sof_reti1 in the brain of a juvenile *S. officinalis*. These genes were also significantly expressed in the CNS (brain + optic lobes) of the adult as well as Sof_v-arr in the optic lobes. *In situ* data seem to indicate that Sof_r-opsin1 could be found in a few cells of the cortex of the optic lobes but this needs to be confirmed. In the literature, numerous non-image forming roles are described in a large variety of tissues [review in mammals by Leung and Montell (2017)]. As an example, in *D. melanogaster*, opsins are also known to entertain the circadian rhythm in the clock neurons of the brain, together with other photosensitive receptors such as cryptochromes (Szular et al., 2012). Thus it would be interesting to have a better localization of these receptors up to the cellular levels in order to better understand their functions.

CONCLUSION

For the first time, 6 opsins receptors, 2 cryptochromes and 1 visual arrestin were identified in transcriptomes from *Sepia officinalis* embryos. The evolutionary history of these molecules is intricate with a gene duplication of an arrestin shared at least by all Coleoidea and two duplications of opsins shared by at least all Decabrachia which might have important implication of the functioning of the visual system in some cephalopods. Our results showed that there is an expression of photosensitive receptors in the developing eyes of *S. officinalis* as early as stage 23. Expressions of four of these photosensitive molecules (Sof_r-opsin1, So-reti1, Sof_reti2 and Sof_v-arr) increased significantly when the eyes are developing and starting to be functional (from stage 25 to 28), suggesting they play a role in visual phototransduction cascade. Not only the visual system seemed to be already effective before hatching but this light-detection system set up earlier in the eyes than in other tissues with photosensitive properties (i.e., CNS and skin) and most likely involved part of the same r-opsin transduction cascade. Furthermore, we showed for the first time an eye-specific expression of a cryptochrome in the eye of *S. officinalis* embryos. After hatching the expression of this Sof_CRY_6 is also found in the CNS. This could indicate a indirect or most likely indirect role of CRY_6 in the phototransduction cascade of *S. officinalis*. Finally, this study allows us for the first time to have quantitative data on the expression of these genes in embryos living in standard conditions thus opening the way for comparative studies in the future.

DATA AVAILABILITY STATEMENT

Data are publicly available on the NCBI platform under the accession numbers MN788446 to MN788460.

ETHICS STATEMENT

The eggs were obtained in the Centre de Ressources Biologiques (CRB) in Roscoff (EU0413 – Station Biologique de Roscoff – Sorbonne University) taken in the wild or obtained from animals captured in the wild. The CRB-Station Biologique de Roscoff is an authorized institution, EU-0413, with the agreement number B-29-239-11 (delivered date 2014/04/30) to keep wild animals in captivity and do research and to capture animals in wild (Permit 102-2019 from the Maritime Affairs Directorate of the French Ministry of Ecology). The genitors in Roscoff were used only for eggs providing. They all die after reproduction as they usually do in the wild. The eggs developed in the lab in Paris. The eggs/embryos before hatching of cuttlefish are not under the legislation. **The juveniles** hatched from eggs obtained from the CREC, Université Caen Normandie in 2015. The CREC has all the authorization required to keep *Sepia officinalis* in the marine station (CREC- agreement A14384001) (delivered date 2014/12/24). Eggs were kept in aquarium of "Le Palais de la découverte" (EU 75-576) until hatching. Juveniles were kept under controlled conditions and killed at 1 month using MgCl2 as anesthetics. This experiment took place in 2015 and we had obtained an official notification from our local Ethical Committee Cuvier n°68. At that time, an authorization was not required because nothing was done that leads to suffering of animals and all were done to avoid pain. The subadults fished were used only for personal consumption by the fisherman. We have taken the target organs when the animals were just dead and the animals were kept by the fisherman. There is no need of a permit to fish in the sea.

AUTHOR CONTRIBUTIONS

MB designed and planned the experiment, performed data collection and analysis, as well as manuscript preparation and editing. AO performed bio-informatics analysis and supervised data collection in Japan, as well as manuscript editing. EC assembled the transcriptome of juveniles. LB-P and YB wrote the project, supervised the experiments, and assisted with the data interpretation and manuscript editing. All authors gave final approval for publication and agree to be held accountable for the work performed therein.

FUNDING

This work was partially supported by the JSPS International Fellowship (Nagahama Institute of Bio-Science and Technology _ SP18204) and JSPS Grant-in-Aid for Scientific Research.

This was funded by an EMBRC-France grant. Eggs for *in situ* hybridization and juvenile transcriptome were obtained from CREC marine station-Université de Caen Normandie, thanks to C. Bellanger and C. Le Pabic. Adult organs were obtained thanks to a fisherman, J. Lochon. Transcriptomes of juveniles were obtained from an ATM-MNHN grant (SEPIOME-2015).

ACKNOWLEDGMENTS

The authors would like to thank G. Schires and the Centre de Ressources Biologiques in Biological Marine Station of Roscoff/Sorbonne Université for providing eggs. The authors want to thank C. LePabic and P.-J. Lopez who have contributed to obtain (unpublished) transcriptomic databases essential for assembling the transcriptomes of the juveniles. We are grateful to M. Tosches, for providing some unpublished data of expression in adult *S. officinalis*. For help with the experiments the authors want to thank I. Takemura, R. Minei, V. Hossard, S. Chaouch, I. Seugnet and C. Angée. For help with the figures the authors want to thank Dr. M. T. Sanders.

SUPPLEMENTARY MATERIAL

The Supplementary Material for this article can be found online at: https://www.frontiersin.org/articles/10.3389/fphys.2020.521989/full#supplementary-material

FIGURE S1 | Table of all the sequences used for phylogenetic analyses.

FIGURE S2 | Full alignment used for phylogenetic analyses: opsins tree (1), cryptochromes tree (2) and arrestins tree (3).

FIGURE S3 | Prediction of transmembrane helices in opsin proteins: Sof_r-opsin1 (1), Sof_r-opsin2 (2), Sof_reti1 (3), Sof_reti2 (4), Sof_xeno1 (5) and Sof_xeno2 (6).

FIGURE S4 | Alignment of photosensitive molecules with emphasis on important features. 1. opsins: Alignment of the six opsins from *Sepia officinalis*. The seven transmembrane domains are indicated in gray boxes (based on *S. officinalis* rhodopsin annotation-Uniprot O16005). Important features of GPCR from the rhodopsin family are highlighted (black boxes): the two cysteines forming a dissulfide brigde for protein stability (1 and 3), the conserved lysine (4) of the predictive chromophore binding site (K296 in bovine rhodopsin and K305 in *S. officinalis* rhodopsin/r-opsin1) and the D/ERY domain (2) and NPXXY motif (5) for interaction with G-protein. 2. Cryptochromes: Alignment of cryptochrome sequences from *S. officinalis* annotated with the two conserved domains: the photolyase domain (dark gray) and the FAD-binding domain (light gray).

REFERENCES

Arendt, D. (2017). The enigmatic xenopsins. *eLife* 6:e31781.

Bellingham, J., Morris, A. G., and Hunt, D. M. (1998). The rhodopsin gene of the cuttlefish *Sepia officinalis*: sequence and spectral tuning. *J. Exp. Biol.* 201, 2299–2306.

Benito, J., Houl, J. H., Roman, G. W., and Hardin, P. E. (2008). The blue-light photoreceptor CRYPTOCHROME is expressed in a subset of circadian oscillator neurons in the *Drosophila* CNS. *J. Biol. Rhythms* 23, 296–307. doi: 10.1177/0748730408318588

Biscontin, A., Martini, P., Costa, R., Kramer, A., Meyer, B., Kawaguchi, S., et al. (2019). Analysis of the circadian transcriptome of the Antarctic krill *Euphausia superba*. *Sci. Rep.* 9:13894.

Biscontin, A., Wallach, T., Sales, G., Grudziecki, A., Janke, L., Sartori, E., et al. (2017). Functional characterization of the circadian clock in the Antarctic krill, *Euphausia superba*. *Sci. Rep.* 7:17742.

Boletzky, S. V., Andouche, A., and Bonnaud-Ponticelli, L. (2016). A developmental table of embryogenesis in *Sepia officinalis*. *Vie Milieu* 66, 11–23.

Bolger, A. M., Lohse, M., and Usadel, B. (2014). Trimmomatic: a flexible trimmer for Illumina sequence data. *Bioinformatics* 30, 2114–2120. doi: 10.1093/bioinformatics/btu170

Boycott, B. B. (1961). The functional organization of the brain of the cuttlefish *Sepia officinalis*. *Proc. R. Soc. Lond. B Biol. Sci.* 153, 503–534. doi: 10.1098/rspb.1961.0015

Cao, Z., Sun, L., Chi, C., Liu, H., Zhou, L., Lv, Z., et al. (2016). Molecular cloning, expression analysis and cellular localization of an LFRFamide gene in the cuttlefish *Sepiella japonica*. *Peptides* 80, 40–47. doi: 10.1016/j.peptides.2015.10.005

Chaves, I., Pokorny, R., Byrdin, M., Hoang, N., Ritz, T., Brettel, K., et al. (2011). The cryptochromes: blue light photoreceptors in plants and animals. *Annu. Rev. Plant Biol.* 62, 335–364. doi: 10.1146/annurev-arplant-042110-103759

Craft, C. M., and Whitmore, D. H. (1995). The arrestin superfamily: cone arrestins are a fourth family. *FEBS Lett.* 362, 247–255. doi: 10.1016/0014-5793(95)00213-s

Darriba, D., Taboada, G. L., Doallo, R., and Posada, D. (2011). ProtTest 3: fast selection of best-fit models of protein evolution. *Bioinformatics* 27, 1164–1165. doi: 10.1093/bioinformatics/btr088

Duback, V. E., Pankey, M. S., Thomas, R. I., Huyck, T. L., Mbarani, I. M., Bernier, K. R., et al. (2018). Localization and expression of putative circadian clock transcripts in the brain of the nudibranch *Melibe leonina*. *Comp. Biochem. Physiol. A Mol. Integr. Physiol.* 223, 52–59. doi: 10.1016/j.cbpa.2018.05.002

El-Gebali, S., Mistry, J., Bateman, A., Eddy, S. R., Luciani, A., Potter, S. C., et al. (2019). The Pfam protein families database in 2019. *Nucleic Acids Res.* 47, D427–D432.

Feuda, R., Hamilton, S. C., McInerney, J. O., and Pisani, D. (2012). Metazoan opsin evolution reveals a simple route to animal vision. *Proc. Natl. Acad. Sci. U.S.A.* 109, 18868–18872. doi: 10.1073/pnas.1204609109

Gomez, P. M., Espinosa, L., Ramirez, N., and Nasi, E. (2011). Arrestin in ciliary invertebrate photoreceptors: molecular identification and functional analysis *in vivo*. *J. Neurosci.* 31, 1811–1819. doi: 10.1523/jneurosci.3320-10.2011

Grabherr, M. G., Haas, B. J., Yassour, M., Levin, J. Z., Thompson, D. A., Amit, I., et al. (2011). Trinity: reconstructing a full-length transcriptome without a genome from RNA-Seq data. *Nat. Biotechnol.* 29, 644–652.

Guindon, S., and Gascuel, O. (2003). A simple, fast, and accurate algorithm to estimate large phylogenies by maximum likelihood. *Syst. Biol.* 52, 696–704. doi: 10.1080/10635150390235520

Gurevich, E. V., and Gurevich, V. V. (2006). Arrestins: ubiquitous regulators of cellular signaling pathways. *Genome Biol.* 7:236.

Gurevich, V. V., Dion, S. B., Onorato, J. J., Ptasienski, J., Kim, C. M., Sterne-Marr, R., et al. (1995). Arrestin Interactions with G Protein-coupled Receptors direct binding studies of wild type and mutant arrestins with rhodopsin, β2-adrenergic, and m2 muscarinic cholinergic receptors. *J. Biol. Chem.* 270, 720–731. doi: 10.1074/jbc.270.2.720

Haug, M. F., Gesemann, M., Lazoviæ, V., and Neuhauss, S. C. (2015). Eumetazoan cryptochrome phylogeny and evolution. *Genome Biol. Evol.* 7, 601–619. doi: 10.1093/gbe/evv010

Heath-Heckman, E. A. C., Peyer, S. M., Whistler, C. A., Apicella, M. A., Goldman, W. E., and McFall-Ngai, M. J. (2013). Bacterial bioluminescence regulates expression of a host cryptochrome gene in the squid-vibrio symbiosis. *mBio* 4:e00167-13.

Imarazene, B., Andouche, A., Bassaglia, Y., Lopez, P.-J., and Bonnaud-Ponticelli, L. (2017). Eye development in *Sepia officinalis* embryo: what the uncommon gene expression profiles tell us about eye evolution. *Front. Physiol.* 8:613. doi: 10.3389/fphys.2017.00613

Kingston, A. C. N., Kuzirian, A. M., Hanlon, R. T., and Cronin, T. W. (2015a). Visual phototransduction components in cephalopod chromatophores suggest dermal photoreception. *J. Exp. Biol.* 218, 1596–1602. doi: 10.1242/jeb.117945

Kingston, A. C. N., Wardill, T. J., Hanlon, R. T., and Cronin, T. W. (2015b). An unexpected diversity of photoreceptor classes in the longfin squid,

Doryteuthis pealeii. *PLoS One* 10:e0135381. doi: 10.1371/journal.pone.0135381

Krogh, A., Larsson, B., von Heijne, G., and Sonnhammer, E. L. (2001). Predicting transmembrane protein topology with a hidden Markov model: application to complete genomes. *J. Mol. Biol.* 305, 567–580. doi: 10.1006/jmbi.2000.4315

Langmead, B., and Salzberg, S. L. (2012). Fast gapped-read alignment with Bowtie 2. *Nat. Methods* 9, 357–359. doi: 10.1038/nmeth.1923

Leung, N. Y., and Montell, C. (2017). Unconventional Roles of Opsins. *Annu. Rev. Cell Dev. Biol.* 33, 241–264. doi: 10.1146/annurev-cellbio-100616-060432

Li, B., and Dewey, C. N. (2011). RSEM: accurate transcript quantification from RNA-Seq data with or without a reference genome. *BMC Bioinformatics* 12:323. doi: 10.1186/1471-2105-12-323

Liscovitch-Brauer, N., Alon, S., Porath, H. T., Elstein, B., Unger, R., Ziv, T., et al. (2017). Trade-off between transcriptome plasticity and genome evolution in cephalopods. *Cell* 169, 191–202.e11.

Mäthger, L. M., Roberts, S. B., and Hanlon, R. T. (2010). Evidence for distributed light sensing in the skin of cuttlefish, *Sepia officinalis*. *Biol. Lett.* 6, 600–603. doi: 10.1098/rsbl.2010.0223

Matsui, S., Seidou, M., Horiuchi, S., Uchiyama, I., and Kito, Y. (1988). Adaptation of a deep-sea cephalopod to the photic environment. Evidence for three visual pigments. *J. Gen. Physiol.* 92, 55–66. doi: 10.1085/jgp.92.1.55

Matsuo, R., Koyanagi, M., Nagata, A., and Matsuo, Y. (2019). Co-expression of opsins in the eye photoreceptor cells of the terrestrial slug *Limax valentianus*. *J. Comp. Neurol.* 527, 3073–3086. doi: 10.1002/cne.24732

Matsuo, R., Takatori, Y., Hamada, S., Koyanagi, M., and Matsuo, Y. (2017). Expression and light-dependent translocation of β-arrestin in the visual system of the terrestrial slug *Limax valentianus*. *J. Exp. Biol.* 220, 3301–3314. doi: 10.1242/jeb.162701

Mayeenuddin, L. H., and Mitchell, J. (2003). Squid visual arrestin: cDNA cloning and calcium-dependent phosphorylation by rhodopsin kinase (SQRK). *J. Neurochem.* 85, 592–600. doi: 10.1046/j.1471-4159.2003.01726.x

Mazzotta, G., Rossi, A., Leonardi, E., Mason, M., Bertolucci, C., Caccin, L., et al. (2013). Fly cryptochrome and the visual system. *Proc. Natl. Acad. Sci. U.S.A.* 110, 6163–6168. doi: 10.1073/pnas.1212317110

Mazzotta, G. M., and Costa, R. (2016). Circadian control of visual plasticity in arthropods. *Ethol. Ecol. Evol.* 28, 1–19. doi: 10.1080/03949370.2015.1064037

Merrill, C. E., Pitts, R. J., and Zwiebel, L. J. (2003). Molecular characterization of arrestin family members in the malaria vector mosquito, *Anopheles gambiae*. *Insect Mol. Biol.* 12, 641–650. doi: 10.1046/j.1365-2583.2003.00450.x

Montell, C. (1999). Visual transduction in *Drosophila*. *Annu. Rev. Cell Dev. Biol.* 15, 231–268. doi: 10.1146/annurev.cellbio.15.1.231

Nießner, C., Denzau, S., Malkemper, E. P., Gross, J. C., Burda, H., Winklhofer, M., et al. (2016). Cryptochrome 1 in retinal cone photoreceptors suggests a novel functional role in mammals. *Sci. Rep.* 6:21848.

Nixon, M., and Young, J. Z. (2003). *The Brains and Lives of Cephalopods*. Oxford: Oxford University Press.

Oliveri, P., Fortunato, A. E., Petrone, L., Ishikawa-Fujiwara, T., Kobayashi, Y., Todo, T., et al. (2014). The cryptochrome/photolyase family in aquatic organisms. *Mar. Genomics* 14, 23–37. doi: 10.1016/j.margen.2014.02.001

Passamaneck, Y. J., Furchheim, N., Hejnol, A., Martindale, M. Q., and Lüter, C. (2011). Ciliary photoreceptors in the cerebral eyes of a protostome larva. *EvoDevo* 2:6. doi: 10.1186/2041-9139-2-6

Porter, M. L., Blasic, J. R., Bok, M. J., Cameron, E. G., Pringle, T., Cronin, T. W., et al. (2011). Shedding new light on opsin evolution. *Proc. Biol. Sci.* 279, 3–14. doi: <PMID<PMID:NOPMID</PMID<

Ramirez, M. D., and Oakley, T. H. (2015). Eye-independent, light-activated chromatophore expansion (LACE) and expression of phototransduction genes in the skin of *Octopus bimaculoides*. *J. Exp. Biol.* 218, 1513–1520. doi: 10.1242/jeb.110908

Ramirez, M. D., Pairett, A. N., Pankey, M. S., Serb, J. M., Speiser, D. I., Swafford, A. J., et al. (2016). The last common ancestor of most bilaterian animals possessed at least nine opsins. *Genome Biol. Evol.* 8, 3640–3652.

Rawlinson, K. A., Lapraz, F., Ballister, E. R., Terasaki, M., Rodgers, J., McDowell, R. J., et al. (2019). Extraocular, rod-like photoreceptors in a flatworm express xenopsin photopigment. *eLife* 8:e45465.

Romagny, S., Darmaillacq, A.-S., Guibé, M., Bellanger, C., and Dickel, L. (2012). Feel, smell and see in an egg: emergence of perception and learning in an immature invertebrate, the cuttlefish embryo. *J. Exp. Biol.* 215, 4125–4130. doi: 10.1242/jeb.078295

Ronquist, F., Teslenko, M., van der Mark, P., Ayres, D. L., Darling, A., Höhna, S., et al. (2012). MrBayes 3.2: efficient Bayesian phylogenetic inference and model choice across a large model space. *Syst. Biol.* 61, 539–542. doi: 10.1093/sysbio/sys029

Schurch, N. J., Schofield, P., Gierliński, M., Cole, C., Sherstnev, A., Singh, V., et al. (2016). How many biological replicates are needed in an RNA-seq experiment and which differential expression tool should you use? *RNA* 22, 839–851. doi: 10.1261/rna.053959.115

Siwick, K. K., Strack, S., Rosbash, M., Hall, J. C., and Jacklet, J. W. (1989). An antibody to the *Drosophila* period protein recognizes circadian pacemaker neurons in *Aplysia* and *Bulla*. *Neuron* 3, 51–58. doi: 10.1016/0896-6273(89)90114-1

Song, W., Mu, C., Li, R., and Wang, C. (2017). Peroxiredoxin 1 from cuttlefish (*Sepiella maindroni*): Molecular characterization of development and its immune response against *Vibrio alginolyticus*. *Fish Shellfish Immunol.* 67, 596–603. doi: 10.1016/j.fsi.2017.06.034

Stamatakis, A. (2014). RAxML version 8: a tool for phylogenetic analysis and post-analysis of large phylogenies. *Bioinformatics* 30, 1312–1313. doi: 10.1093/bioinformatics/btu033

Stöger, I., Sigwart, J. D., Kano, Y., Knebelsberger, T., Marshall, B. A., Schwabe, E., et al. (2013). The continuing debate on deep molluscan phylogeny: evidence for Serialia (Mollusca, Monoplacophora + Polyplacophora). *Biomed Res. Int.* 2013:407072.

Stubbs, A. L., and Stubbs, C. W. (2016). Spectral discrimination in color blind animals via chromatic aberration and pupil shape. *Proc. Natl. Acad. Sci. U.S.A.* 113, 8206–8211. doi: 10.1073/pnas.1524578113

Szular, J., Sehadova, H., Gentile, C., Szabo, G., Chou, W.-H., Britt, S. G., et al. (2012). Rhodopsin 5– and Rhodopsin 6–mediated clock synchronization in *Drosophila melanogaster* is independent of retinal phospholipase C-β signaling. *J. Biol. Rhythms* 27, 25–36. doi: 10.1177/0748730411431673

Terakita, A., Hara, R., and Hara, T. (1989). Retinal-binding protein as a shuttle for retinal in the rhodopsin-retinochrome system of the squid visual cells. *Vision Res.* 29, 639–652. doi: 10.1016/0042-6989(89)90026-6

Tosini, G., Davidson, A. J., Fukuhara, C., Kasamatsu, M., and Castanon-Cervantes, O. (2007). Localization of a circadian clock in mammalian photoreceptors. *FASEB J.* 21, 3866–3871. doi: 10.1096/fj.07-8371com

Troshin, P. V., Procter, J. B., and Barton, G. J. (2011). Java bioinformatics analysis web services for multiple sequence alignment—JABAWS:MSA. *Bioinformatics* 27, 2001–2002. doi: 10.1093/bioinformatics/btr304

Vöcking, O., Kourtesis, I., Tumu, S. C., and Hausen, H. (2017). Co-expression of xenopsin and rhabdomeric opsin in photoreceptors bearing microvilli and cilia. *eLife* 6:e23435.

Waterhouse, A. M., Procter, J. B., Martin, D., Clamp, M., and Barton, G. J. (2009). Jalview version 2—a multiple sequence alignment editor and analysis workbench. *Bioinformatics* 25, 1189–1191. doi: 10.1093/bioinformatics/btp033

Wiltschko, R., and Wiltschko, W. (2014). Sensing magnetic directions in birds: radical pair processes involving cryptochrome. *Biosensors* 4, 221–242. doi: 10.3390/bios4030221

Xu, R., and Zheng, X. (2018). Selection of reference genes for quantitative real-time PCR in *Octopus minor* (Cephalopoda: Octopoda) under acute ammonia stress. *Environ. Toxicol. Pharmacol.* 60, 76–81. doi: 10.1016/j.etap.2018.04.010

Yamamoto, M. (1985). Ontogeny of the visual system in the cuttlefish, *Sepiella japonica*. I. Morphological differentiation of the visual cell. *J. Comp. Neurol.* 232, 347–361. doi: 10.1002/cne.902320307

Yamamoto, M., Takasu, N., and Uragami, I. (1985). Ontogeny of the visual system in the cuttlefish, *Sepiella japonica*. II. Intramembrane particles, histofluorescence, and electrical responses in the developing retina. *J. Comp. Neurol.* 232, 362–371. doi: 10.1002/cne.902320308

Yau, K.-W., and Hardie, R. C. (2009). Phototransduction motifs and variations. *Cell* 139, 246–264. doi: 10.1016/j.cell.2009.09.029

Yoshida, M. A., Ogura, A., Ikeo, K., Shigeno, S., Moritaki, T., Winters, G. C., et al. (2015). Molecular evidence for convergence and parallelism in evolution of complex brains of *Cephalopod Molluscs*: insights from visual systems. *Integr. Comp. Biol.* 55, 1070–1083. doi: 10.1093/icb/icv049

Yoshii, T., Todo, T., Wülbeck, C., Stanewsky, R., and Helfrich-Förster, C. (2008). Cryptochrome is present in the compound eyes and a subset of *Drosophila*'s clock neurons. *J. Comp. Neurol.* 508, 952–966. doi: 10.1002/cne.21702

Young, J. Z. (1962). The optic lobes of *Octopus vulgaris*. *Philos. Trans. R. Soc. Lond. B Biol. Sci.* 245, 19–58. doi: 10.1098/rstb.1962.0005

Young, J. Z. (1974). The central nervous system of Loligo I. The optic lobe. *Philos. Trans. R. Soc. Lond. B Biol. Sci.* 267, 263–302. doi: 10.1098/rstb.1974.0002

Zaccardi, G., Kelber, A., Sison-Mangus, M. P., and Briscoe, A. D. (2006). Color discrimination in the red range with only one long-wavelength sensitive opsin. *J. Exp. Biol.* 209, 1944–1955. doi: 10.1242/jeb.02207

Zhu, H., and Green, C. B. (2001). Three cryptochromes are rhythmically expressed in *Xenopus laevis* retinal photoreceptors. *Mol. Vis.* 7, 210–215.

Zhu, H., Sauman, I., Yuan, Q., Casselman, A., Emery-Le, M., Emery, P., et al. (2008). Cryptochromes define a novel circadian clock mechanism in monarch butterflies that may underlie sun compass navigation. *PLoS Biol.* 6:e4. doi: 10.1371/journal.pbio.0060004

Zhu, H., Yuan, Q., Froy, O., Casselman, A., and Reppert, S. M. (2005). The two CRYs of the butterfly. *Curr. Biol.* 15, R953–R954.

Conflict of Interest: The authors declare that the research was conducted in the absence of any commercial or financial relationships that could be construed as a potential conflict of interest.

frontiers in Physiology

BRIEF RESEARCH REPORT
published: 10 February 2021
doi: 10.3389/fphys.2021.622126

Early Exposure to Water Turbidity Affects Visual Capacities in Cuttlefish (*Sepia officinalis*)

*Alice Goerger[1], Anne-Sophie Darmaillacq[1], Nadav Shashar[2] and Ludovic Dickel[1]**

[1] Normandie Univ., UNICAEN, Ethos (Ethologie Animale et Humaine) UMR 6552, Caen, France, [2] Department of Life Sciences, Ben Gurion University of the Negev, Eilat, Israel

In La Manche (English Channel) the level of turbidity changes, not only seasonally and daily in seawater but also along the coast. As a consequence, vision in marine species is limited when based only on contrast-intensity. It is hypothesized that polarization sensitivity (PS) may help individuals detect preys and predators in turbid environments. In the cuttlefish, *Sepia officinalis*, to date, all behavioral studies have been conducted on animals reared in clear water. But the cuttlefish sensory system is adapted to a range of turbid environments. Our hypothesis was that rearing cuttlefish in clear water may affect the development of their visual system, and potentially affect their visually guided behaviors. To test this, newly-hatched cuttlefish, from eggs laid by females brought in from the wild, were reared for 1 month under three different conditions: clear water (C group), low turbidity (0.1 g / l of clay, 50–80 NTU, LT group) and high turbidity (0.5 g / l of clay, 300–400 NTU, HT group). The visual capacities of cuttlefish were tested with an optomotor apparatus at 7 days and at 1 month post-hatching. Optomotor responses of juveniles were measured by using three screen patterns (black and white stripes, linearly polarized stripes set at different orientations, and a uniform gray screen). Optomotor responses of juveniles suggest that exposure to turbid water improves the development of their PS when tested in clear water (especially in LT group) but not when tested in turbid water. We suggest that the use of slightly turbid water in rearing systems may improve the development of vision in young cuttlefish with no detrimental effect to their survival rate. Future research will consider water turbidity as a possible factor for the improvement of cuttlefish well-being in artificial rearing systems.

Keywords: optomotor response, linear polarization, vision, cephalopods, development

OPEN ACCESS

Edited by:
Daniel Osorio, University of Sussex, United Kingdom

Reviewed by:
Angelique Christine Paulk, Massachusetts General Hospital, Harvard Medical School, United States
Michael Kuba, Okinawa International University, Japan

***Correspondence:**
Ludovic Dickel
ludovic.dickel@unicaen.fr

Specialty section:
This article was submitted to Invertebrate Physiology, a section of the journal Frontiers in Physiology

Received: *27 October 2020*
Accepted: *18 January 2021*
Published: *10 February 2021*

Citation:
Goerger A, Darmaillacq A-S, Shashar N and Dickel L (2021) Early Exposure to Water Turbidity Affects Visual Capacities in Cuttlefish (Sepia officinalis). Front. Physiol. 12:622126. doi: 10.3389/fphys.2021.622126

INTRODUCTION

Water turbidity is caused by various mixtures of suspended particles such as sediments, sand/clay (mineral), zooplankton (animal) or algae (plant). These particles absorb and/or scatter the incoming light from the sun. They are also crucial for light and color attenuation in the water column. Light is partially linearly polarized under water. Many factors, such as scattering and the absorption properties of the medium, directionality of the incoming light and the presence of waves on the water surface, can change the orientation of light polarization and induce or reduce polarization [reviewed in Sabbah et al. (2005)]. For example, a little scattering induces polarization

but too much scattering reduces the polarization signal (Shashar et al., 2011; Lerner et al., 2012). Turbidity alone and/or combined with other factors may impair the availability and reliability of visual cues for aquatic animals, and thus potentially alter some of their visually guided behaviors.

Visual information is widely used for predator avoidance and/or prey detection in aquatic animals (Luczkovich, 1988; Fuiman and Magurran, 1994; Gall and Fernandez-Juricic, 2010). As a consequence, water turbidity is probably a strong evolutionary constraint for aquatic organisms. In their natural environments, numerous species living in turbid water quite simply reduce their use of vision. For example, the river dolphin living in turbid rivers has eyes of a reduced size (used only as light sensors) as compared to sea dolphins. Some species of river dolphins are blind (Herald et al., 1969; Pilleri, 1979) and rely only on their biosonars to find prey. In other species, the lack of visual information may be balanced by the use of other senses: this is "sensory compensation" (Hartman and Abrahams, 2000). For example, zebrafish reared in clear water rely on visual information in foraging behavior but the ones reared for 2 weeks in turbid water mainly rely on odor information (Suriyampola et al., 2018). In some species, turbidity differences, which are often coupled with spectral changes, affect the developmental plasticity of the visual system. For example, Ehlman et al. (2015) demonstrated a shift from mid-wave-sensitive opsins to long wave-sensitive opsins in guppies (*Poecilia reticulata*) previously reared in turbid water. The visual system has different roles, including but not limited to: detecting brightness, colors, shapes, and motion (Gegenfurtner and Hawken, 1996; Derrington, 2000). In guppies, the change of opsin may increase motion-detecting abilities in this species to balance the loss of color and brightness cues in turbid water. It follows that in order to investigate the effects of turbidity on the development of the visual system, it is appropriate to work with animal models that live in a variety of natural water turbidity conditions and mainly relying on visual information in their basic behaviors.

Cephalopods have keen vision and many of their behaviors are guided by visual information. There is a great plasticity of their visual capacities and subsequent behaviors depend on experience during the early life stages (Huffard, 2013; Darmaillacq et al., 2017; Marini et al., 2017; Mather and Dickel, 2017; Villanueva et al., 2017). Cephalopods are colorblind (Marshall and Messenger, 1996; Mäthger et al., 2006) but most species have polarization sensitivity (PS), i.e., they can detect the *e*-vector orientation and the degree (percent) of linear polarization of the incoming light. Since no cephalopod is known to be sensitive to the circular polarization component of light, we refer here only to linear polarization without specifying this further. Cuttlefish probably show the finest *e*-vector angle discrimination of all cephalopods (Temple et al., 2012) and are consequently a particularly valuable model for the study of PS. In cuttlefish, PS is potentially involved in various functions such as communication (Shashar et al., 1996; Boal et al., 2004), orientation (Cartron et al., 2012), prey detection (Shashar et al., 1998, 2000) and predator detection (Cartron et al., 2013b,c). Cartron et al. (2013c) demonstrated that PS increases visual capacities in a turbid environment in cuttlefish (*S. officinalis*, *S. pharaonis*, and *S. prashadi*).

A powerful and simple way to study the visual capacities of animals is to measure their optomotor response (OMR) to different visual stimuli (mostly a screen with contrasted patterns rotating around the animal, McCann and MacGinitie, 1965; Groeger et al., 2005; Rinner et al., 2005). When presented with a moving stimulus an individual exhibits unconditioned movements of its eyes, head or whole body following the direction of the moving stimulus (Darmaillacq and Shashar, 2008). OMR can be used to examine sensitivity to contrasts, spectral sensitivity or PS (Darmaillacq and Shashar, 2008). Cartron et al. (2013a) used OMR to show differences of visual capacities based on intensity and polarization contrasts in young cuttlefish previously reared in clear water (from hatching to 30 days of age). Sensitivity to contrast was high from the time of hatching. By contrast, only 20% of individuals responded to polarized stripes patterns at the hatchling stage but all responded to the polarized signal at 1 month. This can be linked, at least partially, to the delay between hatching and first prey catching (Dickel et al., 1997).

Sepia officinalis, a common species, breeds, hatches, and develops in the turbid water of La Manche (English Channel). Up to now, developmental studies on cuttlefish vision (including our own) have always been conducted on animals previously reared in clear water. The present study will investigate the development of visual capacities in young cuttlefish previously reared in different water turbidities. We hypothesize that (1) In turbid water, information based on intensity contrast will be less well perceived than that based on PS. (2) Cuttlefish reared in turbid water will develop PS faster and will consequently display better vision in turbid water than those reared in clear water. These results could provide valuable information about the water quality standards to be used in cuttlefish rearing systems under laboratory conditions according to current European regulations (Directive 2010/63/EU).

METHODS

Animals

Eggs from the wild were collected from several egg batches in Luc-sur-Mer/Villers-sur-Mer and Arcachon vicinities in France (Normandy and Gironde, respectively). They were separated and put randomly in baskets in shallow tanks at the Centre de Recherches en Environnement Côtier (CREC, Luc sur Mer, France). The system is an open system with a flow rate of about one liter/min to avoid any recycling of turbidity. All tanks were then supplied with running oxygenated clear sea water at 19 $\pm$ 1°C. After hatching, cuttlefish were reared for 1 month under three conditions: clear water (C), slightly turbid water (LT), and highly turbid water (HT) in tanks (40 cm $\times$ 60 cm $\times$ 32 cm) providing an enriched habitat (artificial plants, stones, and shells). Each tank contained a maximum of 30 animals at the same time. All tanks were cleaned daily to avoid the proliferation of bacteria and waste

matter. Cleaning was done when the water was clear to avoid damaging the animals. The procedure was the same for all groups. Then, one liter of seawater, without clay (C) or with clay (LT and HT), was added each day. The amount of clay was calculated to obtain a turbidity of 0.1 g/l (50–80 NTU) in the LT and 0.5 g/l (300–400 NTU) in the HT. Turbidity of the water of each tank was measured using a turbidimeter (Turbidimeter 2016LM). Animals were fed daily *ad libidum* with live shrimps (*Crangon crangon*) just after the daily turbidity measurement. Sixty-two cuttlefish were tested at 7 days post hatching (n = 20 for C and HT group and n = 22 for LT group) and 30 other cuttlefish at 30 days of age post hatching (n = 10 in each group). These ages were chosen in accordance with Cartron et al. (2013a) that showed that the visual system critically develops during the month of life. Animal maintenance and experimentation were in compliance with the Directive 2010/63/EU on the protection of animals used for scientific purposes, and following the recommendations of the 3Rs (Fiorito et al., 2014).

Optomotor Apparatus and Behavioral Tests

The optomotor system was described in detail in Darmaillacq and Shashar (2008). In short, the method is based on evoking conditioned OMR (eye or body movements) of cuttlefish with the rotation of contrasting stripes. When rotated stripes are perceived, the cuttlefish will follow the direction of the pattern movements with its eyes or its whole body in order to stabilize the moving visual field. Briefly, the optomotor apparatus consists of a cylinder (40 cm diameter) rotated by a controllable, reversible motor. The patterned screen was placed on the interior wall of the cylinder and a light diffuser was put on the exterior wall. In the center of the apparatus two glass cylinders (one holding the animal, 12 cm diameter and the other containing either clear or turbid water, 24 cm diameter) were placed on a stationary platform. Adding another compartment to the Darmaillacq and Shashar (2008) OMR device allowed us to test the visual ability of young cuttlefish in both clear and turbid water. To avoid any experimenter disturbance, the entire apparatus was covered with an opaque curtain with a single hole for a video camera just above the glass cylinder containing the animal. A LED band placed around the tank with light diffusers provided uniform and stable lighting of the pattern during the experiment. We tested two patterns with 10 mm wide stripes: black and white alternating stripes (BW) and polarized stripes (Pol). The latter consisted of alternating stripes with different orientations of linear polarization (see methods in Cartron et al., 2013a): 0°, 45°, 90°, and 135° (sheet #318, Frank Woolley & Co.). As a control, cuttlefish were tested with a uniform sheet of gray paper (G) (**Figure 1**). Preliminary tests showed the same OMR for cuttlefish when using black and white alternating stripes or black, white and two shades of gray alternating stripes used in Cartron et al. (2013a). Thus it seems that the complexity of the pattern did not interfere with the visual ability of cuttlefish. To check whether the use of two glass cylinders in the apparatus could interfere with stripe detection a video camera was put inside the apparatus instead of the cuttlefish. The contrast between the stripes was measured using ImageJ software and Michelson formula for both stripes (BW and Pol). In clear water there was no difference between contrasts measured through a single or double cylinder (respectively, 43 and 37% contrast difference between the polarized stripes).

Following Cartron et al. (2013a), each cuttlefish was gently moved from its home tank to the experimental cylinder. It was allowed 2 min to calm down before the beginning of the experiment. Following preliminary tests, one speed 30°/s was used for each pattern turning in two directions (clockwise and counter-clockwise). Each cuttlefish was tested twice: first surrounded by clear water and then by turbid water (0.1 g/l of clay mixed with water i.e., low turbidity), in a random order. For both conditions the cuttlefish was submitted to six trials (three patterns × two directions × one speed) for a maximum duration of 15 min each. Between tests in clear and turbid water, the cuttlefish was supplied with new, oxygenated water from its home tank (this water was taken before the turbid event in order to keep the water in the experimental cylinder clear for all groups). Patterns (BW, Pol, and G), directions (clockwise and counter-clockwise) and conditions (turbid or not) were chosen for each session (see the **Figure 1** for a combination example). The interval between two directions was 30 s. There were 1-min intervals between two patterns and 2-min intervals between two conditions. Responses were considered as positive when a cuttlefish followed the patterns over at least 180° in both directions and did not show any response to the control sheet (G) i.e., as in Cartron et al. (2013a) (**Figure 1**). It must be specified that we were stricter in scoring than in previous studies. A response was only considered to be positive with at least a 180° rotation of the tested animal instead of the 90° cutoff in Groeger et al. (2005) and Darmaillacq and Shashar (2008). Furthermore, in the present study a response was only considered to be positive when the animal responded to both rotational directions, single responses being ignored (for an example of a positive response see the video in **Supplementary Material**).

Statistical Analyses

Data were analyzed using R version 3.5.2. Non-parametric McNemar test for paired data with continuity correction was used to compare responses between the two experimental conditions (turbid or not) as well as the responses for the two patterns. For comparison between the three groups a Fisher–Freeman–Halton test (Fisher's exact test for count data with simulated p-value based on 10^5 replicates) was used in addition to a *post-hoc* pairwise Fisher's test with Bonferroni corrections. Comparisons between ages were determined with Fisher's test. Cutoff for significance was decided as $p < 0.05$.

Ethics Statement

This research followed the guidance by Directive 2010/63/EU, and French regulations regarding the use of animals for experimental procedures, and was approved by the Regional Ethical Committee Cenomexa [Project agreement number: APAFIS 2019100316587299 _V2 (#20662)]. The experiment

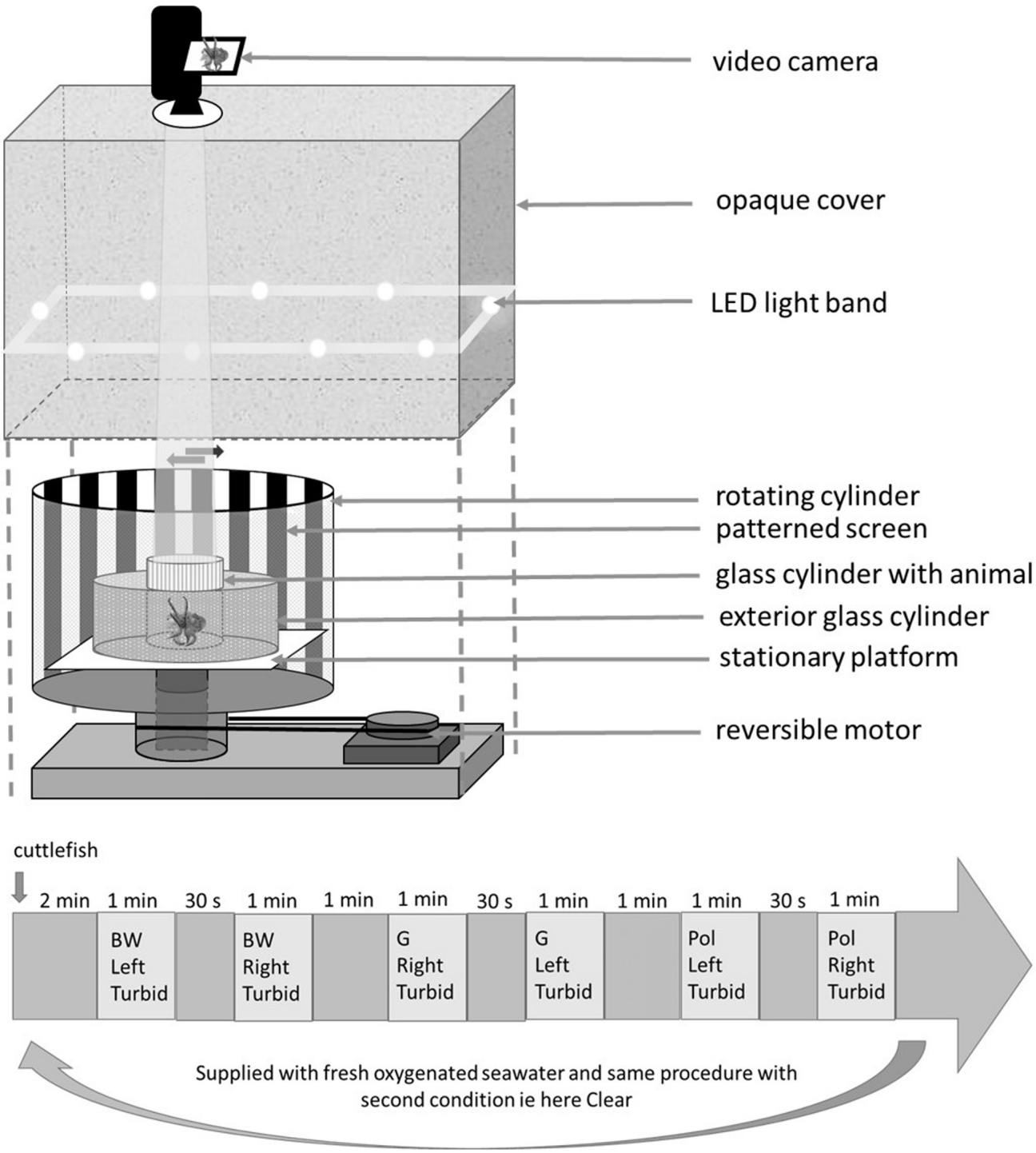

FIGURE 1 | Optomotor apparatus and an example of a procedure for which the order was randomized. The apparatus consisted of a cylinder showing three patterns (BW, black and white; G, gray; Pol, polarized stripes.) and rotated by a reversible motor placed on the inner wall of the apparatus. Two glass cylinders, one holding the animal and the other with more or less turbid water, were placed on a stationary platform in the center of the apparatus. In the procedure, the external cylinder was supplied with turbid seawater (condition 1) and for condition 2 the same experiment was done with clear seawater. Between the two conditions the cylinder holding the animal was supplied with fresh oxygenated seawater.

was designed to decrease animal distress by minimizing the number of animal.

RESULTS

The OMR was recorded in three groups of cuttlefish: a control group reared in constantly clear seawater (C group) and two groups reared in turbid sea water; one group with low turbidity (LT group) and one with high turbidity (HT group). All animals were tested at two ages: 7 days and 1 month post hatching. To assess the effect of turbidity on the development of luminance and PS, we used two patterns, respectively, a BW pattern (black and white stripes) and a Pol pattern (polarized stripes). A uniform gray sheet served as a control pattern (no response expected). Each pattern was tested in two experimental conditions: clear water and turbid water.

At 1 month, the LT group had a somewhat higher survival rate (C group survival = 87.5%; LT group survival = 95%; HT group survival = 85%). Mean cuttlefish size (Dorsal Mantle Length, DML) was slightly greater in the C group at both ages (at 7 days C DML = 10.9 ± 1.1 mm, n_{C7} = 20; LT DML = 10.8 ± 1.0 mm, n_{LT7} = 22; HT DML = 10.6 ± 1.4 mm, n_{HT7} = 20; at 1 month C DML = 18.4 ± 1.5 mm, n_{C30} = 10; LT DML = 17.6 ± 1.9 mm, n_{LT30} = 10; HT DML = 17.9 ± 2.2 mm, n_{HT30} = 10).

In clear water all animals (both ages) showed sensitivity to light intensity (BW) (Fisher-Freeman–Halton test, 7 days-clear water, $P = 1.00$, $n_C = n_{HT} = 20$, and $n_{LT} = 22$; 1 month-clear water, $P = 1.00$, $n_C = n_{LT} = n_{HT} = 10$) (**Figure 2**).

However, in clear water PS improved with development, especially in group C (Fisher test; $P = 0.019$, $n_{C7} = 20$, and $n_{C30} = 10$) (data not shown). At 7 days in clear water the response rate was higher (70–80%) in HT and LT groups (70 and 80%, respectively) with significant PS difference between the group LT (80%) and the group C (30%) ($P = 0.0044$, $n_{LT} = 22$, and $n_C = 20$) (**Figure 2**).

At 7 days and in clear water, the groups C and HT had a higher response rate for the intensity pattern than for the polarized pattern (McNemar test; C, $\chi^2 = 12.07$, df = 1, $P < 0.001$; HT, $\chi^2 = 5.14$, df = 1, $P = 0.023$, $n_C = n_{HT} = 20$) (data not shown). At 1 month, this difference disappeared (McNemar test; C, $\chi^2 = 0.5$, df = 1, $P = 0.48$; HT, $\chi^2 = 1.33$, df = 1, $P = 0.25$, $n_C = n_{HT} = 10$) (**Figure 2**).

In turbid conditions sensitivity to intensity (BW) increased with development (McNemar test; C, χ^2 = NaN, df = 1, $P = 1.00$, $n_{C7} = 20$, and $n_{C30} = 10$; LT, χ^2 = NaN, df = 1, $P = 1.00$, $n_{LT7} = 22$, and $n_{LT30} = 10$; HT, χ^2 = NaN, df = 1, $P = 1.00$, $n_{HT7} = 20$, and $n_{HT30} = 10$) (**Figure 2**). Indeed, under turbid conditions only 70% (group C) to 85% (group HT) of the 1-week old cuttlefish showed a response. The groups C and LT had lower response rate in these experimental conditions than in clear water conditions (McNemar test; C, $\chi^2 = 4.17$, df = 1, $P = 0.041$, $n_C = 20$; LT, $\chi^2 = 4.17$, df = 1, $P = 0.041$, $n_{LT} = 22$) (**Figure 2**).

Polarization sensitivity in turbid water was significantly lower than in clear water (McNemar test; C-7 days, $\chi^2 = 4.17$, df = 1, $P = 0.042$, $n_{C7} = 20$; LT-7 days, $\chi^2 = 16.06$, df = 1, $P < 0.001$, $n_{LT7} = 22$; HT-7 days, $\chi^2 = 8.64$, df = 1, $P = 0.0033$, $n_{HT7} = 20$; C-1 month, $\chi^2 = 6.13$, df = 1, $P = 0.013$, $n_{C30} = 10$; LT-1 month, $\chi^2 = 7.11$, df = 1, $P = 0.0077$, $n_{LT30} = 10$; HT-1 month, $\chi^2 = 5.14$, df = 1, $P = 0.023$, $n_{HT30} = 10$) (**Figure 2**). In fact, in turbid water, at 7 days, no animal showed any OMR, with the exception of one cuttlefish from HT group.

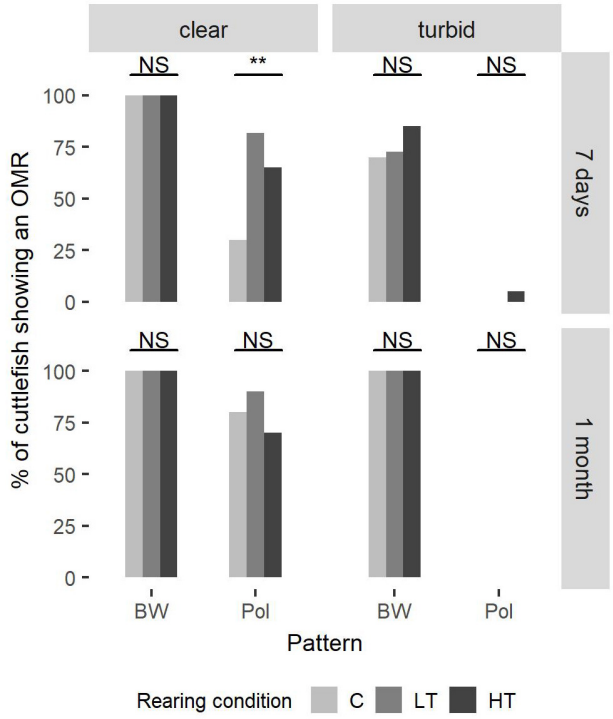

FIGURE 2 | The percentage of cuttlefish showing an optomotor response under three rearing conditions. At 7 days post hatching, 20 cuttlefish were tested in groups C and HT and 22 cuttlefish in group LT. At 1 month post hatching, 10 cuttlefish were tested in each group. Fisher–Freeman–Halton test (Fisher's exact test for count data with simulated p-value based on 10^5 replicates) was used to compare the three groups, with the addition of a post-hoc pairwise Fisher's test with Bonferroni corrections. At 7 days in clear water there is significant polarization sensitivity (PS) difference between the groups LT (80%) and C (30%) ($P = 0.0044$).

On the other hand, in turbid water the response rate for the intensity pattern was always higher than for the polarized pattern for all groups and both ages (McNemar test; C-7 days, $\chi^2 = 12.07$, df = 1, $P < 0.001$, $n_{C7} = 20$; LT-7 days, $\chi^2 = 14.06$, df = 1, $P < 0.001$, $n_{LT7} = 22$; HT-7 days, $\chi^2 = 12.5$, df = 1, $P < 0.001$, $n_{HT7} = 20$; C-1 month, $\chi^2 = 8{,}1$, df = 1, $P = 0.0044$, $n_{C30} = 10$; LT-1 month, $\chi^2 = 8{,}1$, df = 1, $P = 0.0044$, $n_{LT30} = 10$; HT-1 month, $\chi^2 = 8{,}1$, df = 1, $P = 0.0044$, $n_{HT30} = 10$) (**Figure 2**).

DISCUSSION

The aim of this study was to investigate effects on their visual capacities when rearing young cuttlefish in turbid or clear water. Whatever the water turbidity in the rearing system, no abnormal behavior (abnormal swimming, difficulty to catch prey, skin discoloration or damage) was observed in any animal.

However, the survival rate of juveniles was somewhat better in cuttlefish reared with low turbidity than that of animals kept in clear water.

When tested in clear water, PS improved with development. This is in accordance with the results of Cartron et al. (2013a). However, PS was significantly higher at 7 days in LT group (**Figure 2**). One can hypothesize that exposure to turbid water during early development can improve the development of PS in cuttlefish. Since young cuttlefish mainly prey upon mysids, which are transparent, the earlier their PS development, the higher their predation success. Domingues et al. (2004) showed that when fed transparent shrimps, rather than fish, young cuttlefish show higher growth and survival rates under laboratory conditions. As a consequence, constant use of clear water in a cuttlefish-rearing system may reduce the need of PS improvement to catch preys and may thus negatively impact PS development of juveniles, and hence their fitness. In addition, low turbidity may provide optimized conditions for reducing incoming light from the rearing system, thus reducing individual stress. Low turbidity may also facilitate concealment and mutual avoidance between individuals.

When tested in turbid water, sensitivity to light intensity (BW stripes) improved with development in all groups. However, the higher the turbidity in the rearing system the better the light-intensity sensitivity at 7 days. These results confirm for the first time the link between turbid-water rearing conditions and visual capacity improvement in young cuttlefish. However, in nearly all cases, there was no response to the polarized signal when tested in turbid waters. PS, more than light-intensity sensitivity, seems to be specifically limited by the turbidity of the water in juvenile cuttlefish. This is in contradiction with a paper by Cartron et al. (2013b,c), according to which PS improves vision in turbid water in 5-month old cuttlefish. However, in the case in question turbid water was obtained by mixing fine sand (Cartron et al., 2013a,b) whereas we used clay in the present study. In water, partially polarized light is subjected to scattering and absorption by content in suspension (Lerner, 2014). These effects on PS were size- and concentration-specific but not shape-specific [model with spherical particles hypothesis from Lerner et al. (2012) succeeded in explaining measured data in the field in Lerner et al. (2011)]. Fine sand particles and clay particles vary in size (above 50 and 20 μm, respectively). Mie particles (spherical particles with a size between 2 and 20 microns) depolarize the light (and reduce the polarization contrast) whereas geometric particles (size above 100 microns) increase partial polarization (Lerner, 2014). Therefore, different types of sediment creating turbidity may have a strong impact on the transmission of polarized signals. Indeed, Bainbridge and Waterman (1958) showed that mysid crustacean orientation with polarized stimuli improved with water turbidity, and suggested that turbidity created an additional intensity signal related to the polarization of the incoming light. They further speculated that this intensity signal may have overridden the original polarization signal and influenced the shrimps' behavior.

Our results are unexpected, suggesting that future studies could examine their relevance to the real-life situation of cuttlefish. On the other hand, turbid water may offer an attractive environment for an ambush-predator like cuttlefish. It is interesting to note that fishermen usually collect mysids (cuttlefish preys) in turbid areas (Dickel personal observations from different locations in Luc sur Mer and Galveston, TX vicinities). In the present work, the conditions of turbidity (episodic events) in the rearing tank were maybe less frequent (once a day) than those experienced by wild juveniles in the field. As a consequence, more animals may develop PS in their natural environment. Turbid water in the field comprises a mixture of different particles such as fine sand, clay, other minerals and plankton and may well allow the cuttlefish to use PS to visually discriminate between transparent prey, its surroundings (Sabbah and Shashar, 2006; Johnsen et al., 2011) and predators (Cartron et al., 2013b,c). Future studies should explore the effect of water turbidity on PS when created with two components (algae and clay for example) as well as the single effect of each component. As an example, Nieman et al. (2018) showed that visual detection thresholds of two fishes (*Notropis atherinoides* and *Sander vitreus*) were more altered by algal turbidity compared to sedimentary turbidity. This study also demonstrated that the effect of combination treatment (algal and sedimentary turbidity) not only slightly decreased the amount of light (11%) when compared to the separate component (algal turbidity reduced it by 42% and sedimentary turbidity by 35%) but also green-shifted the light as with the algae treatment. As a result it would be difficult to predict the water turbidity effect on vision based only on the water turbidity concentration. However, direct measurements of stripe contrasts in variegated turbidities (using algae, sand, clay or combined ingredients) would provide valuable information. To state the obvious, cuttlefish possess a range of senses such as hearing (Komak et al., 2005) and smell (Boal and Golden, 1999) which may be used in parallel or alternately when one of the other senses is less efficient.

Multiple studies show that the environmental enrichment of a home tank improves the visual abilities (Cartron, 2012) or cognitive and memory skills (Dickel et al., 2000) of the cuttlefish. Environmental enrichment consists of adding stones, sand, shelters, and artificial plants but there is no study on how water turbidity could have an effect on cuttlefish welfare and fitness. The present study demonstrated that rearing cuttlefish in clear water could alter PS development when compared to low turbidity conditions. In addition low turbidity may reduce incoming light from the rearing system, thus reducing individual stress. Low turbidity may also facilitate concealment and mutual avoidance. It should be noted that a study by O'Brien et al. (2016) showed no difference in either predation or camouflage behaviors between cuttlefish reared in the wild (until 2 weeks before hatching) and those reared in clear water in laboratory conditions. However, there was an exception with a uniform pattern, when laboratory-reared cuttlefish produced better camouflage on a uniform background than those from the field). But in the latter study, the wild cuttlefish spent only the first part of their embryonic development in their natural environment, which may not have been sufficient to elicit behavior plasticity. The present study suggests that creating slight turbidity, possibly as a temporary change of the visual context, may improve rearing conditions for

young cuttlefish. Further study is necessary to assess the long-term effects of rearing-system water turbidity on the sensory skills and behaviors of juvenile and adult cuttlefish. Such a study would first also help to determine the maximum turbidity level the cuttlefish can tolerate (to maximize survival). Second, it has to be checked that the turbidity of the water brings an actual increase of cuttlefish survival (assessed by daily measurement of cuttlefish size, food consumption, survival rate at each age), which would counterbalance the cost for extra maintenance (more cleaning due to the sediment in the pipes, tanks, etc.).

DATA AVAILABILITY STATEMENT

The raw data supporting the conclusions of this article will be made available by the authors, without undue reservation.

AUTHOR CONTRIBUTIONS

AG and LD: conception and design of the experiment. AG: data acquisition and data analysis. All authors have taken active part in data interpretation, discussions, and preparation of the manuscript.

FUNDING

This work was supported by grant number PRC 18763-17 by the French CNRS and Israeli MOST and by a grant to AG from la Région Normandie and MANCHE "Plateformes d'exploitation de ressources marines" cofinanced by European Union and la Région Normandie (FEDER/FSE 2014–2020).

ACKNOWLEDGMENTS

We acknowledge and thank Errol Zarfati, decd., who built the optomotor device, Jane Martin for the correction of English. The experiments performed in this study complied with the French National Legislation for animal experiments and with EU directive 2010/63 on the protection of animals used for scientific purposes.

SUPPLEMENTARY MATERIAL

The Supplementary Material for this article can be found online at: https://www.frontiersin.org/articles/10.3389/fphys.2021.622126/full#supplementary-material

REFERENCES

Bainbridge, R., and Waterman, T. H. (1958). Turbidity and the polarized light orientation of the crustacean mysidium. *J. Exp. Biol.* 35, 487–493.

Boal, J., and Golden, D. (1999). Distance chemoreception in the common cuttlefish, *Sepia officinalis* (Mollusca, Cephalopoda). *J. Exp. Mar. Biol. Ecol.* 235, 307–317. doi: 10.1016/S0022-0981(98)00187-7

Boal, J. G., Shashar, N., Grable, M., Vaughan, K., Loew, E., and Hanlon, R. T. (2004). Behavioural evidence for intraspecific signaling with achromatic and polarized light by cuttlefish (Mollusca: Cephalopoda). *Behaviour* 141, 837–861. doi: 10.1163/1568539042265662

Cartron, L. (2012). *Perception de la Polarisation de la Lumière Chez la Seiche Sepia officinalis : Développement, Fonction et Approche Comparative*, University of Caen-Normandie, Caen. [thesis].

Cartron, L., Darmaillacq, A.-S., Jozet-Alves, C., Shashar, N., and Dickel, L. (2012). Cuttlefish rely on both polarized light and landmarks for orientation. *Anim. Cogn.* 15, 591–596. doi: 10.1007/s10071-012-0487-9

Cartron, L., Dickel, L., Shashar, N., and Darmaillacq, A.-S. (2013a). Maturation of polarization and luminance contrast sensitivities in cuttlefish (*Sepia officinalis*). *J. Exp. Biol.* 216, 2039–2045. doi: 10.1242/jeb.08039

Cartron, L., Dickel, L., Shashar, N., and Darmaillacq, A.-S. (2013b). Effects of stimuli shape and polarization in evoking deimatic patterns in the European cuttlefish, *Sepia officinalis*, under varying turbidity conditions. *Invert. Neurosci.* 13, 19–26. doi: 10.1007/s10158-013-0148-y

Cartron, L., Josef, N., Lerner, A., McCusker, S. D., Darmaillacq, A.-S., Dickel, L., et al. (2013c). Polarization vision can improve object detection in turbid waters by cuttlefish. *J. Exp. Mar. Biol. Ecol.* 447, 80–85. doi: 10.1016/j.jembe.2013.02.013

Darmaillacq, A.-S., Mezrai, N., O'Brien, C. E., and Dickel, L. (2017). Visual ecology and the development of visually guided behavior in the cuttlefish. *Front. Physiol.* 8:402. doi: 10.3389/fphys.2017.00402

Darmaillacq, A.-S., and Shashar, N. (2008). Lack of polarization optomotor response in the cuttlefish *Sepia elongata* (d'Orbigny, 1845). *Physiol. Behav.* 94, 616–620. doi: 10.1016/j.physbeh.2008.01.018

Derrington, A. (2000). Vision: can colour contribute to motion? *Curr. Biol.* 10, R268–R270. doi: 10.1016/S0960-9822(00)00403-6

Dickel, L., Boal, J. G., and Budelmann, B. U. (2000). The effect of early experience on learning and memory in cuttlefish. *Dev. Psychobiol.* 36, 101–110. doi: 10.1002/(SICI)1098-2302(200003)36:2<101::AID-DEV2<3.0.CO;2-L

Dickel, L., Chichery, M. P., and Chichery, R. (1997). Postembryonic maturation of the vertical lobe complex and early development of predatory behavior in the cuttlefish (*Sepia officinalis*). *Neurobiol. Learn. Mem.* 67, 150–160. doi: 10.1006/nlme.1996.3754

Domingues, P., Sykes, A., Sommerfield, A., Almansa, E., Lorenzo, A., and Andradea, J. P. (2004). Growth and survival of cuttlefish (*Sepia officinalis*) of different ages fed crustaceans and fish. Effects of frozen and live prey. *Aquaculture* 229, 239–254. doi: 10.1016/S0044-8486(03)00351-X

Ehlman, S. M., Sandkam, B. A., Breden, F., and Sih, A. (2015). Developmental plasticity in vision and behavior may help guppies overcome increased turbidity. *J. Comp. Physiol. A. Neuroethol. Sens. Neural. Behav. Physiol.* 201, 1125–1135. doi: 10.1007/s00359-015-1041-4

Fiorito, G., Affuso, A., Anderson, D. B., Basil, J., Bonnaud, L., Botta, G., et al. (2014). Cephalopods in neuroscience: regulations, research and the 3Rs. *Invert. Neurosci.* 14, 13–36. doi: 10.1007/s10158-013-0165-x

Fuiman, L. A., and Magurran, A. E. (1994). Development of predator defences in fishes. *Rev. Fish. Biol. Fish.* 4, 145–183. doi: 10.1007/BF00044127

Gall, M., and Fernandez-Juricic, E. (2010). Visual fields, eye movements, and scanning behavior of a sit-and-wait predator, the black phoebe (*Sayornis nigricans*). *J. Comp. Physiol. A* 196, 15–22. doi: 10.1007/s00359-009-0488-6

Gegenfurtner, K. R., and Hawken, M. J. (1996). Interaction of motion and color in the visual pathways. *Trends Neurosci.* 19, 394–401. doi: 10.1016/S0166-2236(96)10036-9

Groeger, G., Cotton, P. A., and Williamson, R. (2005). Ontogenetic changes in the visual acuity of *Sepia officinalis* measured using the optomotor response. *Can. J. Zool.* 83, 274–279. doi: 10.1139/Z05-011

Hartman, E. J., and Abrahams, M. V. (2000). Sensory compensation and the detection of predators: the interaction between chemical and visual information. *Proc. R. Soc. Lond. B Biol. Sci.* 267, 571–575. doi: 10.1098/rspb.2000.1039

Herald, E. S., Brownell, R. L. Jr., Frye, F. L., Morris, E. J., Evans, W. E., and Scott, A. B. (1969). Blind river dolphin: first side-swimming cetacean. *Science* 166, 1408–1410. doi: 10.1126/science.166.3911.1408

Huffard, C. (2013). Cephalopod neurobiology: an introduction for biologists working in other model systems. *Invert. Neurosci.* 13, 11–18. doi: 10.1007/s10158-013-0147-z

Johnsen, S., Marshall, N. J., and Widder, E. A. (2011). Polarization sensitivity as a contrast enhancer in pelagic predators: lessons from in situ polarization imaging of transparent zooplankton. *Philos. T. Roy. Soc. B.* 366, 655–670. doi: 10.1098/rstb.2010.0193

Komak, S., Boal, J., Dickel, L., and Budelmann, B. (2005). Behavioral responses of juvenile cuttlefish (*Sepia officinalis*) to local water movements. *Mar. Freshw. Behav. Physiol.* 38, 117–125. doi: 10.1080/10236240500139206

Lerner, A. (2014). "Underwater polarization by scattering hydrosols," in *Polarized Light and Polarization Vision in Animal Sciences*, Vol. 2, ed. G. Horváth (Berlin: Springer), doi: 10.1007/978-3-642-54718-8_15

Lerner, A., Sabbah, S., Erlick, C., and Shashar, N. (2011). Navigation by light polarization in clear and turbid waters. *Phil. Trans. R. Soc. B* 366, 671–679. doi: 10.1098/rstb.2010.0189

Lerner, A., Shashar, N., and Haspel, C. (2012). Sensitivity study on the effects of hydrosol size and composition on linear polarization in absorbing and nonabsorbing clear and semi-turbid waters. *J. Opt. Soc. Am. A* 29, 2394–2405. doi: 10.1364/JOSAA.29.002394

Luczkovich, J. J. (1988). The role of prey detection in the selection of prey by pinfish *Lagodon rhomboides* (Linnaeus). *J. Exp. Mar. Biol. Ecol.* 123, 15–30.

Marini, G., De Sio, F., Ponte, G., and Fiorito, G. (2017). "Behavioral analysis of learning and memory in cephalopods," in *Learning and Memory: A Comprehensive Reference*, 2nd Edn, Vol. 1, ed. J. H. Byrne (Oxford: Academic Press), 441–462. doi: 10.1016/B978-0-12-809324-5.21024-9

Marshall, N. J., and Messenger, J. B. (1996). Colour-blind camouflage. *Nature* 382, 408–409. doi: 10.1038/382408b0

Mather, J. A., and Dickel, L. (2017). Cephalopod complex cognition. *Curr. Opin. Behav. Sci.* 16, 131–137. doi: 10.1016/j.cobeha.2017.06.008

Mäthger, L. M., Barbosa, A., Miner, S., and Hanlon, R. T. (2006). Color blindness and contrast perception in cuttlefish (*Sepia officinalis*) determined by a visual sensorimotor assay. *Vis. Res.* 46, 1746–1753. doi: 10.1016/j.visres.2005.09.035

McCann, G. D., and MacGinitie, G. F. (1965). Optomotor response studies of insect vision. *Proc. R. Soc. B Biol. Sci.* 163, 369–401. doi: 10.1098/rspb.1965.0074

Nieman, C. L., Oppliger, A. L., McElwain, C. C., and Gray, S. M. (2018). Visual detection thresholds in two trophically distinct fishes are compromised in algal compared to sedimentary turbidity. *Conserv. Physiol.* 6:coy044. doi: 10.1093/conphys/coy044

O'Brien, C. E., Bowie, M., Billard, P., Darmaillacq, A.-S., Jozet-Alves, C., David Benhaïm, D., et al. (2016). The effect of an artificial incubation environment on hatchling size and behavior in the cuttlefish, *Sepia officinalis*. *Vie Milieu Life Environ.* 66, 1–9.

Pilleri, G. (1979). The blind Indus dolphin. *Platanista indi. Endeavour.* 3, 48–56. doi: 10.1016/0160-9327(79)90066-8

Rinner, O., Rick, J. M., and Neuhauss, S. C. F. (2005). Contrast sensitivity, spatial and temporal tuning of the larval zebrafish optokinetic response. *Investig. Ophthalmol. Vis. Sci.* 46, 137–142. doi: 10.1167/iovs.04-0682

Sabbah, S., Lerner, A., Erlick, C., and Shashar, N. (2005). Under water polarization vision-a physical examination. *Recent Res. Dev. Exp. Theor. Biol.* 1, 123–176.

Sabbah, S., and Shashar, N. (2006). Polarization contrast of zooplankton: a model for polarization based sighting distance. *Vis. Res.* 46, 444–456. doi: 10.1016/j.visres.2005.05.017

Shashar, N., Hagan, R., Boal, J. G., and Hanlon, R. T. (2000). Cuttlefish use polarization sensitivity in predation on silvery fish. *Vis. Res.* 40, 71–75. doi: 10.1016/S0042-6989(99)00158-3

Shashar, N., Hanlon, R. T., and Petz, A. (1998). Polarization vision helps detect transparent prey. *Nature* 393, 222–223. doi: 10.1038/30380

Shashar, N., Johnsen, S., Lerner, A., Sabbah, S., Chiao, C. C., Mathger, L. M., et al. (2011). Underwater linear polarization- physical limitations to biological functions. *Phil. Trans. R. Soc. B* 366, 649–654. doi: 10.1098/rstb.2010.0190

Shashar, N., Rutledge, P. S., and Cronin, T. W. (1996). Polarization vision in cuttlefish, a concealed communication channel? *J. Exp. Biol.* 199, 2077–2084.

Suriyampola, P. S., Cacéres, J., and Martins, E. P. (2018). Effects of short-term turbidity on sensory preference and behaviour of adult fish. *Anim. Behav.* 146, 105–111. doi: 10.1016/j.anbehav.2018.10.014

Temple, S., Pignatelli, V., Cook, T., How, M., Chiou, T. H., Roberts, N., et al. (2012). High resolution polarisation vision in a cuttlefish. *Curr. Biol.* 22, R121–R122. doi: 10.1016/j.cub.2012.01.010

Villanueva, R., Perricone, V., and Fiorito, G. (2017). Cephalopods as predators: a short journey among behavioral flexibilities, adaptions, and feeding habits. *Front. Physiol.* 8:598. doi: 10.3389/fphys.2017.00598

Conflict of Interest: The authors declare that the research was conducted in the absence of any commercial or financial relationships that could be construed as a potential conflict of interest.

frontiers in Physiology

BRIEF RESEARCH REPORT
published: 18 June 2021
doi: 10.3389/fphys.2021.675252

Quantifying the Speed of Chromatophore Activity at the Single-Organ Level in Response to a Visual Startle Stimulus in Living, Intact Squid

Stavros P. Hadjisolomou[1], Rita W. El-Haddad[1], Kamil Kloskowski[2], Alla Chavarga[2] and Israel Abramov[2]*

[1] *Department of Social and Behavioral Sciences, College of Arts and Sciences, American University of Kuwait, Salmiya, Kuwait,* [2] *Department of Psychology, Brooklyn College, City University of New York, Brooklyn, NY, United States*

OPEN ACCESS

Edited by:
Daniel Osorio, University of Sussex, United Kingdom

Reviewed by:
Pamela Imperadore, Zoological Station Anton Dohrn, Italy
Cecile Bellanger, Université de Caen Normandie, France

***Correspondence:**
Stavros P. Hadjisolomou
shadjisolomou@gmail.com

Specialty section:
This article was submitted to Invertebrate Physiology, a section of the journal Frontiers in Physiology

Received: *02 March 2021*
Accepted: *27 May 2021*
Published: *18 June 2021*

Citation:
Hadjisolomou SP, El-Haddad RW, Kloskowski K, Chavarga A and Abramov I (2021) Quantifying the Speed of Chromatophore Activity at the Single-Organ Level in Response to a Visual Startle Stimulus in Living, Intact Squid. Front. Physiol. 12:675252. doi: 10.3389/fphys.2021.675252

The speed of adaptive body patterning in coleoid cephalopods is unmatched in the natural world. While the literature frequently reports their remarkable ability to change coloration significantly faster than other species, there is limited research on the temporal dynamics of rapid chromatophore coordination underlying body patterning in living, intact animals. In this exploratory pilot study, we aimed to measure chromatophore activity in response to a light flash stimulus in seven squid, *Doryteuthis pealeii*. We video-recorded the head/arms, mantle, and fin when squid were presented with a light flash startle stimulus. Individual chromatophores were detected and tracked over time using image analysis. We assessed baseline and response chromatophore surface area parameters before and after flash stimulation, respectively. Using change-point analysis, we identified 4,065 chromatophores from 185 trials with significant surface area changes elicited by the flash stimulus. We defined the temporal dynamics of chromatophore activity to flash stimulation as the latency, duration, and magnitude of surface area changes (expansion or retraction) following the flash presentation. Post stimulation, the response's mean latency was at 50 ms (± 16.67 ms), for expansion and retraction, across all body regions. The response duration ranged from 217 ms (fin, retraction) to 384 ms (heads/arms, expansion). While chromatophore expansions had a mean surface area increase of 155.06%, the retractions only caused a mean reduction of 40.46%. Collectively, the methods and results described contribute to our understanding of how cephalopods can employ thousands of chromatophore organs in milliseconds to achieve rapid, dynamic body patterning.

Keywords: cephalopod, chromatophore, camouflage, communication, body pattern, startle response, light flash stimulation, temporal dynamics

INTRODUCTION

Unlike the slower chromatophore control of flatfish (2–8 s; Ramachandran et al., 1996), coleoid cephalopods can change body patterns in milliseconds. For decades, scientists in the field of cephalopod vision have focused on the goal of creating a complete characterization of the sophisticated coleoid body patterning abilities. As a result, existing reports are sufficient to describe and explain several known body patterns in cephalopods for camouflage and communication (Hanlon and Messenger, 1988; Hanlon, 2007; Langridge et al., 2007; Zylinski et al., 2009; How et al., 2017). Nevertheless, a theoretical framework on cephalopod body patterning, which does not include the dimension of time, will be inherently inadequate in modeling, holistically, the range of dynamic, rapid transformations observed in animals living in the wild. One approach toward studying this topic is by stimulating the visual system of a living, intact animal, using a light flash to elicit muscular activation of chromatophores, and quantifying the response dynamics by tracking surface area changes in time.

Experiments conducted in the Gilly laboratory revealed how light flashes elicit startle jet-escape responses in squid, *Doryteuthis opalescens* (Berry, 1911). The brief, intense light stimulus activates the central nervous system (CNS) at the magnocellular and palliovisceral lobes, which relay information to the stellate ganglia to modulate forceful muscle contractions of the mantle expelling water through the funnel in the process (Otis and Gilly, 1990; Gilly et al., 1991; Gilly and Lucero, 1992; Neumeister et al., 2000; Preuss and Gilly, 2000). Within the stellar nerve, a group of non-giant motor axons innervates chromatophore muscles (Ferguson et al., 1988). In one of these studies (Neumeister et al., 2000), which investigated the effects of temperature on escape responses in restrained squid, the flash stimulus produced transient chromatophore expansions. Responding to the light flash startle stimulus, animals exhibited a robust jet-escape startle response with transient chromatophore expansions. However, when light intensity was decreased by "positioning the flash unit further from the squid" (Neumeister et al., 2000, p. 551), the animal showed chromatophore expansions as *sub-jet-threshold* startle responses (in the absence of jetting). Squid are a useful species for studying chromatophores because they have fewer and larger chromatophore organs (density: 8 mm^{-2}, maximum diameter: 120–1,520 μm; Hanlon, 1982) compared to octopus (density: 230 mm^{-2}; maximum diameter: 300 μm; Packard and Sanders, 1971) and Sepia (density: 35–50 mm^{-2}; maximum diameter: 300 μm; Hanlon and Messenger, 1988), offering a simpler model to study chromatophore control.

The Neumeister et al. (2000) study validates a reliable method of using flash stimulation and video-recording the skin, from a close-up perspective, to investigate the synchronicity of chromatophore activity at the single-organ level in squid. Since studying chromatophore response dynamics across all body regions was not the study's primary focus, chromatophore expansions only on the mantle were reported. For this exploratory pilot study, we aim at replicating the sub-jet-threshold behavioral responses to flash stimulation with a different species, *Doryteuthis pealeii* (Lesueur, 1821), to examine the mechanisms and temporal dynamics of the sensorimotor system underlying chromatophore control in intact animals (Hadjisolomou, 2017). Due to ethical and logistical issues involved with long-distance transportation of *D. opalescens* for experimentation, *D. pealeii* was chosen as this species is available to be studied in Woods Hole, Massachusetts.

Further, in addition to the mantle, we expanded observations to include chromatophore activity from the understudied regions of the arms, head, and dorsal fin (**Figure 1**). Young (1976) reported on the CNS control of chromatophores in *D. pealeii,* elaborating that separate chromatophore lobes in the brain control different body regions. Specifically, the posterior chromatophore lobes (PCL) mainly control chromatophores on the mantle and fin regions, while chromatophores on the arms and head are primarily controlled by the anterior chromatophore lobes (ACL) and pedal lobes (PL). Axons from the PCL connect without a synapse to chromatophore organs through the pallial nerve. Electrode stimulation of PCL neurons in *Lolliguncula brevis* (Blainville, 1823) causes chromatophore expansion on the mantle and fin (Dubas et al., 1986), but it did not result in retraction of any expanded chromatophores. Both species are part of the same family, Loliginidae (Lesueur, 1821), and have anatomical similarities (Díaz-Santana-Iturrios et al., 2019), thus allowing for approximations between them. We chose these body regions to observe any discrepancies in timed responses due to circuitry differences. By video-recording all body regions in intact, living squid, we quantified the temporal dynamics from light flash stimulation to expansions and retractions at the single-organ level across thousands of chromatophores. Similar to the Reiter et al. (2018) study, which used unrestrained European cuttlefish (Linnaeus, 1758), we measured chromatophore activity from

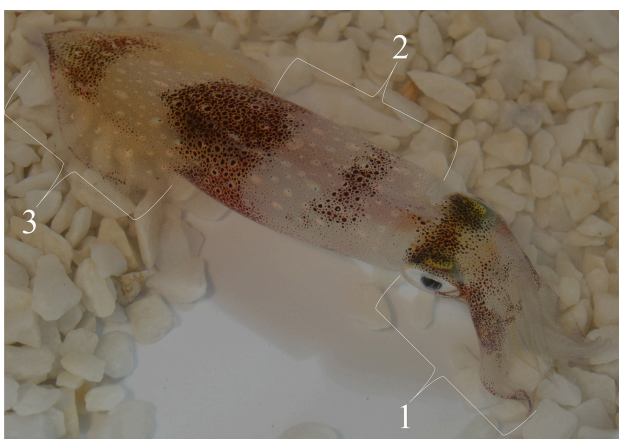

FIGURE 1 | *D. pealeii* (mantle length approximately 14 cm) expressing disruptive body patterning with some chromatophores expanded (dark bands), while others are retracted. Numbers indicate the different body regions measured in the study: 1 = head/arms, 2 = mantle, and 3 = fin.

unrestrained squid. The procedures and methodologies described below enable non-invasive data collection of chromatophore activity from living animals to study behavioral responses in intact organisms.

METHODS

Animals

Adult *D. pealeii* were collected from coastal waters near Woods Hole, Massachusetts, US, in 2014. From large population holding tanks, eight healthy animals (mantle length: 12–15 cm; unknown sex and age) without any visible physical injuries were selected for inclusion. We transported individual squid and housed them together in a 2 m × 1.5 m × 1 m rectangular, light-brown opaque, fiberglass housing chamber connected to an open, temperature-controlled (17–19°C) seawater system. Gravel and sand on the bottom of the housing tank provided a natural substrate for animals to settle. Animals were fed twice a day on an *ad libitum* diet of live *Fundulus* fish and crabs[1].

Experimental Design

Here, *n* refers to the number of different body regions examined (head/arms, mantle, and fin). Each body region, therefore, was considered to be an experimental unit. The study was a within-subjects design consisting of one group of three experimental units, and there were eight animals. One animal was excluded due to a lack of significant chromatophore responses from data analysis (see "Results" section).

Procedure

Experimental Set-Up

To collect measurements, we constructed a rectangular rig covered with a layer of black cloth and an additional layer of an opaque, black tarp to prevent light from entering.

Experimental Tank and Acclimation

The rectangular experimental tank, measuring 53 cm × 43 cm × 18 cm, consisted of white, opaque plastic walls containing 10 L of seawater (**Figure 2**). For each trial, one squid was placed within the experimental tank inside the rig. To establish habituation to the experimental apparatus, each squid was placed in the experimental tank for 10 min then returned to the group home tank, 24 h before experimental trials began. We created a white "V-shaped" partition configuration to enable the squid to settle naturally at the bottom of the tank, thus preventing chromatophore displacement outside of the camera frame. We placed an overhead light source at a 45° angle to illuminate the animal for video recording. The ambient light and visual environment determined the chromatophore's state (expanded or retracted) before light flash stimulation. The animals adopted a lighter skin tone to camouflage in the white, uniformly lit tank during trials. Thus, to allow for a lighter skin tone, most chromatophores were retracted before flash stimulation.

[1]See **Supplementary Material** for the Ethical Note and Experimental Controls sections.

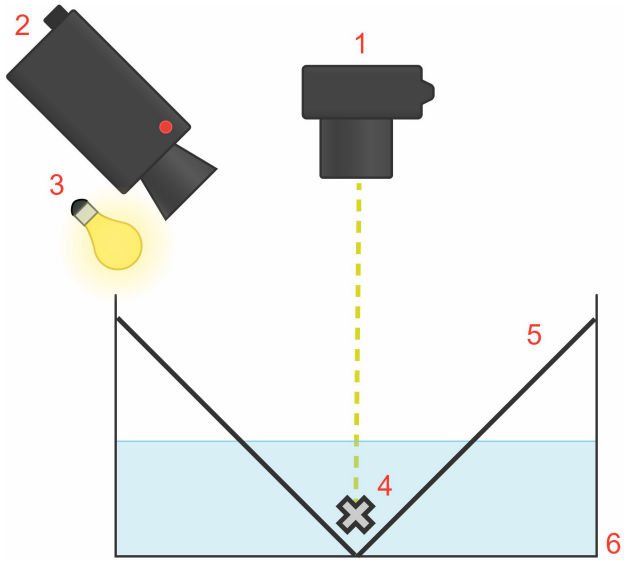

FIGURE 2 | Diagram of the experimental tank set-up, measuring 53 cm × 43 cm × 18 cm (situated inside the rig; external rig structure and black tarp and opaque covers not shown). The flash unit (1) providing the visual startle stimulus was fixed on the rig at a right angle and 50 cm above the animal (4). The camera (2) and light source (3) were at a 45° angle above the animal. The white "V-shaped" partition configuration (5) enabled squid to settle naturally at the bottom of the white, rectangular tank (6).

Startle Stimulus and Sub-Jet-Threshold Startle Response

Animals were presented with light flashes to elicit the startle reflex response. To deliver the startle stimulus in a top-down direction, a Canon SpeedLite 580EX-RT flash unit was fixed on the rig at a right angle and 50 cm above the animal. Similar to the Neumeister et al. (2000) study, we found that *D. pealeii* have jet-escape startle responses and transient chromatophore expansions to intense light flashes. For this study, the duration of each light flash stimulus was ∼100 μs, with an illuminance of 12,500 lx, providing an even exposure of the stimulus on the animal from this distance. The entire animal was illuminated, but we video-recorded only one specific body region per trial for analysis. The stimulus was sufficient in producing muscular contraction but well below the jet-escape sensory threshold to minimize jetting. Thus, this study's behavioral responses comprised of chromatophore expansions and retractions to light flashes in the absence of jetting.

Experimental Trial Procedure

Once in the experimental rig, animals were allowed to procedurally acclimate and settle on the bottom of the tank, as evidenced by the animal remaining motionless for at least 5 min. Once an animal habituated, it received a sequence of approximately 90 flashes. For this study, we used a 10-s inter-stimulus interval (ISI), which does not cause attenuation due to learning, fatigue, or a combination of both (Otis and Gilly, 1990). With an ISI of 10 s, the total sequence duration lasted for 15 min

per body region and each region was tested during different sessions. The duration and ISI were tested in preliminary trials and found to be appropriate for the purposes of this study. The rationale was to reduce testing sessions and have only one per body region since 15 min were sufficient.

Each flash stimulation was considered an individual trial. The purpose was to elicit the sub-jet-threshold startle response. Each animal received 90 trials for each of the three body regions, for a total of 270 trials for each of the eight animals, thus 2,160 trials in total. One body region per animal was tested at a time (we counterbalanced the order of the body regions tested per animal).

For details on video-recording, scoring, image analysis, and statistical analysis see **Supplementary Material**.

RESULTS

Chromatophore Surface Area Changes Following Light Flash Presentation

Out of the 2,160 total trials, 230 were suitable to be analyzed by Change Point Analysis (CPA) (Taylor, 2000). Based on CPA, 185 were identified to have significant chromatophore surface area changes. A total of 4,065 individual chromatophores responded to the startle stimulus with either transient expansion or retraction of the pigment. These chromatophores were further analyzed to characterize response activity pre- and post-stimulation. The remaining 45 trials showed no significant responses by CPA and were excluded, including all Squid #8 trials and all expansion trials in Squid #3.

Additionally, the numbers of trials with chromatophore responses were not equivalent across squid (Squid #2, for example, did not show any retraction responses in any trials). Furthermore, not all squid had all body regions significantly responding to the flash stimulus, and in other cases, there were trials with both significant expansion and retraction instances on the same body region. Thus, there is an unequal distribution of chromatophore numbers and body regions represented in the data (see **Supplementary Figures 2–5**).

The discrepancies in this dataset are the observed behavioral differences between animals; a few animals would swim back and forth often enough to invalidate significant parts of the footage. Additionally, trials were excluded in the process of image analysis if the software was unable to detect chromatophores (Hadjisolomou and El-Haddad, 2017). In such cases, image noise due to fluctuations of color and luminance created artifacts that interfered with chromatophore detection and tracking. However, each significant expansion or retraction followed the same pattern regardless of which body region or squid showed the response.

Chromatophore Expansion

Out of the 185 trials with significant chromatophore surface area changes (from seven animals), 166 (thus, 90% of these trials) showed expansion following the flash stimulus (six animals). Out of these, the head/arms region had 85 trials (Squids #1, 5, and 7), followed by the mantle with 50 (Squids #1 and 4–7), and then the fin with 31 (Squids #2 and 5–6).

Within these 166 trials, 4,000 (98% out of the total 4,065) chromatophores showed significant expansion. On the head/arms, there were 1,598 chromatophores; from the mantle, there were 1,743; and on the fin, there were 659.

Chromatophore Retraction

The remaining 19 trials showed significant chromatophore retractions following the flash stimulus (six animals). The head/arms had nine trials (Squids #1, 3, and 7), the mantle eight (Squids #1 and 4–6), and the fin had two (Squid #1).

Within these 19 trials, we tracked and measured 65 chromatophores showcasing significant retraction. On the head/arms, there were 39 chromatophores; from the mantle 21; and on the fin, there were five.

Descriptive Statistics of Transient Responses

Temporal Dynamics

We calculated descriptive statistics on the temporal dynamics of chromatophore surface area changes following the startle stimulus (see **Table 1** and **Figure 3**). We estimated each value with an estimated margin of error of $\pm$ 16.67 ms, determined by the inter-frame interval when recording at 60 frames per second frequency.

Magnitude of Response

We calculated the magnitude of chromatophore expansion or retraction activity by comparing peak response values of response

TABLE 1 | Descriptive statistics of temporal dynamics in milliseconds (ms).

	Response time (tR)		Delay time (tD)		Rise time (tRt)		Response duration (rD)	
	Expansion (ms)	Retraction (ms)	Expansion (ms)	Retraction (ms)	Expansion (ms)	Retraction (ms)	Expansion (ms)	Retraction (ms)
Head/Arms	50	50	83	83	117	117	300	267
Mantle	67	67	117	100	150	150	384	250
Fin	67	67	100	117	134	134	334	217

Response time (tR) is the time to reach or pass the 5% value of the maximal response;
delay time (tD) is the time to reach or pass the 50% value of the response; rise time (tRt) is the time required to reach the 100% value of the response; response duration (rD) is the time between the 5% values of response before and after the peak.

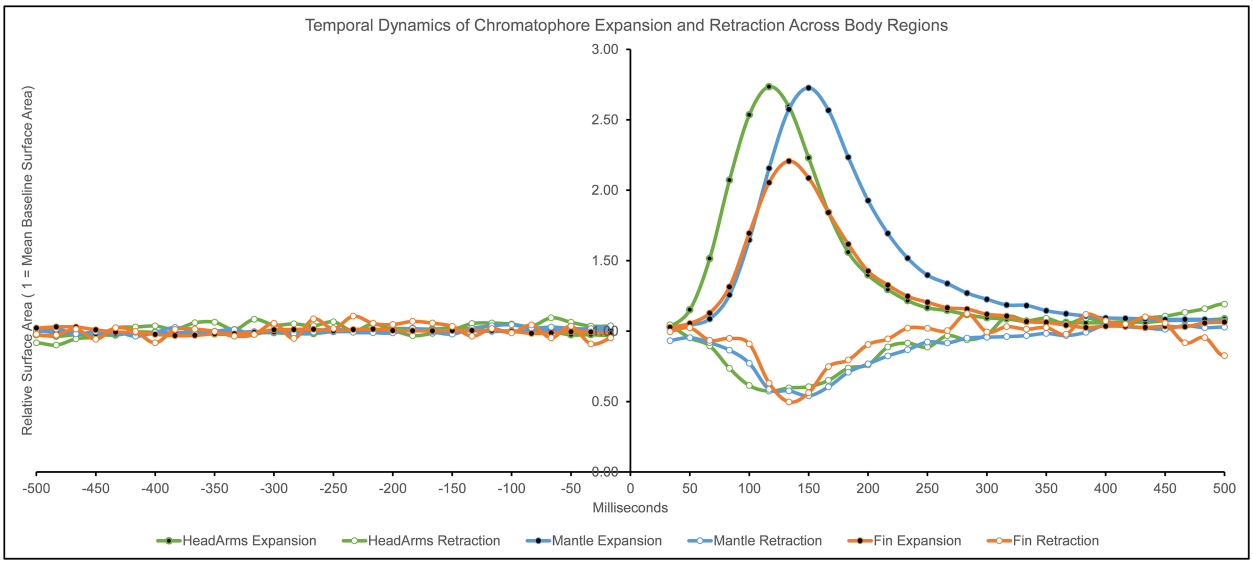

FIGURE 3 | Temporal dynamics (in milliseconds) of chromatophore expansion and retraction across body regions. Surface area values are relative to the average pre-flash chromatophore surface area (1 = average of pre-flash chromatophore surface area; values above 1 = expansion, values below 1 = retraction). Negative values of milliseconds indicate time before the light flash presentation, 0 indicates flash presentation, positive values indicate time after the light flash presentation (The two frames containing the flash stimulus, *t* = 0 ms and t = 17 ms, were removed from analysis due to the animal not being observable).

chromatophore surface area (RCSA) with the pre-flash baseline chromatophore surface area (BCSA) (**Figure 3**).

Expansion

On average, the relative chromatophore surface area increased by 155.06% across all body regions (4,000 chromatophores). Specifically:

Head/arms: 159%
Mantle: 168%
Fin: 116%

Retraction

On average, the relative chromatophore surface area decreased by 40.46% across all body regions (65 chromatophores). Specifically:

Head/arms: 43%
Mantle: 46%
Fin: 50%

DISCUSSION

In this exploratory pilot study, we systematically elicited behavioral responses using a light flash stimulus in intact, living squid and analyzed the temporal dynamics and magnitude of thousands of chromatophore surface area changes at the single-organ level. Here, we report a replication of the following Neumeister et al. (2000) findings using a different squid species. *D. pealeii* with uniform light skin patterns before stimulation responded to flashes with jetting and chromatophore expansion and lower flash intensities triggered transient darkening in the absence of jetting. Our results demonstrate that it is feasible to use intact, living animals, to measure, non-invasively, the temporal dynamics of chromatophore control during body patterning.

We also report the following novel observations: this is the first record of chromatophore activation to light flash stimulation on regions other than the dorsal mantle; our videos show chromatophore activation on the head, arms, and fin, in addition to the mantle. Also, for the first time, we show chromatophore retraction to light flash stimulation: chromatophores that were expanded before stimulation (such as dark bands on the mantle or expanded chromatophores on the head) responded with a transient retraction. Further, we observed synchronous chromatophore expansion and retraction on different parts of the mantle in the same trial (for example, chromatophores on dark bands on the mantle contracted, while chromatophores on light skin expanded).

The general temporal dynamic patterns emerging from this data are the following: the speed of expansion and retraction activation was the same across body regions. Differences in response durations were not dependent on the magnitude of response. Finally, the head/arms were faster in most measurements compared to other body regions. The short latencies reported here are suggestive of a reflexive component of the response.

Light Flash Stimulation Elicits Sub-Jet-Threshold Responses in *D. pealeii*

Chromatophore Expansion

Packard and others have described how flashes of light can elicit responses in chromatophores from dissected octopus skin (Packard and Brancato, 1993; Ramirez and Oakley, 2015). More relevant to this study, Neumeister et al. (2000) reported how light flashes elicit sub-jet-threshold chromatophore expansion in the

squid *D. opalescens*. In agreement with the Neumeister study findings, we demonstrate that the presentation of light flashes elicits chromatophore expansion in a different squid species, *D. pealeii*. Also, we validate a method to measure chromatophore activity from unrestrained squid.

Chromatophore Retraction

This is the first study to report chromatophore retraction in response to presentation of a light flash stimulus. Comparing the two different types of chromatophore activity, expansions and retractions, enables a more thorough characterization of the sensorimotor system since the mechanisms underlying each type of action are not well understood. However, out of 4,065 chromatophores analyzed, only 65 showed retraction. As stated in the "Experimental Tank and Acclimation" section, only a small number of chromatophores were expanded in the original experimental set-up. Therefore, chromatophores responded in the only possible outcome given their original state: retracted chromatophores expanded and expanded chromatophores retracted. These findings demonstrate the method's validity in studying the retraction mechanism, an essential part of the chromatophore system in rapid body patterning.

Characterization of Temporal Dynamics of Sub-Jet-Threshold Responses

Response Time (tR)

Our findings indicate similarities when comparing expansion with retraction and between the different body regions. The average response time to reach or pass the 5% value of the maximal response was 50 ms (± 16.67 ms). This was identical across all body regions and between expansions and retractions. These results echo the timing of the startle response mentioned in previous studies (Neumeister et al., 2000; Mooney et al., 2016). Based on these findings, the speed of the onset of rapid body patterning in squid is characterized by a latency of 50 ms.

Delay Time (tD)

When measuring the average time to reach or pass the 50% value of the response, the head/arms is faster in reaching this mark than the other two body regions in both expansions and retractions. We believe this difference can be explained by the fact that chromatophores on this body region are controlled by separate lobes (ACL and PL; Young, 1976), and thus the temporal discrepancies may be due to the circuitry. The differences between fin and mantle timings average out when we aggregate data for both expansion and retraction.

Rise Time (tRt)

The rise time to reach the 100% value of the response peak is the same within body regions in expansion and retraction, though there are differences between regions. Thus, each body region has specific temporal benchmarks of maximum response regardless of the chromatophore change type. The chromatophores on the head/arms are the fastest between body regions, followed by the fin in second place, and lastly, the mantle. Considering the slight differences in the magnitude of response between the body regions, it is surprising that the chromatophores on the head/arms are about 33 ms faster than those on the mantle. The time difference may not be explained due to response magnitude since these two body regions are almost identical in that dimension. The circuitry's differences (Young, 1976) may explain these temporal discrepancies on the head/arms (ACL and PL) compared to those of the mantle (PCL).

Response Duration (rD)

Most discrepancies were found in the response duration, the time between the 5% values of response before and after the peak, between and within body regions when comparing expansion and retraction. We calculated the duration by finding the time difference between the initial response and the return to the pre-flash state following the peak response. Across the type of responses and body regions, chromatophore change duration is short, between 217 and 384 ms. Compared to color changes seen in other species (Ramachandran et al., 1996), the sub-second cephalopod chromatophore change is unparalleled.

When it comes to expansion, the chromatophores on the head/arms are the fastest to complete the response and reach pre-flash surface area values at 300 ms, followed by the fin (+34 ms) and the mantle (+84 ms). A different pattern was observed with retraction responses: chromatophores on the fin had the shortest duration of response at 217 ms, followed by those on the mantle (+33 ms), and lastly by those on head/arms (+50 ms).

It is worth noting that the response duration was the only dimension in which retraction had a shorter overall interval than expansion. For example, the most prolonged response duration during retraction (267 ms) was still faster than the briefest response duration in expansion (300 ms). One reason to explain this phenomenon is that chromatophore expansion and retraction may depend on separate mechanisms; during expansion, the surrounding radial muscles pull and expand the pigment (Bell et al., 2013). The retraction mechanism, however, is still not fully understood.

Characterization of the Magnitude of Sub-Jet-Threshold Responses

Results indicate differences between the scale of chromatophore surface area changes when a chromatophore expands or retracts. While the surface area increased 155.06% on average during an expansion, the retraction only caused a 40.46% decrease. As discussed in the "Response Duration" section, one reason for this may be the different mechanisms involved in expansion compared to retraction.

Other discrepancies were found when analyzing chromatophores across the body regions. The mantle and head/arms showed the largest surface area expansions with 168% and 159% corresponding changes, respectively. The fin had a 116% increase on average. It is unclear why there is a close to 50% difference between the fin and the other regions. This may be due to differences in the type and distribution of chromatophores on the fin compared to the head/arms and mantle when it comes to body patterning. It is necessary to investigate further if fin chromatophores do not expand as much as those on the mantle and head/arms and why that would be the case.

LIMITATIONS AND FUTURE DIRECTIONS

Unequal Distribution of Trials Between Body Regions and Animals

The number of trials with significant chromatophore responses was not equal per body region within each animal nor between animals, and thus there was an unequal distribution of body regions and chromatophores represented in the dataset. This unequal distribution precludes the possibility to run statistical analyses in determining significant differences in the temporal dynamics and magnitude of responses. Also, due to ethical considerations, we determined that a larger number of animals to be used was not well-warranted. For future studies, we advise scheduling shorter trials over several days so more data can be collected from fewer animals.

Unequal Number of Significant Surface Area Changes Between Expansion and Retraction

Out of the 4,065 chromatophores showing significant responses, only 65 showed retractions. The small sample size makes it difficult to generalize the retraction results. To promote the animal adopting a darker skin tone, we ran additional pilot trials using black tanks and white gravel to generate visual contrast between the substrate and walls. The contrast increased the probability of squid expressing a disruptive or uniformly dark pattern. When squid experienced light flashes while having dark patches of skin, we observed more retractions. However, attempting to replicate these trials using black tanks *within* the rig was impossible due to the video frames' noise resulting from less visibility. Future studies on chromatophore retraction may utilize visual contrast in the environment and appropriate equipment to remove videography noise.

Potential Extraocular Chromatophore Responses

The overall results of our study showed that the response time (tR) was in line with timings from Otis and Gilly (1990). They argue that "[t]he 50-ms delay for giant axon excitation in the startle-escape is similar to that for mantle contraction, indicating that the major source of behavioral delay lies in the central nervous system and not in conduction time along the giant axon (<10 ms) or muscle activation" (p. 2912). Thus, we may conclude that squid chromatophore responses are dependent on the CNS. To test the possibility that squid skin responds directly to light flashes, we used flash stimulation with a recently deceased squid from the main population holding tank. The squid showed spontaneous chromatophore activity before stimulation, and the aim was to observe if there were any extraocular chromatophore responses to the flash stimulus. We found no discernible changes due to stimulation. However, since we only used one deceased squid to test this, we cannot exclude the possibility that extraocular responses may have contributed to chromatophore activity changes in this study.

CONCLUSION

In the natural world, cephalopods are renowned for the dynamic range and speed of adaptive body patterning used in camouflage and communication. In this exploratory study, we used a light flash stimulus to elicit transient chromatophore surface area changes to quantify the chromatophore system's temporal dynamics in living, intact animals. Our measurements here verify the early onset of the sub-second chromatophore changes in body patterning with an unparalleled speed. Based on our findings, we argue that measuring the temporal dynamics of complete behavioral responses during body patterning in intact, living animals is a feasible and essential addition to studies using excised isolated skin of subjects. The unexpected differences between body regions and expansion and retraction responses exemplify the need to continue this research line. Such details of timing the temporal dynamics are essential for comprehensive and quantitative descriptions of body patterning. The methodology and findings described in this study collectively contribute to our understanding of how cephalopods can employ thousands of chromatophore organs within milliseconds for rapid, adaptive body patterning.

DATA AVAILABILITY STATEMENT

The raw data supporting the conclusions of this article will be made available by the authors, without undue reservation.

ETHICS STATEMENT

Ethical review and approval was not required for the animal study because Ethical approval was not required since, at the time this study took place (July, 2014), the Institutional Animal Care and Use Committee (IACUC) protocols were not issued for invertebrate research in the United States and in the Institution where the experiments with live animals were carried out. Nevertheless, procedures were performed to minimize pain and distress of the animals involved.

AUTHOR CONTRIBUTIONS

SH, KK, AC, and IA contributed to the conception and design of the study. SH ran the video trials, collected data, organized the database, and wrote the manuscript's first draft. SH and RE-H performed the statistical analysis. RE-H wrote sections of the manuscript. All authors contributed to manuscript revision, read, and approved the submitted version.

FUNDING

This study was funded by the City University of New York Doctoral Student Research Grant. The funder had no role in study design, data collection and analysis, decision to publish, or manuscript preparation.

ACKNOWLEDGMENTS

SH would like to thank the staff at the Marine Resources Center for providing valuable support in undertaking this study.

SUPPLEMENTARY MATERIAL

The Supplementary Material for this article can be found online at: https://www.frontiersin.org/articles/10.3389/fphys.2021.675252/full#supplementary-material

REFERENCES

Bell, G. R., Kuzirian, A. M., Senft, S. L., Mäthger, L. M., Wardill, T. J., and Hanlon, R. T. (2013). Chromatophore radial muscle fibers anchor in flexible squid skin. *Invertebrate Biol.* 132, 120–132. doi: 10.1111/ivb.12016

Díaz-Santana-Iturrios, M., Salinas-Zavala, C. A., Granados-Amores, J., de la Cruz-Agüero, J., and García-Rodríguez, F. J. (2019). Taxonomic considerations of squids of the family Loliginidae (Cephalopoda: Myopsida) supported by morphological, morphometric, and molecular data. *Mar. Biodivers.* 49, 2401–2409. doi: 10.1007/s12526-019-00979-3

Dubas, F., Hanlon, R. T., Ferguson, G. P., and Pinsker, H. M. (1986). Localization and stimulation of chromatophore motoneurones in the brain of the squid, *Lolliguncula brevis*. *J. Exp. Biol.* 121, 1–25. doi: 10.1242/jeb.121.1.1

Ferguson, G. P., Martini, F. M., and Pinsker, H. M. (1988). Chromatophore motor fields in the squid, *Lolliguncula brevis*. *J. Exp. Biol.* 134, 281–295. doi: 10.1242/jeb.134.1.281

Gilly, W., Hopkins, B., and Mackie, G. O. (1991). Development of giant motor axons and neural control of escape responses in squid embryos and hatchlings. *Biol. Bull.* 180, 209–220. doi: 10.2307/1542390

Gilly, W. F., and Lucero, M. T. (1992). Behavioral responses to chemical stimulation of the olfactory organ in the squid *Loligo opalescens*. *J. Exp. Biol.* 162, 209–229. doi: 10.1242/jeb.162.1.209

Hadjisolomou, S. P. (2017). *Behavioral Responses to Pulses of Light in the Longfin Inshore Squid, Doryteuthis pealeii* (Lesueur, 1821). Ph.D. Dissertation. New York, NY: The Graduate Center, City University of New York.

Hadjisolomou, S. P., and El-Haddad, G. (2017). SpotMetrics: an open-source image-analysis software plugin for automatic chromatophore detection and measurement. *Front. Physiol.* 8:106. doi: 10.3389/fphys.2017.00106

Hanlon, R. (2007). Cephalopod dynamic camouflage. *Curr. Biol.* 17, R400–R404.

Hanlon, R. T. (1982). The functional organization of chromatophores and iridescent cells in the body patterning of *Loligo plei* (Cephalopoda: Myopsida). *Malacologia* 23, 89–119.

Hanlon, R. T., and Messenger, J. B. (1988). Adaptive coloration in young cuttlefish (*Sepia officinalis* L.): the morphology and development of body patterns and their relation to behaviour. *Philos. Trans. R. Soc. Lond. B Biol. Sci.* 320, 437–487. doi: 10.1098/rstb.1988.0087

How, M. J., Norman, M. D., Finn, J., Chung, W. S., and Marshall, N. J. (2017). Dynamic skin patterns in cephalopods. *Front. Physiol.* 8:393. doi: 10.3389/fphys.2017.00393

Langridge, K. V., Broom, M., and Osorio, D. (2007). Selective signalling by cuttlefish to predators. *Curr. Biol.* 17, R1044–R1045.

Mooney, T. A., Samson, J. E., Schlunk, A. D., and Zacarias, S. (2016). Loudness-dependent behavioral responses and habituation to sound by the longfin squid (*Doryteuthis pealeii*). *J. Comp. Physiol. A* 202, 489–501. doi: 10.1007/s00359-016-1092-1

Neumeister, H., Ripley, B., Preuss, T., and Gilly, W. F. (2000). Effects of temperature on escape jetting in the squid *Loligo opalescens*. *J. Exp. Biol.* 203, 547–557. doi: 10.1242/jeb.203.3.547

Otis, T. S., and Gilly, W. (1990). Jet-propelled escape in the squid *Loligo opalescens*: concerted control by giant and non-giant motor axon pathways. *Proc. Natl. Acad. Sci. U.S.A.* 87, 2911–2915. doi: 10.1073/pnas.87.8.2911

Packard, A., and Brancato, D. (1993). Some responses of *Octopus chromatophores* to light. *J. Physiol. Lond.* 459:429.

Packard, A., and Sanders, G. D. (1971). Body patterns of *Octopus vulgaris* and maturation of the response to disturbance. *Anim. Behav.* 19, 780–790. doi: 10.1016/s0003-3472(71)80181-1

Preuss, T., and Gilly, W. F. (2000). Role of prey-capture experience in the development of the escape response in the squid *Loligo opalescens*: a physiological correlate in an identified neuron. *J. Exp. Biol.* 203, 559–565. doi: 10.1242/jeb.203.3.559

Ramachandran, V. S., Tyler, C. W., Gregory, R. L., Rogers-Ramachandran, D., Duensing, S., Pillsbury, C., et al. (1996). Rapid adaptive camouflage in tropical flounders. *Nature* 379, 815–818. doi: 10.1038/379815a0

Ramirez, M. D., and Oakley, T. H. (2015). Eye-independent, light-activated chromatophore expansion (LACE) and expression of phototransduction genes in the skin of *Octopus bimaculoides*. *J. Exp. Biol.* 218, 1513–1520. doi: 10.1242/jeb.110908

Reiter, S., Hülsdunk, P., Woo, T., Lauterbach, M. A., Eberle, J. S., Akay, L. A., et al. (2018). Decomposing the control and development of skin patterning in cuttlefish. *Nature* 562, 361–366. doi: 10.1038/s41586-018-0591-3

Taylor, W. A. (2000). *Change-Point Analysis: A Powerful New Tool for Detecting Changes*. Deerfield, IL: Baxter Healthcare Corporation.

Young, J. Z. (1976). The nervous system of Loligo II. Suboesophageal centres. *Philos. Trans. R. Soc. Lond. B Biol. Sci.* 274, 101–167. doi: 10.1098/rstb.1976.0041

Zylinski, S., Osorio, D., and Shohet, A. J. (2009). Perception of edges and visual texture in the camouflage of the common cuttlefish, *Sepia officinalis*. *Philos. Trans. R. Soc. Lond. B Biol. Sci.* 364, 439–448. doi: 10.1098/rstb.2008.0264

Conflict of Interest: The authors declare that the research was conducted in the absence of any commercial or financial relationships that could be construed as a potential conflict of interest.

Advantages of publishing in Frontiers

OPEN ACCESS
Articles are free to read for greatest visibility and readership

FAST PUBLICATION
Around 90 days from submission to decision

HIGH QUALITY PEER-REVIEW
Rigorous, collaborative, and constructive peer-review

TRANSPARENT PEER-REVIEW
Editors and reviewers acknowledged by name on published articles

Frontiers
Avenue du Tribunal-Fédéral 34
1005 Lausanne | Switzerland

Visit us: www.frontiersin.org
Contact us: frontiersin.org/about/contact

REPRODUCIBILITY OF RESEARCH
Support open data and methods to enhance research reproducibility

DIGITAL PUBLISHING
Articles designed for optimal readership across devices

FOLLOW US
@frontiersin

IMPACT METRICS
Advanced article metrics track visibility across digital media

EXTENSIVE PROMOTION
Marketing and promotion of impactful research

LOOP RESEARCH NETWORK
Our network increases your article's readership